IMPACT OF INTERFERON B AND INTERFERON STIMULATED GENE INDUCTION ON BUNYAMWERA VIRUS REPLICATION

Charles Carlton-Smith

A Thesis Submitted for the Degree of PhD
at the
University of St. Andrews

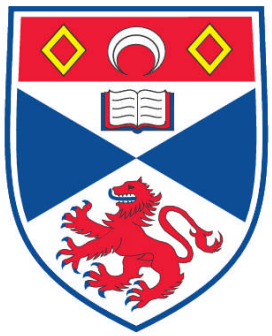

2012

Impact of Interferon β and Interferon Stimulated Gene Induction on Bunyamwera Virus Replication

Charles Carlton-Smith

Biomedical Sciences Research Complex

University of St Andrews

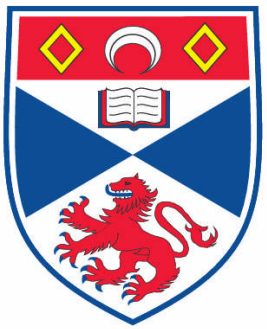

A thesis submitted for the degree of Doctor of Philosophy in Molecular Virology

September 2011

Abstract

The first line of defence against viral infection is the interferon (IFN) response, which must be overcome by a virus for successful replication. Pattern recognition receptors detect virus which triggers induction of IFNβ. Secreted IFNβ stimulates the JAK/STAT signal transduction pathway and the upregulation of IFN stimulated genes (ISGs) culminating with expression of hundreds of antiviral proteins. Bunyamwera virus (BUNV) is the prototype virus for the genus *Orthobunyavirus* and the family *Bunyaviridae*. BUNV is a trisegmented single stranded negative sense RNA virus whose genome comprises the Large (L), Medium (M) and Small (S) RNA segments. The L segment encodes the RNA polymerase, the M segment the two glycoproteins Gn and Gc and a non-structural protein NSm, and the S segment the nucleoprotein and a non-structural protein NSs in overlapping reading frames. The NSs protein interferes with RNA polymerase II mediated transcription thereby inhibiting cellular mRNA production, including IFN mRNA, and hence it is the primary IFN antagonist. A recombinant virus, rBUNdelNSs, that is unable to express the NSs protein, does not inhibit cellular transcription and is thus a strong IFN inducer. The aim of this thesis was to understand how IFN inhibits BUNV replication. Cells stimulated into the antiviral state by IFN treatment were protected against BUNV infection but addition of IFN 6 hours (or later) post infection had little effect on the replication cycle. However, addition of IFN immediately following infection conferred restriction on BUNV replication by initially increasing viral protein synthesis and then by blocking translation of positive sense viral RNA. To identify ISGs with anti-BUNV activity, I screened a panel of 26 cell lines that inducibly express individual ISGs. To aid screening, recombinant BUNV that expressed green fluorescent protein (GFP) were employed, including an NSs deletion virus with GFP fused to the Gc, rBUNGceGFPdelNSs, that I created and characterised. By a combination of virus yield assays, Western blotting and fluorescence techniques, three cell lines that inducibly express PKR, viperin or MTAP44 were shown to restrict BUNV replication. More detailed studies revealed PKR to restrict BUNV RNA and protein synthesis, but when PKR was knocked-down in IFN competent A549 cells viral replication was not blocked in cells pre-treated with IFN. Viperin inhibited viral protein synthesis and virally-induced host cell protein synthesis shut-off. Additionally, viral RNA synthesis was restricted by viperin and this was dependent on the CX_3CX_2C motif 1 of viperin. Taken together, these data show that the restriction of BUNV replication mediated by IFN is an accumulated effect of several different ISGs acting on different stages of the viral life cycle.

Candidate's declarations

I, **Charles Carlton-Smith**, hereby certify that this thesis, which is approximately 52,500 words (excluding references) in length, has been written by me, that it is the record of work carried out by me and that it has not been submitted in any previous application for a higher degree.

I was admitted as a research student in October 2006, and as a candidate for the degree of Doctor of Philosophy (PhD) in Molecular Virology; the higher study for which this is a record was carried out at the University of St Andrews between 2006 and 2011.

Date: ..... signature of candidate: .....

Supervisor's declaration

I hereby certify that the candidate has fulfilled the conditions of the Resolution and Regulations appropriate for the degree of Doctor of Philosophy at the University of St Andrews and that the candidate is qualified to submit this thesis in application for that degree.

Date: ..... signature of supervisor: .....

Prof. R.M. Elliott

Permission for electronic publication

In submitting this thesis to the University of St Andrews I understand that I am giving permission for it to be made available for use in accordance with the regulations of the University Library for the time being in force, subject to any copyright vested in the work not being affected thereby. I also understand that the title and the abstract will be published, and that a copy of the work may be made and supplied to any bona fide library or research worker, that my thesis will be electronically accessible for personal or research use unless exempt by award of an embargo as requested below, and that the library has the right to migrate my thesis into new electronic forms as required to ensure continued access to the thesis. I have obtained any third-party copyright permissions that may be required in order to allow such access and migration, or have requested the appropriate embargo below.

The following is an agreed request by candidate and supervisor regarding the electronic publication of this thesis: **Access to printed copy and electronic publication of thesis through the University of St Andrews**.

Date: ..... signature of candidate: .....

signature of supervisor: .....

Contents

Abbreviations

General

ACE2	angiotensin-converting enzyme 2
ADAR	adenosine Deaminase Acting on RNA
AIM2	absent in melanoma 2
AP-1	activator protein 1
APC	antigen presenting cells
APOBEC	apolipoprotein B mRNA-editing enzyme-catalytic polypeptide-like
ASC	apoptosis-associated Speck-like
ATP	adenosine triphosphate
bp	base pair
BST2	bone marrow stromal cell antigen 2
cAMP	cyclic adenosine monophosphate
CARDif	CARD adaptor inducing IFNβ
CARDs	caspase recruitment domains
CAT	chloramphenicol acetyl transferase
CBP	CREB-binding protein
CID	central interacting domain
CPE	cytopathic effect
CREB	cAMP responsive element binding protein
CTD	C terminal domain
DAI	DNA-dependent activator of IFN
DBD	DNA binding domain
DEV	double enveloped
DIG	digoxigenin
DIs	defective interfering particles
DMEM	Dulbecco’s modified Eagle’s medium
DNA	deoxyribonucleic acid
DTT	dithioreitol
dsRNA	double stranded RNA
eGFP	enhanced green fluorescent protein
eIF2	eukaryotic initiation factor
endo H	endoglycosidase H
ER	endoplasmic reticulum
FACS	fluorescence activated cell sorting
FADD	Fas associated death domain
FERM	four point one, ezrin, radixin, moesin
FPPS	farnesyl diphosphate synthase
g	gram
GAF	gamma activated factor
GAS	γ IFN activated site
GATA3	GATA binding protein 3

GBP	guanylate binding protein
GMEM	Glasgow modified eagle's medium
GPC	glycoprotein precursor
GTP	guanine triphosphate
HEK	human embryonic kidney
HFRS	haemorrhagic fever with renal syndrome
HMG	high mobility group
HPS	hantavirus pulmonary syndrome
IFI	interferon induced protein
IFIT1	IFN induced protein with tetratricopeptide repeats 1
IFITM	interferon induced transmembrane protein
IFN	interferon
IFNAR	interferon α receptor
IFNGR	interferon gamma receptor
IKK	inhibitor of NF-κB kinase
IL	interleukin
IPS-1	IFNβ promoter stimulator protein 1
IRAK	interleukin-1 receptor-associated kinase
IRF	interferon regulatory factor
ISGF3	IFN stimulated gene factor 3
ISGs	interferon stimulated genes
ISRE	interferon stimulated response element
IκB	inhibitor of NF-κB
JAKS	Janus kinase
JH	JAK homology domain
JNKs	c-Jun N-terminal kinases
kb	kilobase
kDa	kiloDalton
kg	kilogram
L	large
LGP2	laboratory of genetics and physiology 2
LRR	leucine-rich repeats
LZ	leucine zipper
M	medium
MAPK	mitogen activated protein kinase
MAVS	mitochondrial antiviral signalling
MDA5	melanoma differentiation-associated gene 5
mDCs	myeloid dendritic cells
MEF	murine embryonic fibroblast
MEM	modified Eagle's medium
MHC	major histocompatibility complex
miRNA	micro RNA
mg	milligram
ml	millilitre

MTAP44	microtubule associated protein
MyD88	myeloid differentiation factor 88
N	nucleoprotein
NBs	nuclear bodies
NEMO	NF-κB essential modifier
NES	nuclear export signal
NF-κB	nuclear factor kappa B
NLS	nuclear localisation signal
NS	non-structural
nt	nucleotide
OAS	oligoadenylate synthetases
OASL	oligoadenylate synthetase-like
ORF	open reading frame
OTU	ovarian tumour domain
PABP	poly(A) binding protein
PAMPs	pathogen associated molecular patterns
PCR	polymerase chain reaction
pDCs	plasmacytoid dendritic cells
PI3K	phosphatidylinositol 3 kinase
PIAS	protein inhibitors of activated STAT
pfu	plaque forming unit
PK	protein kinase
PKC	protein kinase C
PKR	protein kinase R
PLSCR1	phospholipid scramblase 1
PML	promyelocytic leukaemia protein
PRD	positive regulatory domain
PRR	pattern recognition receptor
RE	restriction endonuclease
RER	rough ER
RIG-I	retinoic acid inducible gene I
RIP1	receptor interacting protein 1
RLRs	RIG-I-like receptors
RNA	ribonucleic acid
RNAi	RNA interference
RNaseL	endoribonuclease L
RNP	ribonucleoprotein
RT	room temperature
S	small
SH2	Src-homology 2
shRNA	small hairpin RNA
siRNA	small interfering RNA
SOCS	suppressor of cytokine signalling
SSC	saline sodium citrate

ssRNA	single stranded RNA
stat	signal transduction activator of transcription
STING	stimulator of interferon genes
TAB	TAK1-binding protein
TAD	transcriptional activator domain
TAK1	transforming growth factor β-associated kinase 1
TANK	TRAF associated NF-κB activator
TBK1	TANK binding kinase 1
TGN	*trans*-Golgi network
TH1	T helper 1
TIR	Toll/interleukin-1 resistance
TLRs	Toll-like receptors
TNFR1	tumour necrosis factor receptor 1
TNF-α	tumour necrosis factor alpha
TRADD	TNFR1-associated death domain
TRAF	TNF receptor-associated factor
TRAP	translocon associated protein
TRIF	TIR-domain-containing adapter-inducing interferon-β
TRIM	tripartite motif-containing protein
Tyk	tyrosine protein kinase
UTR	untranslated region
U	unit
UV	ultra-violet
V	volt
v/v	volume per volume
vif	virion infectivity factor
viperin	virus inhibitory protein, endoplasmic reticulum-associated, interferon-inducible
VISA	virus-induced signalling adaptor
VLPs	virus like particles
w/v	weight per volume
µg	microgram
µl	microlitre

Viruses

AKAV	Akabane virus
ANDV	Andes virus
BDV	Borna disease virus
BUNV	Bunyamwera virus
BVDV	bovine viral diarrhoea virus
CCHFV	Crimean-Congo haemorrhagic fever virus
CEV	California encephalitis virus
CMLV	camelpox virus

CPXV	cowpox virus
CSFV	classical swine fever virus
CVV	Cache Valley virus
DENV	Dengue virus
EBOV	Ebola virus
EMCV	encephalomyocarditis virus
FMDV	foot and mouth disease virus
HBV	hepatitis B virus
HCV	hepatitis C virus
HIV-1	human immunodeficiency virus 1
HPIV2	human parainfluenza virus 2
HPV	human papillomavirus
HSV1	herpes simplex virus 1
HTNV	Hantaan virus
IAV	influenza A virus
IBV	influenza B virus
JCV	Jamestown Canyon virus
JEV	Japanese encephalitis virus
LACV	La Crosse virus
LCMV	lymphocytic choriomeningitis virus
LGTV	Langat virus
MARV	Marburg virus
MCMV	murine cytomegalovirus
MeV	measles virus
MHV	mouse hepatitis coronavirus
NDV	Newcastle disease virus
NSDV	Nairobi sheep disease virus
OROV	Oropouche virus
PHV	Prospect Hill virus
PIV3	parainfluenza virus 3
PIV5	parainfluenza virus 5
PTV	Punta Toro virus
PV	polio virus
RVFV	Rift Valley fever virus
SARS	severe acute respiratory syndrome
SeV	Sendai virus
SFV	Semliki Forest virus
SINV	Sindbis virus
SNV	Sin Nombre virus
SSHV	Snowshoe hare virus
THOV	Thogoto virus
TSWV	tomato spotted wilt virus
TULV	Tula virus
UUKV	Uukuniemi virus

VACV	vaccinia virus
VHSV	viral haemorrhagic septicaemia virus
VSV	vesicular stomatitis virus
WNV	West Nile virus

1 Introduction

The immune response

The mammalian immune system is categorised into the innate (non-specific) and the adaptive (specific) immune systems, both of which are able to distinguish between self and non-self. The adaptive immune response is highly specialised and responds only to specific antigens originating from pathogens. It can take several days for this response to get established, and it is not able to prevent or stop the initial infection. However, the adaptive response does provide long-term protection against the same antigens because of the immunological memory provided by memory B and T cells of the adaptive immune response. Furthermore, repeated exposure to the same pathogen/antigen results in a significantly increased and rapid adaptive immune response. This response is mediated by specialised cells called lymphocytes (Braciale, 2007).

The innate immune system is non-specific and comprises various defence mechanisms; physical barriers (such as the skin), physiological barriers (such as the low pH of the stomach), cellular components and proteins which are released by the cells (such as cytokines). This response occurs at the time of exposure to foreign agents and is mediated by phagocytic cells, which ingest and destroy foreign agents, and natural killer cells (NK) which destroy infected cells. All of these cells secrete cytokines, which are small proteins involved in the regulation of the innate immune response. When secreted, the cytokines are able to initiate signalling pathways in neighbouring cells, and to keep the response to the correct magnitude required to clear the infection as efficiently and rapidly as possible, by affecting the growth, differentiation and production of cells in the body (Biron, 2007).

Of considerable importance to the host cell is the counteraction of a viral infection. This begins with the innate response, which must be successful enough to quash the infection, or at the very least suppress it for long enough that the adaptive response has time to be established. Immediately, viruses can be targeted for phagocytosis by the complement cascade system, coating the virions in complement components (Lachmann & Davies, 1997), and circulating neutralising antibodies are highly effective at preventing virus dissemination to vital organs and their subsequent adsorption and entry into cells (Ochsenbein *et al.*, 1999). Viruses that manage to attach and enter cells then have the extremely powerful interferon response to contend with. This response rapidly attempts to stop the viral infection at all levels from replication to egress, and also subsequent entry into surrounding cells, and can even stimulate apoptosis to limit the spread of the virus (Randall & Goodbourn, 2008).

Virus detection by the host cell

Pattern recognition receptors

Pattern recognition receptors (PRRs) are now known to be the main receptors involved in detecting an invading pathogen. They have evolved to detect highly conserved specific pathogen associated molecular patterns (PAMPs) which are located within or on the surface of pathogens. PRRs are able to detect both extracellular and intracellular viruses, and the most intensely studied detect different classes of nucleic acids and include Toll-like receptors (TLRs), and the RNA helicases retinoic acid inducible gene I (RIG-I) (Yoneyama *et al.*, 2004) and melanoma differentiation-associated gene 5 (MDA5) (Andrejeva *et al.*, 2004).

The Toll-like receptors

The Toll-like receptors are type I transmembrane glycoproteins that consist of an intracellular Toll/interleukin-1 resistance (TIR) domain for signal transduction and an extracellular domain of leucine-rich repeats (LRR) for PAMP recognition and binding (Kawai *et al.*, 2005; Takeda & Akira, 2005). Binding of PAMPs to the LRR initiates receptor dimerisation and conformational changes in the receptor, which in turn trigger recruitment of cytosolic adaptor proteins to the TIR domain of the receptor and thereby activate intracellular signal transduction pathways.

TLR3 detects endosomal and extracellular RNA

In 2001, it was determined that TLR3 was the receptor molecule responsible for responses to exogenous dsRNA, leading to the activation of nuclear factor kappa B (NF-κB) and induction of interferon (IFN) expression (Alexopoulou *et al.*, 2001). TLR3 is expressed on a wide variety of cell types, most notably myeloid dendritic cells (mDCs) (Matsumoto *et al.*, 2003). Specifically, TLR3 relocates from the endoplasmic reticulum to the cell surface and the endosome of fibroblasts (Matsumoto *et al.*, 2002; Matsumoto *et al.*, 2003); to the lysosome of bone marrow derived macrophages (de Bouteiller *et al.*, 2005); and to the endosome of mDCs (Johnsen *et al.*, 2006). Thus, the specific location of TLR3 enables it to detect extracellular and intracellular (through endosomal uncoating of the viral protein coat) viral dsRNA irrespective of viral replication or not. It has been shown previously that dsRNA from DNA and positive-stranded RNA viruses is an extremely potent inducer of IFN (Marcus, 1983; Weber *et al.*, 2006), now known to be through TLR3. Knockout mice deficient in TLR3 receptors are resistant to infection by vesicular stomatitis virus (VSV), reovirus and lymphocytic choriomeningitis virus (LCMV) (Edelmann *et al.*, 2004) because these viruses are detected by different PRRs.

Binding of dsRNA to TLR3 initiates receptor dimerisation and the subsequent phosphorylation of its intracellular tyrosine residues, initiating signal transduction within the cell (**Fig 1.1** (Sarkar *et al.*, 2004)). This recruits the TIR

domain-containing adaptor inducing IFN-β (TRIF) adaptor protein and a member of the family of proteins known as TRAFs (TNF receptor-associated factor) leading to either interferon regulatory factor (IRF) 3 or NF-κB activation (Hacker *et al.*, 2006; Hoebe *et al.*, 2003; Jiang *et al.*, 2004; Yamamoto *et al.*, 2002; Yamamoto *et al.*, 2003).

For NF-κB activation, TRIF enlists the E3 ubiquitin ligase TRAF6 and the receptor interacting protein 1 (RIP1) (Cusson-Hermance *et al.*, 2005; Meylan *et al.*, 2004; Sato *et al.*, 2003). This recruitment leads to the oligomerisation and auto-ubiquitination of TRAF6 and the K63-linked poly-ubiquitination of RIP1 (Chen, 2005; Deng *et al.*, 2000). The transforming growth factor β-associated kinase 1 (TAK1), as well as TAK1-binding proteins 2 and 3 (TAB2 and TAB3), interact with TRAF6 and RIP1 *via* recognition of, and binding to, the polyubiquitin chains (Kanayama *et al.*, 2004). The inhibitor of NF-κB (IκB)

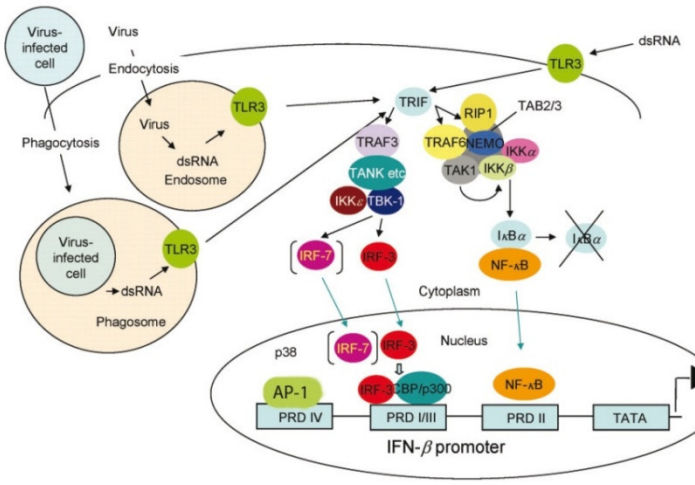

Figure 1.1 : TLR3-dependent signalling in response to dsRNA. TLR3 detects dsRNA and recruits the adaptor protein TRIF that acts as a scaffold to recruit signalling components that feed into either the IRF-3 or the NF-κB pathways. Subsequently IRF-3 and NF-κB and AP-1 assemble on the IFNβ promoter, leading to the recruitment of co-factors such as CBP/p300 and RNA polymerase II, and ultimately IFNβ transcription. Modified from Randall and Goodbourn, 2008.

kinase, IKK, is subsequently recruited to this protein complex (Ea *et al.*, 2006; Li *et al.*, 2006a; Wang *et al.*, 2001; Wu *et al.*, 2006). The subunits IKKα, IKKβ, and the regulatory subunit IKKγ (also known as NF-κB essential modifier (NEMO)) together make up the heterotrimeric IKK complex recruited by polyubiquitinated RIP1 and other members of the aforementioned complex (DiDonato *et al.*, 1997; Mercurio *et al.*, 1997; Rothwarf *et al.*, 1998; Zandi *et al.*, 1998). Now the IKKβ subunit is adjacent to, and thus directly phosphorylated by, TAK1 (Wang *et al.*, 2001). The activated IKK complex then phosphorylates IκB, which is then polyubiquitinated with K48-linked chains and is subsequently degraded. This results in the release of NF-κB from IκB, which allows activated

NF-κB to translocate to the nucleus. This process is regulated by the enzyme A20, which removes ubiquitin from TRAF6 (Boone *et al.*, 2004).

The activation of IRF3 by TLR3 is less well understood than the activation of NF-κB. TRAF3 has been shown to be essential for TLR-stimulated IFN induction (Hacker *et al.*, 2006). For IRF3 activation, TRAF3 is recruited by TRIF, thereby enabling TRAF3 to directly interact with TRAF associated NF-κB activator (TANK) (Li *et al.*, 2002) and TANK can then directly associate with TANK binding kinase 1 (TBK1) (Fitzgerald *et al.*, 2003; Hemmi *et al.*, 2004; Sharma *et al.*, 2003). Together with the related IKKε, TBK1 phosphorylates IRF3, which is then able to translocate to the nucleus. Both IKKε and TBK1 have been shown to activate IRF7 as well (Sharma *et al.*, 2003). TANK has also been shown to interact with IKKγ indicating a possible dual role in both NF-κB and IRF3 activation *via* TLR3 stimulation (Chariot *et al.*, 2002).

TLR7 and TLR9 detect endosomal ssRNA and DNA

TLR3 is not expressed on plasmacytoid dendritic cells (pDCs) (Kadowaki *et al.*, 2001), however pDCs are one of the few cell types to express TLR7 (and also constitutively express IRF7) and they secrete large amounts of IFN during viral infection (Colonna *et al.*, 2004). TLR7 is only expressed in the endosomal compartment of the cells (Diebold *et al.*, 2004; Jarrossay *et al.*, 2001; Kadowaki *et al.*, 2001) and it has been shown that only TLR7 responds to single stranded RNA (ssRNA) in a non-sequence-specific manner (Diebold *et al.*, 2004; Heil *et al.*, 2004). However, this is not always enough to prevent host DNA and RNA from activating the TLR-mediated response (Diebold *et al.*, 2004; Kariko *et al.*, 2005), thus identification of self and non self DNA and RNA is thought to be due to modifications of the nucleosides and their subcellular location (Crozat & Beutler, 2004; Ishii & Akira, 2005; Kariko *et al.*, 2005). It is important to note that the ability to detect self DNA by TLR7 has been linked to auto-immune disorders, such as lupus. Thus, the endosomal localisation and non-sequence specific PAMP are not sufficient to prevent auto-immune activation. Additionally, virus internalisation is required for TLR7 and TLR9 activation (Lund *et al.*, 2003; Lund *et al.*, 2004). It has more recently been observed that TLR7 can also respond to viruses that replicate in the cytoplasm because the cytosolic viral replication intermediates are transported to the lysosome by autophagy and presented internally to the endosomal TLR7 (**Fig 1.2** (Iwasaki, 2007; Lee *et al.*, 2007)). Following ligand binding to TLR7 the adaptor protein myeloid differentiation factor 88 (MyD88) is recruited to the cytosolic domain of the receptor (Lund *et al.*, 2004). MyD88 then recruits the interleukin-1 receptor-associated kinase 4 (IRAK4), IRAK1 and the TRAF6 complex which also involves TRAF3 (Hacker *et al.*, 2006). Once TRAF6 is recruited, the activation of the IKK complex by TAB2/3 and TAK1 and the subsequent activation of NF-κB occurs, as described above for the TLR3 signalling pathway. However, IRF7 is constitutively expressed in pDCs to quite high levels and therefore is the

predominant IRF that is activated in these cells. As such, TRAF6 is able to directly conjugate K63-linked polyubiquitin chains onto IRF7 (Kawai *et al.*, 2004) following formation of the MyD88-IRAK1-IRAK4-TRAF6 complex (Honda *et al.*, 2004; Uematsu *et al.*, 2005), which is also dependent on polyubiquitinated RIP1 (Huye *et al.*, 2007; Uematsu *et al.*, 2005). IRAK1 then phosphorylates IRF7 which can then translocate to the nucleus and alter gene expression (Uematsu *et al.*, 2005).

A role for TLR9 in detection of viral nucleic acids has also been described. TLR9 knockout mice demonstrated a higher susceptibility to murine cytomegalovirus (MCMV) infection which correlated with decreased levels of IFN in the knockout compared to the wild-type mice (**Fig 1.2** (Krug *et al.*, 2004; Tabeta *et al.*, 2004)). TLR9 is present in the endosomal compartment of both

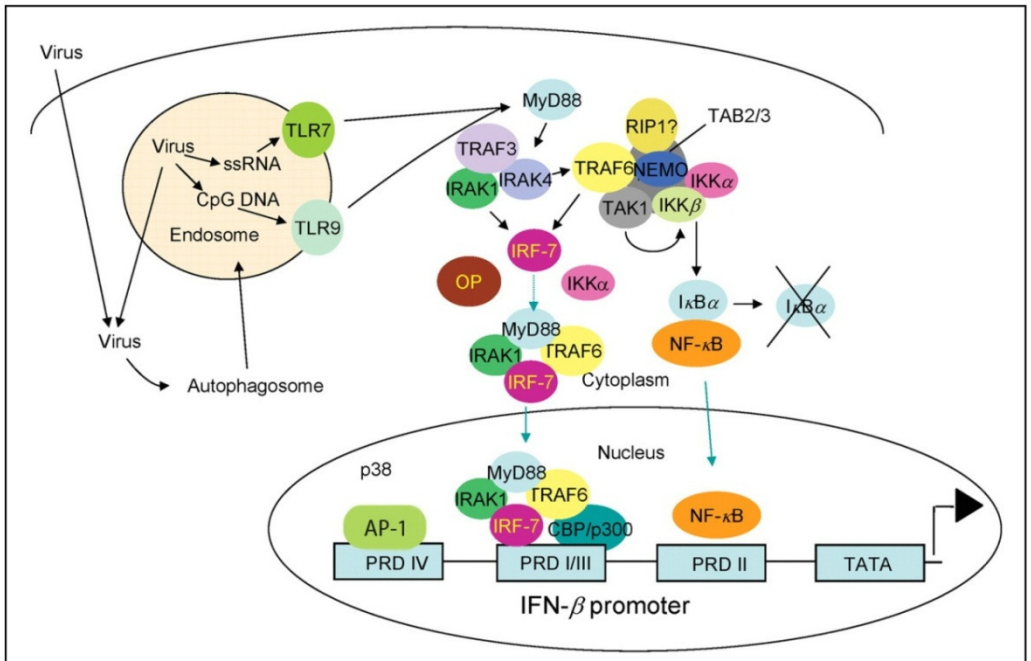

Figure 1.2 : TLR7- and TLR9-dependent signalling. TLR7 detects ssRNA and TLR9 detects CpG DNA. Activated TLRs recruit the adaptor protein MyD88, which further recruits IRAK4 and IRAK5. This complex acts as a scaffold to recruit signalling components for either the IRF-7 or the NF-κB pathways, resulting in nuclear migration and assembly on the IFNβ promoter and the induction of transcription. Modified from Randall and Goodbourn, 2008.

mDCs and pDCs and it detects unmethylated CpG motifs in the lumen of the endosome as foreign viral DNA (Abe *et al.*, 2005; Hemmi *et al.*, 2000; Rutz *et al.*, 2004). However, the signalling pathways are different for each cell type. The mDCs use TLR9 stimulation by the IRF-1-activated MyD88 bound with the IRAK kinases complex to activate the NF-κB pathway (Schmitz *et al.*, 2007), whereas in the pDCs, IFN induction is MyD88-dependent and the CpG ligand must be retained in the endosomal vesicle (Honda *et al.*, 2005). The signalling pathway leading to NF-κB and IRF7 activation is the same as that for TLR7 (Randall & Goodbourn, 2008).

The transcription factor IRF5 has both negative and positive effects on IFN induction depending on which IRF-interacting partner it has (Yanai *et al.*, 2007). TLR7 and TLR9 stimulation can also trigger IFN induction and subsequent secretion into the serum *via* IRF5 (Barnes *et al.*, 2004; Yasuda *et al.*, 2007), and this is also MyD88-dependent as it is for IRF7. IRF5 deficient mice were shown to be more susceptible to viral infection and to have lower levels of IFN in their sera (Yanai *et al.*, 2007).

The RNA helicases RIG-I and MDA5 detect cytoplasmic RNA

Intracellular RNA from replicating viruses can be detected independently of the TLRs (Edelmann *et al.*, 2004) by a class of cytosolic PRRs known as the RIG-I-like receptors (RLRs). The RLRs comprise three proteins, RIG-I, MDA5 and LGP2 (laboratory of genetics and physiology 2). RIG-I was identified as a receptor for dsRNA produced or released into the cytosol during viral infection, as well as being able to detect the dsRNA analogue poly I:C (Yoneyama *et al.*, 2004). MDA5 was originally found to bind to the IFN antagonistic V protein of parainfluenza virus 5 (PIV5) (Andrejeva *et al.*, 2004) and shows similar characteristics to RIG-I (Yoneyama *et al.*, 2005). LGP2 was first identified as a negative regulator of RIG-I and MDA5 (Rothenfusser *et al.*, 2005) but more recently has been shown to facilitate the recognition of viral RNA by MDA5 and RIG-I (Satoh *et al.*, 2010). RIG-I and MDA5 are helicases that have two critical functional domains, one comprising two N-terminal caspase recruitment domains (CARDs) that are conformationally hidden internally, and the other a C terminal RNA helicase domain which has ATPase activity. Detection and subsequent binding of RNA to the RNA binding motif allows a conformational change to occur which exposes the helicase domain for binding of ATP, which itself results in the CARD domains being released to bind to the mitochondrion-associated adaptor protein. This protein was discovered independently by four groups and called IFNβ promoter stimulator protein 1 (IPS-1), mitochondrial antiviral signalling protein (MAVS), CARD adaptor inducing IFNβ (CARDif) and virus-induced signalling adaptor (VISA) (**Fig 1.3** (Kawai *et al.*, 2005; Meylan *et al.*, 2005; Seth *et al.*, 2005; Xu *et al.*, 2005)). The location on the outer mitochondrial membrane of IPS-1 is essential for its function as an adaptor for the recruitment of signalling molecules that result in IFN induction *via* the NF-κB and IRF3 pathways. The association of IPS-1 and tumour necrosis factor receptor 1 (TNFR1)-associated death domain protein (TRADD) coordinates the assembly of the TRAF3-TRAF6-TANK-RIP1-FADD (Fas associated death domain containing protein (FADD)) complex (Michallet *et al.*, 2008). This complex further recruits IKKβ which either activates IKK for NF-κB activation or activates IRF3 by a TBK1/IKKε dependent pathway (Zhao *et al.*, 2007).

MDA5 is negatively regulated by dihydroxyacetone kinase whereas RIG-I is not (Diao *et al.*, 2007). However, RIG-I, but not MDA5, must have its Lys63 residue ubiquitinated by the tripartite motif-containing protein 25 (TRIM25) E3 ligase,

the importance of which was demonstrated by the inability of a TRIM25 knockout cell line to produce IFNβ in response to infection with Sendai virus (SeV) (Gack *et al.*, 2007). Both RIG-I and MDA5, as well as IPS-1, are negatively regulated by Atg5 and Atg12 due to a direct interaction with their CARD domains (Jounai *et al.*, 2007). The same three proteins are also targeted for ubiquitination by the ISG product RNF125, an E3 ligase. This is evidence of a negative feedback mechanism for IFN production following infection with SeV or stimulation with dsRNA that regulates IFN induction and limits or curtails the immune response (Arimoto *et al.*, 2007). Further negative

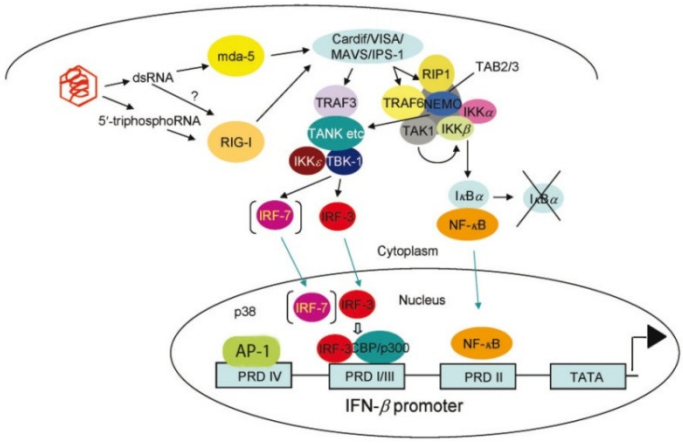

Figure 1.3 : MDA-5- and RIG-I-dependent signalling. Both RNA helicases detect viral dsRNA generated in the cytoplasm and RIG-I also detects RNA molecules with 5' triphosphates. Both helicases have N-terminal CARD domains that recruit the adaptor protein IPS-1 which acts as a scaffold to recruit signalling components that feed either the IRF-3 or NF-κB pathways resulting in assembly on the IFNβ promoter and the induction of transcription. Modified from Randall and Goodbourn, 2008.

regulation of IPS-1 occurs *via* co-localisation of IPS-1 and NLRX1 at mitochondria, which blocks the association of IPS-1 with both MDA5 and RIG-I (Arimoto *et al.*, 2007). The RIG-I-related IFN inducible helicase LGP2 also appears to negatively regulate RIG-I and MDA5 by binding to, and sequestering, RNA but not initiating downstream signalling due to the absence of a CARD domain (Rothenfusser *et al.*, 2005; Yoneyama *et al.*, 2005). However, this is further complicated by studies showing knockout mice lacking LGP2 have a normal negative feedback inhibition of IFNβ transcription and are more susceptible to viruses that activate MDA5 signalling as opposed to RIG-I signalling (Venkataraman *et al.*, 2007).

To establish the differing roles of MDA5 and RIG-I during a viral infection, they were first studied *in vitro* and stimulated with poly I:C. Not only did both respond equally well to poly I:C (Andrejeva *et al.*, 2004; Cardenas *et al.*, 2006; Yamashita *et al.*, 2005; Yoneyama *et al.*, 2004; Yoneyama *et al.*, 2005), but

when the helicase domains were switched between the proteins no difference could be discerned in their capability to respond to the poly I:C stimulus (Childs *et al.*, 2007). Using knockout mice deficient in either MDA5 or RIG-I, studies uncovered that MDA5 dominantly (over RIG-I) recognises poly I:C and that dendritic cells, macrophages and embryonic fibroblasts all respond better *via* MDA5 stimulation after poly I:C treatment (Gitlin *et al.*, 2006; Kato *et al.*, 2006), whereas RIG-I recognises *in vitro* transcribed RNAs (Kato *et al.*, 2006). Further studies revealed that RIG-I recognises self from non-self by being activated by RNAs bearing uncapped 5'-triphosphates (such as viral genomic RNAs) as opposed to cellular RNAs that are post transcriptionally capped (Hornung *et al.*, 2006; Pichlmair *et al.*, 2006), or those RNAs that are transcribed by polymerases I and III which have 5' monophosphates.

This difference in PAMP or ligand detected by MDA5 or RIG-I is supported by evidence from infections with specific viruses. Infection of knockout mice with influenza A virus (IAV) or paramyxoviruses triggers the activation of the RIG-I signalling pathway but not the MDA5 pathway (Kato *et al.*, 2006). However, studies using knockout mice show that infection with picornaviruses leads to the activation of the MDA5 pathway for IFNβ induction and not the RIG-I pathway (Gitlin *et al.*, 2006; Loo *et al.*, 2008). The latter is because throughout the replicative cycle, picornavirus RNA is covalently bound to the VPg protein and thus there is no 5' end available for RIG-I to detect (Lee *et al.*, 1977). During infection both poliovirus (PV) and encephalomyocarditis virus (EMCV) have been shown to produce measurable levels of dsRNA, detectable by MDA5. Conversely, IAV and paramyxoviruses do not produce detectable dsRNA (Pichlmair *et al.*, 2006). Separate studies using overexpression and knockout cell lines have further corroborated MDA5 involvement, and not RIG-I, with picornavirus infection (Kato *et al.*, 2006), but also with measles virus (MeV) infection (Berghall *et al.*, 2006), and both proteins, MDA5 and RIG-I, have been demonstrated to be used in IFN induction by Newcastle disease virus (NDV) and SeV (Andrejeva *et al.*, 2004; Melchjorsen *et al.*, 2005; Yoneyama *et al.*, 2004; Yoneyama *et al.*, 2005), along with flaviviruses and reoviruses (Loo *et al.*, 2008).

DAI detects cytoplasmic DNA

DNA located in the cytosol elicits an immune response, and one of the PRRs responsible for detection is the DNA-dependent activator of IFN regulatory factors (DAI) (also known as DLM1 and ZBP1) (Takaoka *et al.*, 2007). DAI subsequently activates the IFN system independently of TLR9 (Fu *et al.*, 1999; Stetson & Medzhitov, 2006). It has been shown that DAI has three domains that bind to DNA and that they are essential for activation of DAI *in vivo* (Wang *et al.*, 2008). Furthermore, this activation leads to the induction of IFN in a TLR/RIG-I-independent manner, but by a mechanism that requires the kinases TBK1 and IKKε and the transcription factor IRF3 (Ishii *et al.*, 2006; Takaoka *et*

al., 2007). Knockdown of DAI using RNAi demonstrated a reduction in IFNβ when infected, and thus stimulated, with the DNA virus herpes simplex virus 1 (HSV1) but not with the RNA virus NDV (Takaoka *et al.*, 2007). AIM2 (absent in melanoma 2) is another protein recently shown to directly bind DNA from the DNA virus MCMV. Binding of DNA by AIM2 leads to the interaction of the caspase-1-activating adaptor protein ASC (apoptosis-associated Speck-like protein) resulting in the formation of a caspase-1-activating inflammasome, which is partially responsible for the maturation of IL-1β and IL-18 and leads to NK cell-dependent IFNγ synthesis. Using AIM2 and ASC knockout mice it has been shown that MCMV replicates to a higher titre in the knockout mice compared with the wild-type mice and thus that the AIM2-ASC pathway is essential for the innate immune response to MCMV (Rathinam *et al.*, 2010).

STING

More recently the stimulator of interferon genes (STING) protein has been found to play a significant role in the innate immune response to viral infections by detecting non-CpG intracellular DNA species originating from DNA pathogens. STING is normally resident in the ER and has five putative transmembrane domains and is able to stimulate the induction of IFNβ by the signalling pathways of IRF3 and NF-κB (Ishikawa & Barber, 2008). STING knockout murine embryonic fibroblast (MEF) cells were highly sensitive to negative stranded RNA viruses and unable to produce IFN in response to herpes virus infection or B-DNA stimulation, all in a TLR9 independent manner. Also, STING was found to interact with the translocon associated protein (TRAP) β and with RIG-I, and furthermore, RNAi knockdown of TRAPβ inhibited IFN induction by STING (Ishikawa & Barber, 2008).

Interferon

Over fifty years ago Isaacs and Lindenmann described the interference of influenza virus replication by a cytokine released from chick cells which had been infected with a heat inactivated influenza virus (Isaacs & Lindenmann, 1987). Thus this cytokine was called IFN, and since then substantial amounts of work have shown IFN to be involved in many cellular pathways and responses which are generally termed as the IFN response. The last decade has proved enormously successful in providing understanding of the receptors, ligands, signalling pathways, genetic elements and effector proteins involved in this complex response system, and how this is effective against viruses will be discussed in further detail below.

The IFN family is made up of many glycoproteins which, when secreted by cells, are able to elicit an immune response that ultimately leads to the cells going into the ‘antiviral state’. This is achieved by IFN stimulated up-regulation of many antiviral genes involved with inhibition of protein synthesis, cell growth and programmed cell death, apoptosis. There are several types of IFN, which

are grouped into three classes, types I, II and III, based on the sequence of their amino acids and the receptors they bind. Type I human IFNs are further sub-divided into five classes, IFN-α (containing 13 different subtypes), IFN-β, IFN-ε, IFN-κ, and IFN-ω. Of the type I IFNs it is only IFN-α and IFN-β that are directly induced by viral infection, and the level of induction is variable between differing cell types and dependent on the viral stimulus (Pestka *et al.*, 2004). Type II IFN consists of IFN-γ alone, and the type III IFNs consist of IFN-λ1, IFN-λ2 and IFN-λ3, which are also known as IL-29, IL-28A and IL-28B respectively. IFN-γ is not directly induced by viruses and is secreted by activated T lymphocytes and NK cells, whereas type III IFNs are also induced directly by viral infection using pathways similar to IFNs α and β for detection (Onoguchi *et al.*, 2007).

The secreted IFNs α/β bind to the interferon α receptor (IFNAR), which is a heterodimeric receptor comprising IFNAR1 and IFNAR2, and eventually stimulate the viral innate immune response *via* genes known as interferon stimulated genes (ISGs) (**Fig 1.4**). IFN-γ binds to the IFN-γ receptor (IFNGR) which is a tetramer comprising two IFNGR1 chains and two IFNGR2 chains,

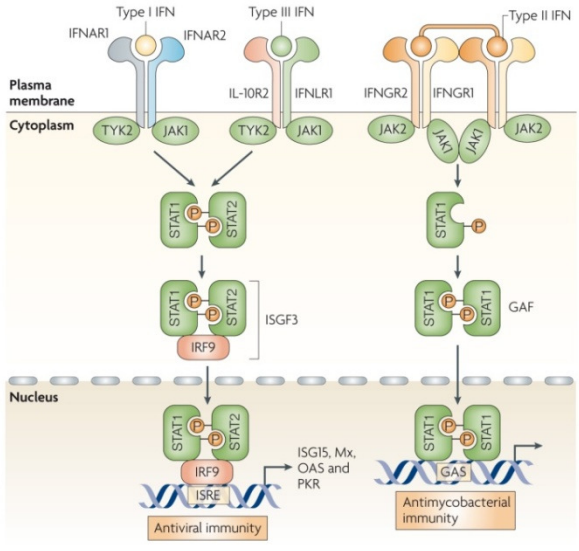

Figure 1.4 : Interferon receptor signalling. The type I, II and III IFNs bind to their respective receptor triggering the JAK/STAT signal transduction pathway, resulting in the formation of ISGF3 or GAF. These complexes translocate to the nucleus to induce IFN-stimulated genes from IFN-stimulated response elements (ISREs) or GAS promoter elements, for type I and type III, or type II IFN responses, respectively. Modified from Sadler and Williams, 2008.

thus mediating an overall innate immune response (**Fig 1.4**). Type III IFNs bind to the heterodimeric receptor consisting of the interleukin 10 receptor 2 (IL-10R2) and the IFN-λ receptor 1 (IFN-λR1). Type I and type III IFNs induce a similar antiviral response once stimulated, and are induced in many cell types; however, there is a reduced number of type III IFN receptors compared with the number of IFNARs (Meager *et al.*, 2005).

Interferon induction

There exists a vast array of viral infection detection methods, along with differing methods of entry into the cell by viruses of different families, and hence, an abundant variety of viral stimuli, from viral nucleic acids to viral proteins (discussed later), to induce the IFN response.

Interferon β induction: the enhanceasome

Immediately upstream of the IFNβ promoter is the IFNβ enhancer element, which controls the activation of IFNβ transcription. The IFNβ enhancer element comprises four binding sites, two for the IRF proteins, one for the activator protein 1 (AP-1) and one for the NF-κB protein. The IRF protein transcription factors, essentially IRF3 and IRF7, bind to the positive regulatory domains (PRD) I and III, the AP-1 complex binds to PRD IV, and the NF-κB complex, comprising of p50/p60 dimers, binds to PRD II. These proteins are activated in the cytoplasm and then translocate to the nucleus where the binding of these proteins and the stability of the resulting structure, the enhanceasome, is additionally improved by non-histone high mobility group (HMG)-I/Y chromatin proteins bending of the DNA. The enhanceasome structure and conformation as it is formed allows for increasing and enhanced recruitment of, and binding of, the transcription factors and coactivators, which further increases the self assembly of the enhanceasome. This additionally augments the recruitment of cAMP responsive element binding protein (CREB)-binding protein (CBP)/p300 and RNA polymerase II to the IFNβ promoter, and crucially completes the activation and transcription of IFNβ mRNA in the stimulated cells.

Interferon α induction

Interferon α induction occurs in leukocytes (by an IFNβ independent pathway) and fibroblast cells (by an IFNβ dependent pathway), and, as with IFNβ induction, IFNα promoters contain binding sites for AP-1 and IRF proteins namely the PRD I site. Unlike the IFNβ enhancer element there is no binding site for NF-κB, but, studies using IFNβ knockout mice have shown that IFNα induction is non functional without IFNβ gene expression (Erlandsson *et al.*, 1998). Thus, because the IFNα genes are switched on by IRF7, and IRF7 is an IFNβ gene product that is induced early on in the IFNβ response (except in pDCs as they constitutively express IRF7) by the activation of the IRF3 signal transduction pathway, the powerful IFNα response is dependent on the IFNβ response (Levy *et al.*, 2002; Marie *et al.*, 1998).

Interferon γ induction

Interferon γ induction occurs in NK cells irrespective of antigen presentation whereas $CD4^+$ T helper 1 (TH1) cells and most $CD8^+$ cells require antigen presentation by antigen presenting cells (APC) (Young, 1996). Consequently, production of IFNγ occurs in these cells but not in cells infected by a virus (Takaoka & Yanai, 2006). This activation is vital for the innate immune response of macrophages, and in NK cells is dependent on production of IL-12 from APCs. In $CD4^+$ cells the IFN promoter comprises two elements, the distal and proximal elements. The distal element is activated by binding of the GATA binding protein 3 (GATA3) and the proximal element is activated by binding of a transcription complex that includes AP-1. However, $CD8^+$ cells only require

activation by the distal regulatory element. Furthermore, both the $CD4^+$ and $CD8^+$ cell's IFN activation is enhanced by the cytokines IL12 and IL18, which are secreted by APCs, although neither IL12 or IL18 is sufficient to stimulate a response on their own (Goodbourn *et al.*, 2000; Singh *et al.*, 2000; Young, 1996).

Interferon λ induction

Interferon λ induction follows the same course as type I IFN induction.

IFN signalling pathways

The STAT proteins

Humans have seven STAT proteins, called STAT1-STAT4, STAT5a, STAT5b and STAT6, which either form stable homodimers or stable heterodimers following activation (Schindler & Plumlee, 2008). The STAT proteins consist of seven structurally conserved domains which comprise the amino terminal domain, coiled coil domain, DNA binding domain (DBD), linker domain, Src-homology 2 (SH2) domain, tyrosine activation motif, and transcriptional activator domain (TAD). The amino terminal domain allows unphosphorylated STATs to homotypically dimerise, and thus aids the recruitment of STAT dimers during receptor activation (Braunstein *et al.*, 2003). The coiled coil domain is thought to control nuclear import and export and to have some involvement with regulatory proteins (Schindler *et al.*, 2007). The DBD is involved in nuclear import and export as well as binding to GAS (McBride & Reich, 2003; Schindler & Plumlee, 2008). The linker domain ensures constant nuclear export in resting cells and translates conformational changes to the DBD (Bhattacharya & Schindler, 2003). The SH2 domain is responsible for receptor recruitment and activation of STAT dimers (Shuai *et al.*, 1994). The tyrosine activation motif assists JAK-dependent phosphorylation of STAT, and then itself is bound to the second STAT, to make the dimer, by the SH2 domain (Mao *et al.*, 2005; Schindler & Plumlee, 2008). TADs are important for the recruitment of coactivators, and to maintain stability of STAT proteins, as some can be targeted for ubiquitination (Schindler & Plumlee, 2008). With regards to the IFN signalling pathway, signalling *via* STAT1 and STAT2 is the most prominent.

There are four members of the JAK family, Jak1, Jak2, Jak3 and Tyk2 and they have seven JAK homology domains, JH1-JH7. JH1 is responsible for tyrosine kinase catalytic activity. JH2 is a pseudokinase domain that inhibits JAK activation (when no suitable ligand is bound), and thus negatively regulates the kinase activity of JH1 (Luo *et al.*, 1997; Saharinen *et al.*, 2000). JH3 and JH4 have a SH2 domain with no known function, and the rest, JH4 to JH7 make up the FERM (four point one, ezrin, radixin, moesin) domain which provides stability and maintains the association with cytokine receptors. The N terminal region of the JAKs allows receptor association in the inactive state (Chen *et al.*, 1997). Much of the downstream signalling stimulated by cytokines, including

IFNs, involves the JAK family (Burfoot *et al.*, 1997; Platanias *et al.*, 1996). For example, Tyk2 binds IFNAR1, whereas Jak1 binds with IFNAR2 and IFNGR1, and Jak3 binds IFNGR2 (Schindler & Plumlee, 2008). Once IFN binds to the receptor, the JAKs are also activated by trans- or auto-phosphorylation (Rane & Reddy, 2000), leading to the phosphorylation of specific tyrosine residues on the cytoplasmic domain of the receptor. Receptor phosphorylation leads to recruitment of SH2 domain-containing proteins, including STATs and phosphatidylinositol 3 kinase (PI3K), resulting in continuation of the signalling pathway and culminating in the antiviral response. JAK knockout mice are unable to survive for very long, illustrating the importance of these proteins (Karaghiosoff *et al.*, 2000; Park *et al.*, 1995; Rodig *et al.*, 1998).

Type I IFN signalling

The 'classical' pathway of IFN signalling is *via* JAK/STAT signal transduction and this pathway is thus well characterised. In unstimulated cells the intracellular domains of the IFNAR subunits are physically associated with the cytoplasmic Tyk2 and JAK1 kinases as well as both the STAT1 (weakly *via* STAT2) and the STAT2 proteins (Abramovich *et al.*, 1994; Muller *et al.*, 1993; Novick *et al.*, 1994; Precious *et al.*, 2005). Once type I IFNs have bound to the IFNARs, they undergo a conformational change which results in Tyr466 of IFNAR1 being phosphorylated by Tyk2, leading to a robust interaction between IFNAR1 and STAT2. This stronger interaction allows phosphorylation of Tyr690 of STAT2 by Tyk2, and consequently the phosphorylation of STAT1 at Tyr701 by JAK1 (Leung *et al.*, 1995). The stable heterodimer of STAT1/STAT2 imparts a conformational change that reveals the nuclear localisation signal (NLS) allowing the dimer to translocate to the nucleus (until it is dephosphorylated and the nuclear export signal (NES) is again exposed and the proteins are exported back to the cytoplasm) (Banninger & Reich, 2004; Fagerlund *et al.*, 2002; McBride *et al.*, 2000; Melen *et al.*, 2003). Tyrosine phosphorylation of the STAT1/STAT2 dimer results in the assembly of the heterotrimeric transcriptional activator complex ISGF3 (IFN stimulated gene factor 3), comprising STAT1/STAT2/IRF9, which enters the nucleus and binds to the interferon stimulated response elements (ISRE) upstream of the type I IFN genes and activates transcription of IFN (Kessler *et al.*, 1990; Levy *et al.*, 1989; Martinez-Moczygemba *et al.*, 1997; Tang *et al.*, 2007; Veals *et al.*, 1992). Whether IRF9 binds to the STAT1/STAT2 dimer at the IFNAR is unknown. However, STAT2 and IRF9 have been shown to interact with each other both before and after IFNα stimulation and in a separate study IRF9 was shown to associate directly with IFNAR2, suggesting ISGF3 complex formation is at the IFNAR (Martinez-Moczygemba *et al.*, 1997; Tang *et al.*, 2007).

It is not only STAT1 and STAT2 which dimerise in response to type I IFNs; homodimers of STAT1, STAT3, STAT4, STAT6, and heterodimers of STAT1/3, STAT1/4, STAT1/5, STAT2/3 and STAT5/6 have been described (Farrar *et al.*,

2000; Platanias, 2005; Torpey *et al.*, 2004). When activated these STAT dimers initiate transcription of ISGs by binding to the upstream ISRE/GAS elements of their promoters. With this diversity in STAT dimer formation comes regulation of which ISGs are upregulated, as expression of some ISGs occurs in response to STAT binding to either the ISRE or to GAS or even to both regulatory elements. In this way optimal ISG expression can be achieved by a combination of STATs binding to different regulatory elements and conversely, some STATs can upregulate one ISG whilst simultaneously downregulating another (Nguyen *et al.*, 2002; Platanias, 2005).

Type II IFN signalling

Type II IFN (IFNγ) binds and stimulates the type II IFN receptors, IFNGR1 and IFNGR2, which are constitutively associated with Jak1 and Jak2, respectively (Bach *et al.*, 1997; Chen *et al.*, 2004; Stark *et al.*, 1998). As for type I IFNs, IFNγ binding to IFNGR1 results in receptor dimerisation, and the subsequent JAK activation stimulates phosphorylation of IFNGR1. This results in a conformational change and two binding sites for STAT1 become exposed. The subsequent binding of STAT1 proteins is *via* the SH2 domains. Phosphorylation of Tyr701 of STAT1 allows its dissociation from the receptor and subsequent SH2 domain-controlled STAT1/STAT1 homodimersiation, the homodimer being called gamma activated factor (GAF) (Decker *et al.*, 1991a; Nguyen *et al.*, 2002). GAF then translocates to the nucleus and binds to the GAS elements and stimulates ISG expression (Decker *et al.*, 1991b).

Type III IFN signalling

Type III IFNs, IFNλ, have their own exclusive receptor, although they still elicit a very similar IFNα/β induced signalling pathway. As with IFNα/β they use the JAK/STAT signal transduction pathway, and as such binding of IFNλ to the type III IFN receptor triggers phosphorylation of the intracellular domain of the receptor by the Janus kinases (JAKs), and subsequently phosphorylation of the signal transducer and activator of transcription (STAT) proteins. These include STAT2, STAT3, STAT4, STAT5 and the formation of STAT1 homodimers, and consequently activation of the γ IFN activated site (GAS) regulated genes, therefore IFNλ induction follows the same course as the typical type I IFN induction pathway (Dumoutier *et al.*, 2004). Thus, both type I and type III IFNs are induced by dsRNA and viral infections and both result in the upregulation of many antiviral proteins and antigen expressing class I major histocompatibility complex (MHC) (Kotenko *et al.*, 2003). IFNλ, however, is not as potent as the other types of IFN due to the low level expression of the type III IFN receptor on only a few, specific cells (Meager *et al.*, 2005).

STAT transactivation

Additionally, for optimal ISG upregulation by IFNs, the STATs need to be further modified either post translationally or by the interaction with other proteins

called transcriptional coactivators. STAT1 needs to be phosphorylated at residue Ser727, and this is done by the serine kinase protein kinase Cδ (PKCδ) (itself a member of the protein kinase C family). Additional serine kinases involved in an IFN dependent manner that phosphorylate Ser727 are PKCε and the calcium/calmodulin dependent protein kinase (PK) II. Phosphorylation of STAT1 in this manner results in enhanced interaction between STAT1 and nMYC and STAT interactor (NM1) (Zhu *et al.*, 1999), which itself enhances the interaction between STAT1 and transcription factors such as CBP/p300. The latter transcription factor, CBP/p300, further enhances the interactions of several other groups of transcription factors (Janknecht & Hunter, 1996). STAT2 also binds to CBP/p300 and assists with the activation of transcription, although STAT2 is not serine phosphorylated (Bhattacharya *et al.*, 1996)

Negative regulation of IFN signalling

There are several IFN-inducible proteins that interact in a negative feedback loop to control the IFN response. The protein inhibitors of activated STATs (PIAS) protein PIAS1 interacts with STAT1 homodimers, prevents them binding to DNA and therefore inhibits gene expression (Liu *et al.*, 1998). The ubiquitin-like protein ISG15, itself an ISG, becomes conjugated to STAT1 and targets STAT1 for degradation (Malakhov *et al.*, 2003). The suppressor of cytokine signalling (SOCS) family of protein phosphatases target JAK proteins for proteasomal degradation or directly inhibit their activity (Rui *et al.*, 2002; Sasaki *et al.*, 1999; Yasukawa *et al.*, 1999). Furthermore, the protein tyrosine phosphatases SHP1 and SHP2 contain SH2 domains and as such are able to dephosphorylate the tyrosine residues of both the STATs and the receptor, thereby returning the STATs to their inactive state (Mustelin *et al.*, 2005).

Other interferon signalling mechanisms

As discussed above the JAK/STAT signal transduction pathway is the ‘classical’ and fundamental IFN induction pathway, resulting in the upregulation of many antiviral proteins. However, this is not the complete story; there are other pathways that have been shown to produce signalling molecules and cascades that help in optimising the IFN response. These include the mitogen activated protein kinase (MAPK) p38 cascade (Platanias, 2005), the CRK proteins which are able to interact with Tyk2 (Ahmad *et al.*, 1997; Feller, 2001), and the PI3K proteins which exert negative regulatory effects on the JAK/STAT signalling pathway (Hawkins *et al.*, 2006; Platanias, 2005).

ISGs and IFN induced antiviral proteins

IFN stimulated genes

Interferon production, secretion and subsequent binding and stimulation of the IFN receptors, IFNAR and IFNGR, promote the upregulation of over 300 ISGs which mediate the antiviral response within IFN-stimulated cells. These ISGs are involved in numerous functions within the stimulated cell, as well as in

neighbouring cells and in cells mediating the adaptive immune response. The ISGs promote the antiviral response as well as being antiproliferative and immunomodulatory, and include proteins that regulate transcription and translation of gene expression, and proteins that regulate apoptosis and the cell cycle such as chemokines, cytokines and enzymes (de Veer *et al.*, 2001; Der *et al.*, 1998). Many of the identified ISGs have not been characterised as yet. However, several ISGs that play an essential role in establishing the antiviral state have been well characterised, including Mx GTPases, protein kinase R (PKR), and 2', 5' oligoadenylate synthetases (OAS)/endoribonuclease L (RNaseL), while some others, such as viperin, are just beginning to be studied. Upregulation of ISGs is an essential aspect of the innate immune response. Using knockout mice which are deficient in either IFNAR or IFNGR it was shown that despite the mice seeming to be healthy and able to mount an adaptive immune response with T cells, they were extremely susceptible to viral infections, with Semliki Forest virus (SFV) titres being undetectable after 24 hours in the wild type mice but extremely high in the knockout mice (Huang *et al.*, 1993; Hwang *et al.*, 1995). Added together, the IFN induced and subsequent expression of ISGs, the antiviral state that cells are put into becomes a highly inhospitable place for viruses, inhibiting their replicative cycle and allowing extra time to be gained by the cell and neighbouring cells in order to give the adaptive immune response a chance to be activated.

The OAS and RNaseL pathway

The 2',5' OAS proteins are IFN inducible though are constitutively present within the cytoplasm in small quantities, where they are able to act as PRRs for the sensing of viral dsRNA (**Fig 1.5** (Hoenen *et al.*, 2007; Sadler & Williams, 2008)).

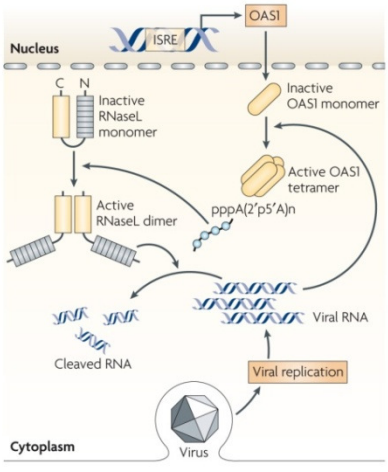

Figure 1.5 : The OAS1-RNaseL antiviral pathway. OAS1 is expressed constitutively at low levels and accumulates in the cytoplasm as an inactive monomer. OAS1 activation by dsRNA results in oligomerisation into a tetramer which synthesises 2',5'-oligoadenylates which activate the constitutively expressed inactive RNaseL which dimerises and cleaves dsRNA. Modified from Sadler and Williams, 2008.

They are characterised by their ability to catalyse the polymerisation of ATP into oligomers of adenosine by synthesising a 2',5'-linked phosphodiester linkage (Rebouillat & Hovanessian, 1999). These oligomers then initiate the activation of the constitutively expressed endonuclease RNaseL (Zhou *et al.*, 1993) which

is able to degrade RNAs of both cellular and viral origin, and thus inhibit the synthesis of proteins. The smaller RNA molecules can then, in turn, further activate the induction of type I IFNs *via* RIG-I and MDA5, which are also in the cytoplasm, leading to an increased antiviral response (Malathi *et al.*, 2007). The engineering of RNaseL-deficient mice and the subsequent exposure to RNA viruses from the families of *Paramyxoviridae*, *Togaviridae*, *Picornaviridae*, *Reoviridae*, *Flaviviridae*, *Orthomyxoviridae* and *Retroviridae* showed an increase in susceptibility to infection (Silverman, 2007). Furthermore, Zhou *et al.* (1999) showed that parainfluenza virus 3 (PIV3), EMCV, VSV and vaccinia virus (VACV) replication was suppressed in the presence of RNaseL over-expression.

Mx GTPases

There are four families of proteins in the class of guanine hydrolysing proteins: the p65 GBPs, the very large inducible GTPases, the p47 guanylate-binding proteins and the Mx proteins. It is only the Mx proteins which have a proven role in antiviral immunity (Haller *et al.*, 1980). The Mx GTPase family consists of two human proteins, MxA and MxB, and two murine proteins, Mx1 and Mx2.

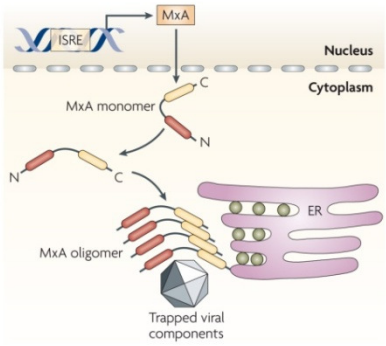

Figure 1.6 : Mechanism of action of MxA. Induction of MxA occurs through IFN signalling pathways. MxA accumulates in the cytoplasm on intracellular membranes as oligomers which bind to viral nucleocapsids or other viral components to trap and then degrade them. Modified from Sadler and Williams, 2008.

These were discovered after inbreeding of mice led to an increase in susceptibility to orthomyxovirus infection, which was subsequently shown to be due to mutations in the Mx gene (Haller *et al.*, 1979). Of the four proteins, only Mx2 localises to the nucleus, whereas the other three are cytoplasmic, and only MxA shows antiviral activity in humans (Haller *et al.*, 1995). The Mx proteins comprise a large N-terminal GTPase domain along with a central interacting domain (CID) and a leucine zipper (LZ) domain at the C-terminal end, and the latter two domains are essential for recognition of viral targets (Kochs & Haller, 1999). Due to the subcellular localisation of Mx proteins next to the smooth ER and their apparent affinity for nucleocapsid-like structures, they are able to halt viral replication considerably early on in the infection by binding to viral components (**Fig 1.6** (Accola *et al.*, 2002)). This has been shown with influenza virus, and constitutes a particularly effective mechanism for counteracting the generation of viruses able to escape the antiviral mechanisms of MxA (Turan *et*

al., 2004). More recently Haller *et al.* have shown MxA tetramers to form filamentous or ring-like structures on the viral nucleoprotein consequently inhibiting viral polymerase activity (Haller *et al.*, 2010). Other viruses to be affected by Mx proteins include rhabdoviruses, togaviruses, paramyxoviruses, orthomyxoviruses and bunyaviruses. In the latter, animal-infecting viruses from each genus (excluding tospoviruses) have been shown to be inhibited by MxA (Bridgen *et al.*, 2004; Frese *et al.*, 1996; Kanerva *et al.*, 1996), leading Andersson *et al.* (2004) to conclude that all animal bunyaviruses are restricted by MxA.

PKR

PKR was first discovered when a translational block was identified in a cell-free *in vitro* translation system using a lysate from VACV-infected cells that had been treated with IFN and had been supplemented with exogenous RNA (Kerr *et al.*, 1977; Metz & Esteban, 1972). PKR has been found to be encoded on a single gene (Barber *et al.*, 1993) and is constitutively expressed in quiescent mammalian cells at relatively low levels, in a monomeric state, and, as expected for a translation inhibitor, is associated with ribosomes (Zhu *et al.*, 1997b). PKR belongs to the family of kinases responsible for phosphorylating the eIF2α subunit in response to stress, in particular that mediated by viral infections. It has two specific kinase activities, one of which autophosphorylates to activate

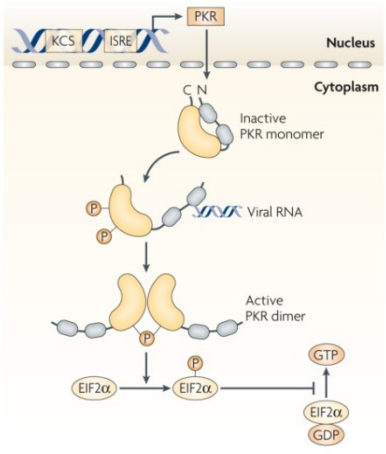

Figure 1.7 : Mechanism of action of PKR. PKR is constitutively expressed in the cell and accumulates in the nucleus and the cytoplasm as an inactive monomer which is activated by viral RNAs and several other ligands. Following activation PKR monomers are phosphorylated and dimerise and subsequently inhibit translation by the phosphorylation of eIF2α. Modified from Sadler and Williams, 2008.

PKR, and the second to phosphorylate the eIF2α subunit of eIF2, which in turn blocks eIF2 activity and thus protein synthesis. As well as the kinase domain, PKR also has a dsRNA binding domain which activates PKR when RNA binds to it (**Fig 1.7**). Activation of PKR can occur by dsRNA of viral, synthetic or cellular origin binding to the N terminus of PKR, causing activation by autophosphorylation and homodimersiation (Dar *et al.*, 2005). PKR has been shown to be optimally activated by dsRNA longer than 30 bp (base pairs), as well as by ssRNAs containing 5' triphosphates greater than 47 bases in length (Nanduri *et al.*, 1998). This permits PKR to distinguish self from non-self since

most cellular RNAs have 5' monophosphates or 5' cap structures. In normal mammalian cells, eIF2 comprises three subunits, α, β and γ, and is responsible for delivering the Met-tRNAi to the ribosome to initiate GTP-dependent translation. On arrival, the GTP is hydrolysed by eIF5, which in turn releases the eIF2-GDP from the initiation complex. The eIF2B then catalyses the regeneration of the eIF2-GTP from the eIF2-GDP. PKR is a serine/threonine kinase and as such phosphorylates residue Ser51 of the eIF2α subunit which subsequently binds strongly to the eIF2B subunit, inhibiting the capacity for eIF2B to catalyse regeneration of eIF2-GTP from eIF2-GDP (Roberts *et al.*, 1976). As the ratio of eIF2B to eIF2 is very low, only a small amount of phosphorylated eIF2α is required to severely inhibit translation (Hershey, 1991). Once the recycling of eIF2 is halted, protein translation is blocked. Thus, the inhibition of protein synthesis is the basic mechanism of antiviral activity of PKR. Furthermore, PKR acts as a PRR by detecting and binding dsRNA and initiating the IκB/NF-κB signal transduction pathway (Kumar *et al.*, 1994). Viruses known to be affected by PKR are hepatitis C virus (HCV), West Nile virus (WNV), human immunodeficiency virus 1 (HIV-1), Sindbis virus (SinV) and EMCV (Gorchakov *et al.*, 2004; Nagai *et al.*, 1997; Noguchi *et al.*, 2001; Samuel *et al.*, 2006; Yeung *et al.*, 1999).

ISG15

The highly IFN-inducible protein ISG15 is approximately 15 kDa in size and is a ubiquitin homologue (Loeb & Haas, 1992) that was first isolated over 20 years ago. ISG15 expression gives a 165 amino acid precursor which is further processed to reveal the C terminal sequence LRLRGG. Ubiquitylation occurs through the adenylation of the two glycine residues within this sequence which are then linked *via* a thioester bond to the cysteine residues on the three ubiquitin enzymes, ubiquitin activating enzyme (E1), ubiquitin conjugating enzyme (E2), and ubiquitin ligase enzyme (E3). This ubiquitin ligation complex can then attach ubiquitin to the lysine residues on target proteins. Ubiquitylation is essential within the immune response, aiding intracellular signal transduction, and, when under the control of IFNs and ISGs, it is termed ISGylation (**Fig 1.8**). The process is much the same as ubiquitylation, however, the ubiquitin E1 enzyme is unable to form a thioester linkage with ISG15, and it is now known that there are several enzymes that catalyse the reactions required to conjugate ISG15 to substrate proteins. UBE1L is the E1-like ubiquitin-activating enzyme and is responsible for activating ISG15. The two enzymes UBE2E1 and UBE2L6 serve the equivalent role of E2 in conjugation, and the two E3 ligase enzymes HerC5 and TRIM25 are able to conjugate the target proteins to ISG15 *via* their HECT and RING domains. De-ISGylation is the reversal of this process and enzymes involved in the hydrolysis of ISG15 are the ubiquitin specific proteases such as USP2, USP5, and USP18 (Sadler & Williams, 2008). Unlike ubiquitylation, ISGylation leads to protein stabilisation, translocation or non-degradative negative feedback (Kim *et al.*, 2008; Loeb & Haas, 1994; Lu *et*

al., 2006). Many proteins involved in the type I IFN response undergo ISG15 conjugation, such as JAK1, STAT1, RIG-I, PKR, MxA and RNaseL (Zhao *et al.*, 2005). Furthermore, ISG15 has been shown to have cytokine characteristics and is secreted in large amounts (D'Cunha *et al.*, 1996). The antiviral effects of ISG15 have been demonstrated with several viruses by using knockout mice deficient in ISG15. Such viruses include HSV-1, SV and IAV and IBV (influenza B virus) (Lenschow *et al.*, 2005; Osiak *et al.*, 2005). In addition, Lenschow *et al.* (2005) showed that IFNAR1 deficient mice infected with an engineered SV that

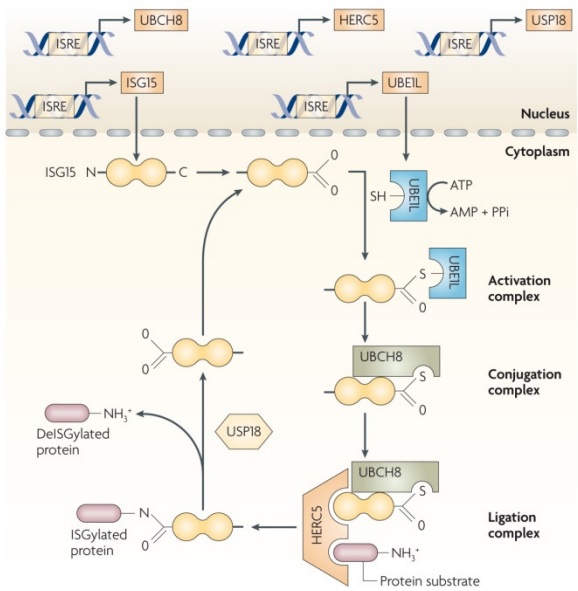

Figure 1.8 : Mechanism of action of ISG15. E1, E2 and E3 proteins sequentially catalyse the conjugation of ISG15 to numerous protein substrates to modulate pleiotropic cellular responses to inhibit virus production. This process is termed ISGylation and is reversibly regulated by proteases. UBE1L is E1, UBCH8 is E2, HERC5 is E3, and USP18 is the protease. Modified from Sadler and Williams, 2008.

expressed ISG15 subsequently protected the mice from a lethal dose of wild type SV. Knockdown of USP18 by siRNA enhances cellular resistance to HCV and VSV (Randall *et al.*, 2006). Furthermore, USP18 knockout mice showed an increase in IFN and poly I:C sensitivity compared to wild type mice (Malakhova *et al.*, 2003), and Ritchie *et al.* (2004) demonstrated resistance in these mice to LCMV and VSV infection.

PML

Promyelocytic leukaemia (PML) protein is an essential component of PML nuclear bodies (NBs), although there are many other proteins involved, and many of these are also IFN inducible, such as Sp100 and PA28. PML NBs are heterogeneous in both the type of proteins comprising the NBs and the size of the bodies. Treatment with IFN directly induces transcription of PML and leads to an increase in the number and size of the NBs (Everett & Chelbi-Alix, 2007). The PML protein has been shown to be involved in higher order chromatin loop structure organisation and gene regulation (Kumar *et al.*, 2007). In an over-expression system, both the PML III protein and the PML IV protein isoforms inhibited the replication of RNA and DNA viruses. PML protein knockout MEFs

were more susceptible to infection with LCMV, giving a higher viral titre than the naive MEFs, thus demonstrating the importance of PML (Djavani *et al.*, 2001).

Other ISGs

Triple knockout mice that are deficient in the Mx, RNaseL and PKR proteins were still able to mount a limited IFN-induced antiviral response, providing evidence that further mechanisms of innate immunity exist (Zhou *et al.*, 1999). There are now known to be numerous IFN-inducible proteins that are involved in the antiviral response, including ISG20, Viperin, ISG56, adenosine deaminases and the restriction factors apolipoprotein B mRNA-editing enzyme-catalytic polypeptide-like (APOBEC) 3F and 3G (APOBEC 3F and 3G) and the tripartite motif-5α (TRIM5α). ISG20 is a 3', 5' exonuclease that specifically degrades ssRNA (Degols *et al.*, 2007). Viperin has been shown to disrupt lipid raft formation and hence to inhibit the budding of IAV (Wang *et al.*, 2007). ISG56 (IFN induced protein with tetratricopeptide repeats 1 (IFIT1)) disrupts translation through its interaction with multiprotein complexes essential to translation. The interaction of ISG56 with the eIF3e subunit renders it unable to stabilise the eIF2-GTP-tRNAi^{Met} complex (Hui *et al.*, 2003). The adenosine deaminases are directly mutagenic to dsRNA, converting adenosines to inosines (Zahn *et al.*, 2007). The APOBEC enzymes both deaminate cytidine and hence mutate the viral template and then inhibit the reverse transcription of retroviruses (Randall & Goodbourn, 2008; Ying *et al.*, 2007). TRIM5α binds to infectious retroviral capsids and targets them for proteasomal degradation (Towers, 2007). These pathways and many more have yet to be fully characterised.

Control of apoptosis

Once a cell is infected with a virus, one of the specific functions of IFN is to induce apoptosis, not only within the infected cell, but also to induce the pro-apoptotic state in neighbouring cells, thus ensuring that the spread of the viral infection is limited. The ISG proteins PKR, OAS/RNaseL and PML are all involved in the induction of apoptosis. Furthermore, it is known that IFNs induce expression of the cellular enzymes caspases, which are key proteins in the induction of apoptosis (Balachandran *et al.*, 2000; Chin *et al.*, 1997; Schindler, 1998; Subramaniam *et al.*, 1998).

Viral countermeasures to IFN

Soon after Isaacs and Lindenmann's discovery of IFN, Lindenmann noticed another phenomenon in infected cells: prior infection with a live virus was enough to suppress the subsequent IFN induction by an attenuated virus. He called it inverse interference (Lindenmann, 1960). Fifty years later, it is now known that all viruses must either circumvent or overcome the IFN response for successful replication, and the range of viral IFN antagonists stretches across all the components of the IFN system. There are five ways that viruses use to

circumvent the IFN response: global inhibition of cellular gene and or protein expression; inhibition of IFN induction by inhibiting signalling pathways or masking exposure of viral PAMPs; blocking signalling of IFN; blocking ISGs; and by being inherently insensitive to IFNs. Some viruses interfere with the IFN system with a combination of the above and some encode one or more individual viral proteins that antagonise the IFN system in several different ways (Randall & Goodbourn, 2008). Furthermore, there must be a temporal control exerted during the viral replicative cycle to ensure that the virus is able to produce the IFN antagonist without inducing the IFN response too early by producing other viral proteins/PAMPs. This also demonstrates that the virus will be constantly under selective pressure. Therefore cell tropism is fundamental to viral pathogenicity but virulence of the virus depends on the ability of its IFN antagonist to counteract the IFN response (Young *et al.*, 2003).

Protein shutoff

Inhibition of cellular gene expression and/or protein synthesis is a strategy used by several viruses. This is particularly advantageous as it completely removes the inhibitory effects of IFN on the virus, not only in the infected cell but also in the neighbouring cells which will not be stimulated into the antiviral response. However by "switching off" the cell, apoptosis is induced more rapidly, the virus is unable to utilise the cell's transcriptional and translational machinery and the virus will not be able to establish a persistent infection. The IFN antagonist NSs protein of viruses in the family *Bunyaviridae* is particularly efficient at causing host cell protein shut-off and, interestingly, the NSs proteins of viruses in two distinct genera have the same function but with a different mechanism (discussed later). The matrix (M) protein of VSV inhibits host cell transcription by blocking the basal transcription factor TFIID and then also by inactivating translation factors, as well as interfering with the intracellular transport of RNAs and proteins (Ahmed & Lyles, 1998; Black & Lyles, 1992; Petersen *et al.*, 2000). IFN gene transcription is inhibited by PV, IAV and HSV1 as they encode antagonists which shut-off host cell transcription and translation. Likewise, foot and mouth disease virus (FMDV) expresses the leader protein which induces host cell protein shut-off (Chinsangaram *et al.*, 1999). Often, mutations in the viral IFN antagonist gene are enough to attenuate these viruses.

Blocking IFN cascades and PAMPs

There are several factors to consider when looking at the amount of IFN induced in response to viral infection. The preparation of the virus can have an effect, due to a high number of defective interfering particles (DIs) or chemokines in the viral innoculum (Strahle *et al.*, 2006). Factors from the virus point of view are, firstly, the type and amount, of IFN inducer, such as dsRNA, that is produced. Secondly, whether the viral antagonist counteracts the induction of IFN and its mode of action, and how quickly the virus can express the antagonist. Thirdly, the type of cell that the virus is infecting as specific cell

types produce differing amounts of IFN. Viruses address these factors in numerous ways. PAMPs produced during replication may be protected by capping the RNA or 'cap snatching' as with paramyxoviruses and influenza viruses respectively. Hantavirus genomic RNA does not have 5' triphosphates, and picornaviruses attach the Vpg protein to the end of their RNAs, both of which will protect the RNA from detection by RIG-I. Furthermore some positive-stranded RNA viruses replicate in intracellular vesicles, and retroviruses integrate their genomes into the host cell genome. Some viruses express IFN antagonists that sequester dsRNA such as the VP35 protein of Ebola virus (EBOV) (Cardenas *et al.*, 2006; Hartman *et al.*, 2006), the NS1 protein of IAV (Lu *et al.*, 1995), and the vaccinia virus E3 protein (Chang *et al.*, 1992). There are viruses which express IFN antagonists that target specific IFN induction pathway points. For example, HCV virus targets TLR3 signalling by cleaving TRIF with NS3/4a (Li *et al.*, 2005a) which also cleaves IPS-1 at Cys508 thus disrupting RLR signalling (Li *et al.*, 2005b). In addition, many paramyxoviruses inhibit MDA5 activity by expressing the V protein which directly interacts with MDA5 but not RIG-I (Andrejeva *et al.*, 2004). In contrast, IAV expresses a protein called NS1 that inhibits RIG-I-mediated signalling (Mibayashi *et al.*, 2007). Inhibition also occurs further downstream, with some viruses blocking the regulatory proteins such as IRF3 which is targeted for proteasomal degradation by the NPro protein of bovine viral diarrhoea virus (BVDV) and classical swine fever virus (CSFV) (Bauhofer *et al.*, 2007), whereas the P protein of Borna disease virus (BDV), rabies virus and the Gc protein of Hantaan virus (HTNV) target TBK1 to prevent IRF3 activation (Alff *et al.*, 2006; Brzozka *et al.*, 2005). IRF3 is also targeted by Thogoto virus (THOV) at a transcriptional level by preventing dimerisation of IRF3 and its association with CBP (Jennings *et al.*, 2005).

IFN signalling inhibition

Blocking the IFN signalling pathway enables some viruses to inhibit more than one type of IFN pathway, as the three known pathways do have some overlap, and it further reduces the response of cytotoxic T cells through lack of MHC I upregulation, and hence the infected cells would no longer respond to the IFNs. There are many ways in which viruses are able to inhibit IFN signalling, and many do it on several different levels. Firstly, viruses such as Japanese encephalitis virus (JEV), Dengue virus (DENV) and Langat virus (LGTV) all interfere with IFN receptors. JEV protein NS5 impedes protein tyrosine kinase Tyk2 (Lin *et al.*, 2006), while DENV and LGTV disrupt IFNGR complexes (Ho *et al.*, 2005; Park *et al.*, 2007). Type I and II IFN signalling is inhibited by polyomavirus T antigen binding to JAK1 (Weihua *et al.*, 1998). Several poxviruses, such as cowpox virus (CPXV) and camelpox virus (CMLV), express proteins that are usually secreted by infected cells and that can bind directly to extracellular IFNγ. Other poxviruses, such as VACV, express proteins that can bind to IFNα/β and some even express proteins that mimic the IFNGR which

are able to sequester IFNγ, thus preventing neighbouring cells from entering the antiviral state (Alcami & Smith, 1995; Alcami *et al.*, 2000; Symons *et al.*, 1995). Many viruses inhibit the function of the STAT proteins; rabies virus P protein binds to, and thereby inactivates, STAT1 and STAT2 (Vidy *et al.*, 2007). The paramyxoviruses use several different mechanisms to block the STAT proteins; mumps virus targets STAT1 and STAT3 for degradation, whereas PIV5 targets STAT1, and human parainfluenza virus 2 (HPIV2) targets STAT2. However, the henipaviruses V and P proteins sequester the STAT1 and STAT2 proteins (Conzelmann, 2005; Horvath, 2004; Nagai & Kato, 2004). Additionally, PIV5 is able to overcome cells in the antiviral state because the virion-associated V protein begins to target STAT1 for degradation immediately after infection, thus dismantling the antiviral state (Carlos *et al.*, 2005). The EBOV protein VP24 inhibits nuclear import of STATs by binding to the nuclear localisation signal receptor karyopherin α1 (Reid *et al.*, 2006), whereas HSV1 inhibits JAK/STAT signalling by inducing SOCS3 expression soon after infection (Yokota *et al.*, 2004). Human papillomavirus (HPV) inhibits the formation of the ISGF3 complex and subsequent IFNα/β activation by a direct interaction between IRF9 and the viral E7 protein (Barnard & McMillan, 1999).

Viral inhibitors of ISGs

Many viruses have also evolved ways of overcoming the ISGs that they induce through their earlier infection. As stated above, there are over 300 ISGs identified and many of them still have unknown functions and mechanisms, so some of the counter measures that different viruses use for the more characterised pathways shall be briefly described. Clearly ISG15 has antiviral properties as several viruses specifically target it for inhibition, most notably IBV. This virus prevents ISG15 from being conjugated to its target proteins by expressing the viral protein NS1 which interacts with, and sequesters, the E3 ligase (Yuan & Krug, 2001). The cytidine deaminase proteins APOBEC 3G and 3F are targeted by the virion infectivity factor (vif) protein of many lentiviruses (including HIV) which recruits E3 ligases to ubiquitinate the APOBECs and thus ensure their subsequent proteasomal degradation (Soros & Greene, 2007). HIV-1 also inhibits the OAS RNaseL response by activating the inhibitor of RNaseL, thus eliminating the activation of the OAS response (Martinand *et al.*, 1999). Due to the low affinity of OAS for dsRNA, the OAS ISGs can be easily targeted for inhibition by viral proteins that sequester dsRNA, like the NS1 protein of IAV. Numerous other viruses express viral proteins that are able to sequester dsRNA and not only inhibit the OAS response, but they are also particularly useful in counteracting the PKR and ADAR ISG responses.

Known effects of IFN on viruses

Many viruses have been intensively studied over the past few years for the virus specific effects of IFNs on their replication cycle, and this has led to successful treatments of some viral diseases such as hepatitis caused by HCV. The

paramyxovirus PIV5 encodes the viral V protein that inhibits IFN signalling by targeting STAT1 for proteasomal degradation and also limits the amount of IFN synthesised by blocking the nuclear translocation of IRF-3 (Andrejeva *et al.*, 2002; He *et al.*, 2002). The PIV5 strain CPI- is unable to block IFN signalling and was used to study the effects of IFN in cells unable to synthesise IFN that were infected with CPI- or CPI+ (the latter is able to block IFN signalling) strains. The study showed several results: the virus protein synthesis profile was altered and proteins encoded downstream of the V/P gene were downregulated; the transcription gradient was altered such that an increase in viral genes at the 3' end of the genome occurred, whilst there was a decrease in transcription of genes towards the 5' end of the genome (Carlos *et al.*, 2005); the polymerase was also affected as the mRNAs of CPI- virus were shown to have longer poly(A) tails; and viral proteins were shown to be redistributed within IFN treated infected cells which further enhanced the formation of inclusion bodies (Carlos *et al.*, 2005). Treatment of Vero cells with IFNγ downregulated the mRNA and cellular expression of the SARS-Co-V receptor angiotensin-converting enzyme 2 (ACE2) thereby inhibiting the virus at the level of attachment (de Lang *et al.*, 2006). Primary human macrophages that were infected with HIV-1 and subsequently treated with IFNα were shown to have a reduced accumulation of nascent cDNA which correlated with a loss of infectivity of the virus, and was linked to the ubiquitin-proteasomal degradation pathway (Goujon & Malim, 2010). IFNβ treated neuronal cells infected with the highly IFN sensitive VSV produced viral particles with hyperphosphorylated matrix proteins, detected in both the cell lysate and the budded virions (D'Agostino P *et al.*, 2009). Further analysis showed that hyperphosphorylation of the matrix protein inhibited its interaction with the nucleocapsid protein thereby disrupting viral assembly. These studies show that the viral specific effects of IFNs cover the whole spectrum across the viral replication cycle from adsorption right through to egress.

The *Bunyaviridae*

Classification

In 1975 the family *Bunyaviridae* was formally established and now contains over 350 serologically-distinct viruses. All the viruses in this family share morphological and molecular characteristics (Fenner, 1976) in that the genome is tri-segmented and comprises single stranded negative sense RNA; they are surrounded by a membrane-derived lipoprotein envelope containing viral glycoprotein spikes; each virion is usually spherical in shape and is between 80 nm and 100 nm in diameter; viral replication occurs in the cytoplasm and viral morphogenesis takes place at the smooth inner membranes of the Golgi apparatus without prior core formation (Schmaljohn, 2007). There are five genera within this family: *Hantavirus*, *Nairovirus*, *Phlebovirus*, *Orthobunyavirus* and *Tospovirus*. While the term bunyaviruses refers to the whole family, each genus is usually referred to individually as hantaviruses, nairoviruses, phleboviruses, orthobunyaviruses and tospoviruses, respectively (Elliott, 1997). Excluding the hantaviruses, which are spread *via* aerosolised rodent excreta, all the viruses are arthropod-borne viruses. Aside from the tospoviruses, which infect plants, all members of the bunyavirus family infect animals, and viruses in each of the five genera cause huge socio-economical costs annually, with over 60 causing disease in livestock and humans (Schmaljohn, 2007).

Genus Hantavirus

The name for the *Hantavirus* genus is derived from the prototype virus of this genus, Hantaan virus (HTNV), which was so named after the river near the initial outbreaks of the disease known then as Korean haemorrhagic fever. This virus was originally discovered during the Korean war with over 3000 reported cases of an acute febrile illness, of which approximately 33% progressed into haemorrhagic fevers, with a 5% to 10% mortality rate (Lee, 1989). The disease is now known as haemorrhagic fever with renal syndrome (HFRS) and there are several etiological viruses, such as Hantaan, Seoul and Puumala virus. The latter was identified as the causative agent of a milder illness known for over 50 years in northern Europe before the virus that caused it was isolated (Niklasson *et al.*, 1987). In 1993 another outbreak of disease occurred in the south western USA in an area known as the four corners (southwest Colorado, northwest New Mexico, northeast Arizona and southeast Utah), but this time the disease progressed rapidly to severe respiratory problems resulting in death in over 50% of the people infected. The etiological agent of the outbreak was quickly isolated and analysed and found to be another new hantavirus causing what is now known as hantavirus pulmonary syndrome (HPS). It was subsequently named Sin Nombre (Spanish for “no name”) virus (Nichol *et al.*, 1993). Since then HPS has been diagnosed across the USA and more than ten separate strains of hantaviruses have been isolated from various species of

rodent, which are now known to be the animal reservoir of this genus (Childs *et al.*, 1994; Douglass *et al.*, 2005; Khan *et al.*, 1996; Smithee *et al.*, 2007). Unlike the other four genera of the *Bunyaviridae*, the hantaviruses are not transmitted by arthropods but instead by the excreted faeces, urine and saliva from rodents. The route of transmission is through the respiratory tract for rodents and humans *via* inhalation of dust and or aerosolised excreta (Elliott, 1996).

Genus Nairovirus

Apart from some isolates from culicoid flies and mosquitoes, the nairoviruses are exclusively tick-borne viruses, and are so called after the original isolation of the etiological agent in the outbreak of Nairobi sheep disease in Kenya in 1910 (Schmaljohn, 2007). Nairobi sheep disease virus (NSDV) has a mortality rate of over 90% in sheep and goats, causing acute haemorrhagic gastroenteritis (Davies, 1997; Marczinke & Nichol, 2002). Crimean-Congo haemorrhagic fever virus (CCHFV), infects humans and a variety of livestock, and has a mortality rate of 10% in humans but is asymptomatic in livestock. The first known outbreak occurred in the 1940s in the Crimean peninsula, and since then there have been several more outbreaks throughout Europe, Asia and Africa, with the first isolation of the virus in 1956 in Kisangani, Africa. Recent studies of the age and evolution of CCHFV using virus strains from a wide geographical area and spanning nearly fifty years (1956-2005) suggest that the virus is over 3000 years old (Carroll *et al.*, 2010). The predominant reservoir of these viruses is the arthropod host, in which transovarial transmission (vertical transmission from mother to offspring) occurs thus maintaining the viral reservoir. Transmission to vertebrates occurs primarily through biting by infected ticks but can also occur *via* contact with infected blood and tissues. The subsequent replication of the virus in vertebrates results in amplification of the virus which itself further increases the likelihood of transmission to more ticks.

Genus Phlebovirus

Most of the viruses in this genus are transmitted *via* the phlebotomine sandfly, hence the name of the genus, and are found throughout the world except in Australia. However, the most notable member of this genus, Rift Valley fever virus (RVFV), is transmitted primarily by the *Aedes* mosquito species and was first isolated from a newborn lamb in 1930. This disease causes huge devastation to livestock as infection results in abortion and high mortality. Infection of humans often occurs through close contact with livestock and causes haemorrhagic fever and death in 0.5% of cases. Uukuniemi virus (UUKV) is carried by the *Ixodes ricinus* tick and is non-pathogenic for humans, making it a good model virus for studying this genus under minimal containment. Sandfly fever Sicilian and Naples viruses were first isolated in the 1940s in Italy and are known to cause self limiting febrile illnesses throughout Europe, Asia and Africa and are suspected to have done so for many years. From this genus, transovarial transmission of RVFV has been shown in *Aedes*

mcintoshi mosquitoes suggesting a possible reservoir, which can also explain the seasonal nature of the outbreaks of RVFV (Schmaljohn, 2007).

Genus Tospovirus

The isolation of the tomato spotted wilt virus (TSWV) was in 1930, although the associated disease was first recognised in Australia in 1915, and this virus also gives the genus name (Schmaljohn, 2007). There are 8 species of tospovirus, which are transmitted by several species of thrips, and they are found worldwide, in the wild as well as in greenhouses of more temperate zones (Wijkamp *et al.*, 1993). Despite several campaigns to reduce the thrips vector population, tospoviruses account for more than one billion US dollars of crop losses each year as they infect in excess of 900 species of plants belonging to 82 distinct botanical families (Schmaljohn, 2007). Thus there is an enormous economic impact of tospovirus infection on agricultural production. Intriguingly, transmission between plants and thrips differs from other members of the family *Bunyaviridae* in that infectious viral particles are not thought to be required. The ribonucleoprotein (RNP) forms aggregates within the plant cells which are subsequently consumed by the thrips (Kitajima *et al.*, 1992). Complete viral replication then occurs in the thrips enabling them to infect new plant hosts. Once new plant host cells are infected the virus no longer needs to complete its full replication cycle to further infect neighbouring cells as cell-to-cell spread of RNP is achieved with just the movement protein NSm (Kormelink *et al.*, 1994; Sin *et al.*, 2005). Furthermore, only the larvae of the thrips can be infected as during the maturation process the midgut muscle tissue and the salivary glands are separated, but the infection does survive through these stages (transstadial transmission). Thus both adults and larvae can infect plants, and there is no reported vertical transmission (Schmaljohn, 2007).

Genus Orthobunyavirus

The *Orthobunyavirus* genus is by far the largest genus in the family *Bunyaviridae*, containing over 170 isolates that are found throughout the world. Most members of this genus are carried by mosquitoes and are transmitted to a vast range of vertebrate hosts. The prototype virus, Bunyamwera virus (BUNV), for the genus and the family *Bunyaviridae* was originally isolated in the 1940s in Uganda and causes acute febrile illness (Smithburn *et al.*, 1946). BUNV is now known to infect many mammals, such as goats, horses, cows and humans, and recently neutralising antibodies for BUNV were found in birds, in particular the red ovenbird *Furnarius rufus* (Tauro *et al.*, 2009). The viruses of this genus were originally categorised by their serological properties, giving rise to such groups as the California, Simbu and Bunyamwera serogroups. Further, viruses in this genus are responsible for many diseases of humans and livestock. Cache Valley virus (CVV), now endemic across North America, causes abortions and congenital deformations in sheep and was isolated in Utah in 1956 (Chung *et al.*, 1990). California encephalitis virus (CEV) has been linked

with three cases of encephalitis in California, although not recently. After the death from encephalitis of a child in the USA in 1960 La Crosse virus (LACV) was isolated from his brain and is now known to be a significant contributor to viral encephalitis in the USA (Schmaljohn, 2007). Jamestown Canyon virus (JCV) was isolated in Colorado from *Culiseta inornata* mosquitoes and found to cause many cases of encephalitis in adults (Schmaljohn, 2007). Oropouche virus (OROV) was isolated in 1955 in Trinidad and is responsible for many acute febrile illness epidemics in South America, particularly Brazil (Schmaljohn, 2007). The isolation of Akabane virus (AKAV) in Japan in 1959 established the cause of foetal malformations of cattle in Australasia, Israel and Japan. Snowshoe hare virus (SSHV), now found across North America, causes encephalitic disease in both children and adults, and was isolated in 1959 in Montana (Schmaljohn, 2007).

Transmission of orthobunyaviruses occurs when an infected mosquito bites a vertebrate host in which the virus can then replicate to a high titre, possibly resulting in disease symptoms like the examples given above. Humans are considered dead end hosts as they are unlikely to transmit the virus back into the mosquito population thus, the transmission between mosquitoes is essential to the maintenance of the infected mosquito population and survival of the virus (Gonzalez-Scarano, 1996). However, the high viremia in humans infected with OROV allows transmission to uninfected midges. There is horizontal transmission of orthobunyaviruses *via* the infection of a vertebrate host followed by the subsequent feeding on the same host by other mosquitoes. In addition, systemic infection of the mosquito allows transovarial vertical transmission and venereal transmission from males to females (Thompson & Beaty, 1977; Watts *et al.*, 1975). Thus, transmission of viruses between mosquitoes, either with or without a vertebrate intermediate, allows the persistence of the virus in a vector which itself shows no symptoms of infection and thus makes it difficult to eradicate only the infected mosquitoes.

Virion structure

Virions range in size between 80-120 nm in diameter; Orthobunyavirus virions are about 100 nm and are spherical to pleiomorphic in shape (Martin *et al.*, 1985; Murphy *et al.*, 1968). Viruses assemble at the Golgi apparatus and thus take their membrane envelope from the Golgi membrane. The envelope of LACV is a single lipid bilayer 4 nm thick containing heterodimeric glycoprotein spikes (glycoproteins Gn and Gc) that are 10 nm long and constitute an even distribution across the surface of the whole virion (Obijeski *et al.*, 1976a; Talmon *et al.*, 1987)(**Fig 1.9**). Contained within the envelope of bunyaviruses are three RNPs comprising the nucleocapsid protein (N) which encapsidates the three single stranded RNA (ssRNA) genomic segments designated small (S), medium (M) and large (L), in a ratio of 12 nucleotides per monomer of N, and in a helical formation (Mohl & Barr, 2009; Obijeski *et al.*, 1976b). Bound

onto the ends of the RNPs is the L protein which is the viral RNA-dependent RNA polymerase, completing the RNPs into the appearance of a closed circle (Obijeski *et al.*, 1976b). For the viral particle to be infectious it must contain at

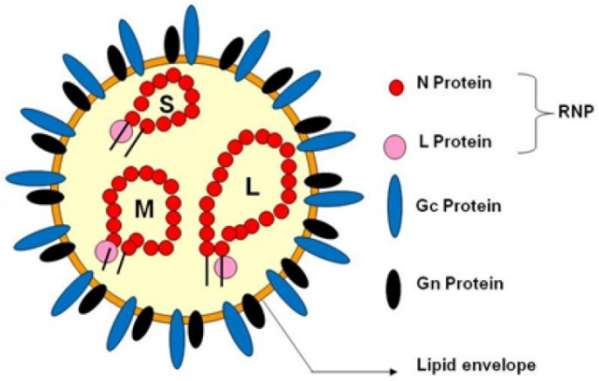

Figure 1.9 : The structure of a bunyavirus virion. The two glycoproteins Gn (black) and Gc (blue) are embedded in the lipid envelope (orange) as heterodimers. Within this, the three RNA segments are individually encapsidated by the nucleocapsid protein (red) in a circular conformation, and are associated with the polymerase protein (pink) to form ribonucleoproteins.

least one of each segment, however, these are not necessarily in equimolar quantities and could help to explain the variety in particle size which is seen in electron microscopy (Hutchinson *et al.*, 1996; Talmon *et al.*, 1987).

The surface structure of the virion appears to differ significantly across the genera (**Fig 1.10**). The orthobunyaviruses appear with small knob-like protrusions, whilst HTNV shows a gridlike pattern and CCHFV has very small morphological units forming a fringe around the virions (Martin *et al.*, 1985).

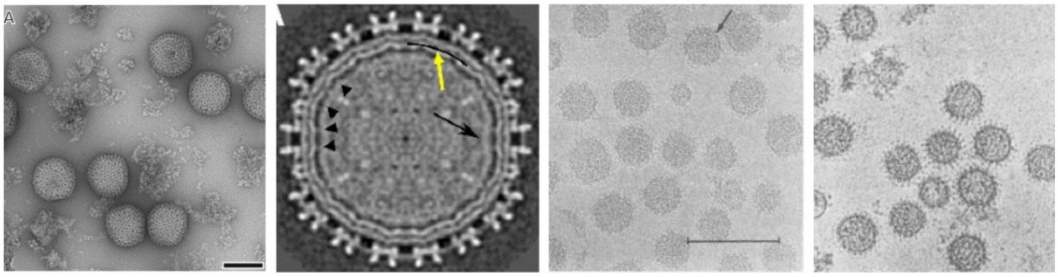

Figure 1.10 : Electron micrographs of members of the *Bunyaviridae*. **(A)** Purified RVFV particles stained with 2% uranyl acetate. Bar is 100 nm. Taken from Huiskonen *et al.*, 2009. **(B)** Central section through the RVFV MP-12 map showing glycoprotein surface protrusions, the lipid envelope and the unstructured core. The black arrow points to an underlying higher density layer which may represent a higher occupancy layer where RNP segments are tethered by cytoplasmic tails of Gn and Gc glycoproteins. Arrowheads point to connecting densities protruding through the envelope, most likely representing the glycoprotein cytoplasmic tails. For yellow arrow and black arc see original publication. Protein is shown in white. Taken from Sherman *et al.*, 2010. **(C)** and **(D)** Vitrified hydrated LACV. Arrow points to membrane bilayers **(C)** and glycoprotein spikes are visible in **(D)**. Bar is 200 nm. Taken from Talmon *et al.*, 1987.

Recently the MP-12 vaccine strain of RVFV, a phlebovirus, has been analysed using cryo-electron microscopy which showed that the glycoproteins are arranged in an icosahedral formation with T=12 symmetry. There are 122 individual capsomers consisting of 110 hexons and 12 pentons comprising 12 and 10 glycoproteins each respectively. However, the specific composition and location of Gc and Gn within the capsomers was not found (Sherman *et al.*,

2009). Furthermore, they were unable to resolve RNPs, but did observe transmembrane densities of Gn cytoplasmic tail domains crossing the lipid bilayer and interacting with the RNPs that were situated directly below these transmembrane densities which is consistent with other studies on UUKV and BUNV (Huiskonen *et al.*, 2009; Overby *et al.*, 2007; Sherman *et al.*, 2009; Shi *et al.*, 2007). Similar work on UUKV also showed the spikes to have two distinct pH dependent conformations; being 8 nm at pH 6.0 and 13 nm at pH 7.0 (Overby *et al.*, 2008).

Genome organisation and viral proteins

Bunyavirus genomes range in size from ~12 kb to ~19 kb (Table 1.1) and all members of the *Bunyaviridae* have a negative-sense coding strategy for their structural proteins: the L protein (the RNA dependent RNA polymerase) is encoded on the L segment; the glycoproteins Gc and Gn are encoded on the M segment; and the nucleocapsid (N) protein is encoded on the S segment (Nichol *et al.*, 2005). Additionally, viruses in the genera *Orthobunyavirus*,

Table 1.1: Terminal nucleotide sequences of the S, M, and L genome segment of representative members of the family *Bunyaviridae.*

Genus- Virus	Consensus S, M, L terminal nucleotides	Genome size	L segment	M segment	S segment
Orthobunya- Bunyamwera	3' UCAUCACAUG- 5' AGUAGUGUGC-	12294	6875	4458	961
Hanta- Hantaan	3' AUCAUCAUCUG- 5' UAGUAGUAUGC-	11845	6533	3616	1696
Nairo- Dugbe	3' AGAGUUUCU- 5' UCUCAAAGA	18855	12255	4888	1712
Phlebo- Rift Valley fever	3' UGUGUUUC- 5' ACACAAAG-	11979	6404	3885	1690
Tospo- Tomato spotted wilt	3' UCUCGUUA- 5' AGAGCAAU-	16634	8897	4821	2916

Size and segments are in nucleotides. Taken from (Schmaljohn, 2007).

Phlebovirus and *Tospovirus* all encode a non-structural (NSs) protein on their S segment. The tospoviruses and phleboviruses use an ambisense coding strategy for the NSs protein, whereas the orthobunyavirus NSs protein is in an overlapping reading frame with the N protein. Furthermore, orthobunyaviruses, tospoviruses and some phleboviruses encode another non structural protein, NSm, on their M segment. Thus, bunyaviruses use both negative sense and ambisense coding strategies. Some viruses also encapsidate some anti-genomic RNAs in to the virions; the UUKV virion contains S segment anti-genomic RNA, while RVFV has anti-genomic RNA for all three segments in the

virion (Ikegami *et al.*, 2005; Simons *et al.*, 1990). TSWV virions contained S and M segment anti-genomic RNAs, and LACV progeny from insect cells had S segment anti-genomic RNA in the virions (Kormelink *et al.*, 1992a; Raju & Kolakofsky, 1989).

The untranslated regions

The coding region of each segment is flanked by a 3' and a 5' untranslated region (UTR). There are several mini-replicon based systems in use to study bunyaviruses and these have helped to elucidate the role of the UTRs in the bunyavirus replication cycle. Within each genus the viral UTR terminal sequences are not only complementary but also conserved (Table 1.1), however they are not conserved either by sequence, length, or degree of complementarity across the different genera. The 11 terminal nucleotides (nt) of the orthobunyavirus UTRs are complementary except at position 9 where the pair is G-U, and as the segment size increases so too does the extent of complementarity. This complementarity leads to pan handle structures and the non-covalently linked circularisation of each segment, as observed by electron microscopy (Hewlett *et al.*, 1977; Kolakofsky & Hacker, 1991; Obijeski *et al.*, 1976b; Pardigon *et al.*, 1982; Patterson *et al.*, 1983; Samso *et al.*, 1975).

The UTRs have a direct effect on transcription and replication of bunyavirus RNAs. Mutagenesis of the UTRs that altered the complementarity of the segments by changing either nucleotide identity or base-pairing potential inhibited transcription and translation and demonstrated the importance of the UTRs in promoter strength (Barr & Wertz, 2004; Kohl *et al.*, 2004). Furthermore, the strength of the promoters for transcription of each segment is different, with a ratio of 100:10:1 for the S, M and L segments of LACV, respectively (Rossier *et al.*, 1988). However, the genomic RNA levels were found to be equimolar. Studies into the RNA synthesis of BUNV genomic and antigenomic RNA synthesis showed that the promoter strength decreased in the order M>L>S (Barr *et al.*, 2003), which was later shown for UUKV also (Flick *et al.*, 2004). Thus the UTRs play an essential role in initiating transcription but also with distinguishing the different degrees of gene expression for each segment.

In addition to the aforementioned role of the UTRs in the initiation of transcription and translation, they have also been found to have critical functions in termination of transcription, as well as in viral RNA encapsidation and packaging. Transcription termination signals have been mapped to the UTRs, and for those phleboviruses and tospoviruses using an ambisense strategy, hairpin structures within the intergenic regions act as termination signals. Barr *et al.* (2006) mapped a 6 nt termination signal within a 33 nt region of the UTR of the BUNV S segment. Further investigation revealed a second termination signal that was also found in the L segment UTR. Using

competitive binding assays, the terminal 32 nt of the 5' end of the BUNV S segment were found to be essential for the encapsidation of RNA by the N protein and thus to contain an RNA encapsidation signal (Osborne & Elliott, 2000). Studies have demonstrated that the UTRs are sufficient to mediate packaging of the genome segments although the specific sequences and the mechanism have yet to be elucidated. Furthermore, the efficiency of packaging by the UTRs of UUKV was found to vary by segment, with it being greater for the L segment than the M and S segments (L was stable over seven passages compared with M and S segments being lost after three passages) (Blakqori *et al.*, 2003; Flick *et al.*, 2004). Thus, while the UTRs do not encode viral proteins, they do provide necessary signals for the modulation of viral gene expression, as well as packaging RNA segments into new virions.

Viral genes and expression

The L segment and the L protein

As mentioned above, the L segments of all the orthobunyaviruses encode the L protein, which is the viral RNA dependent RNA polymerase. There is no evidence of any other coding within these segments and they have a negative sense coding strategy. The L segments of the orthobunyaviruses, hantaviruses and phleboviruses are about 6.5 kb in length, whereas the tospoviruses and nairoviruses have L segments of about 9 kb and 12 kb respectively (Table 1.1 (Schmaljohn, 2007)). The L proteins expressed by the nairoviruses are the largest at 459 kDa, followed by the tospovirus L protein which is 331 kDa, and the L protein from hantaviruses, orthobunyaviruses and the phleboviruses are 250 kDa (Table 1.2 (de Haan *et al.*, 1991; Elliott, 1989; Marriott & Nuttall, 1996; Muller *et al.*, 1991; Schmaljohn, 1990)). The shape of the L protein polymerase domain resembles a right hand, in that it has a thumb, palm and fingers domain, and sequence alignments also show that four motifs within the palm domain are conserved. In fact these "polymerase motifs" are conserved among many different viral polymerases as they are involved in binding divalent cations, selection of nucleosides and sugars, and in catalysis. However, despite this conservation based on the functional requirements of the enzyme, there is evidence that some sequence motifs are found only in some genera. For example, first identified in RVFV the L protein contains two regions at the N terminus which are only conserved in the *Bunyaviridae* and the *Arenaviridae* (Muller *et al.*, 1994). To prove the RNA dependent RNA polymerase function of the bunyavirus L protein, it was first expressed in recombinant vaccinia virus and subsequently used to synthesise RNA from transfected BUNV RNPs (Jin & Elliott, 1991). The authors did further analysis using the same system and found that the mRNAs contained non-viral heterogeneous sequences, demonstrating that the L protein has endonuclease activity to generate the primers as well as transcriptional activity. They further showed that the L protein utilises the method of "cap snatching" to generate capped 5' mRNAs

(Jin & Elliott, 1993). Shi and Elliott (2009) generated two recombinant viruses with the V5 epitope tag positioned towards the C terminus of the L protein, that were infectious and also functional in a minireplicon assay. They further showed that the L protein was distributed in the cytoplasm, colocalised with N protein, and was more concentrated in the perinuclear region of the cell.

The M segment and the glycoproteins Gn and Gc

All members of the *Bunyaviridae* family encode the two glycoproteins (Gn and Gc) as a polyprotein from a single ORF on the M segment.

The glycoproteins are located within the membrane-derived envelope of the virion and constitute the viral projections (spikes) (Schmaljohn, 2007). Initially the glycoproteins were named G1 and G2 based on their migration through a polyacrylamide gel. However, it was subsequently found that these proteins were interchangeable between genera of some viruses, and thus the nomenclature was changed to the current system based on the coding location

Table 1.2: Viral proteins of representative members of the family *Bunyaviridae*

Genus Virus	L segment		M segment		S segment	
	Protein	Size	Protein	Size	Protein	Size
Orthobunya- Bunyamwera	L	259	Gn Gc NSm	32 110 18	N NSs	26 11
Hanta- Hantaan	L	247	Gn Gc	70 55	N	48
Nairo- Dugbe	L	459	Gn Gc	35 73	N	50
Phlebo- Rift valley fever	L	238	Gn Gc NSm	55 62 14	N NSs	28 32
Tospo- Tomato spotted wilt	L	332	Gn Gc NSm	46 75 37	N NSs	29 52

Protein sizes are in kDa

either at the N terminus or the C terminus of the polyprotein (Lappin *et al.*, 1994). The polyprotein precursor is co-translationally cleaved to give the two integral transmembrane glycoproteins which are further modified by N-linked glycosylation (Nichol *et al.*, 2005; Shi *et al.*, 2005). The existence of conserved cysteine residues (comprising around 4-7% of the expressed gene product) implies the polypeptide secondary structure is determined by disulphide bridges (Schmaljohn, 2007). The N terminus of the glycoproteins protrudes from the virion while the C terminus of the proteins anchors them into the envelope. Each of the glycoproteins is preceded by a signal peptide, indicating that polyprotein cleavage is carried out by a cellular signal peptidase. The

glycoproteins are transported to the Golgi complex *via* a Golgi targeting and retention signal in the Gn protein and not in the Gc protein (which does not traffic to the Golgi without interacting with Gn) (Erickson *et al.*, 2007; Shi *et al.*, 2004; Shi *et al.*, 2005). As mentioned above, the two glycoproteins are not equal in molecular mass and the sizes vary among the bunyaviruses (Table 1.2). BUNV encodes a Gn protein that, at 32 kDa, is considerably smaller than the 110 kDa Gc protein. The BUNV Gn comprises 302 residues and has a cytoplasmic tail of 78 residues, whereas the Gc protein comprises 957 residues and has a cytoplasmic tail of just 25 residues (Elliott, 1990; Lees *et al.*, 1986).

The M segment and the NSm protein

For members of the *Orthobunyavirus*, *Phlebovirus* and *Tospovirus* genera, the M segment also encodes the non-structural protein NSm (Table 1.2). BUNV encodes an NSm protein that co-localises to the Golgi with other viral proteins. It has been found to be able to interact with other viral proteins and to be essential for virion assembly. The loss of NSm or the selective deletion of any of 3 of the 5 putative domains within NSm (identified as domains I, II and V) prevents synthesis of virus-like particles, showing that NSm has a crucial role in BUNV assembly (Shi *et al.*, 2006).

While one or more NSm proteins have been identified in other genera within the bunyavirus family, the function of all of these proteins has not been determined. The phleboviruses produce a variety of NSm proteins, from the UUKV which does not express an NSm protein (but does produce a Gn protein analogous to the NSm-Gn fusion polypeptide of RVFV) to the 30 kDa NSm protein produced by the Punta Toro virus (PTV) (Matsuoka *et al.*, 1988; Schmaljohn, 2007). RVFV encodes two NSm proteins: a distinct 14 kDa protein and a 78 kDa NSm protein, which is cleaved from the N-terminus of the M segment precursor polyprotein. Studies established that there are two start codons upstream of the N terminus of the Gn protein that produce either the NSm protein or the NSm-Gn uncleaved polyprotein of 78 kDa, with no precursor/product relationship between the two proteins (Kakach *et al.*, 1989). The function of both of the NSm proteins is not yet clear for RVFV. Nairoviruses have a more complex processing of the M segment proteins compared with the rest of the family (Marriott *et al.*, 1992). CCHFV polyproteins are proteolytically cleaved to yield the precursor proteins of pre-Gn (140 kDa) and pre-Gc (85 kDa) which contain the cellular protease cleavage site SKI-1 and are subsequently cleaved to the mature Gn (37 kDa) and Gc (75 kDa) by cellular secretory pathway proteases (Bergeron *et al.*, 2007; Schmaljohn, 2007). The NSm protein is cleaved from the precursor protein pre-Gn. The tospovirus TSWV synthesises an NSm protein using an ambisense coding strategy and thus an anti-genomic template-derived mRNA. The TSWV NSm facilitates virus spread from one plant cell to another since NSm localises to the cell wall and interacts with the

plasmodesmata-penetrating tubules to allow transport of the RNPs across the cell wall (Kormelink *et al.*, 1992b).

The S segment and the N protein

The size of the S segment varies across the five genera from the smallest, in the orthobunyaviruses (around 1 kb) to the largest in the tospoviruses (around 3 kb (Table 1.2)). In the *Orthobunyavirus* genus, the S segment encodes two proteins: the N protein and the NSs protein from overlapping open reading frames in the sub-genomic mRNA. Translation occurs *via* the recognition of the distinct start codons by the ribosome and thus the synthesis of two separate proteins (Bishop *et al.*, 1982).

All viruses in the family *Bunyaviridae* encode an N protein on their S segment and this is the most abundant protein found in both the virions and infected cells. The functions of the N protein are to protect the viral RNA from degradation and to facilitate the replication of the RNA, both of which are achieved by the encapsidation of both genomic and anti-genomic RNA into the RNPs, which are required for replication by the L protein. The encapsidation of RNA by the N protein depends upon the ability of individual N protein monomers to oligomerise and this process of oligomerisation differs among the genera. The N proteins of hantaviruses and nairoviruses are the largest in the family. It has been shown that the homotypic interactions between the C and N termini of the N protein of hantaviruses is responsible for the trimerisation of the N protein, which can then encapsidate the RNA (Alfadhli *et al.*, 2002; Alminaite *et al.*, 2008; Yoshimatsu *et al.*, 2003), whereas the RVFV N protein forms stable dimers for encapsidation (Le May *et al.*, 2005). However, TSWV appears to encapsidate RNA by building multimers of the N protein by one N protein addition at a time (Kainz *et al.*, 2004; Uhrig *et al.*, 1999). BUNV N multimerisation also occurs by the addition of one N protein at a time, and the first 10 and last 17 residues are responsible for this process (Leonard *et al.*, 2005).

The S segment and the NSs protein

Only nairoviruses have not been shown to produce a functional NSs protein, *ergo* viruses in the *Tospovirus*, *Phlebovirus*, *Hantavirus*, and *Orthobunyavirus* genera encode a NSs protein and these vary in size from 10 kDa for the orthobunyaviruses to greater than 50 kDa for the tospoviruses (Table 1.2). The NSs proteins in the four genera show no sequence homology; indeed, there is little conservation within the same genus, with the exception of some highly conserved domains within several strains of a single virus (Giorgi *et al.*, 1991; Sall *et al.*, 1997). Unlike the orthobunyaviruses, both the tospoviruses and phleboviruses translate their NSs protein from mRNA transcribed from anti-genomic RNA and thus use an ambisense coding strategy. Furthermore, studies have shown that RVFV NSs is transcribed from anti-genomic RNA

which is carried in the virion (anti-genomic RNAs for all three segments of RVFV have been found in virions) (Ikegami *et al.*, 2005). The NSs protein of the orthobunyaviruses has been shown to play a role in the control of the L protein and decreasing transcription, whereas the NSs protein of RVFV has been shown to enhance RNA transcription (Ikegami *et al.*, 2005; Weber *et al.*, 2001). Importantly, in all four genera, the NSs proteins display roles in antagonising the host cell antiviral responses and for some the mechanism of antagonism has been widely studied.

One well characterised example is that of the RVFV NSs protein, a potent IFN antagonist with several distinct mechanisms. Uniquely the RVFV NSs protein forms ribbon like structures within the nucleus of infected cells (Struthers *et al.*, 1984). This observation was subsequently linked to a critical function of RVFV NSs in host cell protein shut-off. This is achieved through the interaction of RVFV NSs with the p44 subunit of transcription factor TFIIH, resulting in the production of the filamentous structures seen in the nucleus. As a consequence of this interaction of TFIIH and NSs, there is a reduction in the concentration of TFIIH and a subsequent decrease in transcription mediated by both polymerases I and II (Bouloy & Weber, 2010; Le May *et al.*, 2004). Furthermore, NSs interacts with the cellular protein SAP30 in the nucleus and thus disrupts IFNβ transcription (Le May *et al.*, 2008). Several RVFV mutants have been propagated in order to examine the effects of NSs protein on the host cell and viral infection, such as a virus that was engineered to lack the SAP30 interaction domain on the NSs protein and as such was avirulent for mice and unable to counteract the IFN response (Le May *et al.*, 2008). The natural RVFV isolate Clone 13 contains a large deletion in the NSs gene and as such is a strong IFNα/β inducer and is highly pathogenic in $IFNAR^{-/-}$ knockout mice (Bouloy *et al.*, 2001). Subsequently Habjan *et al.* (2009) and Ikegami *et al*. (2009) showed that the NSs protein of RVFV targets PKR for proteasomal degradation whereas Clone 13 NSs does not (discussed later).

The NSs protein of BUNV has also been targeted for further analysis. In minireplicon assays, inhibition of BUNV NSs translation was shown to enhance reporter activity while over-expression of NSs reduced reporter activity (Weber *et al.*, 2001). In the same study, BUNV NSs protein was shown to localise predominantly in the cytoplasm with some found in the nucleus, which was further confirmed more recently by Thomas *et al.* (2004). Further to this, the rescue of a NSs-deficient recombinant BUNV showed the NSs protein to be non-essential to viral viability, although the virus was severely restricted in IFN competent cell lines and was shown to be a strong inducer of the IFNβ promoter (Bridgen *et al.*, 2001). Moreover, Weber *et al.* (2002) demonstrated that the NSs-deficient virus induced over 1000 units (U) of IFNα/β per ml of medium (compared with under 50 U IFNα/β for BUNV) and was dependent on virally produced dsRNA and IRF3. Subsequently a study has shown that IFN

treatment prior to infection has more effect on BUNV replication and that the loss of NSs confers a 10-fold reduction in viral titre (Streitenfeld *et al.*, 2003). Interestingly the same study showed BUNV NSs inhibited dsRNA-dependent IFN induction and yet was ineffectual on the dsRNA-activated PKR and RNase L systems. Like the NSs of RVFV, BUNV NSs protein has been found to cause host cell protein shut-off and the mechanism is by interacting with the cellular protein MED8, a component of the mediator complex which is involved in mRNA synthesis. This interaction ultimately leads to inhibition of phosphorylation of the C terminal domain (CTD) of RNA polymerase II and subsequently to the inhibition of transcription mediated by RNA polymerase II (Leonard *et al.*, 2006; Thomas *et al.*, 2004). Consequently, BUNV NSs blocks the IFN response at the level of transcription. Additionally, the NSs protein of BUNV inhibits the induction of apoptosis by interacting with the IRF3 signalling pathway and inhibiting an IRF3-dependent promoter (Kohl *et al.*, 2003). The inhibition of apoptosis is another mechanism by which BUNV NSs counteracts the host antiviral response.

Finally, the NSs protein of TSWV forms into fibrils or fibrous structures within the cytoplasm of plant cells and sequesters siRNAs and miRNAs, thereby preventing the cellular RNAi pathway from counteracting the infection (Schnettler *et al.*, 2010). Thus, even the bunyaviruses that infect plants have been shown to use the NSs protein to block cellular antiviral mechanisms, suggesting a conservation of function for NSs despite divergent sequences and coding strategies.

The replication cycle

There are several stages to the replication cycle of bunyaviruses: adsorption and entry; primary transcription and translation; amplification of genomic RNA; assembly, budding and release (**Fig 1.11**).

Adsorption and entry

Many enveloped viruses employ similar mechanisms to gain internal access to the host cell. The projections comprising the two viral glycoproteins interact with receptors on the cell surface. For most members of the family, the cell surface receptors have yet to be identified. However, it has been demonstrated that pathogenic hantaviruses bind to β3 integrins and non-pathogenic hantaviruses bind to β1 integrins on endothelial cells (Gavrilovskaya *et al.*, 1999). The orthobunyavirus Gc protein principally mediates the attachment and entry of virus into mammalian and mosquito cells (Plassmeyer *et al.*, 2005). Once bound to the cell surface, entry is by receptor-mediated endocytosis and uncoating occurs by Gc-mediated fusion with endosomal membranes in a pH-dependent manner (Shi *et al.*, 2009). Entry of CCHFV is dependent on clathrin-associated endocytosis, and requires the presence of cholesterol in the plasma membrane and the acidic pH of the endosomal lumen (Simon *et al.*, 2009).

OROV has also been shown to gain entry *via* clathrin-coated pits and endocytosis into HeLa cells, which further requires low pH in the endosome (Santos *et al.*, 2008).

Primary transcription and translation

After uncoating and release of the viral genome into the cytoplasm, primary transcription of genomic RNA to mRNA can take place. There are promoters for genome transcription in the 3'- and 5'- termini of each segment which show

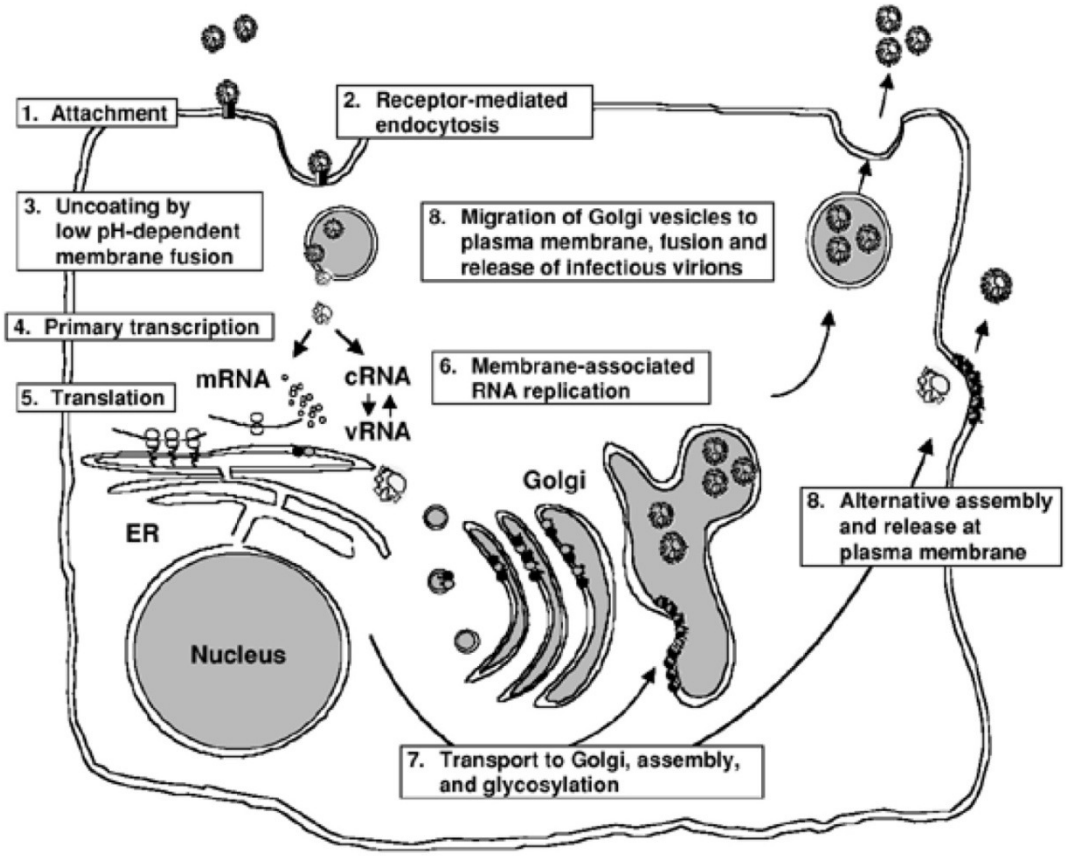

Figure 1.11 : Replication cycle of viruses in the family *Bunyaviridae*. Steps in the replication cycle are: 1. Attachment, mediated by an interaction of viral proteins and host receptors; 2. Receptor-mediated endocytosis; 3. Uncoating, by acidification of endocytic vesicles, and fusion of viral membranes with endosomal membranes; 4. Primary transcription of viral-complementary mRNA species from genome templates using host-cell-derived primers and the virion-associated polymerase; 5. Translation of L, M, and S mRNAs, cotranslational cleavage of the M segment polyprotein, dimerization of Gn and Gc in the ER; 6. Membrane associated RNA replication, synthesis, and encapsidation of cRNA to serve as templates for vRNA or, for ambisense genes, templates for subgenomic mRNA, Genome replication; 7. Morphogenesis including transport of the structural proteins to the Golgi, glycosylation of Gn and Gc, budding into the Golgi cisternae; 8. migration of Golgi vesicles containing viruses to the cell surface, fusion of vesicular membranes with the plasma membrane and release of infectious virions. Some viruses in some cell types can bud both into intracellular vesicles and also from the plasma membrane. ER denotes the endoplasmic reticulum, black and white squares represent the receptor; o represents the N protein, and pairs of black and white circles represent Gn and Gc. Taken from Schmaljohn, 2007.

high sequence complementarity and only the RNA encapsidated by the N protein can act as a template for transcription (Bouloy & Hannoun, 1976; Dunn *et al.*, 1995; Lopez *et al.*, 1995). Minigenome assays with BUNV revealed that complementary 3'- and 5'- termini and some sequence was required for optimal

transcription (Kohl *et al.*, 2004), and Lowen and Elliott (2005) deleted parts of the S segment UTR sequence and revealed that the minimal UTR sequence required for viable BUNV is 29/85 at the 3' end, and 112/174 at the 5' end (where 85 and 174 are the full length 3' and 5' UTRs respectively). Thus, optimal transcription requires the panhandle structure formed by the terminal regions, while specific sequences define promoter strength (Barr & Wertz, 2005). Additionally, minigenome RNAs co-expressed with viral proteins established that only the L and N proteins are required for successful transcription (Dunn *et al.*, 1995). Initially, the L protein functions as an endonuclease and cleaves cytoplasmic host cell mRNA to produce capped primers to initiate mRNA transcription, which produces viral mRNA with a 10-20 heterogeneous nucleotide 5' terminal extension (Bishop *et al.*, 1983; Patterson *et al.*, 1984). Nascent mRNAs are truncated by approximately 50-100 nt compared with the full transcript (anti-genome RNA), implying a specific signal for termination of transcription, and the transcripts are not polyadenylated (Dunn *et al.*, 1994; Patterson & Kolakofsky, 1984; Patterson *et al.*, 1984). BUNV translation is mediated by the UTRs and occurs independently of poly(A) tails and poly(A) binding protein (PABP) as BUNV targets PABP for degradation in order to stop host protein synthesis (Blakqori *et al.*, 2009). The transcription termination signal for BUNV has been mapped to a 33 nt sequence in the 5'-UTR of the S segment. Smaller regions and individual nucleotides within this sequence have been shown to be essential. Furthermore, a second termination signal, of 9 nt in length, has been mapped 32 nt downstream of the BUNV S segment UTR and this second signal has also been found in other orthobunyavirus S segments (Barr *et al.*, 2006).

For optimal efficiency of bunyavirus transcription there must be simultaneous translation. This was demonstrated by the synthesis of incomplete viral transcripts when translation was blocked with protein synthesis inhibitors (such as cycloheximide) (Patterson & Kolakofsky, 1984; Raju & Kolakofsky, 1986) and further by *in vitro* studies showing viral mRNA synthesis only occurred in the presence of actively translating rabbit reticulocyte lysate (Bellocq & Kolakofsky, 1987; Bouloy, 1991). The initial transcription and translation of the viral genes occurs very rapidly, with the M segments being translated at the rough ER (RER) and the S and L segments at the cytosolic (or free) ribosomes. Newly-synthesised viral proteins can be detected within two hours of infection (Kariwa *et al.*, 2003; Madoff & Lenard, 1982; Pennington *et al.*, 1977).

Viral genome amplification

Eventually, the polymerase L protein must change from primed transcription of mRNAs to the transcription of full length RNA transcripts, and thus change from viral transcription to viral replication. As with primary transcription above, this requires both the L and N proteins. However, transcription must now be initiated from the precise start of the 3' terminal end to synthesise a full-length

transcript, which is encapsidated as it is synthesised and not translated. The transcription termination signals within the sequences are overcome by encapsidation with the N protein for viruses such as VSV and SeV (Lamb, 2007; Lyles, 2007) and it is hypothesised that the same occurs for bunyavirus replication. It was also shown with VSV that the polymerase complex the transcriptase, involved with primary transcription, comprised viral L and P proteins along with two cellular proteins and submolar amounts of mRNA cap guanylyltransferase (Qanungo *et al.*, 2004). However, the replicase, the polymerase complex involved with genome replication, was different to the transcriptase and comprised viral L, P and N proteins only. Therefore a similar mechanism of using distinct enzyme complexes for transcription and replication could be employed by bunyaviruses.

The mechanism of prime and realign for genome replication has been proposed to be used by hantaviruses and nairoviruses to justify the monophosphorylated U residue at the 5' end of HTNV genomic RNA. In this case, without a host-derived oligonucleotide primer, the polymerase initiates transcription with pppG and proceeds with the addition of several nucleotides, and then slips backwards and realigns. This produces an overhang with the initial G residue which can then be cleaved off the transcript by the L protein (Garcin *et al.*, 1995b; Prehaud *et al.*, 1997).

Assembly, budding and release

Morphogenesis and subsequent maturation by budding of virions occurs at the smooth Golgi membrane for members of the *Bunyaviridae* (Kuismanen *et al.*, 1982; Salanueva *et al.*, 2003; Smith & Pifat, 1982), although budding at the plasma membrane has been observed for some hantaviruses and RVFV (Anderson & Smith, 1987; Goldsmith *et al.*, 1995; Ravkov *et al.*, 1997). As described above, both of the BUNV glycoproteins localise in the Golgi, though only the Gn protein has a Golgi targeting signal. Thus, without the complex formation of Gn and Gc, Gc would remain in the ER. The Golgi-targeting signal for BUNV has been mapped to the transmembrane domain of the Gn protein, while for two phleboviruses PTV and RVFV it was mapped to the transmembrane domain and part of the cytoplasmic tail of Gn (Gerrard & Nichol, 2002; Matsuoka *et al.*, 1994; Shi & Elliott, 2002; Shi *et al.*, 2004). For HTNV it was shown that mutations in both the Gn and Gc sequences resulted in loss of transport of the Gn-Gc complex to the Golgi, demonstrating the importance of the correct conformation of this complex for transport (Shi & Elliott, 2002). However, studies on nairoviruses revealed that loss of the transmembrane domain and cytoplasmic tail of Gn did not result in the loss of Gn-Gc dimerisation or subsequent transport to the Golgi, thus nairoviruses could have a targeting signal in their Gn ectodomain (Erickson *et al.*, 2007; Haferkamp *et al.*, 2005).

The glycoproteins of PTV and BUNV are transported to the *cis*/medial Golgi compartment, followed by transport through the Golgi and the acquisition of resistance to endoglycosidase H (endo H), an enzyme that cleaves sugars high in mannose. Since BUNV has endo H resistance, it is likely that it progressed through the *trans*-Golgi network (TGN), whereas HTNV and CCHFV retain their susceptibility to endo H and thus likely have not passed through the TGN (Bertolotti-Ciarlet *et al.*, 2005; Novoa *et al.*, 2005a; Shi & Elliott, 2004). Mutational studies of the glycosylation sites of HTNV Gn and Gc proteins revealed the importance of the sites for the ER exit signal and Golgi targeting signal. Further investigation into the glycosylation sites of BUNV Gn and Gc revealed that the Gn site N60 is essential for trafficking both glycoproteins (Gn and Gc) through the Golgi. In contrast, the two glycosylation sites identified on the Gc protein increase viral infection efficiency but are not essential for viral replication (Shi *et al.*, 2005).

Assembly can only occur when the N protein and the two glycoproteins have been transported to the same location, the RNPs are on the cytoplasmic side of the Golgi membrane and the glycoproteins are on the luminal side (Pettersson, 1991; Smith & Pifat, 1982). The interaction between the transmembrane domains of the glycoproteins and the RNPs is the facilitator of virion envelope development, while it is the cytoplasmic tails of the glycoproteins that attract the RNPs to the Golgi membrane. Bunyaviruses are able to concentrate their replication complexes and assembly sites in specific locations inside a cell building a viral factory (Novoa *et al.*, 2005a; Novoa *et al.*, 2005b; Salanueva *et al.*, 2003). The factory consists of multiple units of Golgi stacks, RER elements, mitochondria and tubular structures (tubes) which provide links between these organelles. The structure and function of the tubes are dependent on viral NSm protein and have been shown to number 50 or more per cell. Aggregation of the NSm protein stimulates inward movement from the cytosolic face of the Golgi thus the interaction of the viral NSm protein with host cell actin and giantin provides a scaffold for the assembly of virus particles (Fontana *et al.*, 2008).

Release of the virions occurs by exocytosis; immature particles bud into the Golgi cisternae, where they are transported in vesicles in the secretory pathway, to the plasma membrane where the vesicles fuse and release the virions to the exterior (Fontana *et al.*, 2008).

Assembly and release of tospoviruses differs from the other viruses in the family. The glycoproteins accumulate Golgi membranes which surround the viral RNPs forming double enveloped particles (DEVs). The DEVs then fuse with other DEVs or with the ER and are subsequently released by exocytosis or are ingested by thrips (Kikkert *et al.*, 1999; Wijkamp *et al.*, 1993).

Effects of infection on the host cell and the host response

Excluding the hantaviruses, the viruses of the other four genera all have alternating replication cycles in vertebrate (plant cells for the tospoviruses) and invertebrate host cells, and cytopathology is only seen in the vertebrate/plant cells as opposed to the invertebrate cells (Beaty & Calisher, 1991; Carvalho *et al.*, 1986; Wijkamp *et al.*, 1993). As discussed above, viruses from the *Orthobunyavirus* and *Phlebovirus* genera encode and express a NSs protein that causes host cell protein synthesis to cease. This is known as host cell protein shut-off and can be extremely acute (Bridgen *et al.*, 2001; Thomas *et al.*, 2004). However, UUKV is not able to cause protein shut-off (despite encoding a NSs protein), while the nairoviruses do not cause protein shut-off and, not surprisingly, also do not encode an NSs protein (Pettersson, 1974). For BUNV, host cell protein shut-off is clearly visible by 5 hours post infection and at 7 hours there is little host cell protein synthesis at all, whereas for RVFV the reduction in host cell protein synthesis occurs from 4 to 20 hours post-infection (depending on the MOI used (Pennington *et al.*, 1977)). The hantaviruses are able to cause persistent infections both in their rodent hosts and in mammalian cells in tissue culture, while the members of the family transmitted by arthropods cause persistent infections in the arthropod host and in insect cells in tissue culture.

The primary mammalian host cell response to a viral infection is the IFN response and many bunyaviruses have evolved ways of counteracting this very powerful response. The NSs protein of BUNV is the primary interferon antagonist during the viral replicative cycle. Expression of NSs is predominantly in the cytoplasm, where it interacts with and disrupts the C-terminal domain of RNA polymerase II by inhibiting phosphorylation of the residue serine 2 of the heptapeptide repeat YSPTSPS (Thomas *et al.*, 2004). The C-terminal domain of RNA polymerase II contains 52 repeats of the heptapeptide repeat YSPTSPS; phosphorylation of the serine 2 residue is required for elongation of the mRNA and 3' end processing, and phosphorylation of the serine 5 residue is required for transcription initiation (Ahn *et al.*, 2004; Kobor & Greenblatt, 2002; Komarnitsky *et al.*, 2000). RNA polymerase II-directed protein synthesis requires the multiprotein Mediator complex for mRNA synthesis activation and repression (Kornberg, 2005). The Mediator complex is comprised three modules called the head, middle and the tail (Blazek *et al.*, 2005; Chadick & Asturias, 2005; Conaway *et al.*, 2005; Dotson *et al.*, 2000). The tail interacts with transcriptional activators and repressors and, as such, is the sensor element. The middle module of the complex binds to the polymerase and is in contact with the C-terminal domain of RNA polymerase II, and facilitates the transfer of information from the tail to the head modules. The head module contains the protein MED8 which interacts directly with the polymerase enzyme and appears to regulate the polymerase by recruiting it to the promoter-bound preinitiation complex (Myers *et al.*, 1998). The transcription factor TFIIH kinase

phosphorylates serine 5 residues, and the Cdk9 kinase activity of P-TEFb phosphorylates serine 2 residues of RNA polymerase II, both kinases being activated first by Mediator. Mutational studies showed that the C-terminus of BUNV NSs protein directly interacts with MED8 resulting in inhibition of transcription and, further, that the region stipulated contains amino acids conserved among many orthobunyavirus NSs proteins (Leonard *et al.*, 2006). Several mutant viruses that either lack NSs or express a truncated form of NSs have been shown to be potent IFN inducers and are severely attenuated in IFN competent cell lines. Additionally, the mutant virus mBUNNSs22 is unable to block RNA polymerase II activity even though it contains the MED8 interaction domain, implying a further role of the N-terminus of NSs in counteracting the IFN response (van Knippenberg *et al.*, 2010).

Virus evolution

The capability of this family of viruses to evolve is clearly demonstrated by the numerous serologically distinct virus members and the high divergence seen amongst the viruses. For segmented RNA viruses, there are two methods by which genetic variation can occur, namely genetic drift and genetic shift. Genetic drift arises from deletions, inversions, duplications and point mutations that are accumulated over time through the lack of the proof-reading ability of RNA dependent RNA polymerases. Genetic shift occurs through the dual infection of the same cell and subsequent reassortment of one or more of the viral segments, resulting in a large and immediate genetic change. Genetic reassortment amongst the *Bunyaviridae* is possible in the laboratory, although only between serologically similar viruses. Garissa virus is a natural reassortant orthobunyavirus, isolated in Africa from haemorrhagic fever cases in 1997-98, that had L and S segments from BUNV and an M segment from Ngari virus (Gerrard *et al.*, 2004). Ngari virus itself is a reassortant virus containing BUNV L and S segments and an M segment that Briese *et al.* suggest to be donated by Batai virus (Briese *et al.*, 2006). Recent studies show reassortment in nature with LACV with 25% of mosquitoes infected with a LACV reassortant (Briese *et al.*, 2007; Elliott, 1996; Reese *et al.*, 2008). It is common that reassortants retain their original S and L segments but change their M segment, which can lead to variants with altered pathogenicity and new tropisms. The chances of reassortment occurring in nature are greatly increased by the requirement for arthropod vectors, since the arthropods feed on a variety of vertebrates thereby increasing the possibility of a dual (or more) infection. Furthermore, the possibility of genetic variation within the arthropod vectors is enhanced by transovarial transmission of viruses over several generations that can accumulate genetic alterations (drift), thus making the resulting population of progeny viruses even more distinct (Briese *et al.*, 2006; Gerrard *et al.*, 2004; Kobayashi *et al.*, 2007; Reese *et al.*, 2008).

Reverse genetics of bunyaviruses

Virologists use reverse genetics systems to manipulate cDNAs of viral genomes to better understand the replicative cycle of a virus. It is extremely useful with regards to RNA viruses as direct manipulation of RNA is very difficult. Reverse genetics permits mutational analysis of the viral genomic RNA which would otherwise be impossible. The system of reverse genetics with negative-strand RNA viruses is yet more complicated as the viral genome is not sufficient for replication; the genome needs to be encapsidated by the N protein and there needs to be an RNA dependent RNA polymerase present. The first negative strand RNA virus to be rescued by reverse genetics was rabies virus in 1994 (Schnell *et al.*, 1994). The method used was to infect cells with a recombinant vaccinia virus encoding T7 RNA polymerase (vTF7-3) and then to transfect into the cells four plasmids each under the control of a T7 promoter, one consisting of the full length rabies virus anti-genome followed by a ribozyme, and three expression plasmids encoding the rabies virus L, P and N protein. This led to the production of fully infectious rabies virus 'de novo' and also some genetically modified recombinant (r) rabies virus, thus fully proving the methodology. Subsequently other non segmented negative strand RNA viruses were rescued: VSV (Lawson *et al.*, 1995), MeV (Radecke *et al.*, 1995), SeV (Garcin *et al.*, 1995a), and RSV (Collins *et al.*, 1995). Having established reverse genetics systems for non-segmented negative-strand RNA viruses, the next step was to overcome the inherent difficulties of rescuing a segmented virus, notably the efficiency of the large number of plasmids thought to be required to be transfected into cells. This was overcome by Bridgen and Elliott (Bridgen & Elliott, 1996) who managed to rescue the trisegmented BUNV from cloned cDNAs. The method that they used was very similar to the rabies virus rescue system: HeLa cells were infected with vTF7-3 for T7 RNA polymerase expression, followed by transfection of plasmids containing the BUNV L, M and S ORFs under a T7 promoter, to express all the viral proteins of BUNV. Next, an additional transfection was carried out using plasmids containing the full length anti-genomic BUNV L, M and S segments, also under a T7 promoter and with a hepatitis δ ribozyme and T7 terminator immediately after the viral sequence, to produce BUNV anti-genomes for transcription and replication. Approximately 42 hours later the cells and supernatant were harvested, clarified and used to infect the *Aedes albopictus* C6/36 insect cell line in order to isolate BUNV from VACV since only BUNV can replicate in the insect cells. Several days later, released virions were plaque purified on BHK21 cells. Since the first breakthrough, not only have several other bunyaviruses been rescued, LACV, (Blakqori & Weber, 2005) RVFV, (Billecocq *et al.*, 2008; Gerrard *et al.*, 2007; Habjan *et al.*, 2008; Ikegami *et al.*, 2006) and AKAV (Ogawa *et al.*, 2007), but viruses from other families have as well, namely the orthomyxovirus IAV (Fodor *et al.*, 1999; Neumann *et al.*, 1999). The systems have also been updated and are constantly being refined. The current BUNV rescue protocol is based on

the work of Lowen *et al.* (2004) who significantly improved the yield of virus and decreased the time taken for the whole rescue (Lowen *et al.*, 2004). This method uses the BSR-T7/5 cell line which constitutively expresses the T7 RNA polymerase. These cells are transfected with the pT7ribo plasmids, which express anti-genomic viral L, M and S segments under a T7 promoter and with the hepatitis δ ribozyme immediately after the coding sequence. There is also a T7 termination signal. This system generates high viral yield several days later. With the establishment of a reverse genetics system, comes the opportunities for rescuing mutant viruses, and the first significant virus of this sort was a BUNV with the NSs ORF mutated such that NSs was no longer expressed. This allowed investigations into the functions of NSs, and the differences between the wild-type and deletion viruses. To date many recombinant viruses have been rescued and used in studies to establish if they can be propagated and to investigate the consequences of the mutations on all stages of the virus replication cycle. Furthermore, many viruses now have reporter genes inserted such as renilla luciferase or GFP, so that expression can be quantified using a luminometer and or visualised using microscopy.

Aims

To investigate the effect of type I IFNs on BUNV replication in more detail and to identify specific ISGs that show inhibitory effects on BUNV.

To define the efficacy of fluorescently tagged viruses for screening cell lines for their anti-BUNV properties, and to increase the number of tools available for such purposes. Thus attempt to engineer, rescue and characterise a GcGFP tagged NSs deletion virus, rBUNGceGFPdelNSs.

2 Materials and Methods

Materials and reagents

All chemicals and reagents were purchased from BDH chemicals ltd or Sigma unless otherwise stated. Plastic-ware was purchased from Greiner and Nunc.

The antibiotics (**Table 2.1**), antibodies (**Table 2.2**), viruses (**Table 2.3**), cells (**Table 2.4**), plasmids (**Table 2.5**), enzymes (**Table 2.6**) and media (**Table 2.7**) used in this study are tabulated below.

Table 2.1: Antibiotics

Antibiotic	Description	Manufacturer
Ampicillin	Inhibits bacterial cell wall synthesis by acting as a competitive inhibitor of the transpeptidase enzyme	Promega
Blasticidin	Inhibits protein synthesis at a translational level in prokaryotes and eukaryotes	Invivogen
Geneticin (G418)	Inhibits polypeptide synthesis by inhibiting the elongation step in prokaryotes and eukaryotes	Invitrogen
Hygromycin B	Inhibits protein synthesis by interfering with translocation and promoting mistranslation at the 80S ribosome	Invitrogen
Puromycin	Inhibits protein synthesis by disrupting peptide transfer resulting in premature chain termination on both prokaryotic and eukaryotic ribosome	Invivogen
Tetracycline	Inhibit protein synthesis by blocking the attachment of aminoacyl-tRNA	Sigma

Table 2.2: Antibodies

Antibody	Species	Dilution	Supplier
BUN	Rabbit	IP:1 µl, WB:1/3000	R.M.Elliott
Cy5	Mouse	IF:1/400	Chemicon International Inc
Digoxigenin-AP fab fragment		1/10,000	Roche
GRO	Mouse	1/1000	R.M.Elliott
IgG HRP	Mouse	1/3000	Sigma
IgG HRP	Rabbit	1/3000	Cell signalling

Antibody	Species	Dilution	Supplier
IRF1	Rabbit	1/500	Santa Cruz Biotech
LACV N	rabbit	IP: 1 µl	R.M.Elliott
M2 FLAG	Mouse	1/1000	Sigma
MxA	Rabbit	1/500	Santa Cruz Biotech
BUN N 592	Rabbit	WB:1/6000 IF:1/200	R.M.Elliott
PKR	Mouse	1/3000	Abcam
P-STAT1	Rabbit	1/750	Cell signalling
STAT1	Rabbit	1/750	Cell signalling
Texas red	Rabbit	1/200	AbD Serotec
Tubulin	Mouse	1/3000	Sigma
Viperin	Rabbit	1/500	Abcam

Table 2.3: Viruses

Virus	Description
Wild type Bunyamwera (BUNV)	Naturally occurring Bunyamwera virus. Supplied by R.M.Elliott.
rBUNdelNSs	BUNV with the S segment encoded NSs protein deleted. Supplied by R.M.Elliott.
rBUNGc-eGFP	BUNV with part of the Gc protein replaced with GFP. Supplied by Xiaohong Shi.
rBUNGceGFPdelNSs	rBUNdelNSs virus with part of the Gc protein replaced with GFP. Generated in this study.
rBUNMNSmeGFP	BUNV with part of the NSm protein replaced with GFP. Supplied by Xiaohong Shi.
rBUNM-NSm-EGFPDelNSs	rBUNdelNSs with part of the NSm protein replaced with GFP. Supplied by Xiaohong Shi.
Guaroa (GROV)	Orthobunyavirus isolated in Colombia. Supplied by R.M.Elliott.
La Crosse (LACV)	Naturally occurring Orthobunyavirus. Supplied by R.M.Elliott.
La Crosse del NSs (LACdelNSs)	LACV with the S segment encoded NSs protein deleted. Supplied by R.M.Elliott.

Table 2.4: Cell lines and their maintenance

Cell line	Description	Maintenance	Selection	Reference
2FTGH	Human diploid fibroblast cells	DMEM + 10% (v/v) FBS	N/A	(Pellegrini *et al.*, 1989)
2FTGH/PIV5/V	2FTGH cells that express the V protein of PIV5 w3	DMEM + 10% (v/v) FBS	2 µg/ml blasticidin for PIV5/V protein expression	(Andrejeva *et al.*, 2002)

Cell line	Description	Maintenance	Selection	Reference
A549	Human epithelial cells from a human lung carcinoma	DMEM + 10% (v/v) FBS	N/A	ECACC
A549/PIV5/V (w3)	A549 cells that express the V protein of PIV5 w3	DMEM + 10% (v/v) FBS	2 µg/ml puromycin for PIV5/V protein expression	(Andrejeva *et al.*, 2002; Hilton *et al.*, 2006)
A549/BVDV/NPro	A549 cells that express the BVDV/Npro protein	DMEM + 10% (v/v) FBS	2 µg/ml puromycin for BVDV/NPro protein expression	(Hale *et al.*, 2009; Hilton *et al.*, 2006)
A549shPKR	A549 cells that express shRNA that knocks down PKR expression	DMEM + 10% (v/v) FBS	2 µg/ml puromycin for shPKR expression	Prof R Randall, University of St Andrews, UK
BHK-21 clone 13	Baby hamster kidney cells	GMEM + 10% (v/v) NCS	N/A	(Macpherson & Stoker, 1962)
BSR-T7/5	BHK-21 clone 13 cells that have been stably transfected with the T7 RNA polymerase gene	GMEM + 10% (v/v) FBS	1 mg/ml G418-SO_4	(Buchholz *et al.*, 1999)
HEK 293 ISG *	Human embryo kidney epithelial cells that express an ISG	DMEM + 10% (v/v) FBS	250 µg/ml hygromycin, 5 µg/ml blasticidin, 1 µg/ml tetracycline for ISG expression	(Jiang *et al.*, 2008)
HEp2	Human cervix carcinoma cells	DMEM + 10% (v/v) FBS	N/A	ECACC
HEp2/PIV5/V	Human cervix carcinoma cells that express the V protein of PIV5 w3	DMEM + 10% (v/v) FBS	2 µg/ml puromycin for PIV5/V protein expression	(Andrejeva *et al.*, 2002; Young *et al.*, 2003)
MA104	Epithelial African green monkey foetal kidney cells	DMEM + 10% (v/v) FBS	N/A	ECACC
MA104/PIV5/V	MA104 cells that express the V protein of PIV5 w3	DMEM + 10% (v/v) FBS	2 µg/ml puromycin for PIV5/V protein expression	Prof R Randall, University of St Andrews, UK
P2.1	Derived from U4C cells and are deficient in dsRNA signalling	DMEM + 10% (v/v) FBS	N/A	(Leaman *et al.*, 1998)
U4C	Derived from 2FTGH cells	DMEM + 10% (v/v) FBS	N/A	(Kohlhuber *et al.*, 1997)

Cell line	Description	Maintenance	Selection	Reference
	and are unresponsive to all IFN			
Vero	Fibroblast-like African green monkey kidney cells	DMEM + 10% (v/v) FBS	N/A	ATCC No. CRL-1586

*These cells were used to make 29 ISG inducible cell lines, which are listed in the reference.

Table 2.5: Plasmids

Plasmid	Description	Manufacturer
pT7ribo	Bacteriophage T7 promoter followed by Stu I and Sma I restriction enzymes and the hepatitis δ ribozyme sequence	(Dunn *et al.*, 1995)
pT7riboBUNL(+)	Contains the full BUNV L sequence in the positive sense allowing expression of anti-genomic L	(Bridgen & Elliott, 1996)
pT7riboBUNL(-)	Contains the full BUNV L sequence in the negative sense allowing expression of anti-genomic L	Anice Lowen
pT7riboBUNM(+)	Contains the full BUNV M sequence in the positive sense allowing expression of anti-genomic M	(Bridgen & Elliott, 1996)
pT7riboBUNM(-)	Contains the full BUNV M sequence in the negative sense allowing expression of anti-genomic M	Anice Lowen
pT7riboBUNS(+)	Contains the full BUNV S sequence in the positive sense allowing expression of anti-genomic S	(Bridgen & Elliott, 1996)
pT7riboBUNS(-)	Contains the full BUNV S sequence in the negative sense allowing expression of anti-genomic S	Anice Lowen
pT7riboBUNN	Contains the full BUNV S sequence but only encodes the N ORF	(Bridgen & Elliott, 1996)
TVT7R-BUNM-Δ7-E	The glycoprotein precursor, in pT7riboBUNM(+), residues 501 to 826 were replaced with eGFP	Xiaohong Shi

Table 2.6: Enzymes

Restriction enzymes	Description	Manufacturer
BamHI	G▼GATC C C CTAG▲G	Promega
ClaI	AT▼CG AT TA GC▲TA	Promega
EcoRI	G▼AATT C C TTAA▲G	Promega
HpaI	GTT▼AAC CAA▲TTG	Promega
NcoI	C▼CATG G G GTAC▲C	Promega
PmeI	GTTT▼AAAC CAAA▲TTTG	NEB
StuI	AGG▼CCT TCC▲GGA	Promega
XmnI	GAANN▼NNT TC CT TNN▲NNAAG	Promega
Other Enzymes		
Benzonase® Nuclease	Endonuclease that attacks and degrades all forms of DNA and RNA	Novagen
RQ1 RNase-Free DNase	Endonuclease that degrades DNA	Promega
RNasin	ribonuclease inhibitor	Promega
T7 RNA polymerase	RNA polymerase	Promega

Bacterial strains

E.coli DH5α: Φ80d lacZ ΔM15, recA1, endA1, gyrA96, thi-1, hsdR17 (r_k-, m_k+), supE44, relA1, deoR, Δ(lacZYA-argF) U169, phoA.

JM109: endA1, recA1, gyrA96, thi-1, hsdR17 (r_k-, m_k+), relA1, supE44, Δ(lac-proAB), [F', traD36, proAB, lac/^{q}ZΔM15].

Bacterial culture

- LB agar: L-broth plus 1.5% (w/v) agar
- L-broth (LB): 10 NaCl, 10 g bactopeptone, 5 g yeast extract per litre
- Z-Competent™ cells (Zymo Research): generated as per the manufacturer's instructions

Cell and virus culture

- Overlay: 50% (v/v) 2x MEM (supplemented with FBS (10%)), 50% (v/v) 1.2% HAS agarose (Park Scientific ltd)
- Neutral red: 0.06% (w/v) in PBS
- Giemsa's stain: 10% (v/v) Giemsa's stain in dH_2O
- Fixing buffer: 4% (v/v) formaldehyde in PBS

Transfection reagent

Lipofectamine™ 2000 (Invitrogen)

Table 2.7: Media

Media	Manufacturer
Dulbeccos modified Eagle's medium (DMEM)	Gibco BRL
DMEM without methionine	Gibco BRL
Glasgow modified Eagle's medium (GMEM)	Gibco BRL
Foetal bovine serum (FBS)	Lonza
2x Modified Eagle's medium (MEM)	Gibco BRL
Newborn calf serum (NCS)	PAA
Opti-MEM®	Invitrogen
Tetracycline free FBS	Invitrogen
Tryptose phosphate buffer	Gibco BRL

Immunofluorescence

- 4% Paraformaldehyde fixing buffer
- Permeabilisation buffer: 0.1% (v/v) Triton X-100 in PBS
- Mowiol 4-88
- Phosphate buffered saline (PBS): 170 mM NaCl, 3.4 mM KCl, 10 mM Na_2HPO_4 1.8 mM KH_2PO_4, pH 7.12-7.3, 0.68 mM $CaCl_2$, 0.49 mM $MgCl_2$
- 3x PBS: Mix A and B: A. 72 ml of 30 mM $NaHPO_4$/ 390 mM NaCl
  B. 28 ml of 30 mM NaH_2PO_4/ 390 mM NaCl
- PBS 2%: PBS supplemented with 2% FBS

Protein analysis

In vitro protein labelling, polyacrylamide gel electrophoresis (PAGE) and Western blotting

- 0.5% (w/v) Bromophenol blue
- 2x protein dissociation mix: 12.5% (v/v) SGB, 2% (v/v) SDS, 10% (v/v) β- mercaptoethanol, 20% (v/v) glycerol, 0.02% (v/v) bromophenol blue, 33.5% (v/v) dH_2O
- 10x Tris-glycine running buffer: 2.4 M Tris, 1.9 M glycine
- Acrylamide/bis-acrylamide: 30% (w/v) acrylamide, 0.8% bis-acrylamide 37.5:1 (BioRad)
- 10% (w/v) Ammonium persulphate (APS) (BioRad)
- Blocking buffer: 5% skimmed milk powder (Tesco), 0.1% Tween-20 in PBS
- Chemiluminescent substrate: SuperSignal West Pico Chemiluminescent Substrate (Pierce)

- 25x Complete protease inhibitor (Roche): 1 tablet in 2 ml dH_2O
- Fixing buffer: 20% (v/v) acetic acid, 20% (v/v) methanol, 60% (v/v) dH_2O
- Magic mark XP protein ladder (Invitrogen)
- Transfer buffer: 10% (v/v) methanol, 10% (v/v) 20x NU-PAGE transfer buffer
- Phosphate buffered saline (PBS): 170 mM NaCl, 3.4 mM KCl, 10 mM Na_2HPO_4 1.8 mM KH_2PO_4, pH 7.12-7.3, 0.68 mM $CaCl_2$, 0.49 mM $MgCl_2$
- PBS-Tween: 0.1% Tween-20 in PBS
- RIPA buffer: 5 mM EDTA, 300 mM NaCl, 50 mM Tris pH 7.4, 1% (v/v) Triton X-100
- RIPA wash buffer: 5 mM EDTA, 300 mM NaCl, 50 mM Tris pH 7.4, 0.1% (v/v) Triton X-100
- Resolving gel buffer (RGB): 0.4% (w/v) SDS, 1.5 M Tris, pH 8.9
- 10% (w/v) Sodium dodecylsulphate (SDS)
- Stacking gel buffer (SGB): 0.4% (w/v) SDS, 0.5 M Tris, pH 6.7
- TEMED (N, N, N', N' tetremethylethylenediamine)
- 1.5 M Tris pH 8.9: 181.71 g Trizma Base, 900 ml dH_2O, 21 ml HCl, pH adjusted to 8.9 and volume made up to 1L with dH_2O
- 0.5 M Tris pH 6.7: 60.57 g Trizma Base, 900 ml dH_2O, 34 ml HCl, pH adjusted to 6.7 and volume made up to 1L with dH_2O

Radiochemical

[^{35}S]-methionine (10 µCi/µl) was purchased from (Amersham Pharmacia Biotech)

RNA analysis

Northern blotting and RNA preparation

- 20x SSC: 3 M NaCl, 0.3 M sodium citrate, pH 7.0
- 50% formamide hybridisation buffer: 50% deionised formamide (Ambion), 5x SSC, 0.1% (w/v) n-lauroyl-sarcosine, 0.02% (w/v) SDS, 2% (v/v) blocking buffer
- Agarose electrophoresis grade
- Blocking buffer: 10x blocking powder (Roche) diluted in maleic acid buffer
- Detection buffer: 0.1 M Tris, 0.1 M NaCl, pH 9.5
- Ethidium bromide (Promega)
- RNA loading buffer: 50 mM Tris-HCl, pH 7.6, 0.25% bromophenol blue, 60% glycerol

- Maleic acid buffer: 0.1 M maleic acid, 0.15 M NaCl, ph 7.5
- Sodium dodecylsulphate (SDS): 10% (w/v) in dH_2O
- 10x Tris-acetate-EDTA (TAE) buffer: 400 mM Tris-acetate, 10 mM EDTA
- TRIzol® Reagent (Invitrogen)
- Washing buffer: 0.1 M maleic acid, 0.15 M NaCl, ph 7.5, 0.3% (v/v) Tween-20

Methods

Cell and virus culture

Cell Culture

Mammalian cell lines were maintained in medium (T75) 75cm^2 and or large (T175) 175cm^2 tissue culture flasks and were passaged regularly (when confluent). All medium was removed, and the monolayer was washed with 5 ml (T75) or 10 ml (T175) of PBS and discarded. Next, 3 ml (T75) or 5 ml (T175) of Trypsin was washed over the monolayer and discarded, leaving 1 ml in the flask, which was incubated at 37℃ for 5 minutes. Cells were re-suspended in 5 ml (T75) or 10 ml (T175) of growth medium. Further flasks were seeded using 1 ml of this cell stock into 10 ml (T75) or 20 ml (T175) of growth medium supplemented with 10% FBS and when required, selection antibiotics (see table 1). HEK293 ISG cells were constantly maintained in growth medium containing hygromycin and blasticidin, and for induction of the ISG tetracycline was added for 48 hours.

Cells treated with IFNs were either treated with Roferon recombinant human IFNα-2a (Roche Diagnostics) or Recombinant Human IFNβ 1a mammalian (Hu IFN-β 1a) (PBL Interferon Source) at a concentration of 10^3 U/ml unless otherwise stated.

Cell freezing

Cells were passaged as above only after re-suspension the cells were centrifuged at 3000 rpm for 5 minutes and the supernatant was discarded. The cells were re-suspended in 3 ml (T75) or 6 ml (T175) of growth medium containing 10% DMSO and divided into 1 ml aliquots and stored overnight at -80℃, after which they were transferred to storage in liquid nitrogen.

Cell resuscitation

The vial of cells from the liquid nitrogen store was thawed in a 45℃ water bath and then transferred to a 15 ml falcon tube containing 10 ml of growth medium and centrifuged at 3000 rpm for 5 minutes. The supernatant was removed and

the cell pellet was re-suspended in 5 ml of growth medium and transferred to a small (T25) 25cm^2 tissue culture flask and incubated at 37°C until confluent.

BUNV rescue from cloned DNA

Infectious recombinant BUNV rescue was carried out based on Lowen *et al.* (2004). In a 35 mm diameter dish 1x10^6 BSR-T7/5 cells were transfected with 1.0 µg each of pT7riboBUNL (+), pT7riboBUNM (+) and pT7riboBUNS (+) as stated below (Transfection). Recombinant viruses were rescued by replacing the relative pT7riboBUN plasmid with the plasmid containing the required mutation. The dish was then incubated at 33°C for several days until significant cytopathic effect (CPE) was observed, at which point the culture medium was collected and clarified by centrifugation at 1700 rpm for 3 mins. One hundred microlitres was used for virus infection and elite stock preparation as below (Virus infection, Elite stock preparation/plaque purification**).**

Virus infection

The growth medium was removed and replaced by the inoculum (see below for volume) and returned for incubation at 37°C for 60 minutes with rocking every 10 minutes. Next, the inoculum was removed and replaced with either growth medium or overlay. Unless otherwise stated the volume of inoculum added was as follows:

100 µl per 24-well plate well
200 µl per 35 mm well
400 µl per T25 flask
500 µl per 60 mm well

Virus amplification

One hundred microlitres of elite stock was added to 5 ml of growth medium and transferred to a 90% confluent T175 flask of BHK, Vero or A549/PIV5/V (w3) cells. The flask was incubated at 37°C for 60 minutes with rocking every 10 minutes. Then, 15 ml of growth medium was added and the flask placed in incubation at 33°C. Approximately three days post infection (once 70% CPE or GFP was observed) the growth medium was removed to a 50 ml falcon tube and centrifuged at 3000 rpm to remove the cell debris. The supernatant was divided into 0.5 ml and 1 ml aliquots and stored at -80°C until use.

Titration by plaque assay

One hundred microlitres of virus was serially diluted from 10^{-1} to 10^{-6} in 900 µl PBS 2%. A 35 mm well of confluent cells was inoculated with 200 µl of each dilution and incubated at 37°C for 60 minutes with rocking every 10 minutes.

Next, the inoculum was aspirated and 2 ml of overlay (see below) was added and left to set, and then placed in an incubator at 37°C for four days.

To make the overlay; 25 ml aliquots of 2x MEM supplemented with 4% FBS were warmed to 45°C in a water bath. Sterile 100 ml aliquots of 1.2% HSA agarose were melted in the microwave and then placed in a 55°C water bath for the duration of infection. Next, immediately prior to use, 25 ml agarose was added to 25 ml growth medium and inverted 5 times.

After incubation the cells were fixed by the addition of 2 ml of 4% formaldehyde for 2 to 24 hours. Then, the fixation solution was discarded and the overlay removed by squirting PBS onto the side of the well. One ml of Giemsa's stain, diluted 1/10 with water, was added for 10 minutes and then washed off with tap water and the plates were inverted and left to dry. Plaques were counted, and used to calculate titre in pfu/ml by dividing the number of plaques (n) by the dilution factor (d) multiplied by the inoculum volume (V) in ml:

$$pfu/ml = n/dV$$

Elite stock preparation/plaque purification

As for titration by plaque assay except that after four days incubation at 37°C, 1 ml of 0.6% neutral red was added to each well for 2 hours and then removed. Up to 4 hours later live cells had taken up the neutral red and plaques were visible as clear spots. Using a 200 µl pipette a plaque was picked with an overlay plug and added to 1 ml of growth medium and vortexed to release the virions from the overlay. Next, 500 µl of the plaque pick solution was used to inoculate a T25 flask of confluent cells for 60 minutes at 37°C, with rocking every 10 minutes. Then, 4.5 ml growth medium was added and the flask incubated at 33°C until good CPE was observed. The growth medium was then centrifuged at 3000 rpm to remove the cell debris and the supernatant was divided into 200 µl aliquots and stored at -80°C.

Virus purification by ultracentrifugation

As for virus amplification except that after clarification the supernatant was carefully added to a Beckman tube already containing 18 ml of 20% sucrose (sucrose cushion) and weighed to ensure balance. These were then centrifuged at 26,000 rpm for 120 minutes in a Beckman Coulter centrifuge using the SW28 rotor. Next, the supernatant was aspirated and the virus pellet resuspended in TRIzol for RNA extraction.

Transfection

Transfection was carried out using Lipofectamine™ 2000. Using a previously seeded six-well plate; initially the growth medium was removed and replaced

with 1 ml of fresh medium. DNA (µg) and liposomes (µl) were prepared using a 1:3 ratio. The liposomes were added to 50 µl Opti-MEM® per reaction and left to incubate at room temperature for five mins. The plasmid DNA was added to 50 µl Opti-MEM® per reaction and mixed. The liposome mix was added drop-wise to the DNA mix and gently pipetted up and down five times, and then incubated at room temperature for 20 mins. The DNA-liposome complex (100 µl per reaction/well) was gently added to the well and gently rocked from side to side. The cells were then incubated at 33℃ for five hours and 1 ml of fresh growth medium was added.

Transformation

E.coli transformations were done using E.coli previously prepared for transformation using the Z-Competent™ cell kit as per the instruction manual. Fifty microlitres of E.coli sample was thawed and incubated at room temperature for 30 mins and then 0.5 µg plasmid DNA was added and mixed by flicking 5 times and further incubated on ice for 30 mins. The E.coli were then pipetted onto an ampicillin agar plate and streaked using 5 glass beads and incubated overnight at 37℃.

Plasmid preparation

Plasmid preparation was done using the Qiagen midi- and maxi-prep kits as per the manufacturer's instructions. Midi-preps were started with 100 ml and maxi-preps were started with 300 ml overnight culture grown in LB broth containing 50 µg/ml ampicillin.

Immunofluorescence

Mowiol Mounting Medium

Whilst continually stirring: 4.8 g of Mowiol 4-88 was added to 12 g of glycerol and mixed. This was followed by the addition of 12 ml of ddH_2O and stirring for several hours at RT. Next, 24 ml of 0.2 M Tris-HCl (pH 8.5) was added and stirred, with occasional heating for 10 mins in a 55℃ water bath, until the Mowiol was dissolved. Once dissolved the solution was clarified by centrifugation at 5000 g for 15 mins and the supernatant aspirated and the aliquots stored at -20℃.

4% Paraformaldehyde

One gram of paraformaldehyde was dissolved in 16ml H_2O and 100µl 1N NaOH at 55℃ and stirred occasionally. Once dissolved the pH was adjusted to 7.2 by the addition of dilute HCl and then 8 ml of 3x PBS was added and mixed.

Slide preparation

Coverslips were placed in 24-well plates and seeded with cells. After treatments and or infections (see virus infections above) the coverslips were ready for fixing and mounting onto slides.

For fixing, the growth medium was removed and replaced with 1 ml of 4% paraformaldehyde for 30 mins. The paraformaldehyde was then carefully aspirated and the coverslips were washed 3 times with PBS 2%. One millilitre of permeabilisation solution was added and left at room temperature for 30 mins after which it was aspirated and the coverslip washed 3 times with PBS 2%. Thirty microlitres of the primary antibody stain was then dropped onto the coverslip and left at 4℃ for 60 mins after which the coverslip was washed 3 times with PBS 2%. Thirty microlitres of the secondary antibody stain was dropped on to the coverslip and left at 4℃ for 60 mins after which the coverslip was washed 3 times with PBS 2%. The coverslip was then washed 3 times in dH_2O and placed on 10 µl Mowiol on a glass slide, labelled and left to dry at 4℃. Slides were then visualised using a Zeiss LSM 5 Pascal confocal microscope.

Live cell imaging was carried out in a six-well plate. Cells were infected (see virus infections) and then visualised at the required time points using an AMG Evos microscope.

Protein analysis

In vitro protein labelling, PAGE and Western blotting

SDS-PAG preparation

The required percentage resolving gel solution was prepared (Table 2.8) and 6 ml pipetted into a Novex® empty cassette and isopropanol was layered on top to produce a smooth surface. Once the resolving gel had polymerised, the isopropanol was removed and replaced with 3 ml of stacking gel (Table 2.9) and a comb (10 or 15 well) was inserted and the stacking gel was left to polymerise.

Table 2.8: Resolving gel

Reagents	5%	8%	10%	12.5%	15%	18%
30% Acrylamide	2 ml	3.2 ml	4 ml	5 ml	6 ml	7.2 ml
RGB	3 ml	3 ml	3 ml	3 ml	3 ml	3 ml
H_2O	7 ml	5.8 ml	5 ml	4 ml	3 ml	1.8 ml
10% APS	100 µl	100 µl	100 µl	100 µl	100 µl	100 µl
TEMED	10 µl	10 µl	10 µl	10 µl	10 µl	10 µl

Table 2.9: Stacking gel

Reagents	3 gels	6 gels	9 gels
30% Acrylamide	1.0 ml	2.0 ml	3.0 ml
SGB	1.5 ml	3.0 ml	4.5 ml
H_2O	3.5 ml	7.0 ml	10.5 ml
10% APS	55 µl	110 µl	165 µl
TEMED	10 µl	20 µl	30 µl
0.5% Bromophenol blue	30 µl	30 µl	30 µl

Metabolic labelling of BUNV proteins

Cells at 90% confluency in a 35 mm diameter dish were infected as above and returned to the incubator at 37°C. Two hours prior to the desired time-point the cells were starved of methionine by replacing the culture medium with 1 ml of DMEM without methionine (met-) and incubating at 37°C for 60 minutes. Next, the met- DMEM was replaced with 500 µl of met- DMEM containing 50 µCi [^{35}S]-methionine and the cells were incubated at 37°C for 60 minutes with rocking every 10 minutes.

To lyse the cells the labelling medium was aspirated and the cells were washed once with ice cold PBS and 150 µl of RIPA buffer containing 1/25 Complete was added. The plate was rocked several times and incubated at 4°C for 10 minutes. The cell lysate was transferred to a 1.5 ml microcentrifuge tube and vortexed for 5 seconds and returned to 4°C for 10 minutes. Next, the lysate was centrifuged at 16,000 g for 10 minutes, and then the supernatant was transferred to a fresh microcentrifuge tube, and stored at -20°C until use.

Protein expression

Fifty microlitres of lysate was added to 50 µl of 2x dissociation mix and mixed by pipetting 5 times. Five microlitres of pre-stained protein ladder (Fermentas) or 10 µl of sample was loaded into each well of a 12.5% acrylamide mini-gel. The samples were electrophoresed at 180 V for 50 to 60 minutes in a 1x Tris-glycine running buffer, in the Nu-PAGE tank apparatus (Invitrogen). Gels were then fixed, dried, exposed and developed (see below).

Immunoprecipitation

Antibody conjugated protein A Sepharose beads

To prepare 50% protein A Sepharose beads, 100 mg were added to 800 µl of RIPA buffer, mixed and incubated for 30 mins at room temperature. Then, 30 µl of the 50% protein A Sepharose beads were transferred to a fresh microcentrifuge tube and combined with 1 µl of anti-BUN antibody and 0.5 ml of ice cold PBS and then put on a rotating wheel for 16 hours at 4°C. The microcentrifuge tube was then centrifuged at 16,000 g for 1 min and then the

supernatant was carefully removed and discarded. The antibody conjugated beads were washed three times using 900 µl ice cold RIPA wash buffer and finally once with RIPA buffer.

Immunoprecipitation

Fifty microlitres of lysate was added to the microcentrifuge tube containing the 30 µl of protein A Sepharose beads from the previous step along with 220 µl ice cold PBS and mixed. The microcentrifuge tube was then put on a rotating wheel for 16 hours at 4°C, after which the tube was centrifuged at 16,000 g for 1 min and then the supernatant was carefully removed and discarded. The beads were then washed 4 times with 900 µl of ice cold RIPA wash buffer. One final wash with ice cold PBS was followed with carefully removing the supernatant completely, and discarding it. The beads were resuspended in 30 µl of Dissociation mix and boiled for three mins and then analysed.

Gel Fixing and drying

The stacking gel was cut off and the resolving gel transferred to a plastic box containing 100 ml of fixing buffer, and placed on a rocker for 30 minutes. The gel was then placed on a piece of plastic with a sheet of Whatman on top and dried for 60 mins at 80°C and then exposed to x-ray film or phosphorimager screen overnight, and then developed.

Western blotting

Cells at 90% confluency in a 35 mm diameter dish were infected as above and returned to the incubator at 37°C until the required time for lysis. To lyse the cells the medium was aspirated and the cells were washed once with ice cold PBS and 150 µl of RIPA buffer containing 1/25 Complete was added. The plate was rocked several times and incubated at 4°C for 10 minutes. The cell lysate was transferred to a 1.5 ml microcentrifuge tube and vortexed for 5 seconds and returned to 4°C for 10 minutes. Next, the lysate was centrifuged at 16,000 g for 10 minutes, and then the supernatant was transferred to a fresh microcentrifuge tube, and stored at -20°C until use.

Fifty microlitres of lysate was added to 50 µl of 2x dissociation mix and mixed by pipetting 5 times. Five microlitres of pre-stained protein ladder (Fermentas) or 1 µl of MagicMark XP or 10 µl of sample was loaded per well of a 12.5% acrylamide mini-gel. The samples were electrophoresed at 180 V for 50 to 60 minutes in a 1x Tris-glycine running buffer, in the Nu-PAGE tank apparatus.

Semi-dry transfer

The nitrocellulose membrane and two pieces of blotting pad (Roche) were equilibrated in transfer buffer for 5 mins. Then, using a Trans-Blot® SD Semi-

Dry Electrophoretic Transfer Cell (BioRad), one piece of blotting pad was placed on the platinum anode and then the membrane on top. Having removed the stacking gel the gel was placed on the membrane and a second piece of blotting pad placed on top and rolled with a 10 ml pipette to remove air bubbles. The cathode was then carefully placed on the stack and secured with the latches followed by the safety lid. The transfer was conducted at 20 V for 20 mins.

Detection

The membrane was rinsed three times in PBS-Tween and incubated in blocking buffer for 60 mins, then rinsed three times in PBS-Tween and washed for five mins in PBS-Tween. The three rinse and wash process was repeated three times after which the membrane was incubated with the primary antibody in blocking buffer (Table 2.2). Next, the membrane was rinsed and washed three times as above and incubated with the secondary antibody in blocking buffer for 60 mins. After the secondary incubation the membrane was rinsed and washed three times as above followed by treatment with chemiluminescent substrate for five mins and placed in a cassette with a piece of plastic on top and exposed to x-ray film for 1 s to overnight as required, and developed.

RNA analysis

RNA isolation

Total cell RNA was extracted from a cell cultured monolayer in a T25 flask by removing the growth medium and adding 1 ml of TRIzol. After vigorous shaking and pipetting the resuspended monolayer was transferred to a 1.5 ml microcentrifuge tube and incubated at room temperature for five mins. Subsequently, 200 µl of chloroform was added to the cell lysate, vortexed for 15 s and incubated at room temperature for three mins. Next, the lysate was centrifuged for 15 mins at 4°C and 12,000 g, after which the upper aqueous layer was transferred to a fresh microcentrifuge tube and 0.5 ml isopropanol was added, mixed, and incubated at room temperature for 15 mins to allow precipitation of the RNA. The RNA was then pelleted by centrifugation at 4°C and 12,000 g for 20 mins after which the supernatant was removed and replaced with 1 ml of 75% ethanol. If the RNA was not to be used immediately it was stored at -80°C and then, or otherwise, it was centrifuged for 10 mins at 4°C and 7,500 g. Finally the ethanol was aspirated and the pellet allowed to air dry and subsequently resuspended in RNase-Free H_2O. The concentration and quality (260/280 ratio) was measured using the NanoDrop™ 2000 (Thermo Scientific).

Northern blotting

To make a 1.2% agarose gel, 1.2 g agarose was added to 100 ml of autoclaved water and dissolved by heating in a microwave oven, and then cooled to 55℃ in a water bath. This was poured into a gel casting tray with a comb to produce a fourteen well slab, 11x14x0.6 cm. Once solidified, 1 L of 1x TAE running buffer was added to the gel tank.

Preparation of RNA samples

Ten µg of total cellular RNA was diluted in 20 µl of deionised formamide, 3 µl of 10x loading dye, 1 µl of ethidium bromide and made up to 32 µl with autoclaved water and mixed. The samples were heated to 65℃ for 5 minutes and then rapidly cooled on ice and briefly centrifuged to collect condensation. Thirty microlitres of sample was loaded into a well, and the gel was run at 75 V for 3-5 hours.

Capillary transfer

The gel was washed for 5 minutes and a photograph taken on a UV transilluminator (UVP) to check the rRNA bands. The gel casting tray was inverted and placed in a shallow tray, which was filled up with 10x SSC. Eight centimetres of blotting pad (Roche) was placed on top of the casting tray, followed by 3 pieces of 3MM Whatman paper soaked in 10x SSC which was then rolled with a 10 ml pipette. A piece of positively charged nylon membrane (Sigma), cut to the size of the gel, was soaked in 10x SSC and placed on top of the 3 MM Whatman paper. The gel was carefully placed onto the nylon membrane and rolled using a 10 ml pipette to remove air bubbles. Three more pieces of 3MM Whatman paper were soaked in 10x SSC and placed on top, and then two pieces of 3MM Whatman paper cut to 40 cm long were soaked in 10x SSC and draped over the whole blotting sandwich to act as a wick. A 1 kg weight was placed on top and the tray was covered with cling film to minimise evaporation, and the whole apparatus was left overnight.

U.V crosslinking

Once blotting was complete, the top right hand corner of the membrane was clipped for orientation, and the membrane was washed in 2x SSC for 5 minutes, and hung up to dry. When dry, the membrane was placed face down in the transilluminator and irradiated for 3 minutes at 305 nm and RNA transfer was confirmed by visualising the rRNA bands. The membrane was then stored in a plastic bag at 4℃ until use.

Hybridisation using DIG labelled probes

The membrane was placed in a cylindrical hybridisation bottle with 10 ml of pre-warmed to 68℃ 50% formamide hybridisation buffer. The membrane was pre-

hybridised at 68°C for 30 minutes in a hybridisation oven with constant rotation. The DIG labelled RNA probes were made up to 30 µl with autoclaved water and denatured by boiling for 5 minutes, and then cooled rapidly on ice. The probes were added to 10 ml of prewarmed to 68°C 50% formamide hybridisation buffer and this was used to replace the pre-hybridisation buffer. Hybridisation was carried out overnight at 68°C under constant rotation.

Washes

The membrane was washed under:

Low stringency conditions: 2x10 minutes in 25 ml 2x SSC, 0.1% SDS at RT

High stringency conditions: 2x25 minutes in 25 ml 0.1x SSC, 0.1% SDS at 68°C

Detection

Detection was largely based on the DIG Northern Starter kit (Roche) instruction manual and was optimised as follows:

5 minutes in 25 ml washing buffer
60 minutes in 10 ml 1x blocking solution
60 minutes in 10 ml 1x antibody solution
2x30 minutes in 25 ml washing buffer
5 minutes in 25 ml detection buffer

The membrane was placed on a piece of translucent plastic and 1 ml of CDP Star (Roche) was added drop-wise and the plastic folded over to give a uniform film of CDP Star over the membrane, and left for 5 minutes at room temperature. The excess liquid was squeezed out and the membrane sealed inside the plastic. The membrane was then exposed to x-ray film for 1 second to overnight as required, and developed.

Generation of DIG labelled probes

The plasmid containing the desired probe sequence downstream of a T7 promoter was linearised approximately 1 kb downstream of the T7 promoter by restriction endonuclease digestion. More efficient in-vitro transcription is achieved with a 5' overhang at the cleavage site (Roche), thus enzymes that produce a 5' overhang were chosen over those that produce a 3' overhang or blunt end. The digested DNA was then run on an agarose gel, the desired band excised and purified using the wizard PCR gel purification kit (Promega).

Restriction endonuclease digestion

One microgram of plasmid DNA was added with 1 µl 10x RE buffer, 5-10 units of RE and made up to 10 µl with dH_2O in a microcentrifuge tube and mixed gently by pipetting. The mixture was centrifuged for a few seconds and incubated at the optimum temperature for 2 hours. The mixture was centrifuged again for a few seconds and 2 µl of 6x loading buffer was added and mixed before being electrophoresed on a TAE 1% agarose gel containing ethidium bromide for ~60 mins.

In-vitro transcription

The following was mixed in an RNase free microcentrifuge tube:

1 µg DNA in 20 µl dH_2O
8 µl 5x transcription buffer (Promega)
4 µl 100 mM DTT (Promega)
4 µl DIG labelling mix (Roche)
80 U T7 RNA polymerase (Promega)

The reaction mixture was incubated at 37℃ for 2 hours. Two units of RQ1 RNase-free DNase was added and the mixture incubated at 37℃ for 15 minutes, then diluted up 10 fold to 400 µl and stored at -80℃ until use.

Quantification of DIG labelled probes

Quantification of the DIG labelled probes was carried out as per the manufacturer's instructions in the DIG Northern Starter kit (Roche) manual.

3 The effect of type I IFN on Bunyamwera virus replication

Introduction

Chapter One described the IFN system and the anti-viral proteins that are upregulated *via* IFN signalling. Over the last decade, much progress has been made in studying the effects of IFNs on viruses and the mechanisms viruses use to counteract the IFN response. Infection by most viruses is known to trigger IFN production and the *Bunyaviridae* family is no exception. To this end, human-disease causing viruses from each genus have been studied in more detail in order to determine how they escape the IFN response. For example, type I IFNs have been shown to inhibit CCHFV (Andersson *et al.*, 2006), OROV, Caraparu, Guama, GROV and Tacaiuma viruses (Livonesi *et al.*, 2007), BUNV (Streitenfeld *et al.*, 2003) and several other members of the *Bunyaviridae* family. Successful replication within mammalian cells means that bunyaviruses must overcome the IFN response. The primary IFN antagonist for BUNV is the NSs protein, which blocks host transcription thereby blocking transcription of type I IFNs, and also causes host cell protein synthesis shut-off (Chapter One). Further to this, research into viral countermeasures has helped to elucidate details of the induction of the IFN response to viruses, as well as greatly improving our understanding of the molecular mechanisms of viral pathogenesis. The aim of the work described in this chapter was to investigate the IFN response to BUNV in more detail.

Plaque assays

The most direct method of detecting inhibition of virus replication in host cells is to carry out plaque assays. The plaque assays described here were carried out exactly as stated in Chapter Two; each virus was fully titrated on each cell line at 37°C. BUNV and rBUNdelNSs produce characteristic plaque phenotypes following infection of different cell lines (**Fig 3.1**, compare the top row (BUNV) to the bottom row (rBUNdelNSs) for each cell line indicated). A549 cells are a human lung carcinoma cell line with a fully functional immune response. Since BUNV is able to antagonise the innate immune response *via* the expression of NSs protein, infection of A549 cells produces large (3 mm or more in diameter) plaques (**Fig 3.1**, top row). In contrast, rBUNdelNSs is unable to express NSs protein and therefore no plaques are detected in A549 cells (**Fig 3.1**). HEp2 cells are human cervix carcinoma cells that are also IFN competent. Infection of HEp2 cells with BUNV produced small (1 mm or less in diameter) irregular shaped plaques, while infection with rBUNdelNSs produced no plaques (**Fig 3.1**). HEp2/PIV5/V cells are HEp2 cells that have been transduced to express the PIV5 V protein which targets STAT1 for degradation, thereby blocking IFN signalling. Plaque assays with HEp2/PIV5/V cells infected with either BUNV or

rBUNdelNSs produced small irregular plaques which were difficult to distinguish from uninfected cells (**Fig 3.1**). MA104 cells are African green monkey foetal kidney cells that are IFN competent, while MA104/PIV5/V cells have been

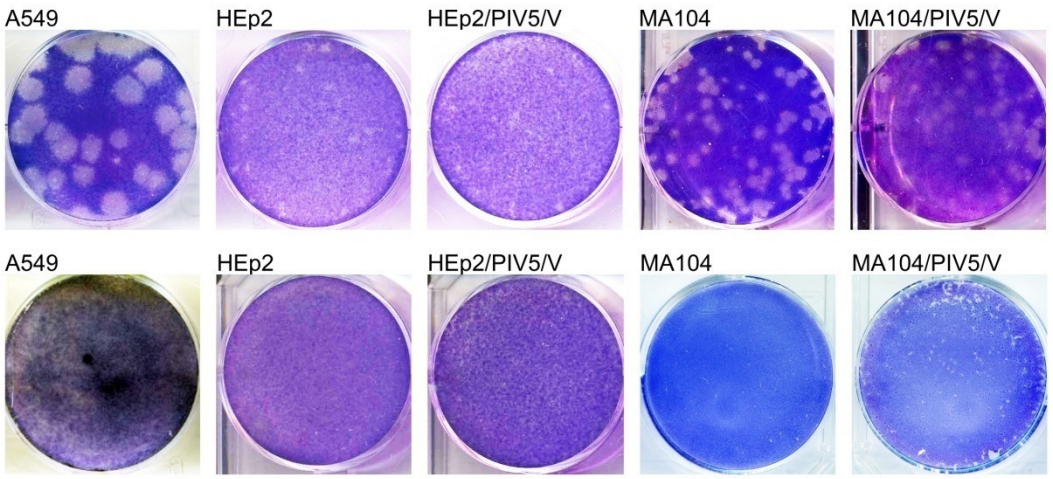

Figure 3.1: BUNV (top row) and rBUNdelNSs (bottom row) plaque phenotypes on A549, HEp2, HEp2/PIV5/V, MA104 and MA104/PIV5/V cells. Cell monolayers were infected with BUNV or rBUNdelNSs and after four days incubation at 37°C were fixed with 4% formaldehyde and stained with 10% Giemsa's solution.

transduced to express the V protein of PIV5 and thus have an attenuated IFN response. The BUNV plaques on MA104 and MA104/PIV5/V cells were medium-sized (2 mm in diameter) and rounded whereas rBUNdelNSs did not form visible plaques on MA104 cells but did form small, irregular shaped plaques on MA104/PIV5/V cells (**Fig 3.1**).

Vero cells are African green monkey kidney epithelial cells that are IFN deficient as they cannot produce type I IFNs but they do have the IFNAR and can respond to exogenous IFN. The plaques produced by BUNV on Vero cells

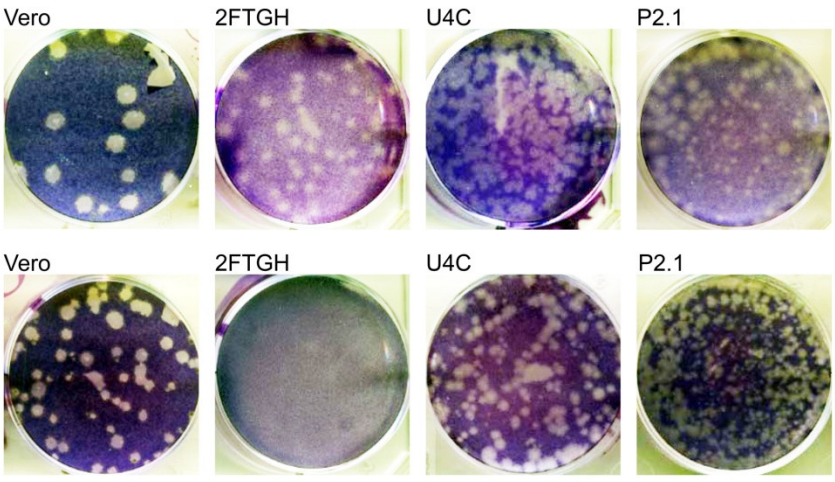

Figure 3.2 : BUNV (top row) and rBUNdelNSs (bottom row) plaque phenotypes on Vero, 2FTGH, U4C and P2.1 cells. Cell monolayers were infected with BUNV or rBUNdelNSs and after four days incubation at 37°C were fixed with 4% formaldehyde and stained with 10% Giemsa's solution.

were typically large and rounded, while those of rBUNdelNSs were of similar shape but were only medium-sized (**Fig 3.2**, compare top row (BUNV) to bottom row (rBUNdelNSs) for each cell line indicated). The 2FTGH cell line is a human fibrosarcoma cell line that is able to produce and respond to IFN. BUNV plaques on 2FTGH cells were medium-sized and round, whereas rBUNdelNSs did not produce any plaques in these cells. However, both viruses do plaque on 2FTGH/PIV5/V cells (Young *et al.*, 2003). U4C cells are derived from the 2FTGH cell line and lack JAK1 and as such are unable to respond to any IFN (Kohlhuber *et al.*, 1997). P2.1 cells are derived from U4C cells and are not only unable to respond to IFN but are also deficient in dsRNA signalling (Leaman *et al.*, 1998). Both BUNV and rBUNdelNSs produced plaques on U4C cells that were small and rounded. BUNV produced plaques on P2.1 cells that were medium-sized and rounded, whereas rBUNdelNSs plaques were small and round-shaped (**Fig 3.2**). Thus, BUNV was able to infect all cell lines whereas those with an intact IFN response (A549, HEp2, MA104 and 2FTGH) were less permissive to rBUNdelNSs infection unless they expressed the PIV5 V protein to restrict IFN signalling (see table 3.1).

Table 3.1: Summary of plaque morphology, size and titre from various mammalian cell lines infected with either BUNV or rBUNdelNSs.

Virus / Cell line	BUNV			rBUNdelNSs		
	Morphology	Size*	Titre†	Morphology	Size*	Titre†
A549	Round	Large	$1.45x10^8$	NP	-	-
HEp2	Irregular	Small	$9x10^6$	NP	-	-
HEp2/PIV5/V	Irregular	Small	$7x10^3$	Irregular	Small	UC
MA104	Round	Medium	$5x10^6$	NP	-	-
MA104/PIV5/V	Round	Medium	$5x10^6$	Irregular	Small	$4.5x10^6$
Vero	Round	Large	$8.5x10^8$	Round	Medium	$2.95x10^6$
2FTGH	Round	Medium	$2.25x10^6$	NP	-	-
U4C	Round	Small	$1.06x10^7$	Round	Small	$6.4x10^5$
P2.1	Round	Medium	$4.8x10^6$	Round	Small	$1.51x10^5$

* Large is 3 mm or greater, medium is 2 mm, small is 1 mm or less.
† Titre (from stock) is in pfu/ml.
NP denotes no plaques and UC denotes plaques were uncountable.

Growth kinetics

Plaque size and morphology is variable between different cell lines and depends on many factors, particularly the IFN response system. Furthermore, investigating the effects on growth of the virus by plaque assay titration is both sensitive and informative. Thus, cells were infected at an MOI of 0.01 pfu/cell,

incubated at 37°C and the released virus was titrated by plaque assay (**Fig 3.3**). Initially, 2FTGH cells were infected with BUNV and after 48 hours the yield of virus plateaued and the final titre was 2.37x10^7 pfu/ml, whilst rBUNdelNSs followed a similar growth pattern but the final titre was 65-fold lower at 3.62x10^5 (**Fig 3.3A**). Growth of BUNV in 2FTGH/PIV5/V cells was not as high as in the *naïve* cells, at 1.03x10^7 pfu/ml at 72 hours, however the growth of rBUNdelNSs was enhanced to 1.08x10^6 pfu/ml but was still 10-fold lower than BUNV (**Fig**

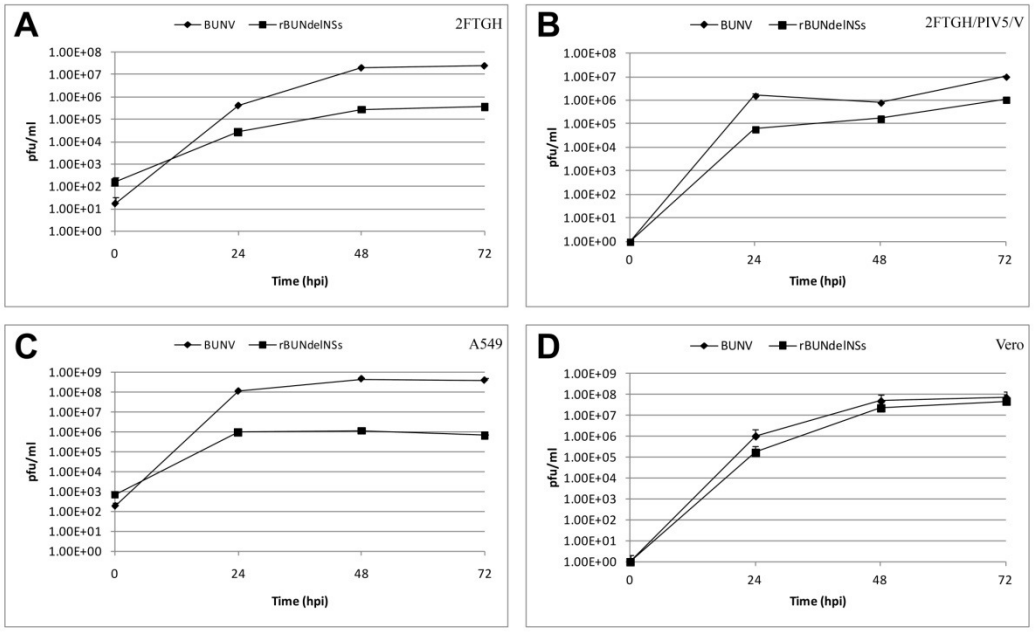

Figure 3.3 : Growth of BUNV and rBUNdelNSs in cell culture at 37°C. 2FTGH **(A)**, 2FTGH/PIV5/V **(B)**, A549 **(C)**, or Vero **(D)** cells were infected with either BUNV or rBUNdelNSs virus at an MOI of 0.01 pfu/cell. At the time points indicated virus in the cell supernatant was collected and titrated by plaque assay. Each value represents the average of triplicate experiments and the error bars show the standard deviation. hpi denotes the hours post infection.

3.3B). The growth kinetics in A549 cells for BUNV showed the virus released peaked and plateaued at 48 hours with a titre of 4.5x10^8 pfu/ml, while rBUNdelNSs was more restricted and released virus plateaued after 24 hours with the titre being over 100-fold lower than BUNV, around 1x10^6 pfu/ml (**Fig 3.3C**). Further to this, the growth kinetics observed in Vero cells showed that BUNV-infected cells produced a final titre of 7.17x10^7 and rBUNdelNSs was completely unrestricted and produced a similar titre of 4.83x10^7 (**Fig 3.3D**).

Effect of IFN concentration and treatment periods

To further investigate the effects of IFN on BUNV, Vero cells were used since they do not synthesise IFN but are able to respond to IFN.

Vero cells were treated with increasing doses of IFN at different times either pre- or post-infection, and incubated at 37°C. The viral titre was then determined at 24 hours post infection by plaque assay, and protein production in infected cells was analysed by Western blotting (**Fig 3.4**). For BUNV, IFN treatment with 0 or 10 U/ml at any time either before or after infection had no

effect on the titre of virus after 24 hours (**Fig 3.4A**). Similar results were observed at 100 and 1000 U/ml for all treatments started after 2 hours prior to infection. However, when pre-treatment began 12 hours prior to infection, a small reduction in viral titre was observed when 100 U/ml were used and a dramatic 400-fold reduction was observed when 1000 U/ml were used. Furthermore, pre-treatment of 100 and 1000 U/ml that began 24 hours prior to infection reduced the BUNV titre 6-fold and more than a 1000-fold respectively (**Fig 3.4A**).

Western blot analysis showed faint N protein bands in cells treated with 100 U/ml started at 24 and 12 hours prior to infection and also for 1000 U/ml treatment started at 2 hours prior to infection (**Fig 3.4C**, top panel). Treatment

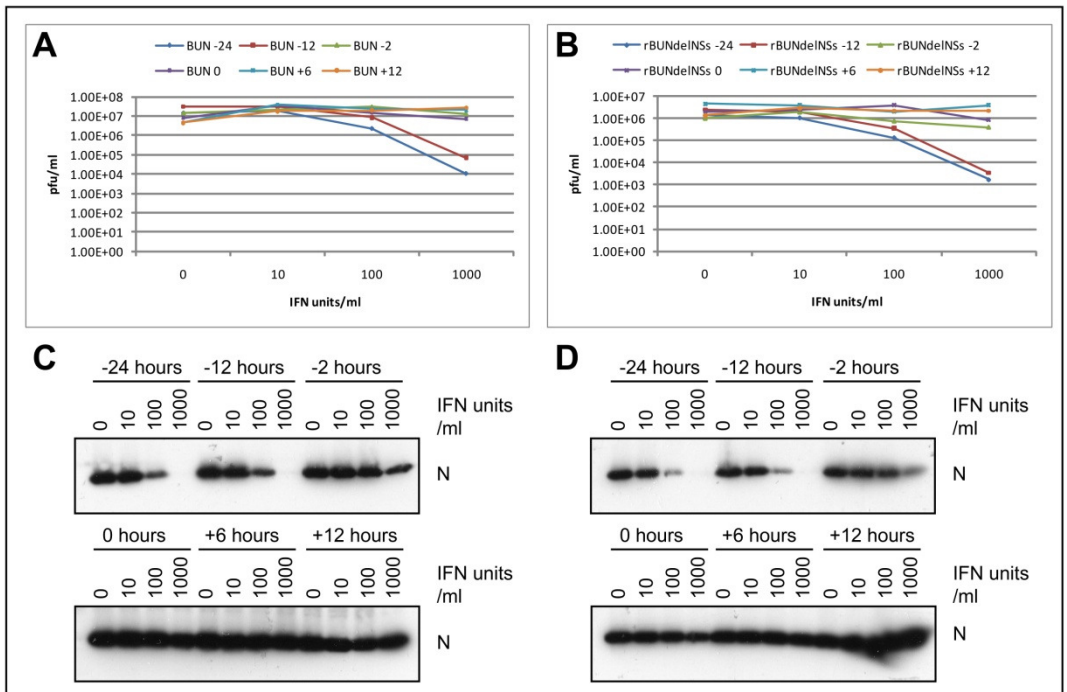

Figure 3.4 : Growth and N protein accumulation at 37°C of BUNV and rBUNdelNSs infected Vero cells treated with increasing concentrations of IFNβ and for different times. Vero cells were either mock treated (0 IFN units/ml) or treated with IFNβ either 24, 12, or 2 hours pre-infection or at the time of infection or 6 or 12 hours post-infection as indicated, and at either 10, 100 or 1000 IFN units/ml as indicated. At the time of infection cells were infected at an MOI of 1 pfu/cell. For virus growth, 24 hours post infection BUNV **(A)** or rBUNdelNSs **(B)** in the cell supernatent was collected and titrated by plaque assay. The infected monolayers were then lysed and 1/30 of the lysate was analysed by SDS-PAGE and then transferred to a nitrocellulose membrane for Western blot analysis. BUNV **(C)** or rBUNdelNSs **(D)** N protein was detected using anti-N (rabbit) antibody. IFN denotes interferon.

of 1000 U/ml that started 12 and 24 hours prior to infection completely inhibited N protein synthesis (**Fig 3.4C**, top panel), but when started at 0 hours there was a slight reduction in the amount of N protein, but treatments that started after infection showed no reduction in the amount of N protein detected (**Fig 3.4C**, bottom panel).

For rBUNdelNSs, treatments of 0 and 10 U/ml at any time point also had little effect on the viral titre after 24 hours and, like BUNV, treatment of 100 U/ml at 12 and 24 hours prior to infection showed only a small reduction in titre (**Fig**

3.4B). However, unlike BUNV, treatment that began 2 hours prior to infection also showed a small reduction in titre. As was seen with BUNV infection, treatment with 1000 U/ml substantially reduced the titre of rBUNdelNSs when the treatment was started 12 (700-fold) and 24 (~800-fold) hours prior to infection, but further reductions in titres were also observed from treatments that began 2 and 0 hours prior to infection. Additionally, as with BUNV, treatment with IFN after infection had no effect on viral titre.

Western blot analysis showed a similar pattern to BUNV but was more pronounced (**Fig 3.4D**). Treatment with 100 U/ml started 24 and 12 hours prior to infection resulted in almost no N protein (**Fig 3.4D**, top panel). Treatment with 1000 U/ml that started 24 and 12 hours before infection resulted in no detectable N protein, and less N protein was detected when started 2 hours before infection. A small reduction in the amount of N protein was observed when IFN was added at 0 hours. Post-infection treatments had no effect on the amount of N protein detected/synthesised/accumulated (**Fig 3.4D**, bottom panel).

Thus, the virus titres correlate with viral N protein production as analysed by western blotting and show that both the dose and time of IFN treatment are important variables when investigating the effects of IFN on the virus replication cycle.

To investigate the effects of both IFNα and IFNβ for their inhibitory effect on BUNV at 37℃, Vero cells were treated at various times with either or both IFNs and then infected with either BUNV or rBUNdelNSs at an MOI of 5 pfu/cell. The cells were harvested and lysed 24 hours post-infection for Western blot analysis (**Fig 3.5**). Treatment with IFNα had little effect on BUNV (**Fig 3.5**, top panel); likely because the IFNα response is dependent on IFNβ induction and Vero

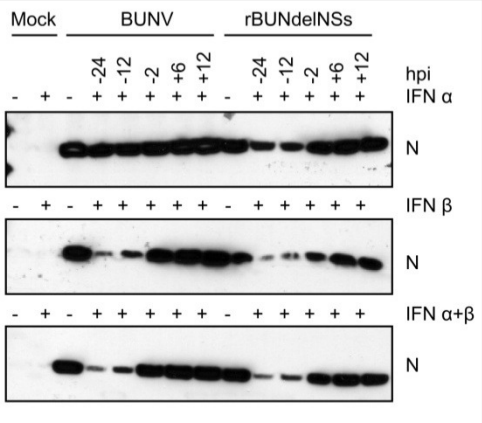

Figure 3.5 : Western blot analysis of mock infected or BUNV or rBUNdelNSs infected Vero cells which have been mock treated or treated with IFN. Vero cells were either mock treated or treated with 1000 U/ml of either IFNα or IFNβ or both, either 24, 12, or 2 hours pre-infection or 6 or 12 hours post-infection, as indicated. Cells were infected at an MOI of 5 pfu/cell and after 24 hours incubation at 37°C the monolayers were lysed and 1/30 of the lysate was analysed by SDS-PAGE and then transferred to a nitrocellulose membrane for Western blot analysis. BUNV or rBUNdelNSs N protein was detected using anti-N (rabbit) antibody. IFN denotes interferon and hpi denotes the hours post infection.

cells cannot produce IFNβ. However, when the cells were pre-treated with IFNα for 24 or 12 hours, rBUNdelNSs infected cells showed some reduction in the amount of N protein produced. In contrast to treatment with IFNα alone, pre-treatment for 24 or 12 hours with IFNβ considerably restricted both BUNV

and rBUNdelNSs (**Fig 3.5**, middle panel) and, as predicted, pre-treatment with both IFNα and IFNβ showed the same inhibition as treatments with IFNβ alone (**Fig 3.5**, bottom panel). The higher MOI used, compared with an MOI of 1 previously, revealed that BUNV was able to overcome IFNβ when the virus concentration was increased.

To establish if exogenous IFNβ has the same effect on BUNV at 37℃ in A549 cells, the cells were pre-treated at various times with IFNβ and then infected with BUNV or rBUNdelNSs at an MOI of 1 pfu/cell. The cells were then harvested 24 hours after infection, lysed and subjected to Western blotting (**Fig 3.6**). N protein was undetectable after pre-treatment for 24 or 12 hours with

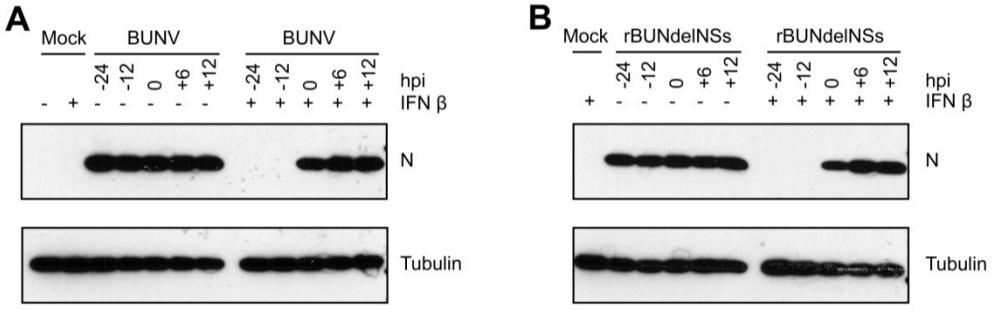

Figure 3.6 : Western blot analysis of mock infected or BUNV (A) or rBUNdelNSs (B) infected A549 cells which have been mock treated or treated with IFNβ. A549 cells were either mock treated or treated with 1000 U/ml IFNβ either 24 or 12 hours pre-infection, at the time of infection or 6 or 12 hours post-infection as indicated. After incubation at 37°C for 24 hours the monolayers were lysed and 1/30 of the lysate was analysed by SDS-PAGE and then transferred to a nitro-cellulose membrane for Western blot analysis. BUNV or rBUNdelNSs N protein was detected using anti-N (rabbit) antibody and tubulin was detected using anti-tubulin (mouse) antibody. IFN denotes interferon and hpi denotes the hours post infection.

IFNβ in BUNV (**Fig 3.6A**) and rBUNdelNSs (**Fig 3.6B**) virus-infected cells. Additionally, treatment that started at 0 hours also showed a reduction in the amount of N protein and there was no observable effect from post-infection treatment for both viruses.

Virus titre in IFNβ pre-treated A549 cells

Pre-treating cells with IFN clearly had a major impact on the replication of BUNV. To elaborate the effect of IFN on viral replication, the growth kinetics of BUNV and rBUNdelNSs at 37℃ were monitored in two cell lines, Vero and A549. After the cells were pre-treated with IFNβ, they were infected with either BUNV or rBUNdelNSs at an MOI of 1 pfu/cell and over a 24 hour period released virus was determined by plaque assay (**Fig 3.7A and B**). The BUNV titre in untreated Vero cells after 24 hours was $1.1x10^8$ pfu/ml (a yield around $1x10^8$ pfu/ml is relatively standard for BUNV) (**Fig 3.7A**). However, in the pre-treated cells the BUNV titre did not increase above $3.5x10^4$ pfu/ml. The rBUNdelNSs virus is attenuated in comparison with BUNV and usually produces a virus titre 10- to 100-fold lower. In the untreated Vero cells the rBUNdelNSs titre was $4.5x10^6$ pfu/ml. Pre-treatment with IFNβ restricted the virus from producing a titre above $9.5x10^4$ pfu/ml. The peak BUNV titre in A549 untreated

cells was $9x10^7$ pfu/ml but from cells pre-treated with IFNβ the titre did not increase above $6.5x10^4$ pfu/ml (**Fig 3.7B**). The peak titre from rBUNdelNSs in

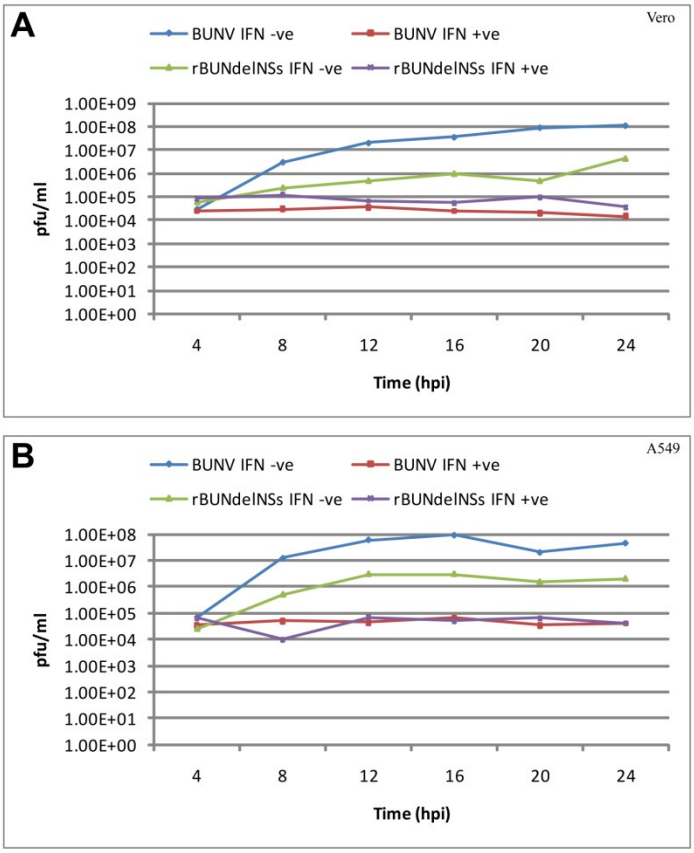

Figure 3.7: Comparison of virus growth in untreated and IFNβ pre-treated Vero (A) or A549 (B) cells at 37°C. Cells were either untreated with or pre-treated with 1000 U/ml IFNβ 24 hours prior to infection. The cells were then infected with BUNV or rBUNdelNSs at 1 pfu/cell and at the time points indicated virus in the cell supernatant was collected and titrated by plaque assay. IFN denotes interferon and hpi denotes the hours post infection.

untreated A549 cells was $3x10^6$ pfu/ml and from pre-treated cells the titre did not increase above $7x10^4$ pfu/ml (**Fig 3.7B**). Thus, pre-treatment with IFNβ appears to fully restrict BUNV replication in both cell lines.

Protein expression in IFNβ pre-treated A549 cells

In order to establish that the restriction on viral titre equates to restriction on viral protein synthesis, A549 cells were pre-treated with IFNβ (1000 U/ml) and then infected with either BUNV or rBUNdelNSs at an MOI of 1 pfu/cell. The cells were then labelled with [^{35}S]-methionine for 1 hour at different times and subsequently analysed by SDS-PAGE and autoradiography (**Fig 3.8**). All the viral proteins (L, Gc, Gn, N, NSm, and NSs) were observed in the untreated cells; however, after IFNβ treatment, none of the viral proteins were readily identified (**Fig 3.8,** BUNV). As with BUNV infection, the untreated rBUNdelNSs-infected cells produced detectable levels of all the viral proteins (except NSs as it has been deleted) but after pre-treatment with IFNβ no viral proteins were detected (**Fig 3.8**, rBUNdelNSs).

Figure 3.8 suggests limited viral protein expression occurred. Therefore, some of the remaining cell lysates from the experiment described above (Fig 3.8) were immunoprecipitated with anti-BUN antibody and the immunoprecipitates

analysed by SDS-PAGE and autoradiography (**Fig 3.9**). As was observed in figure 3.8, viral proteins were detected by 4 hours post infection in untreated

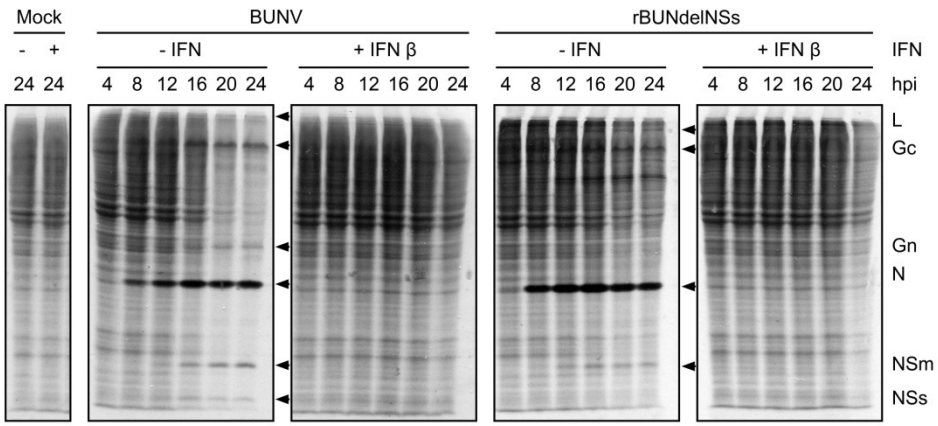

Figure 3.8 : In vivo labelling of A549 cells untreated or pre-treated with IFNβ and infected with BUNV or rBUNdelNSs. At 37°C, cells were either untreated with or pre-treated with 1000 U/ml IFNβ 24 hours prior to infection. The cells were then infected at an MOI of 1 pfu/cell and labelling with ^{35}[S]-methionine was carried out for 1 hour prior to the time points indicated, and then the cells were lysed. 1/30 of the volume of the lysate was loaded per well and analysed by SDS-PAGE and autoradiography. The positions of viral proteins are indicated on the right (with arrows in the centre). IFN denotes interferon and hpi denotes the hours post infection.

cells infected with either BUNV or rBUNdelNSs and the viral proteins L, Gc and N were all clearly visible (**Fig 3.9**, - IFN panels). However, as with earlier data,

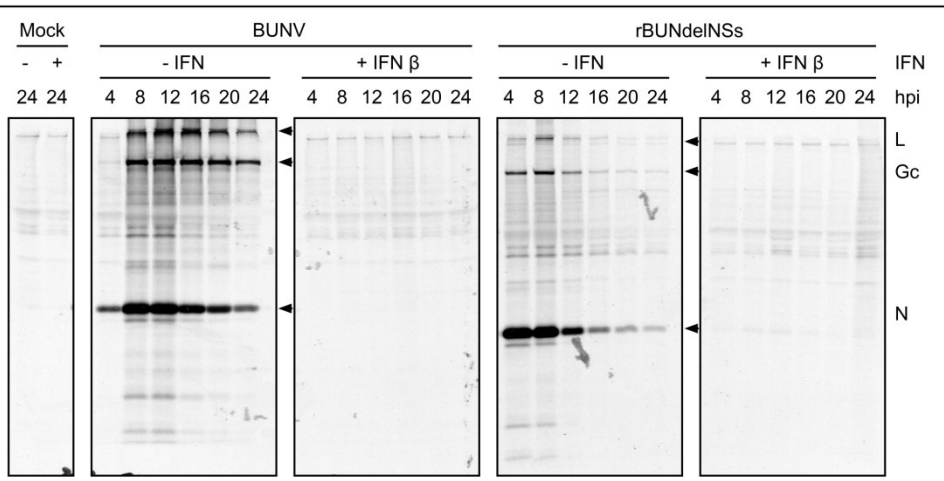

Figure 3.9 : Immunoprecipitation of A549 cells untreated or pre-treated with IFNβ and infected with BUNV or rBUNdelNSs. At 37°C, cells were either untreated with or pre-treated with 1000 U/ml IFNβ 24 hours prior to infection. The cells were then infected at an MOI of 1 pfu/cell and labelling with ^{35}[S]-methionine was carried out for 1 hour prior to the time points indicated, and then the cells were lysed. Using 1/3 of the lysate the soluble antigen extracts were immunoprecipitated with anti-BUN antibody, and the precipitates were analysed by SDS-PAGE and autoradiography. The positions of viral proteins are indicated on the right (with arrows in the centre). IFN denotes interferon and hpi denotes the hours post infection.

no viral proteins were detected in the pre-treated cells infected with either virus. This confirmed that pre-treatment with IFNβ completely restricted detectable viral proteins.

RNA analysis in IFNβ pre-treated A549 cells

The inability of BUNV to produce virions or any detectable viral proteins may stem from a block in virion morphogenesis and or viral protein translation. However, the viral restriction observed previously may have been at the level of RNA transcription and replication. A549 cells were pre-treated with IFNβ (1000

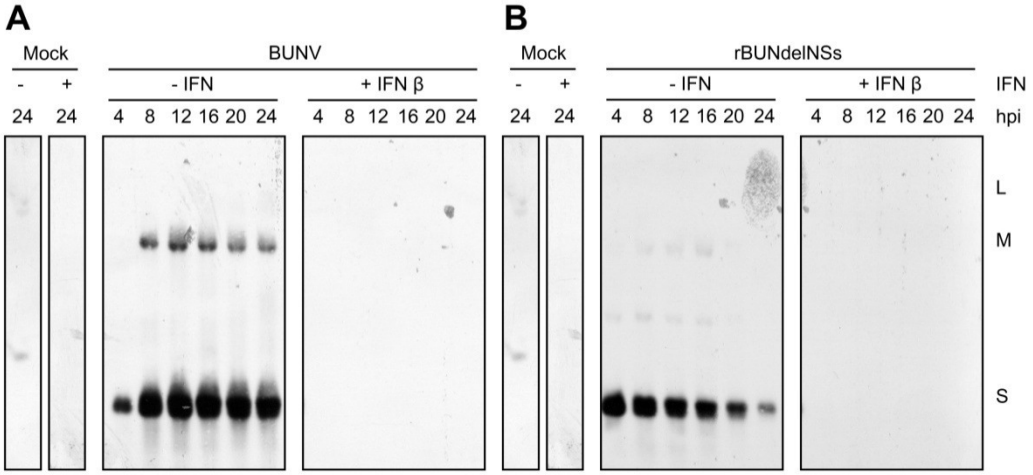

Figure 3.10 : Analysis of viral genomic RNA from A549 cells untreated or pre-treated with IFN and then mock infected or infected with BUNV (A) or rBUNdelNSs (B). At 37°C, cells were either untreated with or pre-treated with 1000 U/ml IFNβ 24 hours prior to infection. The cells were then infected at an MOI of 1 pfu/cell. Total RNA was extracted using Trizol at the time points indicated and 10 µg per well was analysed by Northern blotting using probes complementary to genomic RNA (+ve probes). Viral RNAs are identified on the right. IFN denotes interferon and hpi denotes the hours post infection.

U/ml) and then infected with either BUNV or rBUNdelNSs at an MOI of 1 pfu/cell. Over a 24 hour time period total cellular RNA was extracted at various times and analysed by Northern blotting (**Fig 3.10 and 3.11**). In the untreated cells infected with either BUNV (**Fig 3.10A**) or rBUNdelNSs (**Fig 3.10B**) there were detectable levels of S segment genomic RNA at 4 hours post infection. The M segment was observed in BUNV infected cells by 8 hours whereas the L segment from either virus infection was not detected. From the pre-treated cells infected with either virus there was no detectable viral genomic RNA (**Fig 3.10A and B**, +IFN).

Furthermore, the experiment was repeated for probing with negative orientation probes to detect anti-genomic and mRNA to see whether a block in genome replication and viral protein expression was at the level of transcription (**Fig 3.11A and B**). In untreated cells infected with BUNV S, M and L RNAs were easily detected (**Fig 3.11A**). Cells infected with rBUNdelNSs also showed strong signals and the expected migration pattern for each segment (**Fig 3.11B**) along with two other RNA species whose origin is unknown. After 16 hours the detectable RNA decreased due to virus-induced cell death resulting from a lack of the NSs protein (Kohl *et al.*, 2003). In the IFNβ treated cells, no viral RNAs were detected (**Fig 3.11A and B**, +IFN). Thus, pre-treatment with IFN is

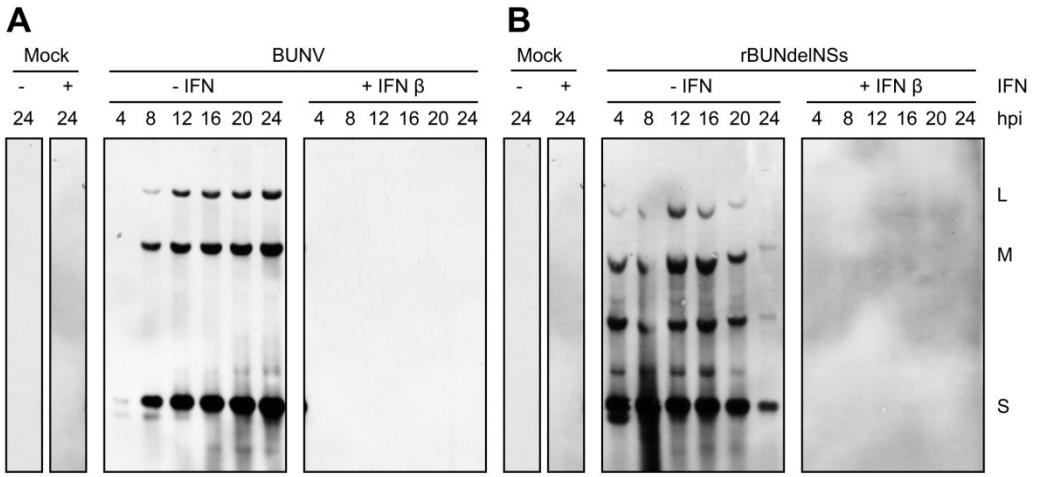

Figure 3.11 : Analysis of viral anti-genomic RNA from A549 cells untreated or pre-treated with IFN and then mock infected or infected with BUNV or rBUNdelNSs. At 37°C, cells were either untreated with or pre-treated with 1000 U/ml IFNβ 24 hours prior to infection. The cells were then infected at an MOI of 1 pfu/cell. Total RNA was extracted using Trizol at the time points indicated and 10 µg per well was analysed by Northern blotting using probes complementary to anti-genomic RNA (-ve probes). Viral RNAs are identified on the right. IFN denotes interferon and hpi denotes the hours post infection.

effective at blocking viral replication at the level of RNA synthesis, as well as abrogating viral protein synthesis.

Quantification of the DIG labelled probes showed differing signal intensities between the L, M and S segment probes. However, the signal intensities of both negative and positive sense probes for each segment were similar. Thus the levels of RNA can be compared for each segment, although this does not account for inefficient RNA transfer from the gel to the membrane.

Protein expression in IFNβ pre-treated Vero cells

Pre-treatment of A549 cells with IFNβ puts the cells in to the antiviral state priming them for defence against a viral infection. However, while Vero cells are unable to synthesise their own IFN, they are able to respond to IFN and can still go into the antiviral state if pre-treated with IFNβ. To investigate whether pre-treated Vero cells are still susceptible to BUNV infection, Vero cells were treated with IFNβ (1000 U/ml) and then infected with either BUNV or rBUNdelNSs at an MOI of 1 pfu/cell. The cells were harvested at various times over 24 hours and the proteins analysed by SDS-PAGE and autoradiography (**Fig 3.12**). The viral proteins L, Gc, Gn, N, NSm and NSs were detected from untreated cells infected with either BUNV or rBUNdelNSs (no NSs) and the N protein was observed by 8 hours post infection. In the BUNV-infected cells, there was visible shut-off at 20 hours post infection (**Fig 3.12**, BUNV -IFN) whereas in rBUNdelNSs infected cells shut-off was barely visible (**Fig 3.12**, rBUNdelNSs –IFN). As seen earlier in A549 cells, there was no discernible viral protein synthesis in IFNβ treated cells infected with either BUNV or rBUNdelNSs (**Fig 3.12**, BUNV and rBUNdelNSs +IFN). For a more specific

examination of the level of protein synthesis in IFNβ treated cells, the samples were immunoprecipitated with anti-BUN antibody and analysed by SDS-PAGE and autoradiography. **Figure 3.13** shows that viral protein synthesis of L, Gc and N protein was detected in untreated cells as early as 4 hours post infection.

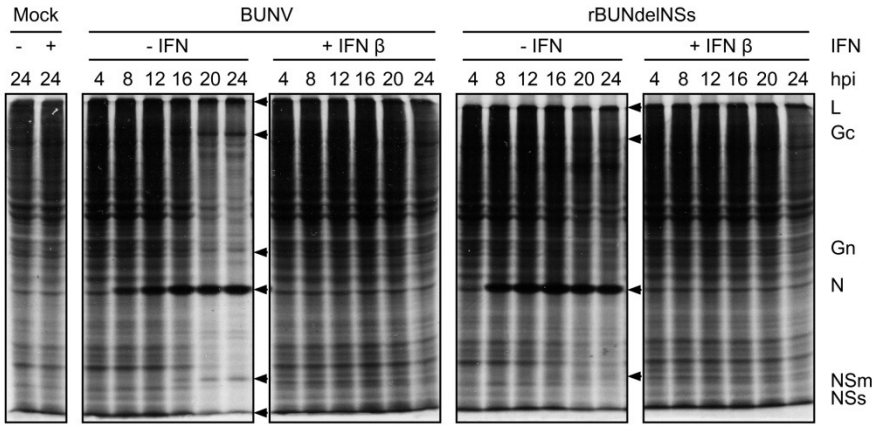

Figure 3.12 : In vivo labelling of Vero cells untreated or pre-treated with IFNβ and infected with BUNV or rBUNdelNSs. At 37°C, cells were either untreated with or pre-treated with 1000 U/ml IFNβ 24 hours prior to infection. The cells were then infected at an MOI of 1 pfu/cell and labelling with ^{35}[S]-methionine was carried out for 1 hour prior to the time points indicated, and then the cells were lysed. 1/30 of the volume of the lysate was loaded per well and analysed by SDS-PAGE and autoradiography. The positions of viral proteins are indicated on the right (with arrows in the centre). IFN denotes interferon and hpi denotes the hours post infection.

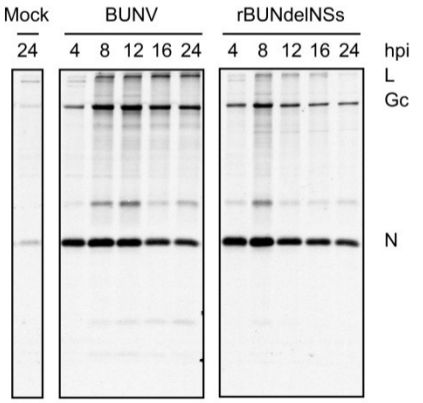

Figure 3.13 : Immunoprecipitation of Vero cells untreated or pre-treated with IFNβ and infected with BUNV or rBUNdelNSs. At 37°C, cells were either untreated with or pre-treated with 1000 U/ml IFNβ 24 hours prior to infection. The cells were then infected at an MOI of 1 pfu/cell and labelling with ^{35}[S]-methionine was carried out for 1 hour prior to the time points indicated, and then the cells were lysed. Using 1/3 of the lysate the soluble antigen extracts were immunoprecipitated with anti-BUN antibody, and the precipitates were analysed by SDS-PAGE and autoradiography. The positions of viral proteins are indicated on the right. IFN denotes interferon and hpi denotes the hours post infection.

However, there was no observed viral protein synthesis in the IFNβ treated cells (data not shown). Thus, treating either A549 or Vero cells with IFNβ 24 hours prior to infection puts the cells into the antiviral state and they appear to be no longer permissive for BUNV replication.

Protein expression in Vero cells subjected to post infection IFNβ treatment

Having ascertained that BUNV is incapable of replicating in Vero cells that have been primed with IFNβ, the next question was whether BUNV would be restricted by the treatment of IFNβ after infection had started. Therefore, Vero cells were infected with either BUNV or rBUNdelNSs at an MOI of 1 pfu/cell and

then treated with IFNβ (1000 U/ml) immediately (synchronous treatment) or 6 or 12 hours post infection. The cells were harvested 24 hours post infection and analysed by SDS-PAGE and autoradiography (**Fig 3.14**). Synchronous treatment with IFNβ considerably restricted both BUNV and rBUNdelNSs protein synthesis: L and NSm proteins were not detectable after treatment, and the Gc and N proteins were only faintly present (**Fig 3.14A**). The level of host

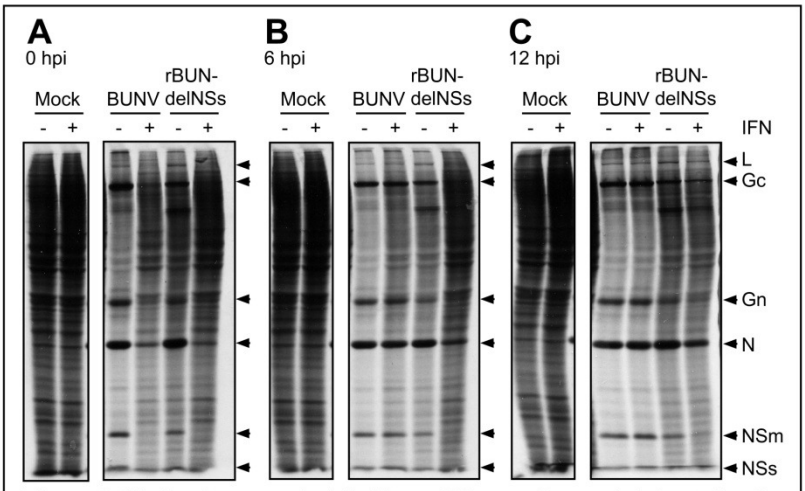

Figure 3.14 : In vivo protein labelling of Vero cells mock infected or infected with BUNV or rBUNdelNSs and treated with IFNβ post infection. At 37°C, cells were infected at an MOI of 1 pfu/cell and then treated with 1000 U/ml IFNβ at the times indicated (**A, B and C**). Labelling with ^{35}[S]-methionine was carried out for 1 h prior to lysis at 24 hours post infection and 1/30 of the volume of the lysate was loaded per well and analysed by SDS-PAGE and autoradiography. The positions of viral proteins are indicated on the right (with arrows in the centre). IFN denotes interferon and hpi denotes the hours post infection.

cell protein synthesis shut-off observed in the treated BUNV infected cells was similar to untreated rBUNdelNSs infected cells but the treated rBUNdelNSs infected cells showed even less shut-off. When treatment was started 6 hours post infection there was no observable effect on BUNV viral protein synthesis although the level of shut-off was slightly reduced (**Fig 3.14B**). However, the treated cells infected with rBUNdelNSs produced less intense viral L, Gc and N protein bands and there was little shut-off observed. As with treatment started 6 hours post infection, treatment that was started 12 hours post infection had no observable effect on BUNV protein synthesis or host protein shut-off (**Fig 3.14C**). Furthermore, cells infected with rBUNdelNSs were only slightly restricted. The level of shut-off was the same as untreated but there was reduced synthesis of all the viral proteins.

The cell lysates were immunoprecipitated with anti-BUN antibody and analysed by SDS-PAGE and autoradiography to gain further understanding of the restriction on protein synthesis observed above (**Fig 3.15**). It was clear that the later the treatment started, the smaller was the effect observed (**Fig 3.15A to B to C**). For BUNV, the level of L, Gc and N protein was reduced considerably by synchronous addition of IFN but not by post-infection treatments. For

rBUNdelNSs, the level of restriction observed on L, Gc and N protein synthesis decreased the longer it was before treatment began; synchronous IFN addition

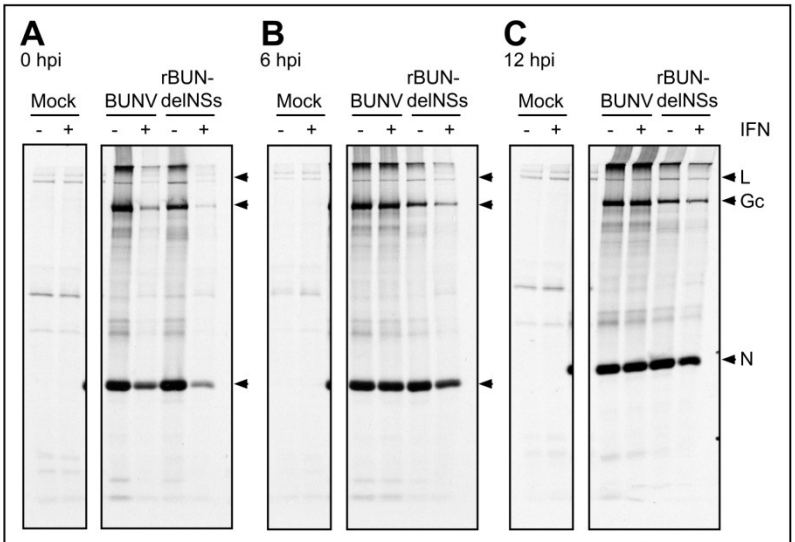

Figure 3.15 : Immunoprecipitation of Vero cells mock infected or infected with BUNV or rBUNdelNSs and treated with IFNβ post infection. At 37°C, cells were infected at an MOI of 1 pfu/cell and then treated with 1000 U/ml IFNβ at the times indicated (**A, B and C**). Labelling with ^{35}[S]-methionine was carried out for 1 h prior to lysis at 24 hours post infection and using 1/3 of the lysate the soluble antigen extracts were immunoprecipitated with anti-BUN antibody, and the precipitates were analysed by SDS-PAGE and autoradiography. The positions of viral proteins are indicated on the right (with arrows in the centre). IFN denotes interferon and hpi denotes the hours post infection.

clearly inhibited viral protein synthesis whereas treatment at 12 hours post infection had little effect on protein levels (**Fig 3.15**, compare A to C).

BUNV protein expression from cells synchronously treated with IFNβ

BUNV replication was restricted by synchronous treatment with IFNβ but not by post infection IFNβ treatment. Therefore, to try to establish at what point in the replication cycle of BUNV the IFN-mediated restriction occurred, Vero cells were infected with BUNV at an MOI of 1 pfu/cell, synchronously treated with IFNβ (1000 U/ml) and labelled for 1 hour with [^{35}S]-methionine at different times over a 24 hour period. Radiolabelled cell extracts were analysed by SDS-PAGE and autoradiography (**Fig 3.16**). The level of detectable viral proteins from untreated cells increased until 12 hours after which the level of N decreased but the level of Gc increased. The level of host cell protein synthesis shut-off increased from 12 hours onwards (**Fig 3.16**, BUNV –IFN). However, the infected treated cells showed an alteration in the pattern of viral protein synthesis. Compared with untreated cells, the level of N and Gc protein synthesis increased 1.7- and 3-fold, respectively (**Fig 3.16B and C**). By 12 hours the addition of IFNβ resulted in a decrease in the level of protein synthesis, and by 24 hours the decrease equated to a 3- and 5-fold reduction for N and Gc protein synthesis, respectively. Following the addition of IFNβ the level of shut-off observed was also reduced by 24 hours post infection (**Fig**

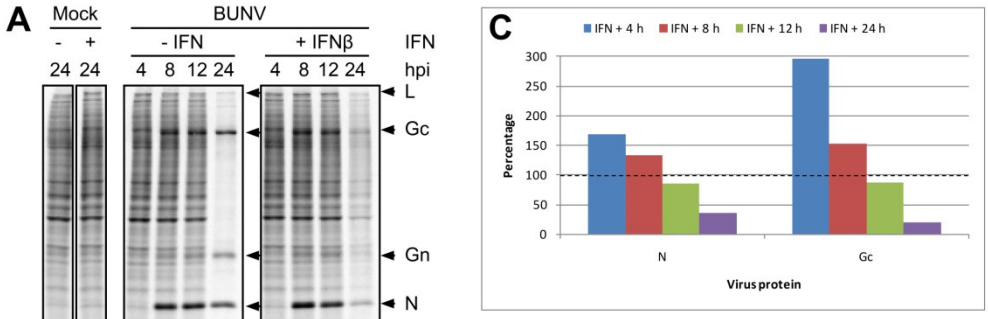

Figure 3.16 : Analysis of Vero cells infected with BUNV and then synchronously either not treated with or treated with IFNβ. At 37°C, the cells were infected at an MOI of 1 pfu/cell and then either not treated or treated with 1000 U/ml IFNβ and then labelling with ^{35}[S]-methionine was carried out 1 hour prior to the time points indicated, and then the cells were lysed. **In vivo labelling (A):** 1/30 of the volume of the lysate was loaded per well and analysed by SDS-PAGE and autoradiography. **Immunoprecipitation (B):** Using 1/3 of the lysate the soluble antigen extracts were immunoprecipitated with anti-BUN antibody, and the precipitates were analysed by SDS-PAGE and autoradiography. The positions of viral proteins are indicated on the right (with arrows in the centre). hpi denotes the hours post infection. **Protein quantification (C):** The BUN samples from panel **B** were quantified using a phosphorimager; the protein in each IFN treated lane was normalised so that its respective untreated protein level was 100% and is represented by the dotted line. IFN denotes interferon.

3.16A). Therefore, these data show that IFNβ treatment alters the level of N and Gc protein synthesis in cells infected with BUNV.

Analysis of BUNV RNA from cells synchronously treated with IFNβ

The observed effect of IFNβ treatment on viral protein synthesis could be at the level of transcription or translation. Therefore, to distinguish these possibilities, Vero cells were infected with BUNV at an MOI of 1 pfu/cell and stimulated synchronously with IFNβ (1000 U/ml), and subsequently, total cellular RNA was extracted at different times post-infection and analysed by Northern blotting (**Fig 3.17)**. The level of BUNV genomic RNA in untreated cells was detectable for each segment by 4 hours, and peaked by 12 hours post-infection (**Fig 3.17A**, –IFN). In the IFNβ-treated cells the RNA levels increased from detection at 4 hours throughout the 24 hour period (**Fig 3.17A**, +IFN). In untreated cells the level of positive-stranded S and M segment RNA was detected at 4 hours and increased up to 8 hours and remained constant, while the L segment RNA was not detected until 8 hours and increased thereafter (**Fig 3.17B**, -IFN). However, all three RNAs were detected in IFNβ-treated cells at 4 hours post infection and at much higher levels suggesting that IFNβ induces increased early transcription of anti-genomic and or mRNA (**Fig 3.17B**, +IFN). This observation

correlates with data described above that showed an increase in early viral protein synthesis of N and Gc protein (**Fig 3.16C**). Protein synthesis shown in figure 3.16C, however, showed significant reduction by 24 hours but the positive

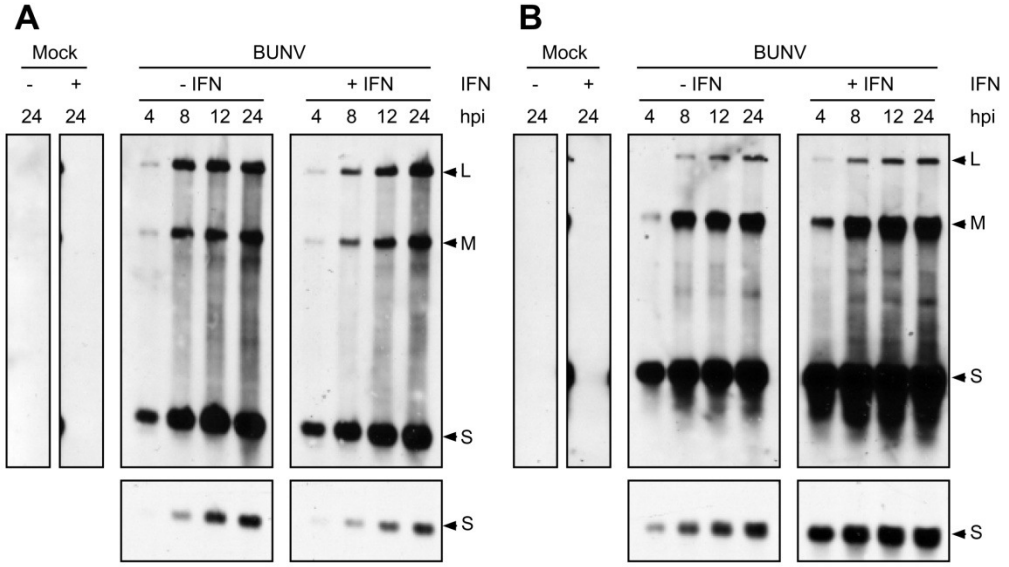

Figure 3.17 : Analysis of viral RNA from Vero cells infected with BUNV and then either not treated with or treated with IFNβ. At 37°C, the cells were infected at an MOI of 1 pfu/cell and then either not treated with or treated with 1000 U/ml IFNβ. Total RNA was extracted using Trizol at the time points indicated and 10 µg per well was analysed by Northern blotting using probes complementary to genomic **(A)** RNA (+ve probes) or to anti-genomic **(B)** RNA (-ve probes). The lower two panels are shorter exposures. Viral RNAs are identified on the right. IFN denotes interferon and hpi denotes the hours post infection.

sense RNA observed in figure 3.17B shows increased RNA synthesis suggesting that IFNβ induced restriction on N and particularly Gc protein synthesis occurs post-transcriptionally.

IFNβ pre-treated Vero cells infected with GRO, LAC or LACdelNSs virus

The above data established that the effect of pre-treating cells with IFNβ renders them non-permissive for BUNV infection. To investigate whether IFNβ has a similar effect on other viruses in the same genus as BUNV, Vero cells were infected with either GROV, LACV or rLACdelNSs virus at an MOI of 1 pfu/cell. The cells were labelled with [^{35}S]-methionine for 1 hour at different times through 24 hours and then harvested for SDS-PAGE and autoradiography analysis. Virus released into the growth medium was titrated by plaque assay.

GROV is an orthobunyavirus first isolated in Colombia and thought to be responsible for a mild febrile illness in humans (Groot *et al.*, 1959). The NSs protein of GROV has a considerably shorter amino acid sequence and is truncated at both N and C termini, compared with other orthobunyaviruses (Elliott, 1996). In untreated Vero cells infected with GROV, N protein synthesis was observed by 8 hours post infection and host-cell protein synthesis shut-off by 12 hours post infection (**Fig 3.18A**, -IFN). At 24 hours, due to significant shut-off, most of the viral proteins were visible. However, in IFNβ-treated cells,

viral proteins were indistinguishable from host cell proteins (**Fig 3.18A**, +IFN). Immunoprecipitation of the same samples using an anti-GRO antibody showed that in untreated cells GROV N protein synthesis was underway by 4 hours post infection and Gc protein synthesis by 8 hours (**Fig 3.18B**, -IFN). After pre-

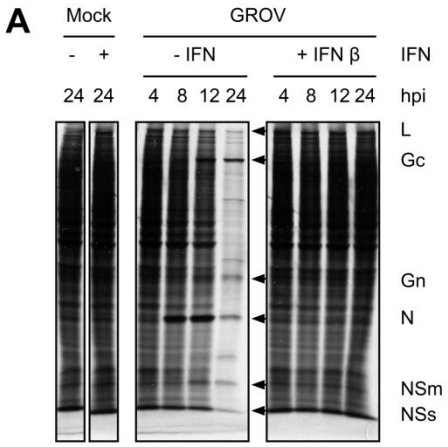

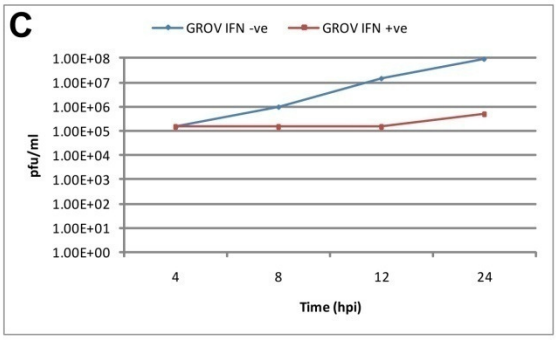

Figure 3.18: Analysis of Vero cells infected with the Orthobunyavirus Guaroa virus (GROV). At 37°C, Vero cells were either not treated or treated with 1000 U/ml IFNβ 24 hours prior to infection. The cells were then infected at an MOI of 1 pfu/cell and labelling with ^{35}[S]-methionine was carried out for 1 hour prior to the time points indicated, and then the cells were lysed. **In vivo labelling (A):** 1/30 of the volume of the lysate was loaded per well and analysed by SDS-PAGE and autoradiography. **Immunoprecipitation (B):** Using 1/3 of the lysate the soluble antigen extracts were immunoprecipitated with anti-GRO antibody, and the precipitates were analysed by SDS-PAGE and autoradiography. The positions of viral proteins are indicated on the right (with arrows in the centre). hpi denotes the hours post infection. **Virus growth (C):** Cells were either untreated with or pre-treated with IFNβ 24 hours prior to infection. The cells were then infected at 0.01 pfu/cell and at the time points indicated virus in the cell supernatants was collected and titrated by plaque assay. Representative growth curve, repeated twice. IFN denotes interferon and hpi denotes the hours post infection.

treatment of cells with IFNβ, GROV was still able to infect and synthesise viral proteins, albeit with greatly reduced levels of viral proteins produced (**Fig 3.18B**, +IFN). This correlates with the viral titre in untreated cells which reached $9.5x10^7$ pfu/ml but was significantly reduced in treated cells and only reached $5x10^5$ pfu/ml (**Fig 3.18C**).

LACV was first isolated in 1960 in the USA (Thompson *et al.*, 1965). It is an Orthobunyavirus responsible for La Crosse encephalitis and is one of the leading contributors to viral encephalitis in the USA (Schmaljohn, 2007). IFNβ untreated cells infected with LACV showed strong host cell protein synthesis shut-off by 12 hours (**Fig 3.19A**, -IFN). Synthesis of viral N protein was detected at 4 hours post infection, peaked at 8 hours, and decreased thereafter (**Fig 3.19B**, -IFN). In IFNβ treated cells, there was no discernible viral protein synthesis or shut-off observed (**Fig 3.19A**, +IFN). After immunoprecipitation with LACV anti-N antibody trace amounts of N protein was detected by 12 hours

post-infection (**Fig 3.19B**, +IFN), though much less protein was produced compared to the same time-point in the untreated cells (**Fig 3.19B**, compare – IFN and +IFN). Furthermore, cells infected with LACV and pre-treated with

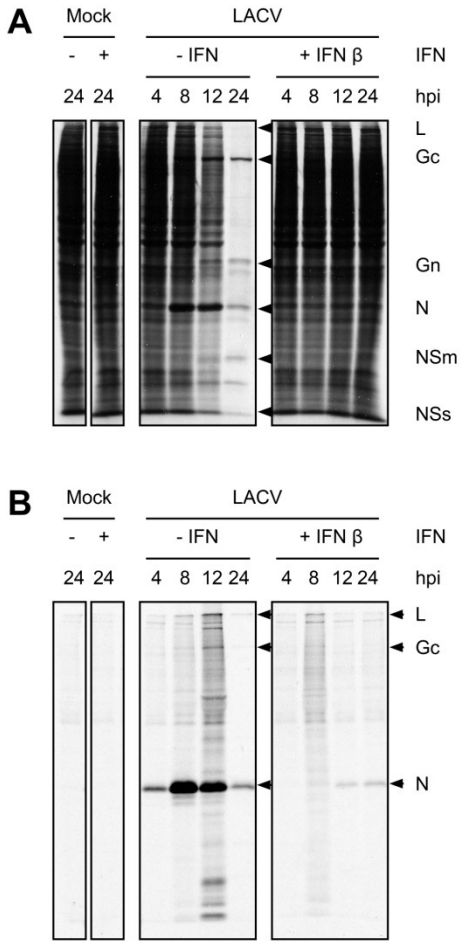

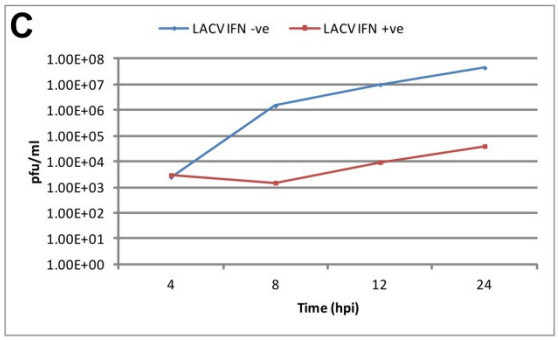

Figure 3.19: Analysis of Vero cells infected with the Orthobunyavirus La Crosse virus (LACV). At 37°C, Vero cells were either not treated or treated with 1000 U/ml IFNβ 24 hours prior to infection. The cells were then infected at an MOI of 1 pfu/cell and labelling with ^{35}[S]-methionine was carried out for 1 hour prior to the time points indicated, and then the cells were lysed. **In vivo labelling (A):** 1/30 of the volume of the lysate was loaded per well and analysed by SDS-PAGE and autoradiography. **Immunoprecipitation (B):** Using 1/3 of the lysate the soluble antigen extracts were immunoprecipitated with LACV anti-N antibody, and the precipitates were analysed by SDS-PAGE and autoradiography. The positions of viral proteins are indicated on the right (with arrows in the centre). hpi denotes the hours post infection. **Virus growth (C):** Cells were either untreated with or pre-treated with IFNβ 24 hours prior to infection. The cells were then infected at 0.01 pfu/cell and at the time points indicated virus in the cell supernatants was collected and titrated by plaque assay. Representative growth curve, repeated twice. IFN denotes interferon and hpi denotes the hours post infection.

IFNβ produced infectious virus ($4x10^4$ pfu/ml) but the titre was 1000-fold lower, thus correlating with the other data presented here (**FIG 3.19A and B**).

rLACdelNSs is a recombinant LACV that is unable to express the NSs protein and therefore cannot antagonise the IFN response as efficiently as LACV. Untreated cells infected with rLACdelNSs still showed some level of host cell protein synthesis shut-off, despite the lack of NSs protein, but not as much as the wild type virus, and in the pre-treated cells there was no observable shut-off or viral protein synthesis (**Fig 3.20A**). Immunoprecipitation with LACV anti-N antibody showed that N protein synthesis was similar to that of the wild type virus, and from IFNβ treated and infected cells trace amounts of N protein were detected (**Fig 3.20B**). Further, rLACdelNSs was severely restricted by IFNβ from producing infectious virus as the viral titre barely increased from $3x10^3$ pfu/ml and was 6000-fold lower than the titre from untreated cells (**Fig 3.20C**).

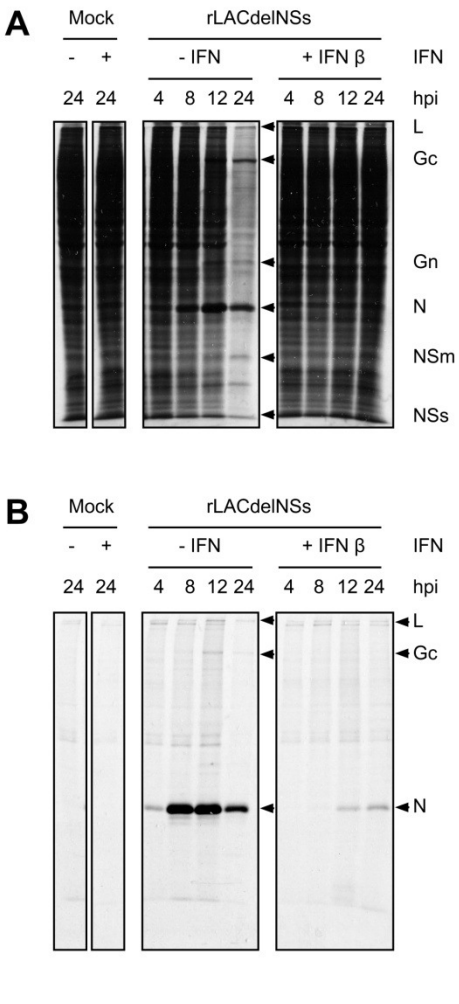

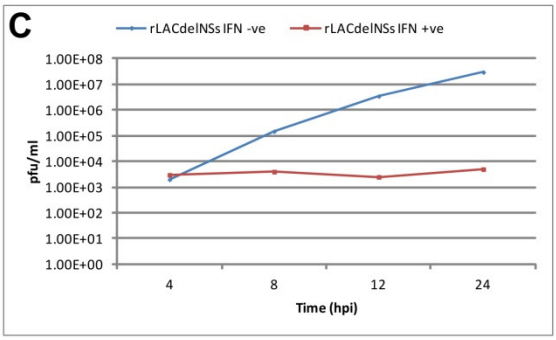

Figure 3.20: Analysis of Vero cells infected with the NSs deletion mutant La Crosse virus (rLACdelNSs). At 37°C, Vero cells were either not treated or treated with 1000 U/ml IFNβ 24 hours prior to infection. The cells were then infected at an MOI of 1 pfu/cell and labelling with ^{35}[S]-methionine was carried out for 1 hour prior to the time points indicated, and then the cells were lysed. **In vivo labelling (A):** 1/30 of the volume of the lysate was loaded per well and analysed by SDS-PAGE and autoradiography. **Immunoprecipitation (B):** Using 1/3 of the lysate the soluble antigen extracts were immunoprecipitated with LACV anti-N antibody, and the precipitates were analysed by SDS-PAGE and autoradiography. The positions of viral proteins are indicated on the right (with arrows in the centre). hpi denotes the hours post infection. **Virus growth (C):** Cells were either untreated with or pre-treated with IFNβ 24 hours prior to infection. The cells were then infected at 0.01 pfu/cell and at the time points indicated virus in the cell supernatants was collected and titrated by plaque assay. Representative growth curve, repeated twice. IFN denotes interferon and hpi denotes the hours post infection.

Discussion

BUNV was able to plaque on all cell lines used in this report, and there are also other cell lines that are permissive to BUNV where infection results in viral plaque formation. Van Knippenberg *et al.* (2010) showed that impairment of the innate immune response, especially the IFN response, in A549 cells results in BUNV producing larger plaques while the NSs deletion virus rBUNdelNSs is also able to plaque on the IFN incompetent cells. Chapter Four shows that rBUNdelNSs grows to a higher titre in A549/BVDV/Npro and A549/PIV5/V cells, both of which have their IFN system impaired (Andrejeva *et al.*, 2002; Hale *et al.*, 2009; Hilton *et al.*, 2006), compared to *naïve* cells (**Fig 4.11A**). Furthermore, the data described earlier (**Fig 3.3**) suggests that the innate immune response in A549 cells is more restrictive on BUNV as there was a 100-fold difference in the BUNV to rBUNdelNSs titre (**Fig 3.3C**) compared with a 10-fold difference in BUNV to rBUNdelNSs titre in 2FTGH cells (**Fig 3.3A**). Also, when the IFN induction system was inhibited by the V protein in 2FTGH/PIV5/V cells, the rBUNdelNSs titre was still 10-fold lower than BUNV,

while lack of IFN production, when using Vero cells, resulted in the titres of both viruses being similar.

Therefore, these data effectively demonstrate the importance of the NSs protein in the fight against the IFN response and how fundamentally vital the IFN response is against BUNV infection. However, as seen here, it is essential that the target cells are able to initiate the antiviral response as early as possible and enter into the antiviral state prior to infection as BUNV appears then to be completely restricted in viral functions. If the cells are pre-treated with IFN, the virus is able to attach and enter the cell (preliminary data not shown) but is then unable to synthesise any RNA and consequently viral proteins and therefore cannot produce any virions. On the other hand, if BUNV infection is already underway before IFN is applied there is little chance of the cell overcoming the virus. The early expression of the viral NSs protein rapidly leads to inhibition of host cell protein synthesis and further exacerbates viral infection. Interestingly though, synchronous treatment with IFNβ enabled partial restriction of BUNV replication by both enhancing positive-strand RNA synthesis and diminishing protein synthesis. The increase in anti-genomic and mRNA did not result in an increase in genomic RNA, but the increase in mRNA appeared to result in a spike in viral protein synthesis which was followed by a decrease.

Viral RNA synthesis requires the N protein and morphogenesis of infectious virus cannot occur without the Gc protein. The early enhancement of Gc and N protein synthesis, as well as positive sense RNA, shows that the block is not initially at the primary transcriptional or the subsequent translational level, suggesting that Gc is sequestered and or degraded. However, the early spike in Gc and N protein synthesis was followed by a considerable reduction, whilst the level of positive sense RNA remained elevated, suggesting translational inhibition of viral mRNA. Therefore, it appears likely that one of the mechanisms of IFNβ induced BUNV inhibition is to enhance the synthesis (and or stability) of BUNV positive sense RNA.

Analysis of Vero cells infected with either of two other orthobunyaviruses, GROV and LACV, showed some faint viral protein bands and slightly elevated titres after pre-treatment with IFNβ. However, an MOI of 1 pfu/cell means that approximately 2/3 of the cells will be infected and therefore slight differences in cell number and or virus titre could result in the differences observed but at the same time a higher MOI allows the virus to overcome the IFN response. It is possible that orthobunyaviruses express protein(s) that have the capability to disassemble the IFN response if given enough time. The paramyxovirus PIV5 has been shown to be able to dismantle the IFN response as the viral V protein targets STAT1 for degradation thus once STAT1 levels drop, the cells are unable to maintain the antiviral state thereby allowing the virus to undergo normal viral replication (Carlos *et al.*, 2005; Carlos *et al.*, 2009; Precious *et al.*, 2007). Perhaps BUNV is able to infect cells and maintain a low, thus far

undetected, level of viral RNA and protein synthesis that eventually could overcome the antiviral state. Since there is no evidence to suggest that BUNV virions are unable to attach and enter the cells in the antiviral state, it is feasible that BUNV could maintain a low level of replication in cells with a robust IFN response.

The concentration of IFN had an impact on virus replication when used to induce the antiviral state. Small doses of IFN such as less than 10 U/ml had no effect on either wild type or mutant virus tested here. However, 100 U/ml was enough to impair both viruses, rBUNdelNSs more so than BUNV, but only when pre-treatment occurred 12 hours or more before infection. Also, the restriction was observed in both A549 (competent IFN system) and Vero (unable to synthesise IFNα/β) cells, although a high MOI did enable detection of some viral N protein even from pre-treated cells. Thus, the loss of NSs was one factor in virus inhibition but as the effect was similar for both BUN and rBUNdelNSs it suggests that there is another more significant factor, which could quite simply be that the antiviral state, once established, is too strong for BUNV to fully overcome unless the cells are saturated with virus. This could be tested by investigating the effects of IFN on protein and RNA synthesis in cells infected over a long time period.

Influenza A virus encodes a non structural protein termed NS1 which has been shown to be a multifunctional protein, though it was originally thought to be primarily an IFN antagonist. The NS1 protein both limits IFNβ production and also limits the activity of the ISGs PKR and OAS. Influenza A virus IFNβ induction is restricted by NS1 as it blocks the activation of IRF3 or the post-transcriptional processing of cellular mRNAs (Kochs *et al.*, 2007). PKR is inhibited by NS1 binding to PKR and preventing the conformational change required for the activation of PKR by either dsRNA or PACT (Li *et al.*, 2006b). Also, OAS antiviral activity is restricted as the NS1 RNA binding domain competes with OAS for dsRNA (Min & Krug, 2006). The RVFV NSs protein is multifunctional as it inhibits host cell protein synthesis, is responsible for suppressing IFN induction, and targets PKR for proteasomal degradation (reviewed in Bouloy and Weber (2010)). Thus it is likely that either BUNV NSs has more than one function in IFN antagonism or that another BUNV protein antagonises the IFN response. This is further evidenced by the observation that there is some host cell protein shut-off in rBUNdelNSs infected cells, probably mediated by the endonuclease cap snatching activity of the polymerase protein. Furthermore, many hantaviruses do not encode functional NSs proteins and therefore have other processes for counteracting the IFN response. The non-pathogenic hantavirus Tula virus (TULV) has recently been shown to inhibit IFN induction *via* the cytoplasmic tail of the Gn glycoprotein interacting with TBK1 (Matthys *et al.*, 2011). The Gn tail of the pathogenic hantavirus NY-1 inhibits RIG-I- and TBK1-dependent IFNβ induction and Andes

virus (ANDV) restricts IFNβ induction by expression of the N protein and the glycoprotein precursor, whereas Sin Nombre virus (SNV) restricts IFNβ induction by expression of the glycoprotein precursor (GPC) alone (Alff *et al.*, 2008; Levine *et al.*, 2010). Furthermore the ANDV N or GPC and the SNV GPC are able to inhibit JAK/STAT signalling (Levine *et al.*, 2010).

Thus, viruses in the family *Bunyaviridae* express several proteins that have been shown to antagonise the IFN response and it is highly possible that the viral proteins of BUNV have more than one function and particularly may be involved in the viral antagonism of the innate immune response of the host cell.

Summary

This chapter shows:

- BUNV is completely inhibited by pre-treatment of cells with IFNβ.
- BUNV is unaffected by post-infection IFNβ treatment.
- BUNV is partially restricted in cells synchronously infected with IFNβ treatment.
- Positive-stranded RNA synthesis increased after synchronous IFNβ treatment.
- Synchronous IFNβ treatment caused an initial spike in N and Gc protein synthesis followed by a drastic reduction of N and particularly Gc protein.

4 The rescue and characterisation of the GFP-tagged virus rBUNGceGFPdelNSs

Introduction

As described in Chapter One, the BUNV rescue system is now very efficient and it takes only a few days to recover infectious virus. Briefly, the method is to transfect 10^6 BSR-T7/5 cells with 1.0 µg each of the plasmids pT7riboBUNL(+), pT7riboBUN(M+) and pT7riboBUN(S+), and then the cells are incubated for four days or until CPE is observed. Thus, direct manipulation of the plasmids and introduction of specific mutations within the cDNA of the virus is possible prior to transfection. The subsequent generation of engineered viruses permits study of the effects, both genotypically and phenotypically, of a mutation on the virus compared with the wild-type strain.

Since the breakthrough of a reverse genetics system for the recovery of BUNV from cDNA in 1996 many mutant viruses have been engineered, most significantly the rBUNdelNSs virus (Bridgen *et al.*, 2001). In addition, the benefits of tagging viruses with GFP have been realised across virology. One group successfully recovered a vaccinia virus that they had engineered to express the envelope glycoprotein BR5 fused to enhanced green fluorescent protein (eGFP) and were then able to track the intracellular movement of the virus in real-time (Ward & Moss, 2001). Bosch *et al.* produced a chimeric mouse hepatitis coronavirus (MHV) that had GFP fused onto the end of the spike (S) protein which was then used to investigate coronaviral entry into cells (Bosch *et al.*, 2004). Thus, the advantages of creating a GFP tagged BUNV for tracking the infectious cycle were clear.

Shi *et al.* (2006) used the reverse genetics system to attempt to generate recombinant viruses containing deletions in the NSm gene. The study found that only viruses with deletions in domains II, III and IV of NSm could be rescued and that deletion of residues 377-426 had no effect on the efficiency of formation of virus like particles (VLPs) compared with wild-type NSm. Thus, they proposed that the internal region of NSm may tolerate insertion of a foreign gene such as GFP. They demonstrated that introduction of a foreign sequence at this point did not interfere with processing of the M segment precursor polyprotein or the function of NSm, and were able to rescue a recombinant virus containing the eGFP ORF fused to the NSm gene between residues 403 to 420 called rBUNM-NSm-EGFP (Shi *et al.*, 2006). This work was taken further by engineering the NSs deletion virus rBUNdelNSs to have an eGFP tag fused to the NSm protein in the same way and the subsequent rescue of an infectious virus called rBUNM-NSm-EGFPDelNSs (Shi *et al.* unpublished).

In more recent work Shi *et al*. looked at the effects of deleting sections of the N terminus of the glycoprotein Gc (Shi *et al*., 2009). Twelve cDNA clones were generated with deletions of the N terminus of Gc ranging in size from 50 to 600 amino acid residues, and the authors were able to rescue four mutant viruses. The rescued viruses were attenuated but they still produced Gc protein that would traffic through the Golgi apparatus and achieve cell fusion. Thus, they demonstrated that the N-terminal half of the Gc ectodomain is not required for virus replication. Of the four rescued viruses, the virus with residues 480 to 826 deleted was the least attenuated and thus chosen to have either eGFP or mCherry fluorescent protein inserted. To achieve this, the amino acid residues from 501 to 826 of the glycoprotein precursor were replaced with either foreign gene in the pT7riboBUNM(+) plasmid by using a unique SacI restriction site that was inserted on the M segment at nt 2534 and a natural Bsu36I site that was found at nt 1549. Both constructs yielded viable viruses by reverse genetics, although both viruses were attenuated in plaque size, growth kinetics and viral titre when compared with wild-type virus (Shi *et al*., 2010). Due to the high number of Gc molecules per virion (approximately 650; Obijeski *et al*., 1976b) it was possible to see virus particles in clarified supernatant from cells infected with either of the tagged viruses under a fluorescence microscope.

The Gc fluorescently tagged viruses have been shown to be invaluable tools in the study of BUNV entry, assembly, intracellular trafficking, egress and host cell interactions (Shi *et al*., 2010). Furthermore, the NSm fluorescently tagged viruses have been useful in the study of virus assembly and morphogenesis (Shi *et al*., 2006). All the aforementioned viruses are detectable when analysed under a fluorescence microscope, however, the viruses fluorescently tagged in the Gc protein produce significantly brighter and clearer signals.

In order to further study the effects of IFN on the replication cycle of BUNV, cells which have been treated with IFN could be infected with any of the fluorescently tagged viruses and the observed GFP signal, or lack of, used as a marker of viral infection and inhibition. The NSm GFP tagged viruses are a useful tool and can be used for such experiments as both the wild-type and the NSs deletion viruses have already been rescued. However the signal from these viruses is less clear than rBUNGc-eGFP, but rBUNdelNSs with a Gc GFP tag has not been rescued. Hence I describe here the creation of this recombinant virus.

Rescue of rBUNGceGFPdelNSs virus

BSR-T7/5 cells were transfected with 1.0 µg pT7riboBUNL(+), 1.0 µg pT7riboBUNN and 1.0 µg TVTM-Δ7-E. The pT7riboBUNL(+) plasmid expresses the viral polymerase and the pT7riboBUNN plasmid contains the mutant S segment which does not encode an NSs protein. The TVTM-Δ7-E plasmid encodes the NSm protein and the glycoproteins Gn and the truncated

Gc with eGFP fused to its N terminus. CPE was observed 18 days post transfection and the cell supernatant used to plaque purify the virus using BHK-21 cells. The infected BHK-21 cells were incubated until green plaques were visible by fluorescence microscopy and individual plaques were picked for purification. Amplification was initially in BHK-21 cells and produced many green cells, but a low and impractical titre of $1x10^5$ or less. Thus Vero cells were used for amplification and produced a better yield and a workable titre of 10^6 pfu/ml.

Virus growth in Vero cells

Initially the growth kinetics of the rescued virus rBUNGceGFPdelNSs (GFPdel) were investigated by multistep virus yield assay in comparison with rBUNdelNSs. As GFPdel appeared to be less able to grow in BHK-21 cells than in Vero cells, many of the subsequent experiments were carried out using Vero cells. Cells were infected with either rBUNdelNSs or GFPdel at an MOI of 0.01 pfu/cell and at various times virus released into the growth medium was

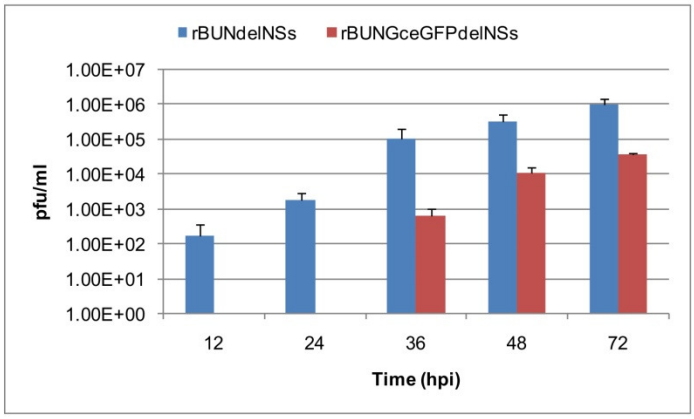

Figure 4.1 : Virus yield from Vero cells infected with rBUNdelNSs or rBUNGceGFPdelNSs. Cells were infected at 0.01 pfu/cell and at the time points indicated a sample of growth medium was removed and used to determine the virus yield by plaque assay. Each value represents the average of triplicate experiments and the error bars show the standard deviation.

collected and titrated by plaque assay. The rBUNdelNSs virus-infected cells released virus that was detected at 12 hours post infection and virus production and release increased throughout the course of the experiment (**Fig 4.1**). However, the GFPdel virus was undetectable for the first 24 hours post infection but did show an overall increase in titre over 72 hours and was significantly attenuated in comparison with rBUNdelNSs (**Fig 4.1**).

To confirm that GFPdel was expressing GFP and that it was detectable under the fluorescence microscope, Vero cells were infected with GFPdel at an MOI of 0.01 pfu/cell and images were taken of the in vivo infection at different times over 72 hours (**Fig 4.2**). At 12 hours post infection there were few green cells which were difficult to find, but at 24 hours post infection GFP expression had increased and there were many clearly observable green cells. After 24 hours the number of cells expressing GFP increased until 72 hours post infection when all the cells were infected and green. This correlates with the increase in titre seen in figure 4.1.

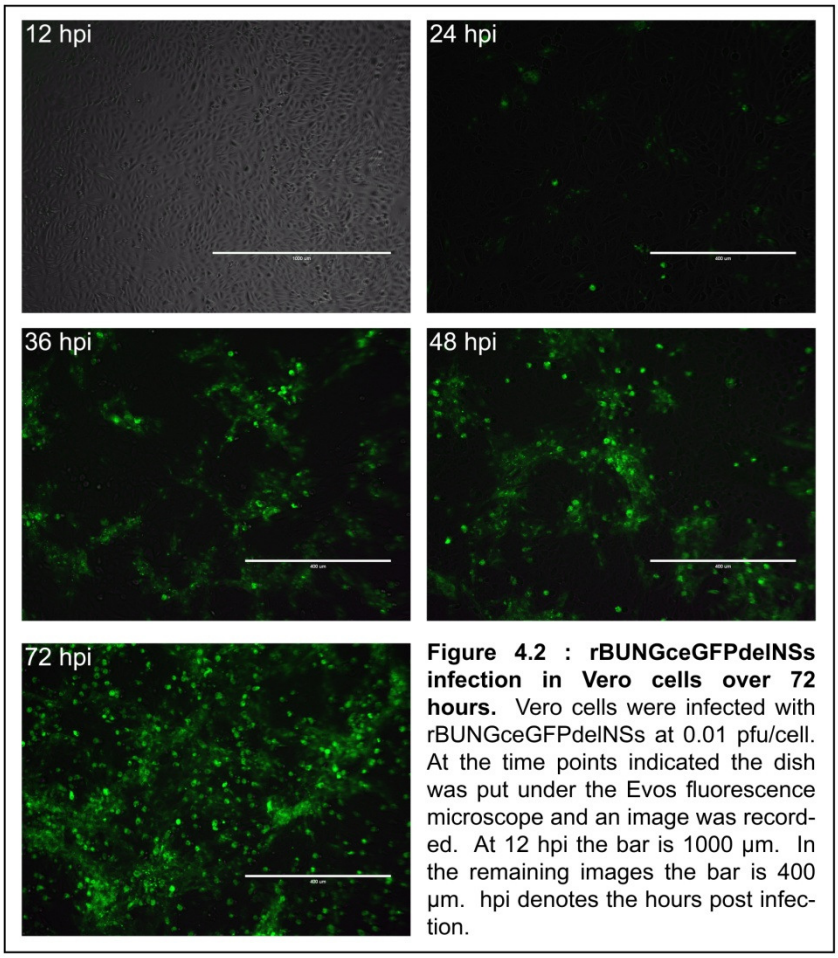

Figure 4.2 : rBUNGceGFPdelNSs infection in Vero cells over 72 hours. Vero cells were infected with rBUNGceGFPdelNSs at 0.01 pfu/cell. At the time points indicated the dish was put under the Evos fluorescence microscope and an image was recorded. At 12 hpi the bar is 1000 µm. In the remaining images the bar is 400 µm. hpi denotes the hours post infection.

GFPdel protein expression

To analyse expression of viral proteins Vero cells were infected at an MOI of 1 pfu/cell with rBUNdelNSs or GFPdel and labelled with [^{35}S]-methionine for one hour at different times. Cell lysates were analysed by SDS-PAGE followed by autoradiography (**Fig 4.3**). Cells infected with rBUNdelNSs showed an increase

Figure 4.3 : In vivo protein labelling of Vero cells mock infected (M) or infected with rBUNdelNSs or rBUNGceGFPdelNSs virus. Cells were infected at 1 pfu/cell and labelling with [^{35}S]-methionine was carried out for 1 h prior to the time points indicated, and then the cells were lysed. 1/30 of the volume of the lysate was loaded per well and analysed by SDS-PAGE and autoradiography. The positions of viral proteins are indicated on the right and by arrows. hpi denotes the hours post infection.

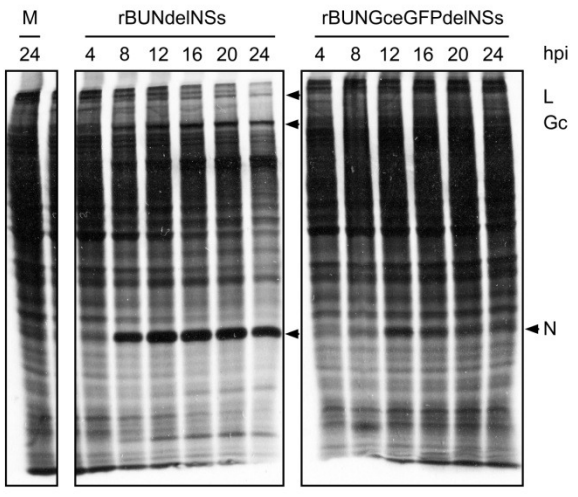

in expression of L, Gc and N proteins up to 16 hours post infection, but then expression was reduced thereafter. In contrast, infection with GFPdel showed significantly reduced expression of L, Gc and N proteins, so that it was difficult to discern viral proteins from cellular proteins except for the N protein; which peaked expression by 12 hours post infection and reduced afterwards. Despite the lack of NSs there was a small degree of host protein synthesis shut-off in rBUNdelNSs infected cells, however shut-off was imperceptible in GFPdel infected cells.

To enable a clearer understanding of the viral protein expression pattern of GFPdel the labelled cell lysate was immunoprecipitated with the anti-BUN antibody and analysed by SDS-PAGE followed by autoradiography (**Fig 4.4**).

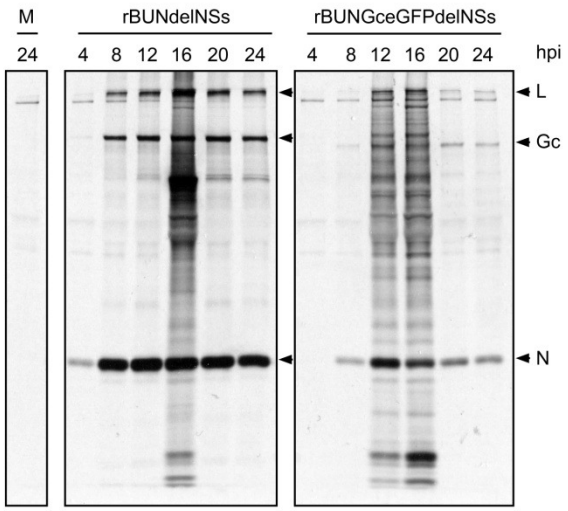

Figure 4.4 : Immunoprecipitation of Vero cells mock infected (M) or infected with rBUNdelNSs or rBUNGceGFPdelNSs. Cells were infected at 1 pfu/cell and labelling with [^{35}S]-methionine was carried out for 1 h prior to the time points indicated, and then the cells were lysed. Using 1/3 of the lysate the soluble antigen extracts were immunoprecipitated with anti-BUN antibody, and the precipitates were analysed by SDS-PAGE and autoradiography. The positions of viral proteins are indicated on the right and by arrows. hpi denotes the hours post infection.

Fig 4.4 shows that infection with rBUNdelNSs yields detectable N, Gc and L protein 4 hours post infection. The levels of N and Gc protein expression peaked at 12 hours post infection and then remained constant until a slight reduction at 24 hours post infection. The L protein expression peaked at 16

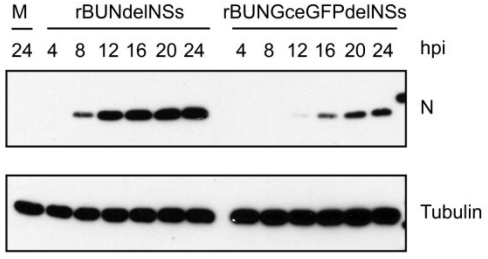

Figure 4.5 : Western blot analysis of Vero cells mock (M) infected or infected with rBUNdelNSs or rBUNGceGFPdelNSs. Cells were infected at 1 pfu/cell and lysed at the time points indicated. 1/30 of the lysate was analysed by SDS-PAGE and then transferred to a nitrocellulose membrane and subjected to Western blotting. N protein (N) was detected using anti-N (rabbit) antibody and tubulin was detected using anti-Tubulin (mouse) antibody. hpi denotes the hours post infection.

hours post infection and decreased thereafter. Viral protein synthesis after infection with GFPdel was much clearer *via* immunoprecipitation. The N and chimeric Gc (which is smaller than wild-type Gc) protein levels peaked at 12 hours post infection and the L protein level peaked at 16 hours post infection

(**Fig 4.4**). After the expression of each of these viral proteins had peaked the expression level then decreased considerably. To further show the GFPdel virus is following a similar replication cycle as rBUNdelNSs only more slowly and thus is attenuated, Western blot analysis was used to detect the viral N protein (**Fig 4.5**). In rBUNdelNSs infected cells N protein was detected at 8 hours post infection and the level increased up to 12 hours after which it remained constant. In GFPdel infected cells, N protein was first detectable at 12 hours and increased in accumulation up to 16 hours and remained constant thereafter. Additionally, Western blot analysis for tubulin was carried out using the same lysate as was used for the protein expression, immunoprecipitation and Western blot experiments and thus acted as a loading control for all three experiments.

RNA analysis of GFPdel

The initial reason for the construction and rescue of GFPdel virus was for use as a tool for screening cell lines for their anti-BUNV effects. As any potential anti-BUNV effects observed could be attributed to an alteration in transcription, the RNA profile of GFPdel was examined, with rBUNdelNSs for comparison. To examine the synthesis of viral genome, anti-genome and mRNA by rBUNdelNSs and GFPdel viruses, Vero cells were infected at an MOI of 1 pfu/cell, lysed for RNA extraction at different times after infection, and the RNA was analysed by Northern blot analysis. The S, M and L segment genomic RNAs for rBUNdelNSs were just detectable at 4 hours post infection and the intensity of the S segment increased throughout the time course whereas the M and L segment intensity increased up to 20 hours and then decreased slightly (**Fig 4.6**). There was an unexplained extra band between the S and M

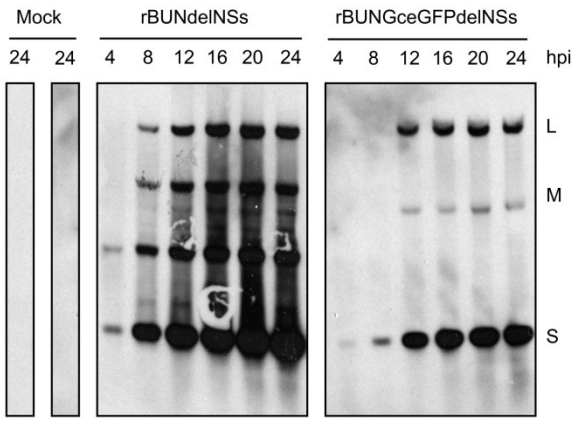

Figure 4.6 : Analysis of genomic viral RNA. Vero cells were mock (M) infected or infected with rBUNdelNSs or rBUNGceGFPdelNSs at 1 pfu/cell. Total RNA was extracted using Trizol at the time points indicated and 10 µg per well was analysed by Northern blotting using probes (+ve probe) complementary to genomic RNA. Viral RNAs are identified on the right. hpi denotes the hours post infection.

segments that has the size of a double-sized S segment, which has been observed previously in some BUNV preparations (R.M.Elliott, personal communication). However, it was not confirmed here as being S segment specific as the blots were carried out using all three segment probes together. The levels of S, M and L genomic RNA of the GFPdel virus were considerably lower than for rBUNdelNSs. The migration of the M segment corresponded with

the replacement of 361 amino acids of Gc with the 238 amino acids of eGFP, a net loss of approximately 400 nucleotides. GFPdel virus replication also appeared to be slower than rBUNdelNSs as S segment RNA was barely detectable at 4 hours post infection and M and L segment RNAs were not detected until 12 hours post infection. Further blots were analysed using probes to detect anti-genomic RNA and mRNA (**Fig 4.7**) and showed that there

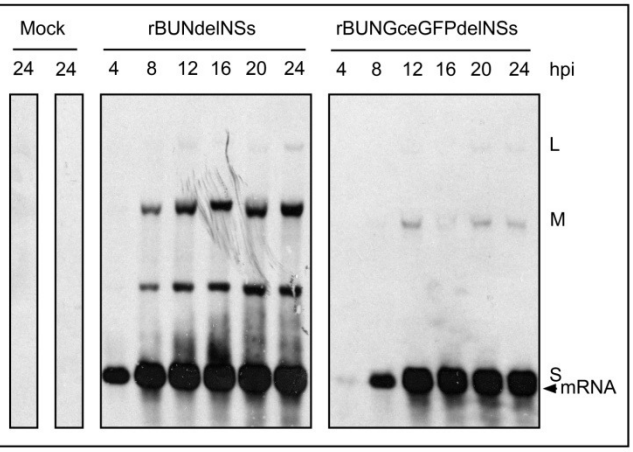

Figure 4.7 : Analysis of anti-genomic viral RNA. Vero cells were mock (M) infected or infected with rBUNdelNSs or rBUNGceGFP-delNSs at 1 pfu/cell. Total RNA was extracted using Trizol at the time points indicated and then 10 µg per well was analysed by Northern blotting using probes (-ve probe) complementary to anti-genomic RNA. Viral RNAs are identified on the right. hpi denotes the hours post infection.

was a strong signal for the S segment anti-genomic RNA and mRNA at 4 hours post infection with rBUNdelNSs, which increased through time points 8 and 12 and then remained fairly constant. The same pattern was seen for the M segment anti-genome and mRNA although it was not detectable until 8 hours post infection, whereas the L segment was not detected. Due to the small differences in size between the L and M segment anti-genomes and their respective mRNAs they are not resolved by electrophoresis. However, there is a difference in size between the S segment anti-genome and the significantly shorter mRNA (961 nt versus approximately 850 nt respectively), which is visible by the broadness of the S segment band in **Fig 4.7**. As was seen with the genomic RNA, the level of anti-genomic RNA and mRNA from GFPdel infected cells was lower than that of rBUNdelNSs infected cells (**Fig 4.7**) and the GFPdel M segment migrated further. The replication of GFPdel was shown to be slower than rBUNdelNSs as S segment anti-genome and mRNA were barely detectable at 4 hours post infection, and M and L segment anti-genome and mRNA were not detectable until 12 hours post infection.

Further to above, the rescued GFPdel virus was also intended for studying the course of infection over 72 hours. To check the stability of GFP in the GFPdel virus the replication cycle was investigated over 72 hours. Vero cells were infected at an MOI of 0.01 pfu/cell with either rBUNdelNSs or GFPdel and labelled with [^{35}S]-methionine for one hour at different times after infection. To enable a clear protein expression profile the cell lysate was immunoprecipitated with anti-BUN antibody and then analysed by SDS-PAGE and autoradiography. It was clear that protein expression with rBUNdelNSs peaked around 36 hours post infection, after which the expression declined and there was much CPE

and cell death, which is characteristic of infection with rBUNdelNSs (**Fig 4.8**). GFPdel infected cells expressed L, Gc and N proteins by 12 hours post infection and the detected levels peaked at 48 hours and then reduced. However, by 48 hours another smaller band was observed which corresponds to the size of the truncated Gc protein minus the GFP tag and, less Gc-eGFP

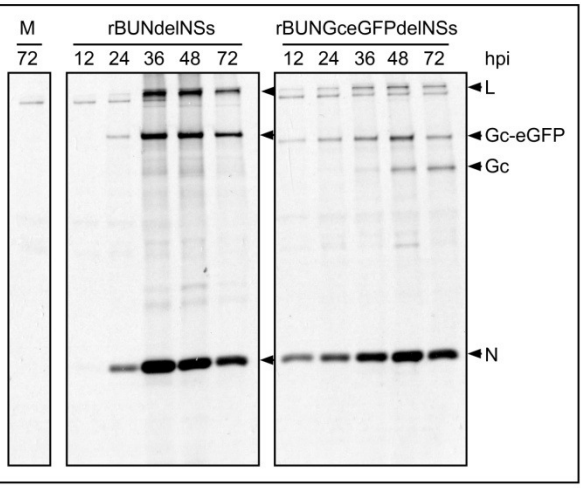

Figure 4.8 : Immunoprecipitation of Vero cells mock infected (M) or infected with rBUNdelNSs or rBUNGceGFPdelNSs. Cells were infected at 0.01 pfu/cell and labelling with [^{35}S]-methionine was carried out for 1 h prior to the time points indicated, and then the cells were lysed. Using 1/3 of the lysate the soluble antigen extracts were immunoprecipitated with anti-BUN antibody, and the precipitates were analysed by SDS-PAGE and autoradiography. The positions of viral proteins are indicated on the right (with arrows in the centre). hpi denotes the hours post infection.

chimeric protein was synthesised at 72 hours compared to truncated Gc. CPE and cell death were not as marked as cells infected with rBUNdelNSs. Western blot analysis to detect N protein accumulation further showed that the pattern was the same for both viruses except that GFPdel accumulated less N protein

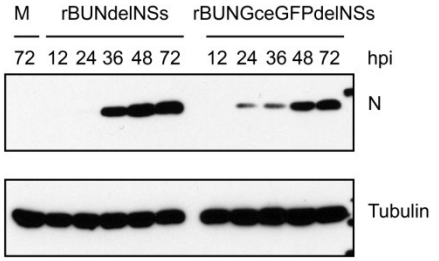

Figure 4.9 : Western blot analysis of Vero cells mock (M) infected or infected with rBUNdelNSs or rBUNGceGFPdelNSs. Cells were infected at 0.01 pfu/cell and lysed at the time points indicated. 1/30 of the lysate was analysed by SDS-PAGE and then transferred to a nitrocellulose membrane and subjected to Western blotting. N protein (N) was detected using anti-N (rabbit) antibody and tubulin was detected using anti-Tubulin (mouse) antibody. hpi denotes the hours post infection.

than rBUNdelNSs (**Fig 4.9**). The tubulin controls confirm that the same amount of protein was loaded into each well for both the labelling experiments and Western blot analysis.

Growth in A549, A549/PIV5/V and A549/BVDV/NPro cells

The attenuation of GFPdel in BHK-21 and Vero cells resulted in a low titre of 10^6 pfu/ml. Although this titre is useable, it had been found that amplifying viruses in A549/PIV5/V cells yielded a higher titre. This is because A549/PIV5/V cells have been transduced to express the PIV5 V protein which blocks IFN signalling by targeting STAT1 for degradation (Andrejeva *et al.*, 2002; Hilton *et al.*, 2006). Another A549 cell line derivative is the A549/BVDV/NPro cells which have been transduced to express the BVDV NPro protease which blocks IFN induction by blocking IRF3 transport into the nucleus by targeting it for degradation (Hale *et al.*, 2009; Hilton *et al.*, 2006).

A549/BVDV/NPro cells are more efficient at blocking IFN production than A549/PIV5/V cells and thus it was thought that they would be the most suitable host for amplification of the GFPdel virus. Multi-step growth cycles of rBUNdelNSs and GFPdel were investigated and compared in these three cell lines. The cells were infected at an MOI of 0.01 pfu/cell and the virus released into the growth medium was collected at different times after infection and titrated by plaque assay. In A549 cells the rBUNdelNSs titre increased by a factor of ten between 12 and 24 hours post infection and then remained

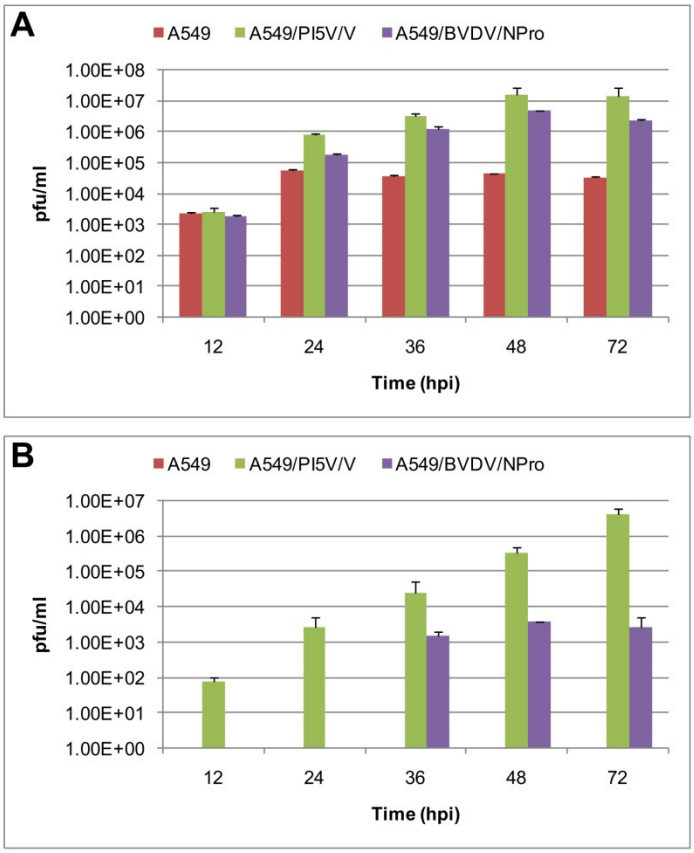

Figure 4.10 : Virus yield from A549, A549/PIV5/V and A549/BVDV/NPro cells infected with rBUNdelNSs (A) or rBUNGceGFPdelNSs (B). Cells were infected at 0.01 pfu/cell and at the time points indicated a sample of growth medium was removed and used to determine the virus yield by plaque assay. Each value represents the average of triplicate experiments and the error bars show the standard deviation.

constant up to 72 hours post infection. However infection in A549/PIV5/V and A549/BVDV/NPro cells yielded higher peak titres of $1.53x10^7$ pfu/ml and $4.75x10^6$ pfu/ml respectively (**Fig 4.10**). In contrast, the GFPdel virus did not grow efficiently in A549 cells, and only reached a peak titre of $3.75x10^3$ pfu/ml in A549/BVDV/NPro cells. However, when grown in A549/PIV5/V cells the titre increased steadily over 72 hours up to $4x10^6$ pfu/ml **(Fig 4.10)**.

In parallel with the virus yield assays above, each of the three cell lines were infected with either rBUNdelNSs or GFPdel and lysed at different times and analysed by Western blotting (**Fig 4.11**). Fig 4.11 confirms that both viruses are unable to synthesise detectable levels of N protein in A549 cells. However, rBUNdelNSs was able to synthesise N protein in both the A549/PIV5/V and A549/BVDV/NPro cell lines, whereas GFPdel was also unable to synthesise detectable levels of N protein in A549/BVDV/NPro, although was able to in

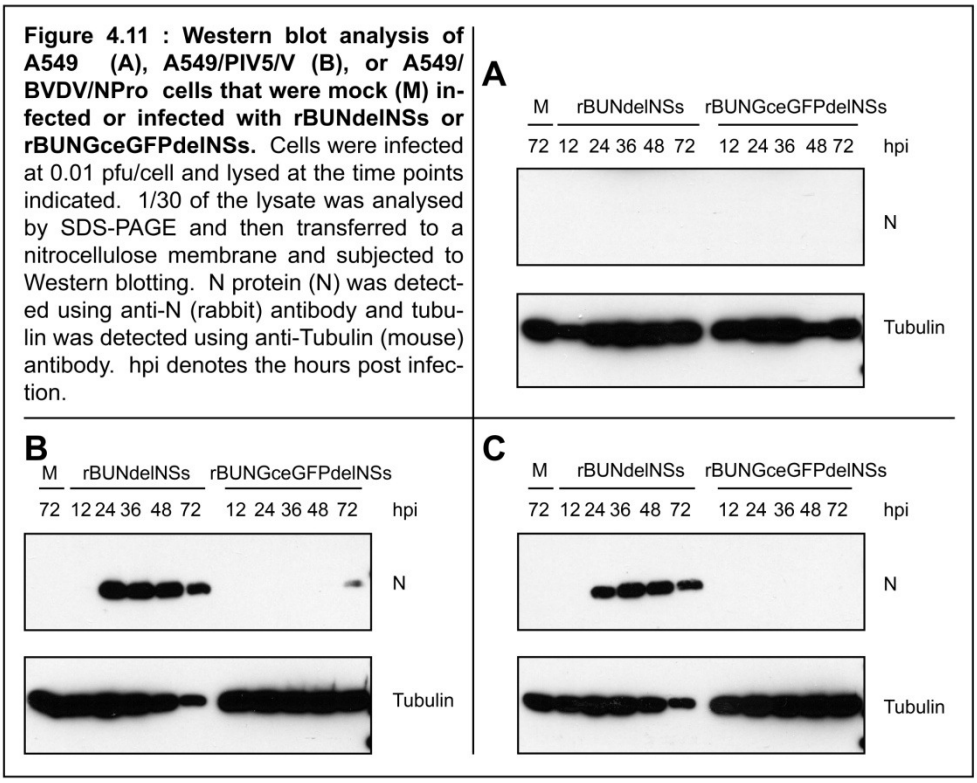

Figure 4.11 : Western blot analysis of A549 (A), A549/PIV5/V (B), or A549/ BVDV/NPro cells that were mock (M) infected or infected with rBUNdelNSs or rBUNGceGFPdelNSs. Cells were infected at 0.01 pfu/cell and lysed at the time points indicated. 1/30 of the lysate was analysed by SDS-PAGE and then transferred to a nitrocellulose membrane and subjected to Western blotting. N protein (N) was detected using anti-N (rabbit) antibody and tubulin was detected using anti-Tubulin (mouse) antibody. hpi denotes the hours post infection.

A549/PIV5/V cells. Thus, N protein synthesis of both viruses in the three cell lines corresponds with the titre of the virus released into the growth medium. Based on these results, GFPdel was amplified in A549/PIV5/V cells.

A549/PIV5/V cells were also infected with GFPdel at an MOI of 0.01 pfu/cell for analysis by fluorescence microscopy. Green cells were visible after 12 hours (**Fig 4.12**) and their number increased up to and peaked at 48 hours. However, at 72 hours there appeared to be less attached cells.

Discussion

The aim for this work was to rescue the GFPdel virus and then to characterise it to ensure that it would be a useful tool for screening cell lines for their anti-BUNV properties. The typical rescue of rBUNV takes approximately four days to yield a titre of around 10^8 pfu/ml, however, the rescue of GFPdel required 18 days and yielded a low viral titre. Furthermore, amplification of GFPdel was inefficient in both BHK-21 and Vero cells, which was unexpected as these cell lines are usually very permissive to bunyavirus infection, replication and subsequent amplification of virus. The GFPdel virus was not expected to replicate in A549 cells as they are fully immunologically functional and this virus is incapable of synthesising the IFN antagonistic NSs protein. However, it was expected to replicate in both A549 cell line derivatives, A549/PIV5/V and A549/BVDV/NPro cells, since these cells express the IFN antagonists the PIV5 V protein and the BVDV NPro protein respectively. In the A549/PIV5/V cells GFPdel grew to a 100-fold higher titre than when grown in Vero cells and, surprisingly, a 1000-fold higher titre than in A549/BVDV/NPro cells. As all three

cell lines have their IFN system inhibited a high viral titre in each was expected. This result implies the innate immune response in Vero and A549/BVDV/NPro cells is sufficient to inhibit the GFPdel virus, whereas the A549/PIV5/V cells are not. This may be because the BVDV/NPro protein blocks IRF3 and thus the

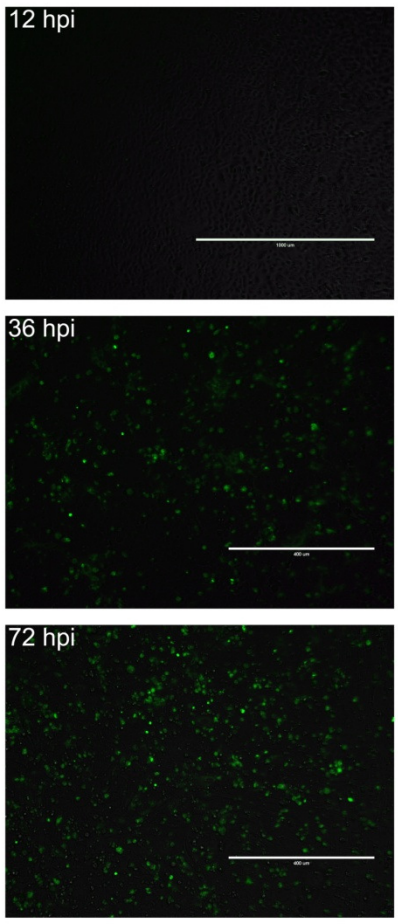

Figure 4.12 : rBUNGceGFPdelNSs infection in A549/PIV5/V cells over 72 hours. A549/PIV5/V cells were infected with rBUNGceGFPdelNSs at 0.01 pfu/cell. At the time points indicated the dish was put under the Evos fluorescence microscope and an image was recorded. At 12 hpi the bar is 1000 µm. In the remaining images the bar is 400 µm. hpi denotes the hours post infection.

synthesis of IFN beta *via* IRF3-induced gene transcription. This does however still allow the synthesis of IFN beta *via* NFκB and thus the antiviral response, whereas the PIV5/V protein blocks IFN signalling and efficiently blocks the antiviral response after the synthesis of IFN and GFPdel virus is able to replicate more easily in the A549/PIV5/V cells. Vero cells are unable to synthesise type I IFN but can produce other types of IFN which can mount the antiviral response. Additionally, the NSs protein has a role in regulation of the viral polymerase protein such that rBUNdelNSs produces more N protein than wt BUNV, which also leads to an earlier onset of apoptosis. However, the double mutation (no NSs and partial deletion of Gc) in GFPdel is further and more severely attenuated compared with rBUNdelNSs. Tracking viral infection by immunofluorescence of the expressed GFP tag shows that GFPdel produces a viable and sustained infection in both Vero and A549/PIV5/V cells and also does not cause the extensive CPE that would be seen in rBUNdelNSs infected cells.

Over the first 24 hours of infection, GFPdel synthesised lower levels of viral proteins but these were easily detectable and followed the same expression pattern as that of rBUNdelNSs. However, the GFPdel genomic M segment migrated further than rBUNdelNSs M and there was a difference between the genomic RNA expression ratio L:M:S when compared with rBUNdelNSs as the GFPdel M segment band was weaker, showing reduced replication of the M segment. Additionally, GFPdel did not cause as much CPE as rBUNdelNSs because the virus is even more attenuated and was not synthesising viral proteins as rapidly or replicating in and infecting as many cells as rBUNdelNSs. Over the time period of 72 hours GFPdel protein expression had a similar pattern to rBUNdelNSs except that the peak level of L, Gc and N protein expression was at 48 hours for GFPdel but 36 hours for rBUNdelNSs, and the overall protein expression and CPE was significantly lower in GFPdel infected cells. Furthermore, after 36 hours the virus began to lose the GFP tag fused to the Gc protein (**Fig 4.8**) and the appearance of a smaller protein band at 48 hours corresponded with the size of the truncated Gc protein without GFP. This could show a problem with translation or it may be due to misfolding of the Gc-eGFP glycoprotein and the resulting slow maturation of the chimeric glycoprotein occurring post-translationally during protein processing. Shi *et al.* (2010) showed that rBUNGc-eGFP started to lose the GFP tag after six passages but when the GFP in rBUNGc-eGFP was replaced by mCherry, the tag sequence was maintained for at least 10 passages. Therefore it is possible that the loss of GFP from GFPdel could be at a nucleotide level which would be seen by sequencing the M segment and Northern blotting. Additionally, the A549/PIV5/V cells infected with GFPdel showed a reduction in green cells from 48 to 72 hours which could be due to the loss or the degradation of the chimeric Gc-eGFP glycoprotein or apoptosis. Although this was not seen in infected Vero cells but GFPdel is more attenuated in Vero cells than A549/PIV5/V cells.

Thus, despite increased attenuation, GFPdel can still be used to follow the course of infection over 24 and 72 hours, although the fluorescence of GFP may decrease after 36 hours due to either the virus losing the GFP tag or to inhibition of the virus or both. The loss of the GFP tag does make it difficult to assess BUNV inhibition by monitoring changes in GFP levels after 36 hours post infection. Therefore this virus is a useful and reliable tool for tracking the course of a BUNV infection and thus for screening cell lines for their anti-BUNV characteristics over 24 hours but not 72 hours.

Summary

This chapter shows:

- The rescue of GFPdel.
- The GFPdel virus is stable over 24 hours but starts to lose the GFP tag 36 hours after infection.
- The A549/PIV5/V cell line is the most permissive to GFPdel infection.
- This GFPdel virus is a useful indicator of infections over 24 hours.

5 Screening of ISG inducible cell lines for Bunyamwera virus replication

Introduction

Chapter One described the induction of IFN and how it results in the upregulation of several hundred ISGs and the subsequent synthesis of antiviral proteins. This chapter concentrates on the antiviral proteins expressed from ISGs. The first part of this chapter describes the effects of over-expressing particular ISGs on BUNV replication as detected by the highly sensitive plaque assay protocol and further by the less sensitive Western blot analysis of N protein accumulation. The second part of the chapter uses imaging techniques to study anti-BUNV properties of cells that over-express different ISGs and the potential of an image based screening protocol for rapid assessment of BUNV inhibition. The immunofluorescence technique is less sensitive than viral plaque formation assay so it can be compared with the plaque assay and Western blot data to establish the overall effectiveness of the technique for screening.

Transfection of cells with ISG cDNA expressing plasmids or siRNA to knockdown ISG mRNA does not ensure that all of the target cell population expresses the transgenic cDNA or has its ISG mRNA targeted, thus the experimental data collected from such experiments may not be clear cut. There are over 300 antiviral proteins produced from ISGs, and the individual knockdown of one of them may be compensated for by one or many of the other ISGs and antiviral proteins synthesised. Therefore, engineering a cell line to over-express an ISG protein when induced averts these problems. Jiang *et al.* (2008) used the human embryonic kidney (HEK293)-derived cell line FLP-IN T REx (Invitrogen) to engineer cells that were able to over-express FLAG tagged individual ISG proteins when induced by tetracycline (Tet). The FLP-IN T REX cell line contains stable integrations of a single flippase (FLP) recombination target (FRT) site, thus, when Jiang *et al.* cotransfected these cells with a plasmid (pcDNA5/FRT/ISG) that contains a FRT site and encodes an ISG along with a plasmid (pOG44) that expresses the recombinase Flp IN, the ISG cDNA was integrated into the cellular genome through the FRT site with its expression under the control of the TET-on promoter (**Fig 5.1**). This method was used to create 29 cell lines (kindly donated by Ju-Tao Guo, Drexel University College of Medicine, USA); 26 that over-express an individual ISG protein, 2 that over-express a mutant ISG protein, and one that over-expresses the chloramphenicol acetyl transferase (CAT) protein without a FLAG tag. Using these ISG over-expressing cells, the following section investigates the effects of various ISGs on BUNV and rBUNdelNSs replication and further tests the competency of three GFP-tagged viruses for screening these cell lines for

their anti-BUNV characteristics. Chapter Four described the three GFP-tagged viruses rBUNGc-eGFP, rBUNM-NSm-EGFP (BUNGFP) and rBUNM-NSm-EGFPDelNSs (NSmGFPdel) in detail. The practicalities of performing the experiments presented below proved more difficult than expected as the HEK ISG cells adhered loosely to tissue culture plate wells and cover slips thus requiring alterations to standard protocols and extra care throughout. Some of

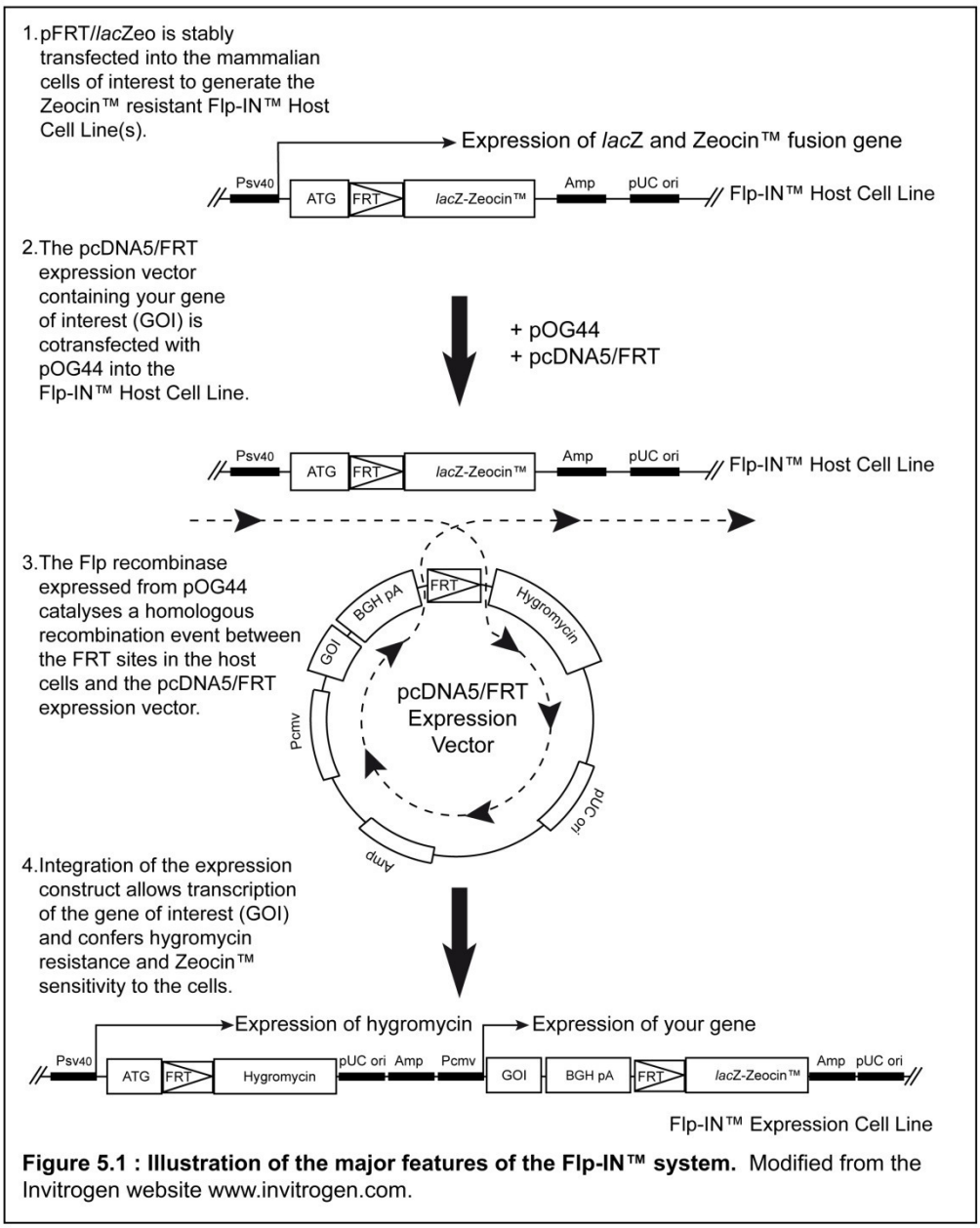

Figure 5.1 : Illustration of the major features of the Flp-IN™ system. Modified from the Invitrogen website www.invitrogen.com.

the cells were extremely sensitive, in culture, particularly requiring high quality cell maintenance. There are over 300 ISGs and many are barely understood, although most used in this study have a known function in innate immunity.

Growth kinetics and N protein synthesis in HEK ISG cells

To induce expression of the ISG in each of the HEK293 ISG expressing cell lines (hereon after the inducible ISG cell line will have the ISG incorporated into

the cell line name e.g. the PKR inducible cell line will be called HEK PKR) the cells were incubated with 1 µg/ml of Tet for 48 hours prior to infection. The cells were then infected with BUNV or rBUNdelNSs at an MOI of 0.01 pfu/ml after which the virus released into the medium at various time points was titrated by plaque assay. Furthermore, duplicate wells were set up and infected with either rBUNGc-eGFP or BUNGFP or NSmGFPdel viruses at an MOI of 1 pfu/ml and lysed 24 hours post infection for Western blot analysis for the ISG, N and tubulin proteins. The data collected for each cell line are presented below.

Negative control

The first cell line tested was the HEK CAT cells which were used as a negative control. Infection of both the uninduced and the induced cells with either BUNV

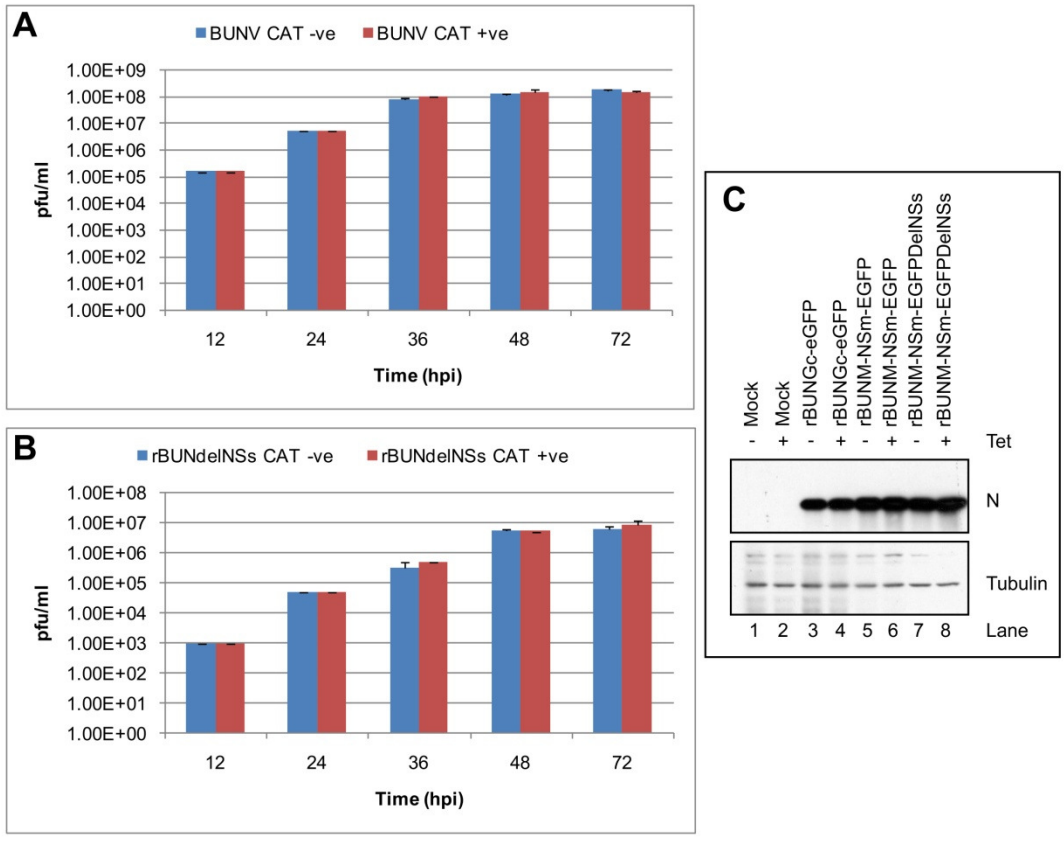

Figure 5.2 : Virus yield and N protein synthesis from virus infected HEK CAT cells. Cells were either not induced (-ve) or induced (+ve) and then infected with BUNV **(A)** or rBUNdelNSs **(B)** at 0.01 pfu/cell and at the time points indicated a sample of growth medium was removed and used to determine the virus yield by plaque assay. Each value represents the average of triplicate experiments and the error bars show the standard deviation. hpi denotes hours post infection. **(C)** Uninduced (-Tet) or induced (+Tet) cells were either mock infected or infected with either rBUNGc-eGFP, rBUNM-NSm-EGFP, or rBUNM-NSm-EGFPDelNSs virus at 1 pfu/cell. Twenty four hours later the cells were lysed and 1/30 of the lysate was analysed by SDS-PAGE and transferred to a nitrocellulose membrane and subjected to Western blotting using anti-FLAG (rabbit) antibody for ISG detection and N and tubulin proteins were detected using anti-N (rabbit) antibody and anti-Tubulin (mouse) antibody respectively. Proteins are labelled on the right hand side.

or rBUNdelNSs showed no change in the viral yield (**Fig 5.2A and 5.2B**) or the amount of N protein synthesised (**Fig 5.2C**). In this cell line the CAT gene has

not been replaced with an ISG thus there is no induced FLAG-tagged protein to detect.

To investigate whether the GFP-tagged viruses would give accurate reflections of the growth kinetics of BUNV and rBUNdelNSs the two cell lines HEK 38348 and HEK PKR cells were selected to be tested with the two NSm GFP-tagged viruses BUNGFP and NSmGFPdel.

FLJ38348

FLJ38348 is also known as coiled-coil domain containing 75 (CCDC75) protein and is 30 kDa in size (Rani *et al.*, 2007). The function of this protein is unknown

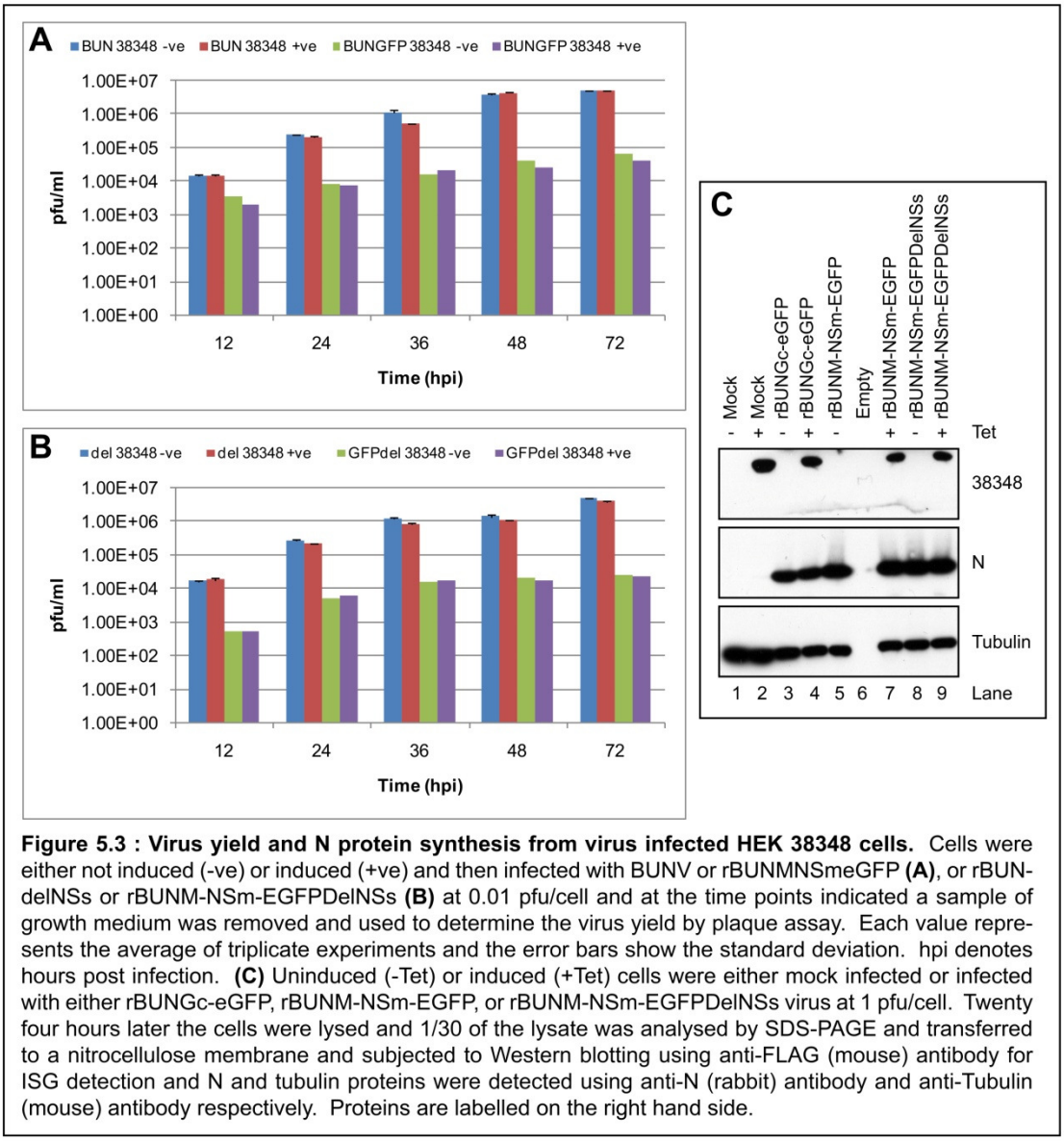

Figure 5.3 : Virus yield and N protein synthesis from virus infected HEK 38348 cells. Cells were either not induced (-ve) or induced (+ve) and then infected with BUNV or rBUNMNSmeGFP **(A)**, or rBUNdelNSs or rBUNM-NSm-EGFPDelNSs **(B)** at 0.01 pfu/cell and at the time points indicated a sample of growth medium was removed and used to determine the virus yield by plaque assay. Each value represents the average of triplicate experiments and the error bars show the standard deviation. hpi denotes hours post infection. **(C)** Uninduced (-Tet) or induced (+Tet) cells were either mock infected or infected with either rBUNGc-eGFP, rBUNM-NSm-EGFP, or rBUNM-NSm-EGFPDelNSs virus at 1 pfu/cell. Twenty four hours later the cells were lysed and 1/30 of the lysate was analysed by SDS-PAGE and transferred to a nitrocellulose membrane and subjected to Western blotting using anti-FLAG (mouse) antibody for ISG detection and N and tubulin proteins were detected using anti-N (rabbit) antibody and anti-Tubulin (mouse) antibody respectively. Proteins are labelled on the right hand side.

but it is induced by IFN (Jiang *et al.*, 2008). FLJ38348 protein contains a short conserved region (~40 amino acids) called a G-patch domain which also occurs in some putative RNA-binding proteins; therefore its function may involve binding to RNA. The induced HEK 38348 cells infected with BUNV and

BUNGFP virus showed no change in viral yield compared with the uninduced cells (**Fig 5.3A**). When infected with rBUNdelNSs or NSmGFPdel the induced cells yielded the same amount of virus as the uninduced cells (**Fig 5.3B**). Although the yield of virus from BUNGFP infected cells was nearly 100-fold lower than BUNV infected cells and the cells infected with NSmGFPdel yielded over 100-fold lower virus than those infected with rBUNdelNSs. This was predicted as, based on previous work, the GFP-tagged viruses are known to be attenuated. The amount of N protein synthesised by the three tagged viruses was the same in uninduced and induced cells (**Fig 5.3C**).

PKR

PKR, described in Chapter One, is activated by dsRNA which results in its autophosphorylation, and phosphorylated PKR phosphorylates eIF2α and this

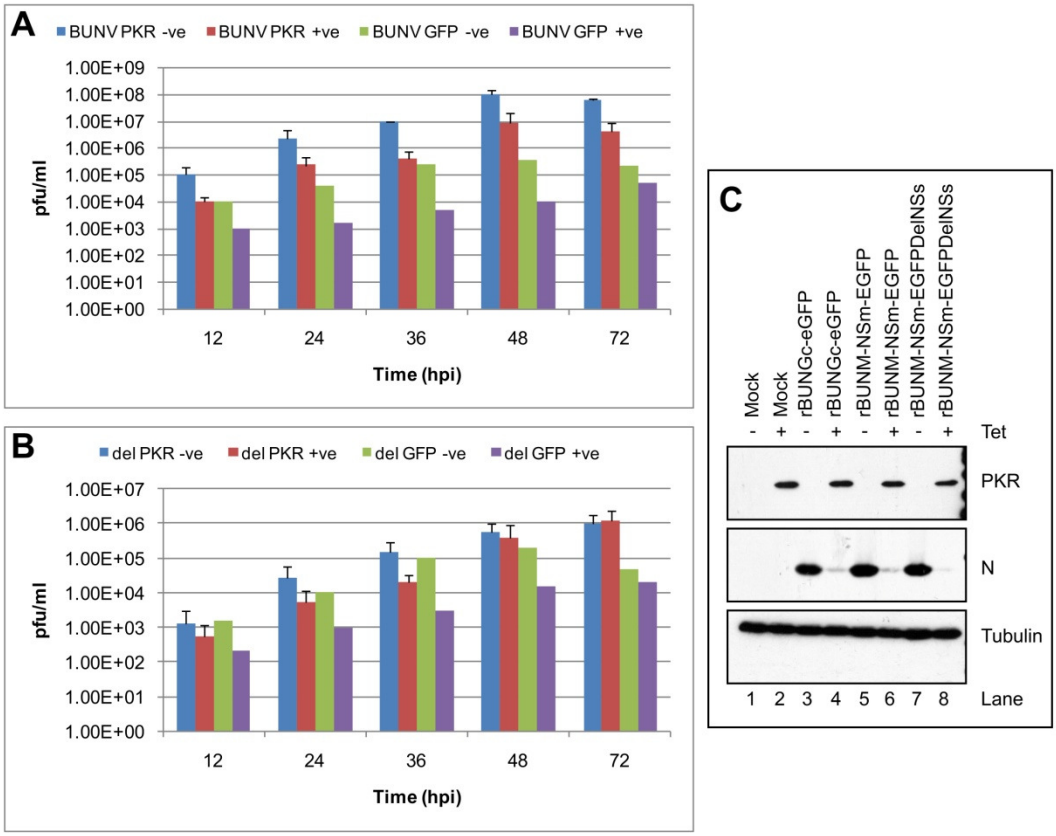

Figure 5.4 : Virus yield and N protein synthesis from virus infected HEK PKR cells. Cells were either not induced (-ve) or induced (+ve) and then infected with BUNV or rBUNMNSmeGFP **(A)**, or rBUNdelNSs or rBUNM-NSm-EGFPDelNSs **(B)** at 0.01 pfu/cell and at the time points indicated a sample of growth medium was removed and used to determine the virus yield by plaque assay. Each value represents the average of triplicate experiments and the error bars show the standard deviation. hpi denotes hours post infection. **(C)** Uninduced (-Tet) or induced (+Tet) cells were either mock infected or infected with either rBUNGc-eGFP, rBUNM-NSm-EGFP, or rBUNM-NSm-EGFPDelNSs virus at 1 pfu/cell. Twenty four hours later the cells were lysed and 1/30 of the lysate was analysed by SDS-PAGE and transferred to a nitrocellulose membrane and subjected to Western blotting using anti-FLAG (mouse) antibody for ISG detection and N and tubulin proteins were detected using anti-N (rabbit) antibody and anti-Tubulin (mouse) antibody respectively. Proteins are labelled on the right hand side.

in turn blocks cell protein synthesis (Garcia *et al.*, 2006). Compared with uninduced cells, induced HEK PKR cells infected with BUNV showed a ten-fold reduction in virus yield in the first 24 hours and this reduction further increased through the rest of the 72 hour infection period (**Fig 5.4A**). A similar trend was observed for the induced cells infected with BUNGFP although the degree of inhibition was larger (**Fig 5.4A**). After infection with rBUNdelNSs the induced HEK PKR cells showed greater restriction on virus yield in the first 36 hours post infection but by 72 hours this was reversed and induced PKR appeared to enhance the yield of virus (**Fig 5.4B**). The level of inhibition on viral yield observed in the induced cells infected with NSmGFPdel peaked at 36 hours and reduced thereafter (**Fig 5.4B)**. Western blot analysis showed a significant

reduction in the amount of N protein produced in induced cells (**Fig 5.4C** lanes 4, 6 and 8) compared with uninduced cells (**Fig 5.4C** lanes 3, 5 and 7) infected with any of the three GFP-tagged viruses. Additionally the intensity of the N protein band for each virus in the uninduced cells was similar (**Fig 5.4C** lanes 3, 5 and 7). Thus the Western blot data correlates with the lower viral yield observed in the induced HEK PKR cells.

HEK PKRM cells over-express a mutant form of PKR that has the conserved lysine residue in the ATP binding pocket replaced with an arginine residue, yielding a dominant negative PKR unable to carry out its protein kinase activity (Jiang *et al.*, 2008). When HEK PKRM cells were induced and infected with BUNV there was no difference in viral yield compared with uninduced cells (**Fig 5.5A**). Furthermore when induced HEK PKRM cells were infected with rBUNdelNSs there was no significant variation in viral yield (**Fig 5.5B**). Western blot analysis of N protein confirmed no change in the amount of N produced in either uninduced or induced cells for all three viruses (**Fig 5.5C**). Thus, there was no effect on the viral yield in the presence of dominant negative PKR in the induced HEK PKRM cells.

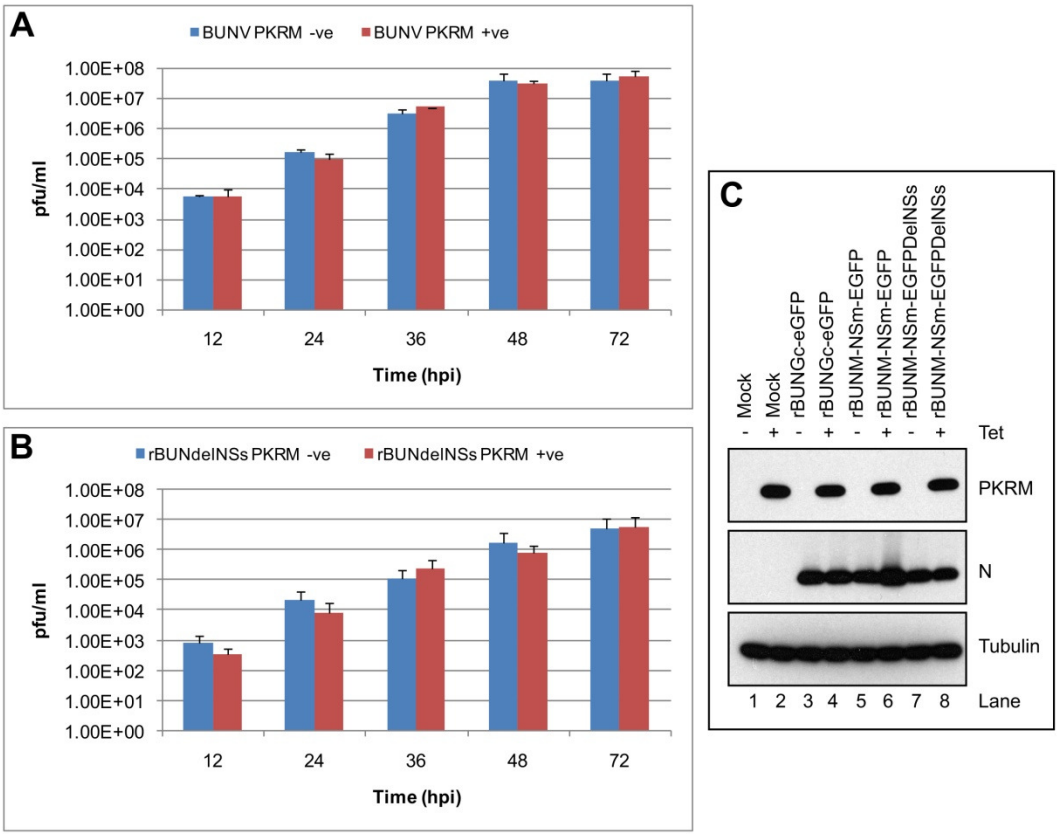

Figure 5.5 : Virus yield and N protein synthesis from virus infected HEK PKRM cells. Cells were either not induced (-ve) or induced (+ve) and then infected with BUNV **(A)** or rBUNdelNSs **(B)** at 0.01 pfu/cell and at the time points indicated a sample of growth medium was removed and used to determine the virus yield by plaque assay. Each value represents the average of triplicate experiments and the error bars show the standard deviation. hpi denotes hours post infection. **(C)** Uninduced (-Tet) or induced (+Tet) cells were either mock infected or infected with either rBUNGc-eGFP, rBUNM-NSm-EGFP, or rBUNM-NSm-EGFPDelNSs at 1 pfu/cell. Twenty four hours later the cells were lysed and 1/30 of the lysate was analysed by SDS-PAGE and transferred to a nitrocellulose membrane and subjected to Western blotting using anti-FLAG (mouse) antibody for ISG detection and N and tubulin proteins were detected using anti-N (rabbit) antibody and anti-Tubulin (mouse) antibody respectively. Proteins are labelled on the right hand side.

ISG56

ISG56 is also known as interferon-induced protein with tetratricopeptide repeats 1 (IFIT1) and is a 55.3 kDa protein that inhibits the ability of the eIF3e subunit, of the eIF3 complex, to stabilise the eIF2-GTP-tRNAi^{Met} complex thereby inhibiting translation (Fensterl & Sen, 2011). Additionally ISG56 contains multiple tetratricopeptide motifs which are able to form scaffolds between

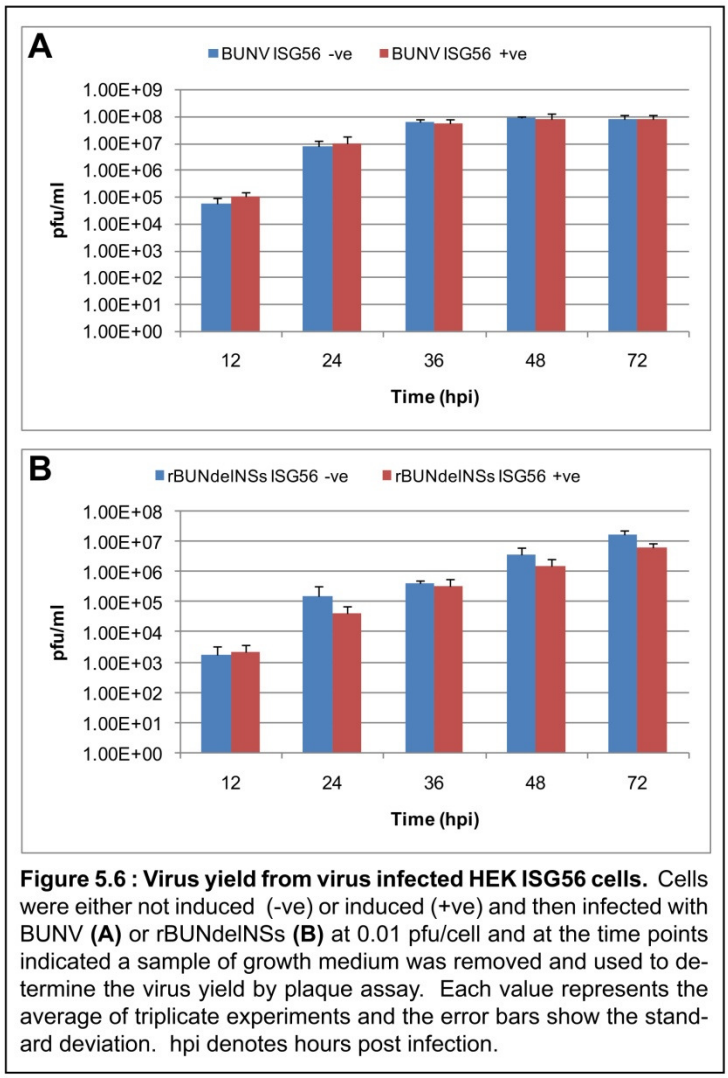

Figure 5.6 : Virus yield from virus infected HEK ISG56 cells. Cells were either not induced (-ve) or induced (+ve) and then infected with BUNV **(A)** or rBUNdelNSs **(B)** at 0.01 pfu/cell and at the time points indicated a sample of growth medium was removed and used to determine the virus yield by plaque assay. Each value represents the average of triplicate experiments and the error bars show the standard deviation. hpi denotes hours post infection.

tandem tetratricopeptide repeats and mediate protein-protein interactions (Lamb *et al.*, 1995). When the induced HEK ISG56 cells were infected with BUNV there was little change in the viral yield compared with uninduced cells (**Fig 5.6A**), but induced cells infected with rBUNdelNSs showed more variation in viral yield (**Fig 5.6B**). Western blot analysis showed no difference in the amount of N protein between infected uninduced or induced cells (data not shown).

PLSCR1 and PLSCR2

Scramblase enzymes are involved in the translocation of phospholipids between the lipid bilayer of the cell membrane and are activated by an increase in cytosolic calcium which results in the redistribution of phospholipids (Sahu *et al.*, 2007). Phospholipid scramblase 1 (PLSCR1) is highly induced by type I and II IFNs and also by various growth factors and is thought to play a role in the upregulation of the IFN response and subsequently induced antiviral proteins. Knockdown of PLSCR1 in human cells by siRNA rendered the cells more susceptible to VSV infection and yielded higher titres (Dong *et al.*, 2004).

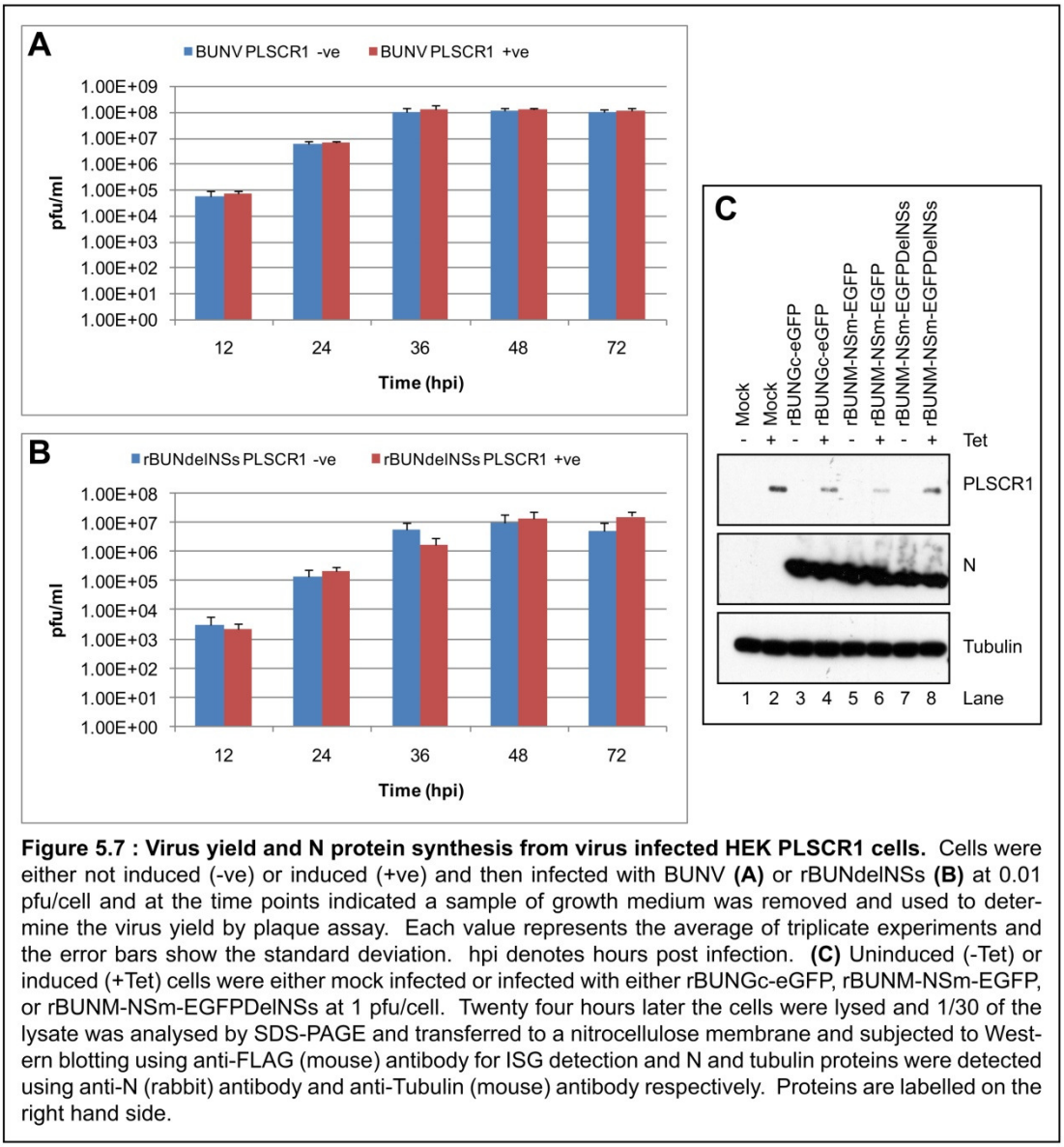

Figure 5.7 : Virus yield and N protein synthesis from virus infected HEK PLSCR1 cells. Cells were either not induced (-ve) or induced (+ve) and then infected with BUNV **(A)** or rBUNdelNSs **(B)** at 0.01 pfu/cell and at the time points indicated a sample of growth medium was removed and used to determine the virus yield by plaque assay. Each value represents the average of triplicate experiments and the error bars show the standard deviation. hpi denotes hours post infection. **(C)** Uninduced (-Tet) or induced (+Tet) cells were either mock infected or infected with either rBUNGc-eGFP, rBUNM-NSm-EGFP, or rBUNM-NSm-EGFPDelNSs at 1 pfu/cell. Twenty four hours later the cells were lysed and 1/30 of the lysate was analysed by SDS-PAGE and transferred to a nitrocellulose membrane and subjected to Western blotting using anti-FLAG (mouse) antibody for ISG detection and N and tubulin proteins were detected using anti-N (rabbit) antibody and anti-Tubulin (mouse) antibody respectively. Proteins are labelled on the right hand side.

Furthermore PLSCR1 requires palmitoylation in order to be inserted into the membrane and when this does not occur, PLSCR1 is relocated to the nucleus where it binds to DNA and ultimately leads to enhanced expression of several antiviral ISGs (Dong *et al.*, 2004). Over the course of 72 hours the HEK PLSCR1 induced cells infected with BUNV showed no change in the viral yield

compared with the uninduced cells (**Fig 5.7A**). Similarly, when infected with rBUNdelNSs there was little variation in viral yield (**Fig 5.7B**). Furthermore, the Western blot showed no change in the accumulation of N protein from any of the three GFP viruses (**Fig 5.7C**). The PLSCR1 related isoform PLSCR2 plays

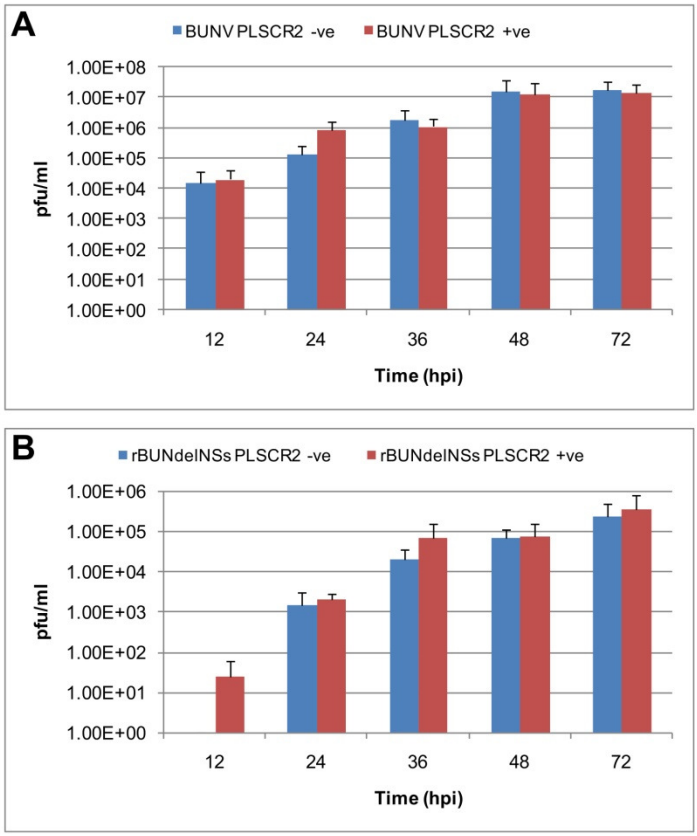

Figure 5.8 : Virus yield from virus infected HEK PLSCR2 cells. Cells were either not induced (-ve) or induced (+ve) and then infected with BUNV **(A)** or rBUNdelNSs **(B)** at 0.01 pfu/cell and at the time points indicated a sample of growth medium was removed and used to determine the virus yield by plaque assay. Each value represents the average of triplicate experiments and the error bars show the standard deviation. hpi denotes hours post infection.

a role in the bidirectional transbilayer migration of phospholipids leading to the loss of asymmetry of the phospholipids of the plasma membrane. The induced HEK PLSCR2 cells infected with BUNV resulted in no significant change in viral yield (**Fig 5.8A**), which was also observed for the induced cells infected with rBUNdelNSs (**Fig 5.8B**).

ADAR1

Members of the adenosine deaminase class of enzymes function to edit RNA by deaminating adenosine residues within double-stranded RNA thus generating inosine residues (Samuel, 2011). One of the consequences of this enzymatic activity is the introduction of mutations into viral RNA genomes. The 136 kDa Adenosine Deaminase Acting on RNA (ADAR) 1 protein is upregulated by IFN, is located in the cytoplasm and is responsible for hypermutation of viral RNA (Gelinas *et al*., 2011). The HEK ADAR1 cells infected with BUNV showed

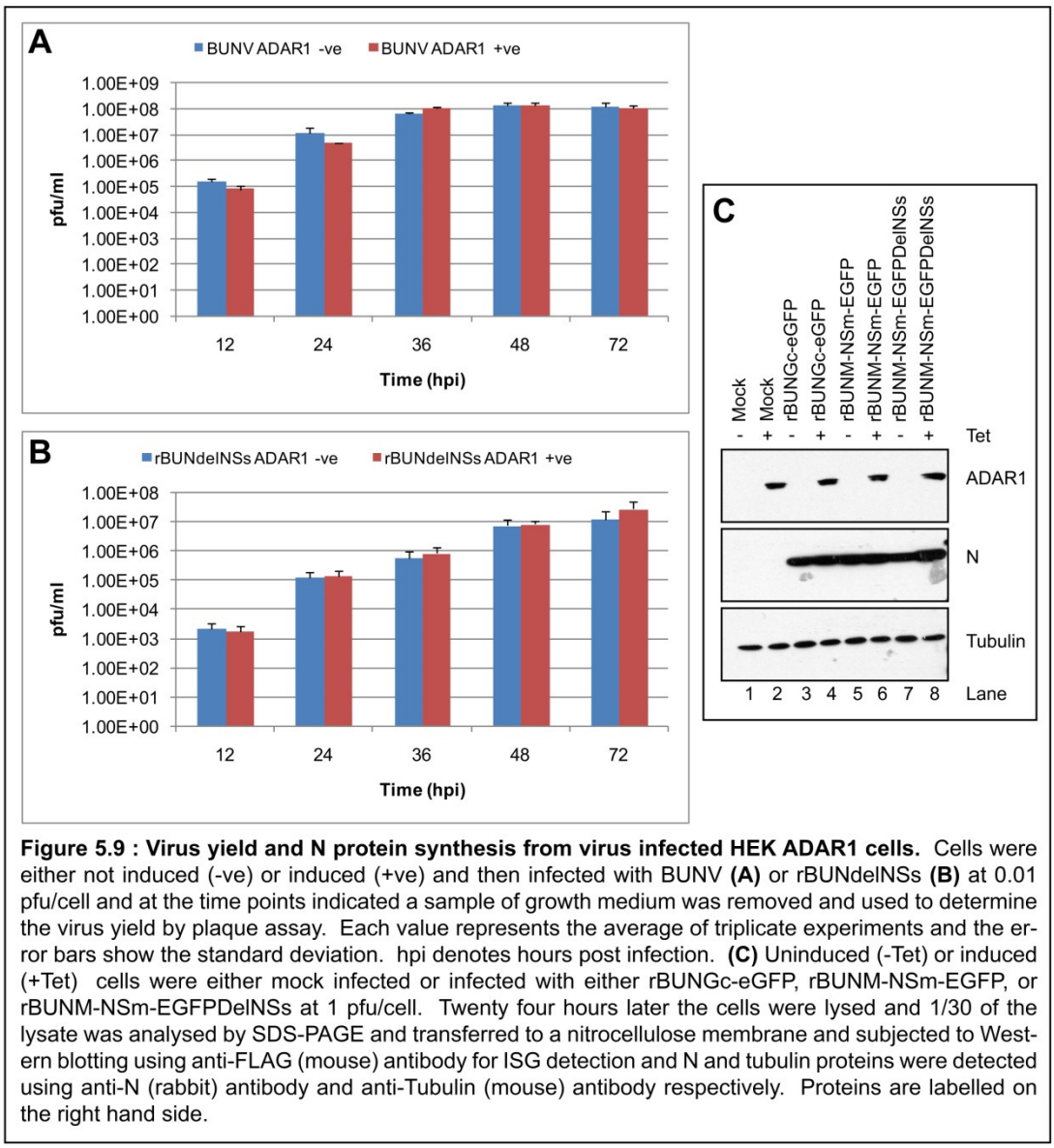

Figure 5.9 : Virus yield and N protein synthesis from virus infected HEK ADAR1 cells. Cells were either not induced (-ve) or induced (+ve) and then infected with BUNV **(A)** or rBUNdelNSs **(B)** at 0.01 pfu/cell and at the time points indicated a sample of growth medium was removed and used to determine the virus yield by plaque assay. Each value represents the average of triplicate experiments and the error bars show the standard deviation. hpi denotes hours post infection. **(C)** Uninduced (-Tet) or induced (+Tet) cells were either mock infected or infected with either rBUNGc-eGFP, rBUNM-NSm-EGFP, or rBUNM-NSm-EGFPDelNSs at 1 pfu/cell. Twenty four hours later the cells were lysed and 1/30 of the lysate was analysed by SDS-PAGE and transferred to a nitrocellulose membrane and subjected to Western blotting using anti-FLAG (mouse) antibody for ISG detection and N and tubulin proteins were detected using anti-N (rabbit) antibody and anti-Tubulin (mouse) antibody respectively. Proteins are labelled on the right hand side.

no significant reduction in BUNV yield between uninduced and induced cells throughout 72 hours (**Fig 5.9A**). Infection with rBUNdelNSs also showed no change in yield between the cells throughout (**Fig 5.9B**), and Western blot analysis detected no alteration in the amount of N protein produced from any of the three GFP-tagged viruses (**Fig 5.9C**).

MTAP44

MTAP44 is also known as IFN-induced protein 44 (IFI44) and is part of the IFI superfamily (Hallen *et al.*, 2007). MTAP44 is a 50 kDa protein comprising 444 amino acids, and it aggregates to form microtubular structures. The induced HEK MTAP44 cells infected with BUNV showed a reduced viral yield from 12 hours through to 72 hours with an 18-fold reduction at 36 hours lowering to a 6-fold reduction by 72 hours (**Fig 5.10A**). However, the induced cells infected with rBUNdelNSs virus showed no inhibition in yield until 36 hours post infection which showed a 4-fold reduction which further increased to a 12-fold reduction

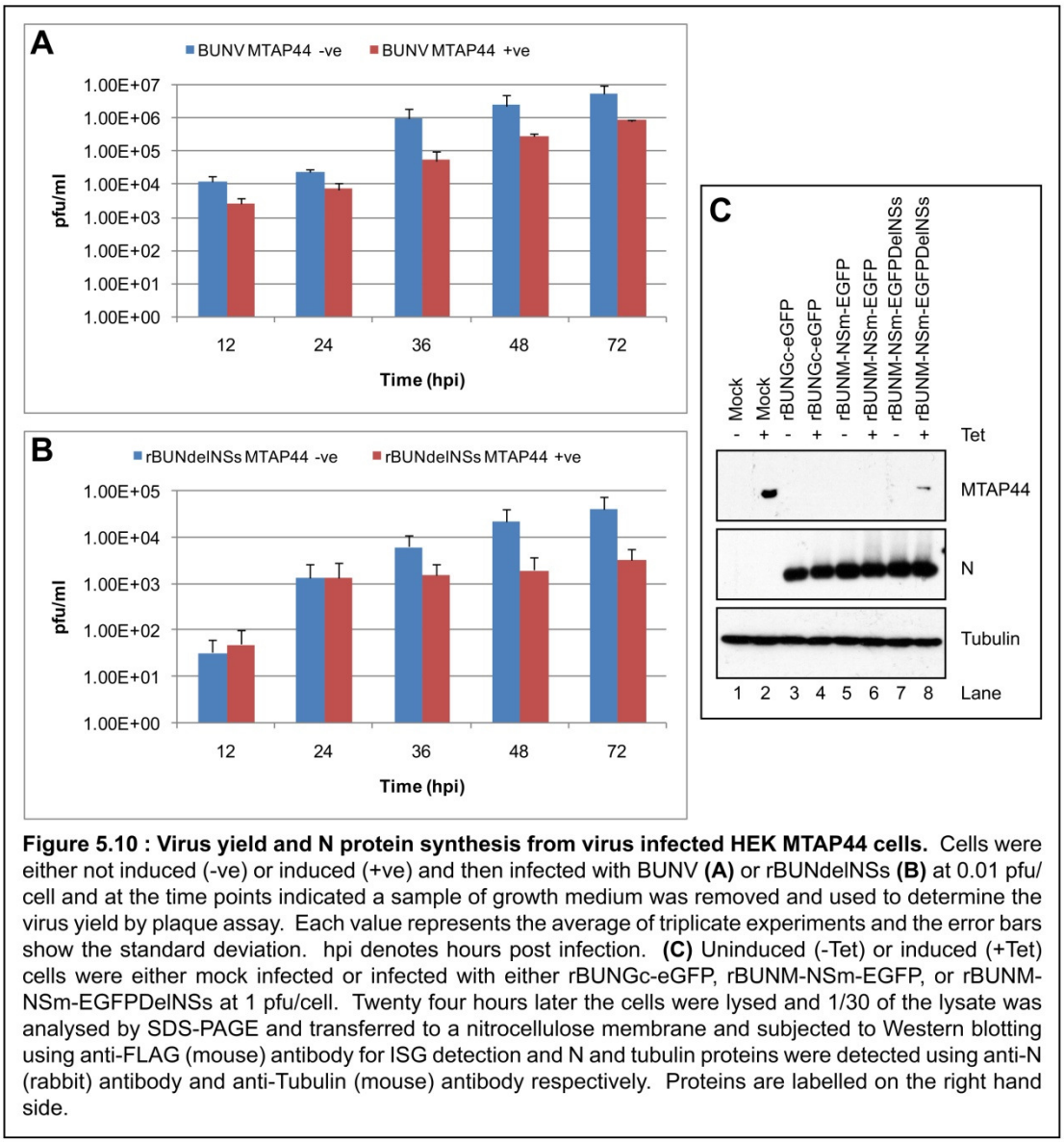

Figure 5.10 : Virus yield and N protein synthesis from virus infected HEK MTAP44 cells. Cells were either not induced (-ve) or induced (+ve) and then infected with BUNV **(A)** or rBUNdelNSs **(B)** at 0.01 pfu/cell and at the time points indicated a sample of growth medium was removed and used to determine the virus yield by plaque assay. Each value represents the average of triplicate experiments and the error bars show the standard deviation. hpi denotes hours post infection. **(C)** Uninduced (-Tet) or induced (+Tet) cells were either mock infected or infected with either rBUNGc-eGFP, rBUNM-NSm-EGFP, or rBUNM-NSm-EGFPDelNSs at 1 pfu/cell. Twenty four hours later the cells were lysed and 1/30 of the lysate was analysed by SDS-PAGE and transferred to a nitrocellulose membrane and subjected to Western blotting using anti-FLAG (mouse) antibody for ISG detection and N and tubulin proteins were detected using anti-N (rabbit) antibody and anti-Tubulin (mouse) antibody respectively. Proteins are labelled on the right hand side.

by 72 hours (**Fig 5.10B**). Western blot analysis detected no change in the amount of N protein produced by any of the three GFP-tagged viruses (**Fig 5.10C**). The FLAG-tagged MTAP44 itself was difficult to detect using Western blotting techniques but was shown to be inducible with Tet pre-treatment (**Fig 5.10**, lane 2). Therefore the system of MTAP44 induction by Tet was reliable

and could be used to test MTAP44 for inhibitory effects on BUNV *via* virus yield assays but the detection of MTAP44 by Western blot was not reliable.

BST2

BST2 also known as tetherin, is a 19.7 kDa type II transmembrane glycoprotein that has been shown to restrict the release of virions from cells by forming a proteinacious link that tethers the virion to the surface of the cell (Kaletsky *et al.*, 2009; Neil *et al.*, 2007; Yondola *et al.*, 2011). The induced HEK BST2 cells infected with BUNV showed a five-fold reduction in viral yield by 48 hours

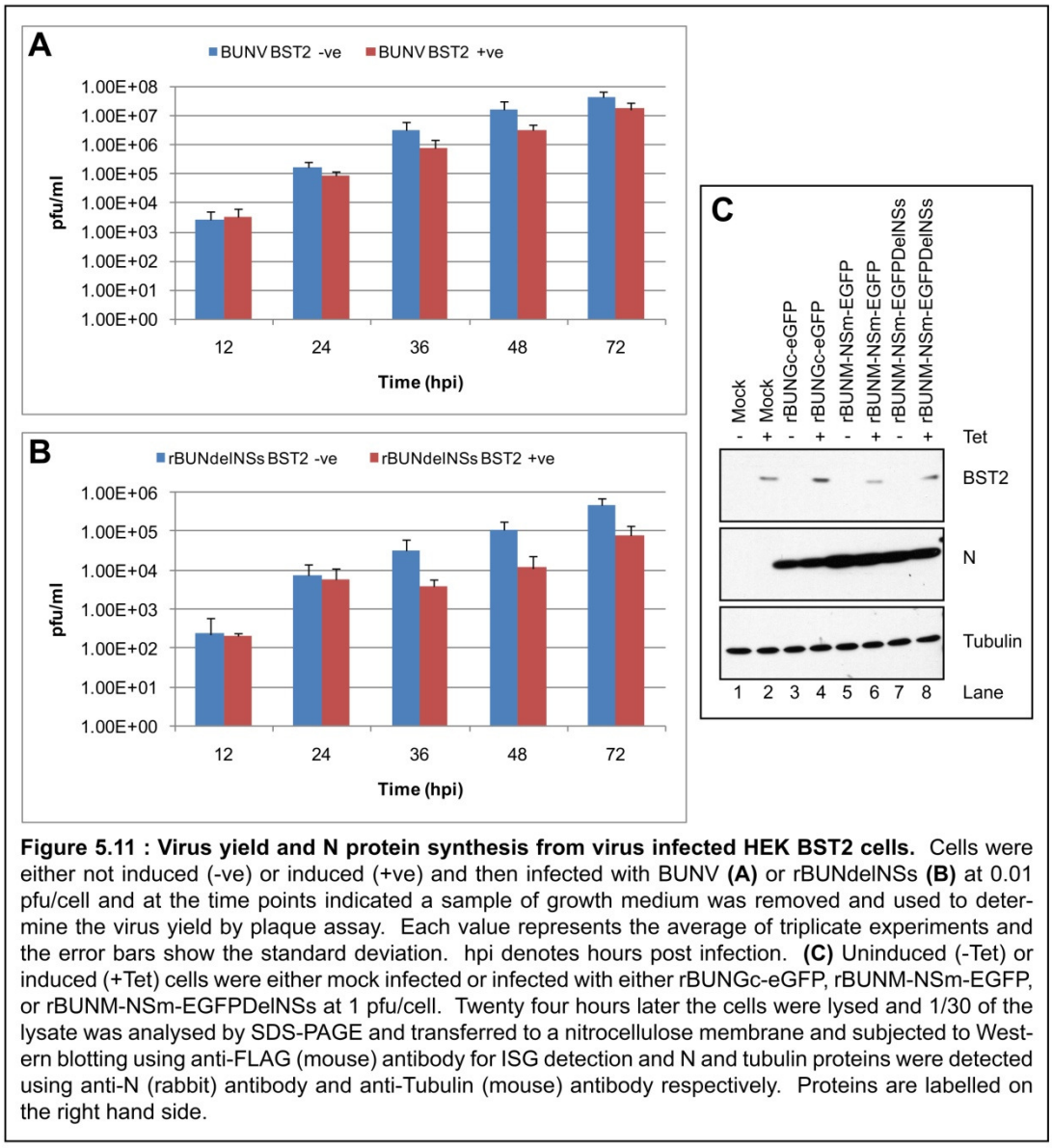

Figure 5.11 : Virus yield and N protein synthesis from virus infected HEK BST2 cells. Cells were either not induced (-ve) or induced (+ve) and then infected with BUNV **(A)** or rBUNdelNSs **(B)** at 0.01 pfu/cell and at the time points indicated a sample of growth medium was removed and used to determine the virus yield by plaque assay. Each value represents the average of triplicate experiments and the error bars show the standard deviation. hpi denotes hours post infection. **(C)** Uninduced (-Tet) or induced (+Tet) cells were either mock infected or infected with either rBUNGc-eGFP, rBUNM-NSm-EGFP, or rBUNM-NSm-EGFPDelNSs at 1 pfu/cell. Twenty four hours later the cells were lysed and 1/30 of the lysate was analysed by SDS-PAGE and transferred to a nitrocellulose membrane and subjected to Western blotting using anti-FLAG (mouse) antibody for ISG detection and N and tubulin proteins were detected using anti-N (rabbit) antibody and anti-Tubulin (mouse) antibody respectively. Proteins are labelled on the right hand side.

compared with uninduced cells (**Fig 5.11A**). There was also a reduction in viral yield from induced HEK BST2 cells infected with rBUNdelNSs virus, compared with uninduced cells, observed to be nearly ten-fold by 36 and 48 hours post infection (**Fig 5.11B**). The Western blot for N protein showed that the amount of N was unchanged between uninduced and induced cells for each of the three GFP-tagged viruses (**Fig 5.11C**).

Ubiquitination

STAF50 is also known as TRIM22 and is a 57 kDa protein located in the nucleus but can localise to the cytoplasm (Kajaste-Rudnitski *et al.*, 2010). It may function as an E3 ubiquitin ligase and is also able to ubiquitinate proteins in a TRIM22-dependent manner. HIV-1 transcription is restricted by STAF50

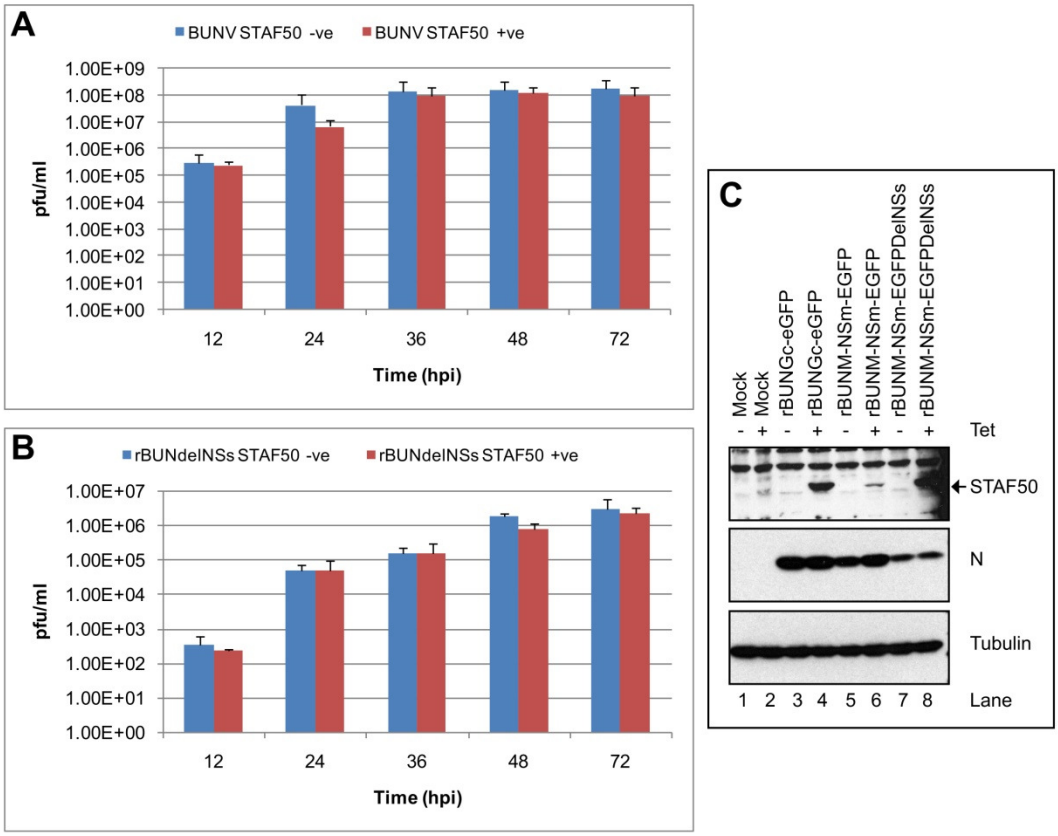

Figure 5.12 : Virus yield and N protein synthesis from virus infected HEK STAF50 cells. Cells were either not induced (-ve) or induced (+ve) and then infected with BUNV **(A)** or rBUNdelNSs **(B)** at 0.01 pfu/cell and at the time points indicated a sample of growth medium was removed and used to determine the virus yield by plaque assay. Each value represents the average of triplicate experiments and the error bars show the standard deviation. hpi denotes hours post infection. **(C)** Uninduced (-Tet) or induced (+Tet) cells were either mock infected or infected with either rBUNGc-eGFP, rBUNM-NSm-EGFP, or rBUNM-NSm-EGFPDelNSs at 1 pfu/cell. Twenty four hours later the cells were lysed and 1/30 of the lysate was analysed by SDS-PAGE and transferred to a nitrocellulose membrane and subjected to Western blotting using anti-FLAG (rabbit) antibody for ISG detection and N and tubulin proteins were detected using anti-N (rabbit) antibody and anti-Tubulin (mouse) antibody respectively. Proteins are labelled on the right hand side.

which also targets the Gag protein by disrupting its trafficking to the cell surface (Barr *et al.*, 2008). The induced HEK STAF50 cells infected with BUNV or rBUNdelNSs produced a similar yield of virus compared with uninduced cells throughout the 72 hours (**Fig 5.12A** and **5.12B** respectively). The amount of N protein produced by the NSs deletion virus (lane 7 and 8) was significantly less than the two GFP-tagged BUNV viruses (lanes 3, 4, 5 and 6) although when comparing each virus in the uninduced and induced cells there was little difference (**Fig 5.12C**).

ISGylation

ISG15

ISG15 was described in more detail in Chapter One; it is strongly induced by IFN and is one of the first and most abundantly expressed proteins, and a key component of ISGylation (Zhang & Zhang, 2011). During ISGylation ISG15 is conjugated onto lysines of target proteins by its C-terminal sequence LRLRGG. Like ubiquitination this involves several enzymatic proteins homologous to the ubiquitin enzymes E1, E2, and E3. **Figure 5.13A** shows the viral yield from

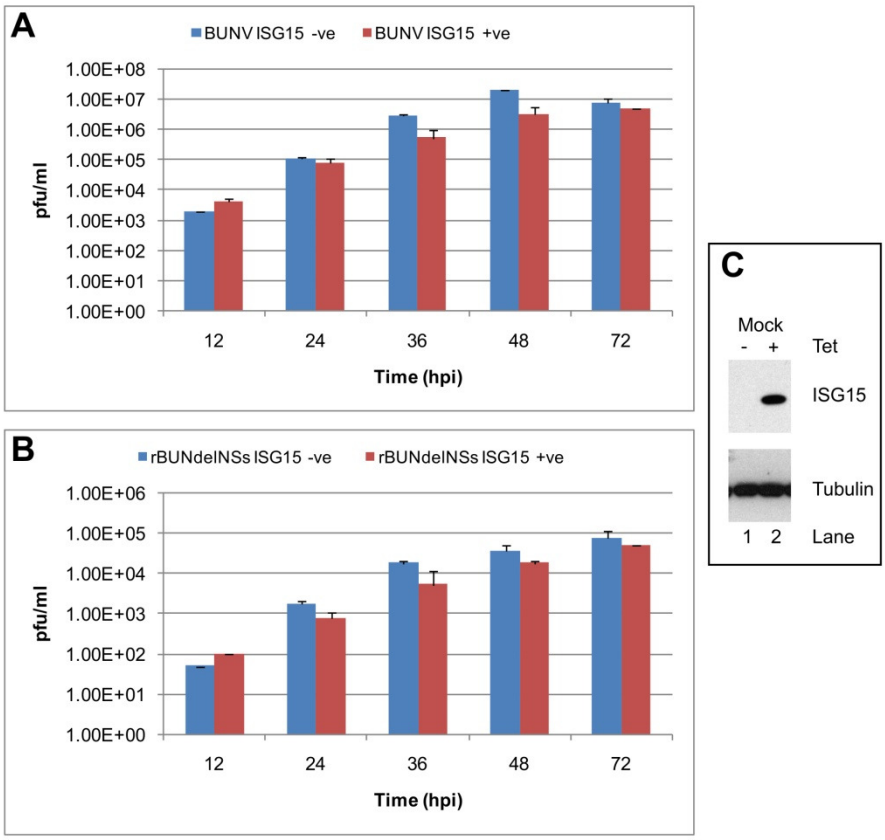

Figure 5.13 : Virus yield from virus infected HEK ISG15 cells. Cells were either not induced (-ve) or induced (+ve) and then infected with BUNV **(A)** or rBUNdelNSs **(B)** at 0.01 pfu/cell and at the time points indicated a sample of growth medium was removed and used to determine the virus yield by plaque assay. Each value represents the average of triplicate experiments and the error bars show the standard deviation. hpi denotes hours post infection. **(C) FLAG-tagged ISG15 detection.** 1/30 of the lysate from uninduced (-Tet) or induced (+Tet) cells was analysed by SDS-PAGE and transferred to a nitrocellulose membrane and subjected to Western blotting using anti-ISG15 (mouse) antibody and anti-Tubulin (mouse) for ISG15 and tubulin detection respectively. Proteins are labelled on the right hand side.

HEK ISG15 cells infected with BUNV and there was little difference until 36 and 48 hours post infection when there was a 5- and 6- fold reduction respectively. A similar slight reduction in viral yield was also apparent in rBUNdelNSs infected HEK ISG15 cells (**Fig 5.13B**). Western blot analysis of the uninduced and induced cells to detect FLAG-tagged ISG15 using two different anti-FLAG antibodies did not detect any protein. However, Western blot analysis using an anti-ISG15 antibody did detect FLAG-tagged ISG15 (**Fig 5.13C**). Thus, this

suggested that the FLAG-tag on ISG15 was not available for binding, but did confirm induction of FLAG-tagged ISG15 by Tet treatment.

UBE2L6

The UBE2L6, also known as ubcH8, protein is a 17.8 kDa protein which is a member of the E2 ubiquitin-conjugating enzyme family that is part of the ISGylation pathway (Zhao *et al.*, 2004). UBE2L6 is responsible for conjugation

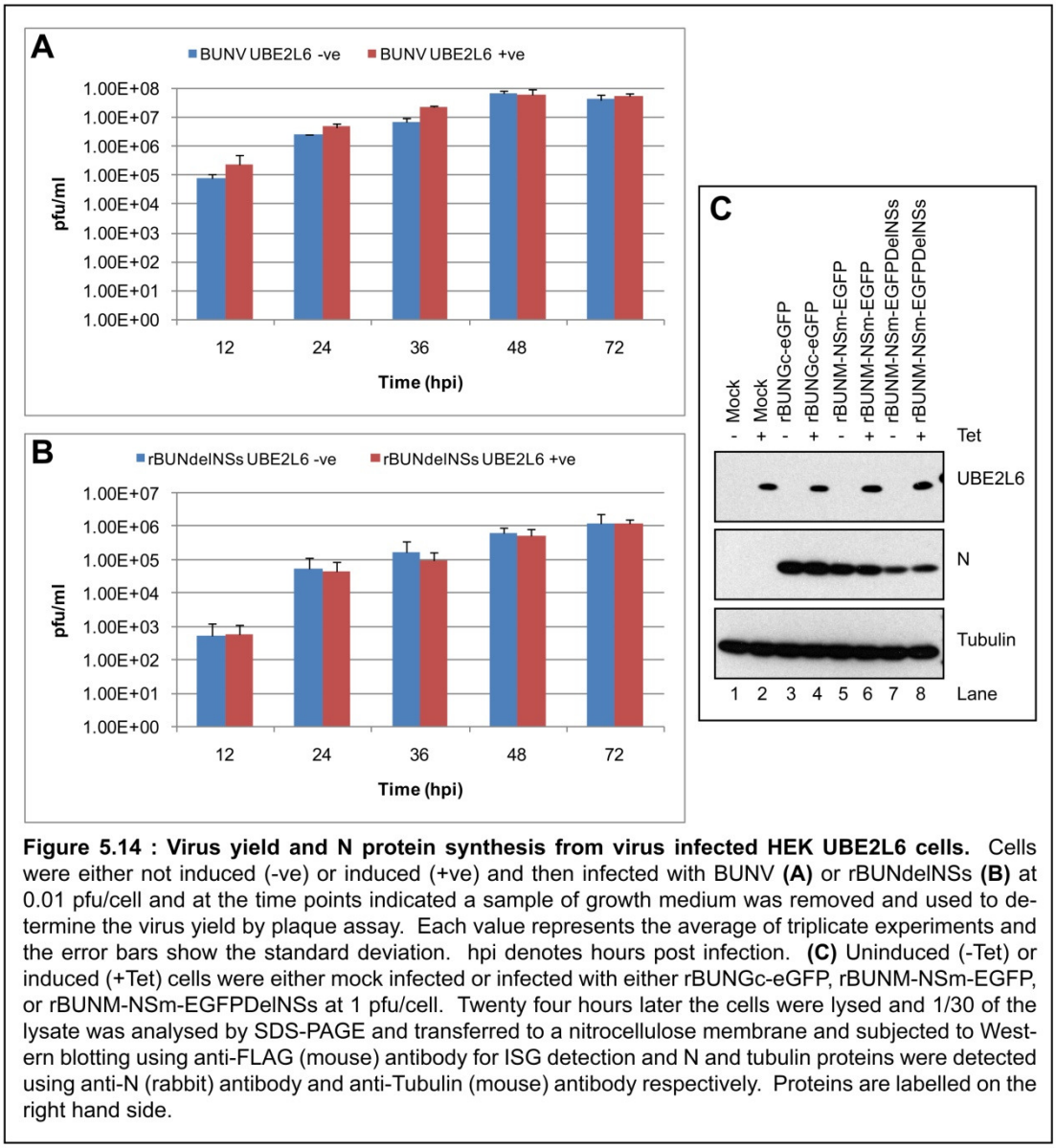

Figure 5.14 : Virus yield and N protein synthesis from virus infected HEK UBE2L6 cells. Cells were either not induced (-ve) or induced (+ve) and then infected with BUNV **(A)** or rBUNdelNSs **(B)** at 0.01 pfu/cell and at the time points indicated a sample of growth medium was removed and used to determine the virus yield by plaque assay. Each value represents the average of triplicate experiments and the error bars show the standard deviation. hpi denotes hours post infection. **(C)** Uninduced (-Tet) or induced (+Tet) cells were either mock infected or infected with either rBUNGc-eGFP, rBUNM-NSm-EGFP, or rBUNM-NSm-EGFPDelNSs at 1 pfu/cell. Twenty four hours later the cells were lysed and 1/30 of the lysate was analysed by SDS-PAGE and transferred to a nitrocellulose membrane and subjected to Western blotting using anti-FLAG (mouse) antibody for ISG detection and N and tubulin proteins were detected using anti-N (rabbit) antibody and anti-Tubulin (mouse) antibody respectively. Proteins are labelled on the right hand side.

of ISG15 to target proteins. The HEK UBE2L6 cells infected with BUNV (**Fig 5.14A**) or rBUNdelNSs (**Fig 5.14B**) showed little difference in viral yield when either uninduced or induced. This was further corroborated by Western blot analysis which showed no change in the amount of N protein from GFP-tagged virus infected uninduced and induced cells (**Fig 5.14C**). However, there was less N protein in the NSs deletion virus infected cells (lanes 7 and 8) compared with the GFP-tagged BUN virus infected cells (lanes 3, 4, 5, and 6), suggesting some further attenuation.

FLJ20637

FLJ20637 is also called HerC6 and is a putative E3 ubiquitin protein ligase that directly transfers ubiquitin from a thioester (E2) to the substrate (ubiquitination target) (Hochrainer *et al.*, 2005). FLJ20637 was thought to be involved in ISGylation as it shares 49% identity with HerC5 which has ISG15 E3 ligase activity (Dastur *et al.*, 2006; Versteeg *et al.*, 2010). A study using siRNA to knockdown FLJ20637 showed little effect on overall ISG15 conjugation but did suggest a role in targeting a small set of proteins compared with Herc5 (Dastur *et al.*, 2006). However, recent studies have shown the mouse homologue to FLJ20637, mHerc6, to be an ISG15 E3 ligase (Versteeg *et al.*, 2010). Both the uninduced and the induced HEK 20637 cells were infected with either BUNGc-eGFP or BUNGFP or NSmGFPdel virus and the amount of N protein after 24 hours was detected by Western blotting (**Fig 5.15**). The amount of N protein

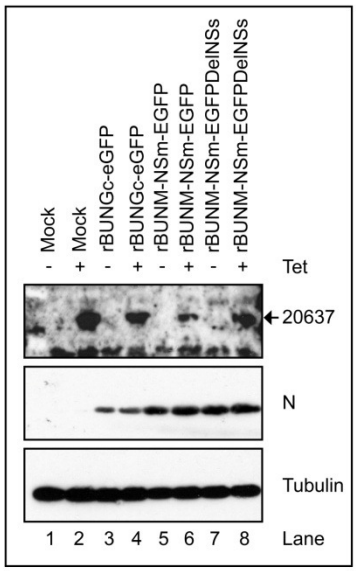

Figure 5.15 : Viral N protein synthesis from virus infected HEK 20637 cells. Uninduced (-Tet) or induced (+Tet) cells were either mock infected or infected with either rBUNGc-eGFP, rBUNM-NSm-EGFP, or rBUNM-NSm-EGFP-DelNSs at 1 pfu/cell. Twenty four hours later the cells were lysed and 1/30 of the lysate was analysed by SDS-PAGE and transferred to a nitrocellulose membrane and subjected to Western blotting using anti-FLAG (mouse) antibody for ISG detection, and N and tubulin proteins were detected using anti-N (rabbit) antibody and anti-Tubulin (mouse) antibody respectively. Proteins are labelled on the right hand side.

synthesised did not change between uninduced and induced cells (compare lanes 3 with 4, and 5 with 6, and 7 with 8), however comparing the amount of N protein synthesised by each virus shows a reduction in BUNGc-eGFP infected cells compared with the NSmGFP-tagged viruses (compare lanes 3 and 4 with lanes 5, 6, 7, and 8). As with some previous cell lines the FLAG-tagged ISG was difficult to detect, thus the bands showed different intensities but are thought to represent equal induction.

USP18

USP18, also known as UBP43, is a 43 kDa protein also involved in ISGylation (Malakhov *et al.*, 2002). This protein is a member of the de-ubiquitinating proteases and is able to efficiently cleave ISG15 fusions. Thus USP18 is involved in reversing the process of ISGylation (termed de-ISGylation) and is vital for maintaining a balance of ISG15 conjugated proteins within a cell. The HEK USP18 induced cells infected with either BUNV (**Fig 5.16A**) or rBUNdelNSs (**Fig 5.16B**) showed little change in viral yield over 72 hours,

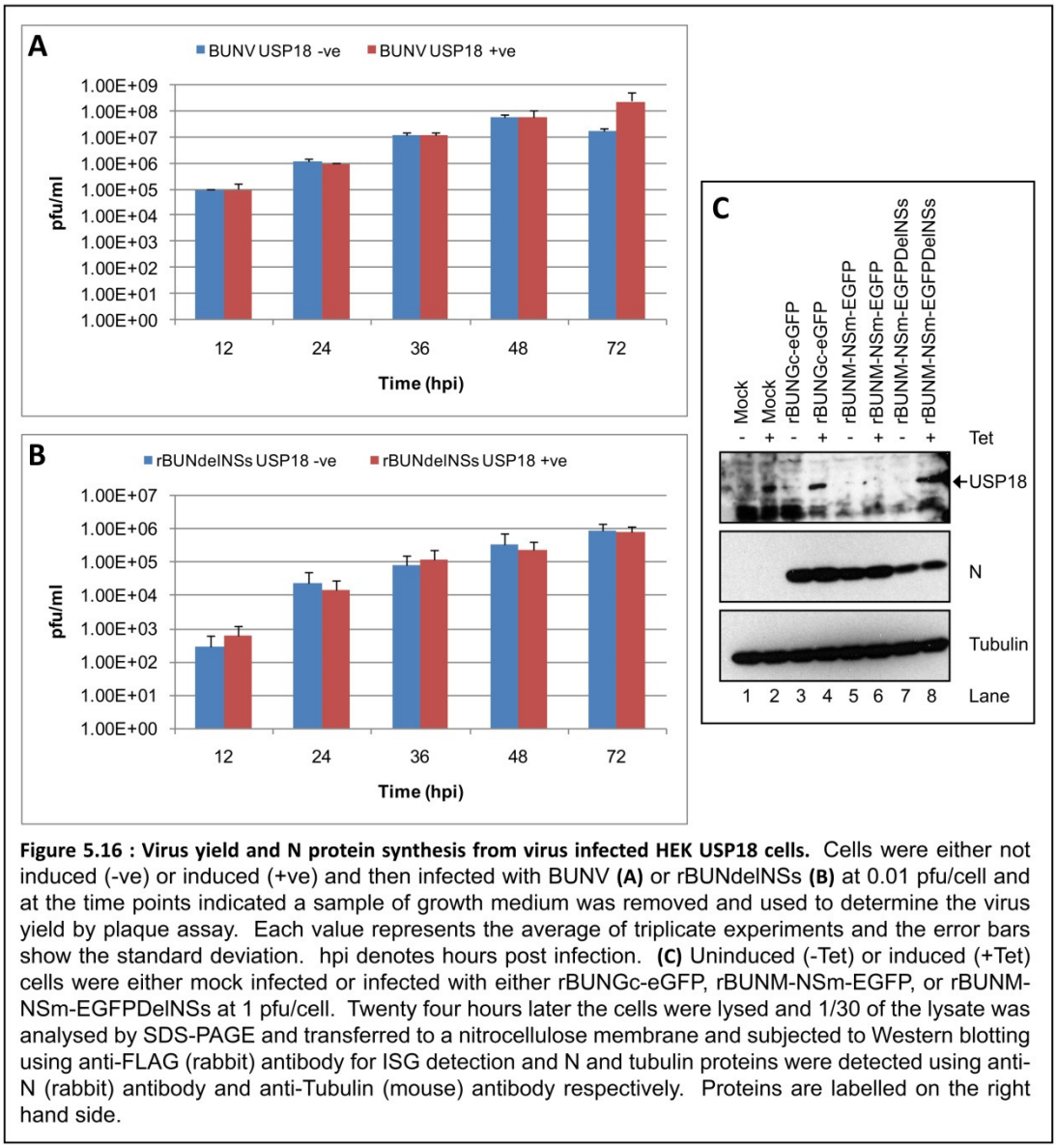

Figure 5.16 : Virus yield and N protein synthesis from virus infected HEK USP18 cells. Cells were either not induced (-ve) or induced (+ve) and then infected with BUNV **(A)** or rBUNdelNSs **(B)** at 0.01 pfu/cell and at the time points indicated a sample of growth medium was removed and used to determine the virus yield by plaque assay. Each value represents the average of triplicate experiments and the error bars show the standard deviation. hpi denotes hours post infection. **(C)** Uninduced (-Tet) or induced (+Tet) cells were either mock infected or infected with either rBUNGc-eGFP, rBUNM-NSm-EGFP, or rBUNM-NSm-EGFPDelNSs at 1 pfu/cell. Twenty four hours later the cells were lysed and 1/30 of the lysate was analysed by SDS-PAGE and transferred to a nitrocellulose membrane and subjected to Western blotting using anti-FLAG (rabbit) antibody for ISG detection and N and tubulin proteins were detected using anti-N (rabbit) antibody and anti-Tubulin (mouse) antibody respectively. Proteins are labelled on the right hand side.

except for an increase in BUNV yield from induced cells at 72 hours. Additionally the amount of N protein produced by GFP-tagged BUNV (**Fig 5.16C**, lanes 3, 4, 5 and 6) was greater than that produced by the NSs deletion virus infected cells (**Fig 5.16C**, lanes 7 and 8). The USP18 band observed was difficult to detect but is clear in lanes 2, 4 and 8 (**Fig 5.16C**) so is thought to have been induced across all induced cells.

ISG12a

The ISG12a protein is also known as IFI27 and is 11.3 kDa in size (Rosebeck & Leaman, 2008). ISG12a promotes IFN induced apoptosis by associating with or inserting into the mitochondrial membrane and rapidly inducing the release of cytochrome c from the mitochondria and the activation of various caspases and Bcl-2-associated X (BAX) protein. Thus, ISG12a enhances IFN-dependent perturbation of normal mitochondrial function. HEK ISG12a-induced cells infected with BUNV showed no reduction in viral yield over 72 hours (**Fig 5.17A**) however, infection with rBUNdelNSs showed a significant reduction in viral yield until 48 hours where there was a 10-fold increase in viral yield

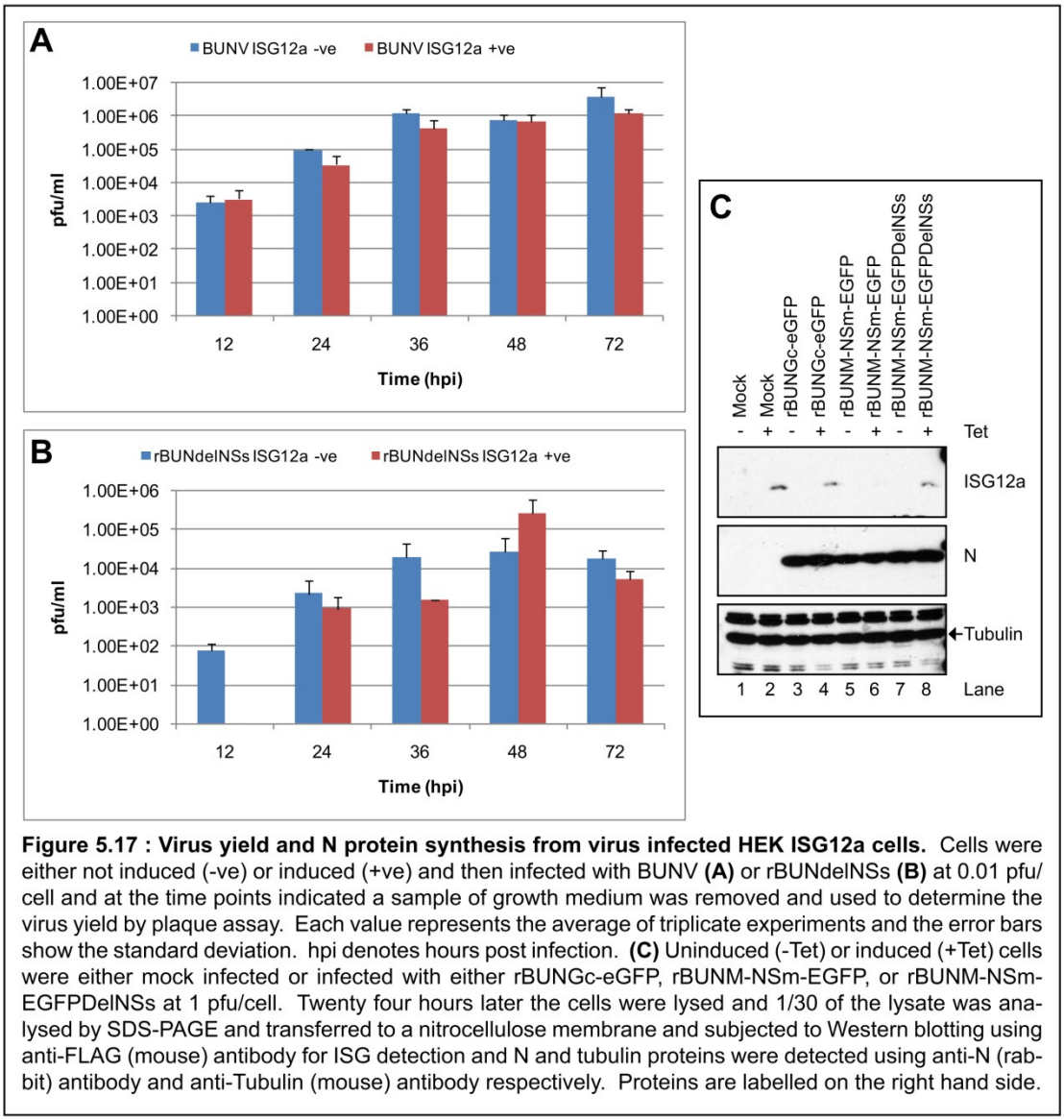

Figure 5.17 : Virus yield and N protein synthesis from virus infected HEK ISG12a cells. Cells were either not induced (-ve) or induced (+ve) and then infected with BUNV **(A)** or rBUNdelNSs **(B)** at 0.01 pfu/cell and at the time points indicated a sample of growth medium was removed and used to determine the virus yield by plaque assay. Each value represents the average of triplicate experiments and the error bars show the standard deviation. hpi denotes hours post infection. **(C)** Uninduced (-Tet) or induced (+Tet) cells were either mock infected or infected with either rBUNGc-eGFP, rBUNM-NSm-EGFP, or rBUNM-NSm-EGFPDelNSs at 1 pfu/cell. Twenty four hours later the cells were lysed and 1/30 of the lysate was analysed by SDS-PAGE and transferred to a nitrocellulose membrane and subjected to Western blotting using anti-FLAG (mouse) antibody for ISG detection and N and tubulin proteins were detected using anti-N (rabbit) antibody and anti-Tubulin (mouse) antibody respectively. Proteins are labelled on the right hand side.

compared with uninduced cells (**Fig 5.17B**). The Western blot for N protein showed no change in the levels of N protein produced from all three GFP-tagged viruses in infected uninduced and induced cells (**Fig 5.17C**). Furthermore the difficulties with detecting FLAG-tagged ISG12a account for the

less intense band in lane 6 (**Fig 5.17C**) although ISG induction is thought to have occurred across all Tet-induced cells.

GBP1

Guanylate binding protein 1 is 67.9 kDa in size and is in the large (p65) GTPase superfamily of proteins which comprises GBP1 to GBP5 (Prakash *et al.*, 2000). Guanylate binding proteins are defined by their ability to bind guanine nucleotides (GMP, GDP and GTP) and they have two binding motifs which differentiates them from GTP-binding proteins that have three binding motifs. Over-expression of GBP1 has been shown to inhibit HCV in cell culture and, further, the NS5B protein of HCV binds GBP1 thereby blocking its GTPase activity and consequently its antiviral effect (Itsui *et al.*, 2006; Itsui *et al.*, 2009).

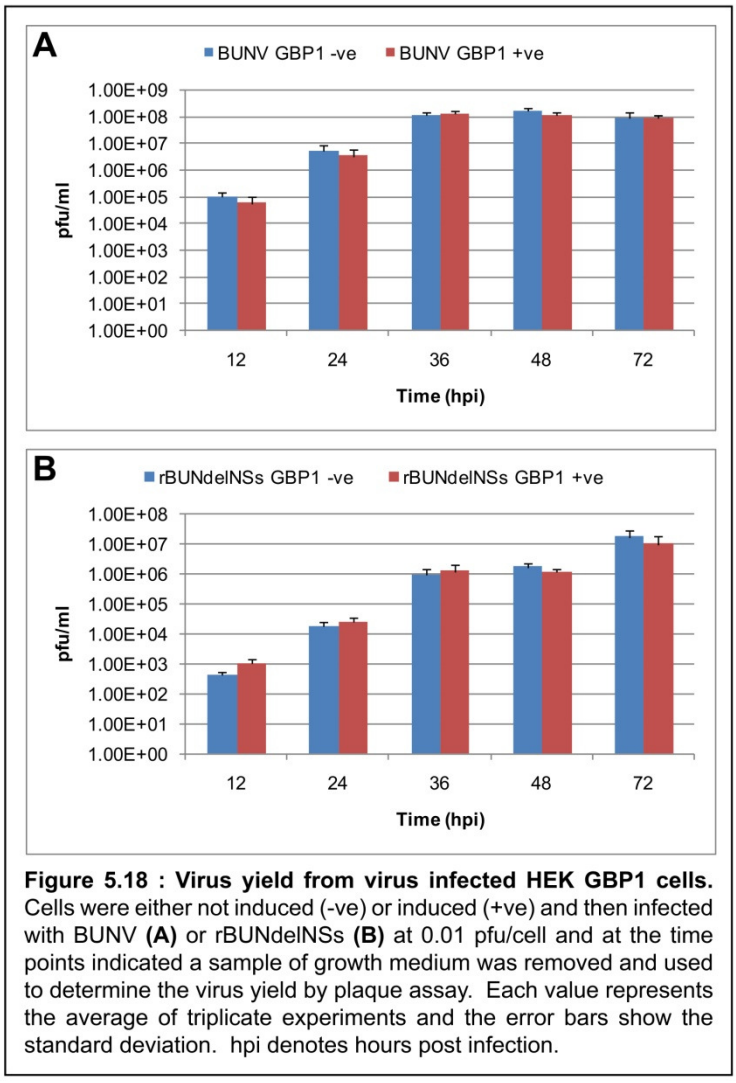

Figure 5.18 : Virus yield from virus infected HEK GBP1 cells. Cells were either not induced (-ve) or induced (+ve) and then infected with BUNV **(A)** or rBUNdelNSs **(B)** at 0.01 pfu/cell and at the time points indicated a sample of growth medium was removed and used to determine the virus yield by plaque assay. Each value represents the average of triplicate experiments and the error bars show the standard deviation. hpi denotes hours post infection.

Thus, similarly with the Mx proteins, GBP1 antiviral activity is mediated through its GTPase activity. The viral yield from induced HEK GBP1 cells infected with either BUNV (**Fig 5.18A**) or rBUNdelNSs (**Fig 5.18B**) showed little restriction when compared with uninduced cells.

FLJ20035

FLJ20035 is also known as DEAD (Asp-Glu-Ala-Asp) box polypeptide 60 (DDX60) and is a probable ATP-dependent RNA helicase induced by type I IFNs (Bigger *et al.*, 2004). The HEK FLJ20035 cells infected with BUNV or rBUNdelNSs showed no change in viral yield between the uninduced and induced cells over

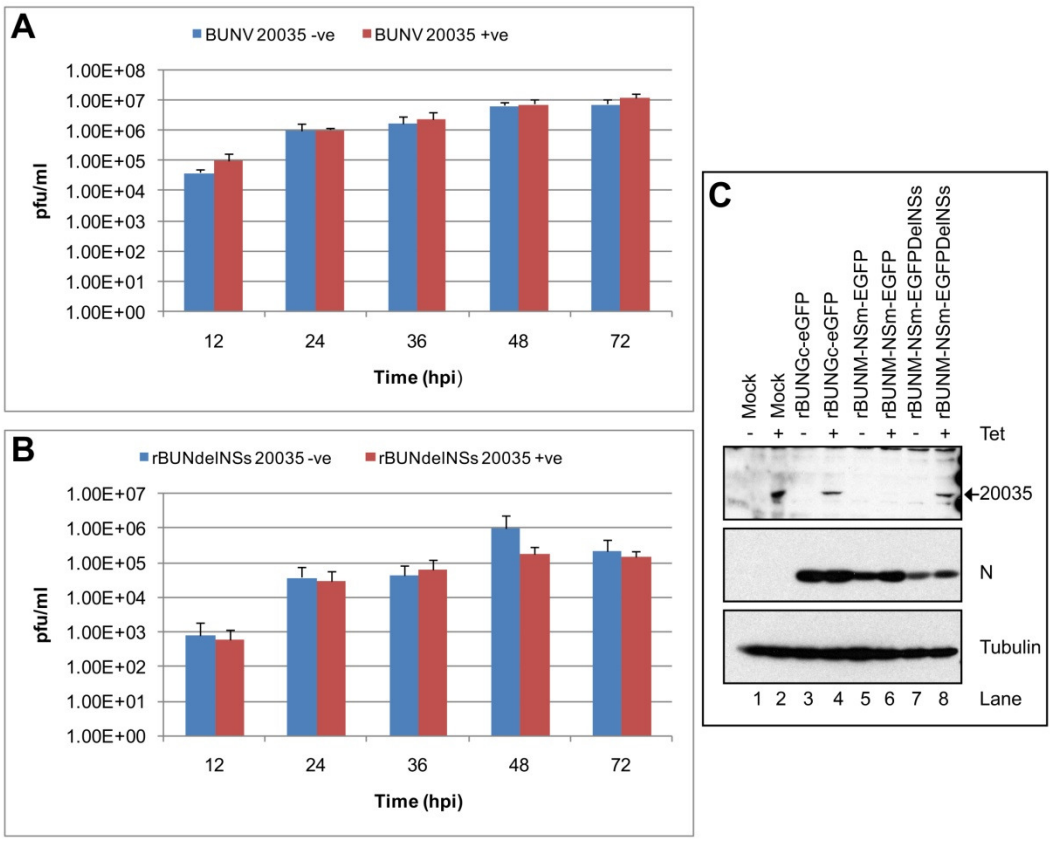

Figure 5.19 : Virus yield and N protein synthesis from virus infected HEK 20035 cells. Cells were either not induced (-ve) or induced (+ve) and then infected with BUNV **(A)** or rBUNdelNSs **(B)** at 0.01 pfu/cell and at the time points indicated a sample of growth medium was removed and used to determine the virus yield by plaque assay. Each value represents the average of triplicate experiments and the error bars show the standard deviation. hpi denotes hours post infection. **(C)** Uninduced (-Tet) or induced (+Tet) cells were either mock infected or infected with either rBUNGc-eGFP, rBUNM-NSm-EGFP, or rBUNM-NSm-EGFPDelNSs at 1 pfu/cell. Twenty four hours later the cells were lysed and 1/30 of the lysate was analysed by SDS-PAGE and transferred to a nitrocellulose membrane and subjected to Western blotting using anti-FLAG (mouse) antibody for ISG detection and N and tubulin proteins were detected using anti-N (rabbit) antibody and anti-Tubulin (mouse) antibody respectively. Proteins are labelled on the right hand side.

72 hours (**Fig 5.19A** and **Fig 5.19B** respectively). The Western blot analysis showed no change in the amount of N protein synthesised in uninduced and induced cells, but there was less N protein in the NSs deletion virus infected cells (**Fig 5.19C**, lanes 7 and 8) than in the GFP-tagged BUNV infected cells (**Fig 5.19C**, lanes 3, 4, 5 and 6). The FLAG-tagged 20035 protein was particularly difficult to detect which could be due to its location at the C-terminus of the DDX60 protein but it was induced following Tet treatment as shown in lanes 4 and 8 on the Western blot (**Fig 5.19C**, upper panel).

MAPK8

Mitogen-activated protein kinases (MAPK) are serine-threonine kinases involved with rapid gene expression in response to extra-cellular stimuli such as cytokines (Dong *et al.*, 2002). The c-Jun N-terminal kinases (JNKs) comprise MAPK8, MAPK9 and MAPK10 and are activated in response to stress stimuli such as UV irradiation, heat shock and cytokines. MAPK8 is induced by IFN and regulates AP-1 transcriptional activity by phosphorylating several of its constituents but is also involved in the TNF-α induced apoptosis pathway.

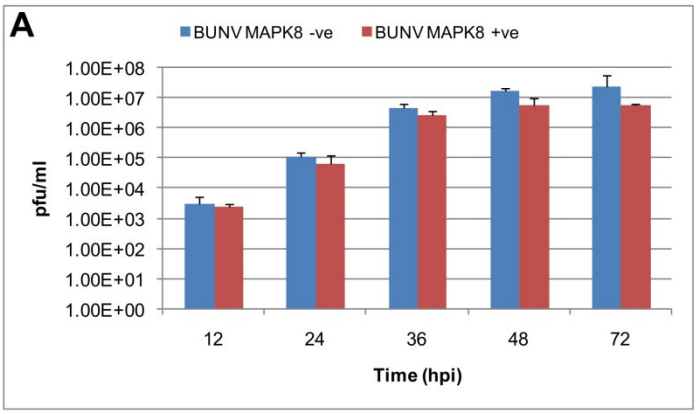

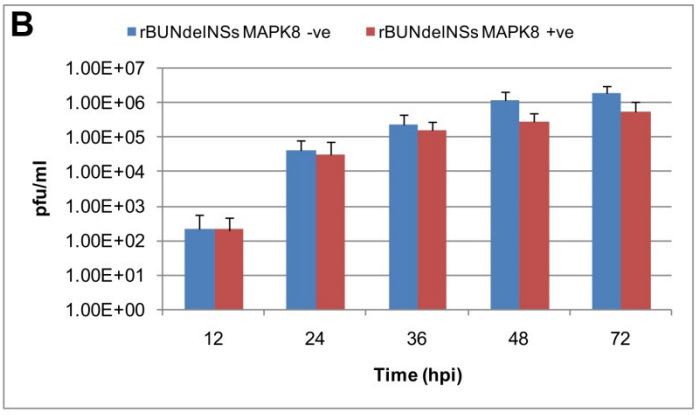

Figure 5.20 : Virus yield from virus infected HEK MAPK8 cells. Cells were either not induced (-ve) or induced (+ve) and then infected with BUNV **(A)** or rBUNdelNSs **(B)** at 0.01 pfu/cell and at the time points indicated a sample of growth medium was removed and used to determine the virus yield by plaque assay. Each value represents the average of triplicate experiments and the error bars show the standard deviation. hpi denotes hours post infection.

MAPK8 is capable of either promoting or inhibiting viruses as it has been shown to restrict varicella-zoster and vaccinia virus replication but to enhance reovirus replication (Clarke *et al.*, 2004; Hu *et al.*, 2008; Rahaus *et al.*, 2004). The HEK MAPK8-induced cells were infected with BUNV or rBUNdelNSs and both infections showed no significant change in viral yield from uninduced infected cells (**Fig 5.20**).

Viperin

Viperin is also known as radical S-adenosyl methionine domain containing (RSAD) 2 protein and is 42 kDa in size (Chin & Cresswell, 2001). This protein has been demonstrated to inhibit IAV by disrupting lipid raft formation at the plasma membrane which is vital for IAV budding and leads to "daisy chain" formation budding (Wang *et al.*, 2007). HEK Viperin cells induced to express

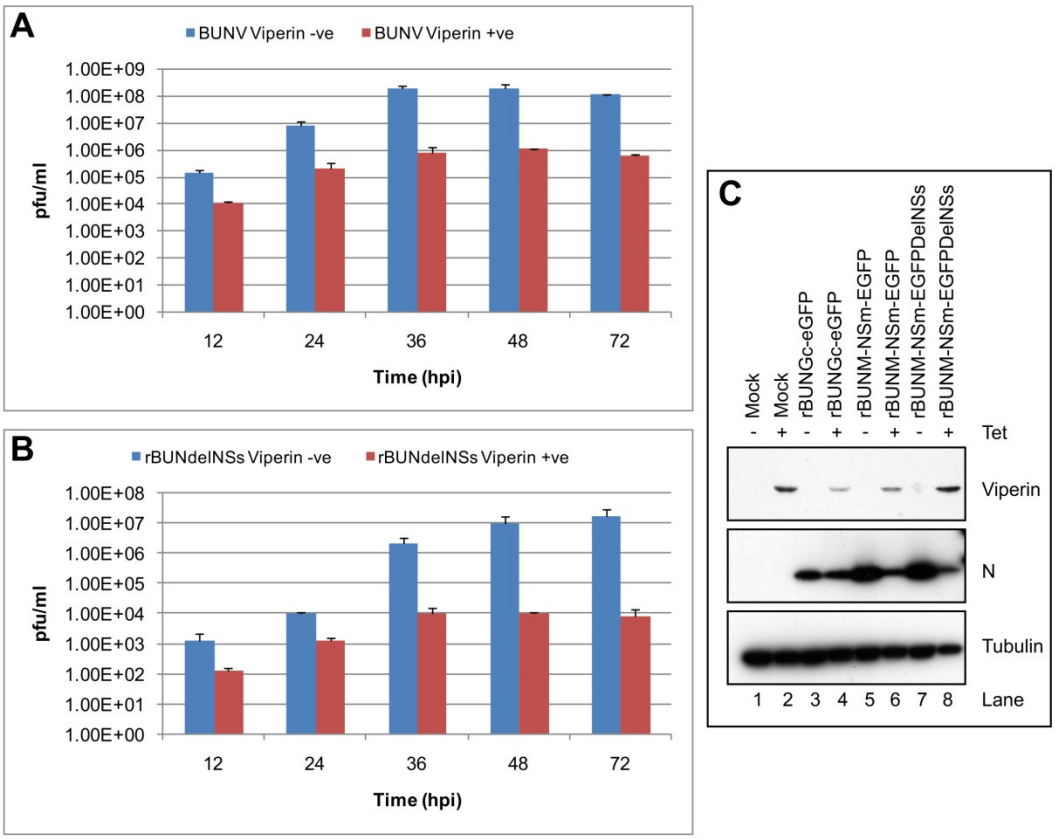

Figure 5.21 : Virus yield and N protein synthesis from virus infected HEK Viperin cells. Cells were either not induced (-ve) or induced (+ve) and then infected with BUNV **(A)** or rBUNdelNSs **(B)** at 0.01 pfu/cell and at the time points indicated a sample of growth medium was removed and used to determine the virus yield by plaque assay. Each value represents the average of triplicate experiments and the error bars show the standard deviation. hpi denotes hours post infection. **(C)** Uninduced (-Tet) or induced (+Tet) cells were either mock infected or infected with either rBUNGc-eGFP, rBUNM-NSm-EGFP, or rBUNM-NSm-EGFPDelNSs at 1 pfu/cell. Twenty four hours later the cells were lysed and 1/30 of the lysate was analysed by SDS-PAGE and transferred to a nitrocellulose membrane and subjected to Western blotting using anti-FLAG (mouse) antibody for ISG detection and N and tubulin proteins were detected using anti-N (rabbit) antibody and anti-Tubulin (mouse) antibody respectively. Proteins are labelled on the right hand side.

viperin and then infected with BUNV showed an inhibition of viral yield throughout the 72 hours. The inhibition increased from 10-fold by 12 hours up to 100-fold by 48 hours compared with uninduced cells (**Fig 5.21A**). When infected with rBUNdelNSs virus the reduction in viral yield increased from 10 fold by 12 hours to 1000-fold by 72 hours (**Fig 5.21B**). Western blot analysis for N protein showed a significant reduction in the amount of N produced by 24 hours post infection (**Fig 5.21C**).

The HEK VPM1 cells when induced over-express a viperin mutant (VPM1) that has had three cysteine residues in the conserved motif I of viperin replaced with three alanine residues thus removing the enzymatic capability of viperin (Jiang *et al.*, 2008). There is no effect on viral replication observed following induction of VPM1 in these cells (**Fig 22A**). Thus, the inhibitory effects of over-expressed

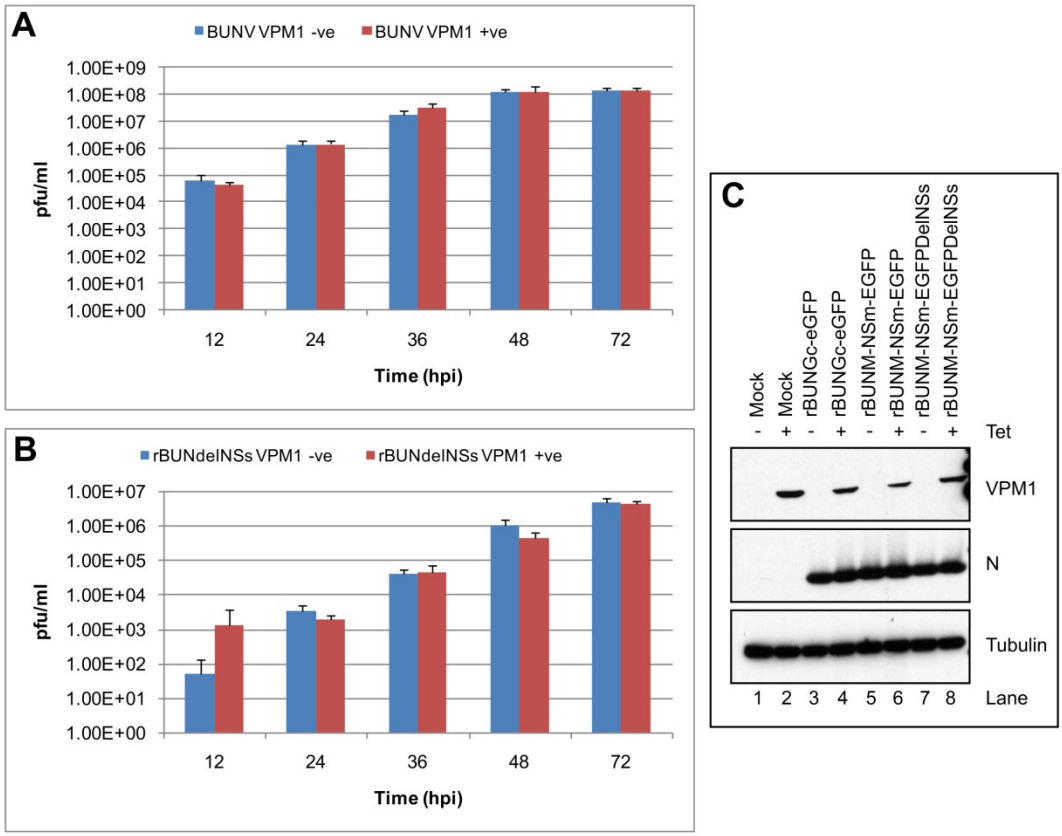

Figure 5.22 : Virus yield and N protein synthesis from virus infected HEK VPM1 cells. Cells were either not induced (-ve) or induced (+ve) and then infected with BUNV **(A)** or rBUNdelNSs **(B)** at 0.01 pfu/cell and at the time points indicated a sample of growth medium was removed and used to determine the virus yield by plaque assay. Each value represents the average of triplicate experiments and the error bars show the standard deviation. hpi denotes hours post infection. **(C)** Uninduced (-Tet) or induced (+Tet) cells were either mock infected or infected with either rBUNGc-eGFP, rBUNM-NSm-EGFP, or rBUNM-NSm-EGFPDelNSs at 1 pfu/cell. Twenty four hours later the cells were lysed and 1/30 of the lysate was analysed by SDS-PAGE and transferred to a nitrocellulose membrane and subjected to Western blotting using anti-FLAG (mouse) antibody for ISG detection and N and tubulin proteins were detected using anti-N (rabbit) antibody and anti-Tubulin (mouse) antibody respectively. Proteins are labelled on the right hand side.

wild-type viperin on BUNV were abrogated when induced HEK VPM1 cells were infected with BUNV (compare Figure **5.21A** and **5.22A**). When HEK VPM1 cells were infected with rBUNdelNSs virus there was an initial 10-fold increase in viral yield in the induced cells but this was reduced to little difference by 24 hours and thereafter (**Fig 5.22B**). This shows that the loss of the enzymatic function of viperin impairs its ability to inhibit BUNV replication. The Western blot analysis confirmed the abrogation of viperin activity did not result in a change in the amount of N protein by 24 hours post infection (**Fig 5.22C**).

IFITM proteins

The interferon induced transmembrane (IFITM) proteins are induced by both type I and II IFNs and they contain two transmembrane domains and a highly conserved cytoplasmic domain with the N- and C- termini in the luminal space. They have been shown to inhibit the endocytic entry of IAV haemagglutinin (HA)-pseudotyped retroviruses and their subsequent early replication as well as restricting DENV and WNV replication at an early stage in their life cycle (Brass *et al.*, 2009). The filoviruses, EBOV and Marburg virus (MARV), and the SARS

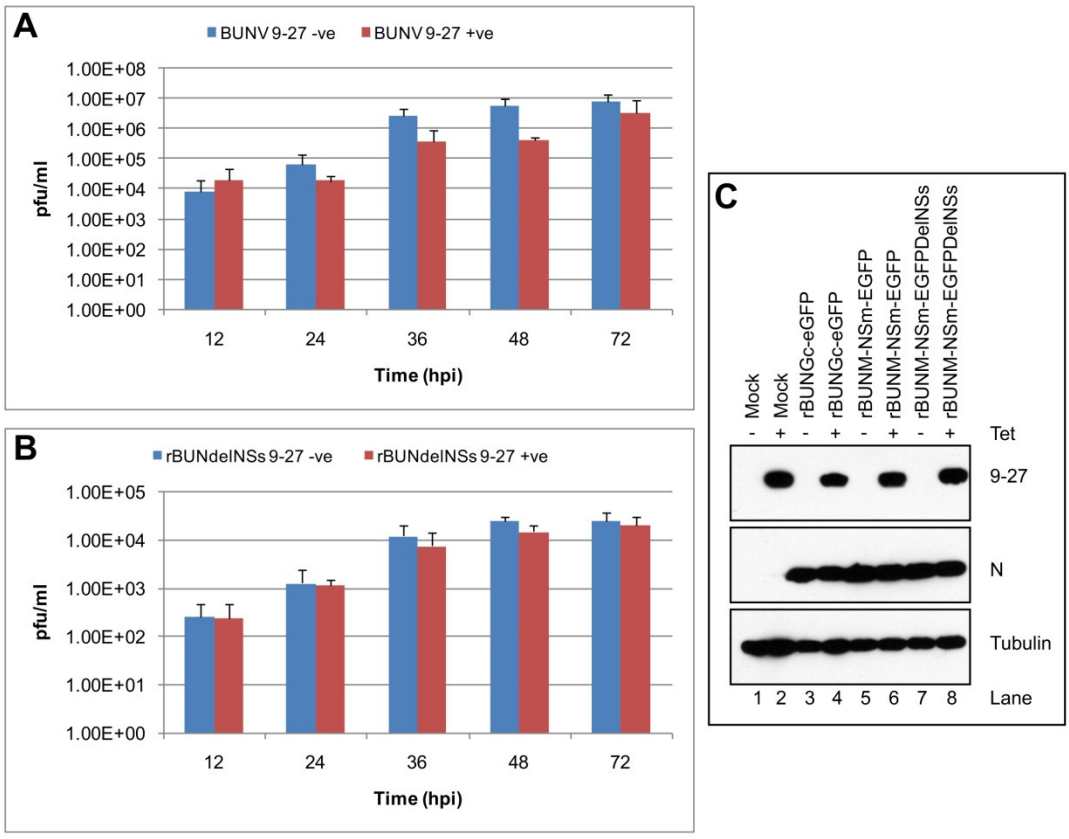

Figure 5.23 : Virus yield and N protein synthesis from virus infected HEK 9-27 cells. Cells were either not induced (-ve) or induced (+ve) and then infected with BUNV **(A)** or rBUNdelNSs **(B)** at 0.01 pfu/cell and at the time points indicated a sample of growth medium was removed and used to determine the virus yield by plaque assay. Each value represents the average of triplicate experiments and the error bars show the standard deviation. hpi denotes hours post infection. **(C)** Uninduced (-Tet) or induced (+Tet) cells were either mock infected or infected with either rBUNGc-eGFP, rBUNM-NSm-EGFP, or rBUNM-NSm-EGFPDelNSs at 1 pfu/cell. Twenty four hours later the cells were lysed and 1/30 of the lysate was analysed by SDS-PAGE and transferred to a nitrocellulose membrane and subjected to Western blotting using anti-FLAG (mouse) antibody for ISG detection and N and tubulin proteins were detected using anti-N (rabbit) antibody and anti-Tubulin (mouse) antibody respectively. Proteins are labelled on the right hand side.

coronavirus were shown to be restricted by IFITM proteins in the late stages of the endocytic pathway, however IFITM proteins have shown little or no effect on the entry of viruses in the *Arenaviridae* family (Huang *et al.*, 2011).

The ISG9-27 protein is also known as IFITM1 and is a 13.9 kDa protein comprising 125 amino acids (Alber & Staeheli, 1996; Lewin *et al.*, 1991). The 1-8D protein is also known as IFITM2 and is a 14.6 kDa protein comprising 132

amino acids and the 1-8U protein is also known as IFITM3 and is a 14.6 kDa protein comprising of 133 amino acids (Lewin *et al.*, 1991).

Figure 5.23A (above) shows the BUNV yield from uninduced and induced HEK 9-27 cells over 72 hours. Twenty-four hours post-infection there was a 5-fold reduction in BUNV yield in induced cells, which further increased through 36 (7-fold) and 48 (14-fold) hours but was reduced at 72 (2-fold) hours. Over the same time-frame, rBUNdelNSs was only slightly restricted by 36 and 48 hours post infection (**Fig 5.23B**). However, Western blot analysis showed no reduction in the accumulation of N protein from any of the three GFP viruses investigated (**Fig 5.23C**). Thus, the reduction in viral yield did not result in a detectable reduction in N protein expression.

The Western blot for the HEK 1-8U cells showed little effect on N protein after the cells were induced but a slight reduction in the amount of N protein produced from rBUNGc-eGFP infected cells warrants further investigation (**Fig 5.24**).

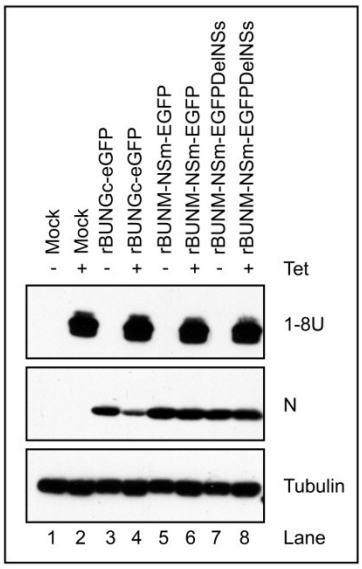

Figure 5.24 : Viral N protein synthesis from virus infected HEK 1-8U cells. Uninduced (-Tet) or induced (+Tet) cells were either mock infected or infected with either rBUNGc-eGFP, rBUNM-NSm-EGFP, or rBUNM-NSm-EGFP-DelNSs at 1 pfu/cell. Twenty four hours later the cells were lysed and 1/30 of the lysate was analysed by SDS-PAGE and transferred to a nitrocellulose membrane and subjected to Western blotting using anti-FLAG (mouse) antibody for ISG detection, and N and tubulin proteins were detected using anti-N (rabbit) antibody and anti-Tubulin (mouse) antibody respectively. Proteins are labelled on the right hand side.

The HEK 1-8D cells showed no difference in BUNV or rBUNdelNSs yield between uninduced and induced cells (**Fig 5.25A and 5.25B**). This was further corroborated by the Western blot which showed no change in the amount of N protein from each virus (**Fig 5.25C**).

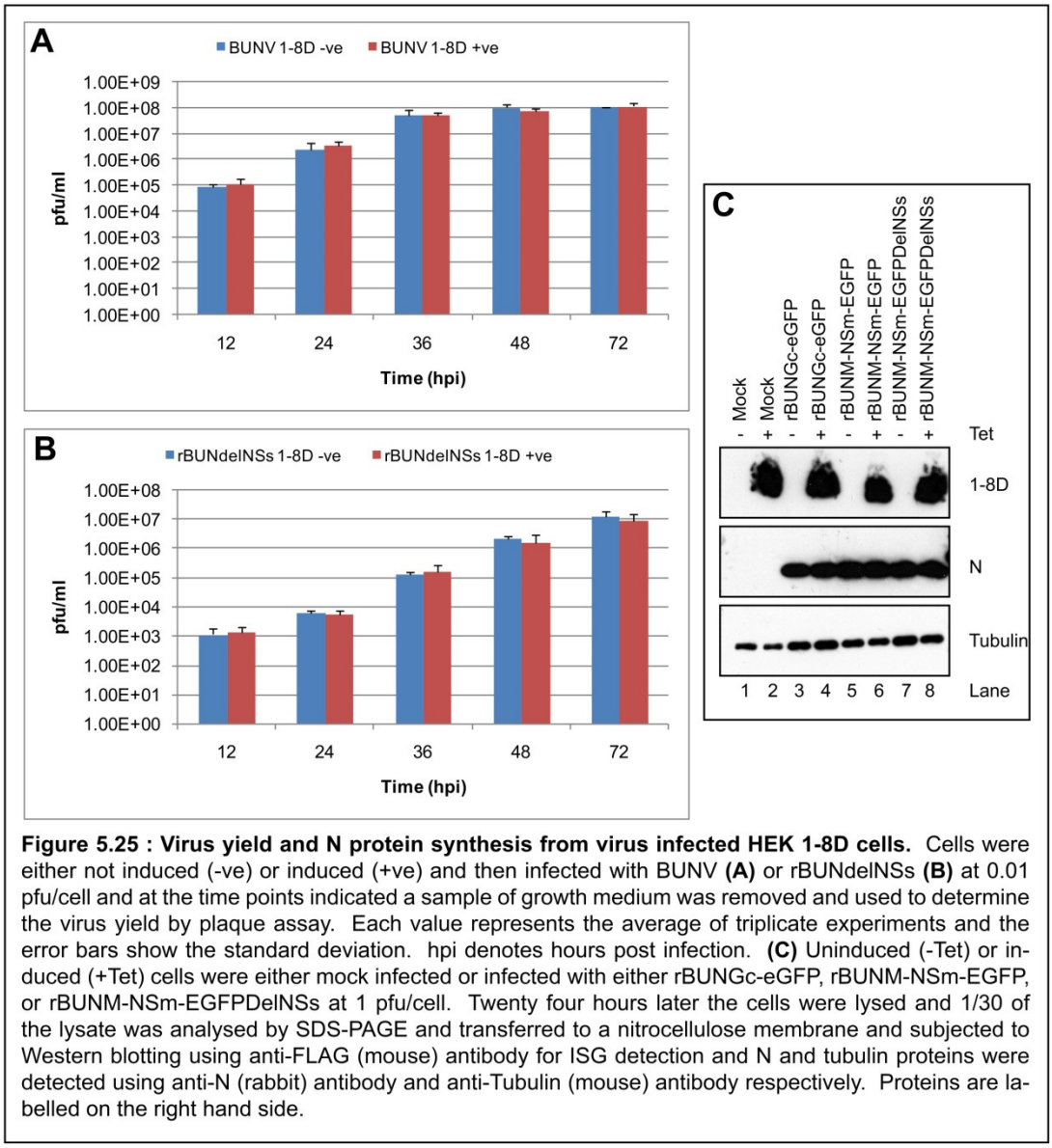

Figure 5.25 : Virus yield and N protein synthesis from virus infected HEK 1-8D cells. Cells were either not induced (-ve) or induced (+ve) and then infected with BUNV **(A)** or rBUNdelNSs **(B)** at 0.01 pfu/cell and at the time points indicated a sample of growth medium was removed and used to determine the virus yield by plaque assay. Each value represents the average of triplicate experiments and the error bars show the standard deviation. hpi denotes hours post infection. **(C)** Uninduced (-Tet) or induced (+Tet) cells were either mock infected or infected with either rBUNGc-eGFP, rBUNM-NSm-EGFP, or rBUNM-NSm-EGFPDelNSs at 1 pfu/cell. Twenty four hours later the cells were lysed and 1/30 of the lysate was analysed by SDS-PAGE and transferred to a nitrocellulose membrane and subjected to Western blotting using anti-FLAG (mouse) antibody for ISG detection and N and tubulin proteins were detected using anti-N (rabbit) antibody and anti-Tubulin (mouse) antibody respectively. Proteins are labelled on the right hand side.

SAMHD1

SAMHD1 is a putative nuclease that is 72 kDa in size. It is involved in the regulation of the innate immune response as it is upregulated in response to a viral infection and seems to act as a negative regulator of the antiviral response (Rice *et al.*, 2009). The accumulation of N protein in both uninduced and induced HEK SAMHD1 cells was the same for each of the three GFP-tagged viruses (**Fig 5.26**).

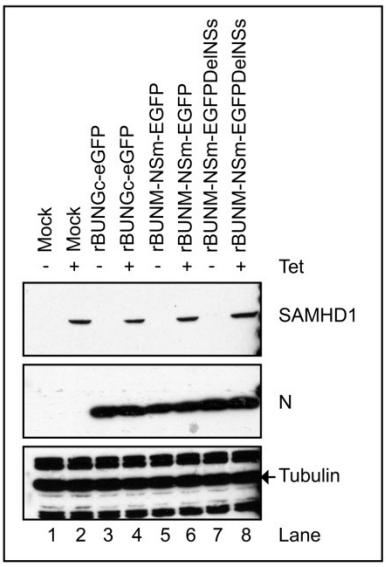

Figure 5.26 : Viral N protein synthesis from virus infected HEK SAMHD1 cells. Uninduced (-Tet) or induced (+Tet) cells were either mock infected or infected with either rBUNGc-eGFP, rBUNM-NSm-EGFP, or rBUNM-NSm-EGFP-DelNSs at 1 pfu/cell. Twenty four hours later the cells were lysed and 1/30 of the lysate was analysed by SDS-PAGE and transferred to a nitrocellulose membrane and subjected to Western blotting using anti-FLAG (mouse) antibody for ISG detection, and N and tubulin proteins were detected using anti-N (rabbit) antibody and anti-Tubulin (mouse) antibody respectively. Proteins are labelled on the right hand side.

OAS proteins

The OAS proteins have been described previously in Chapter One. Essentially, they function by activating RNase L, which then degrades viral RNA and not only directly inhibits the virus but can also further stimulate the IFN response *via* RLR signalling and thus indirectly inhibit viral replication (Malathi *et al*., 2007; Silverman, 2007). The HEK OAS1V1 cells when induced and infected with BUNV showed an overall 5-fold reduction in viral yield, whereas infection with

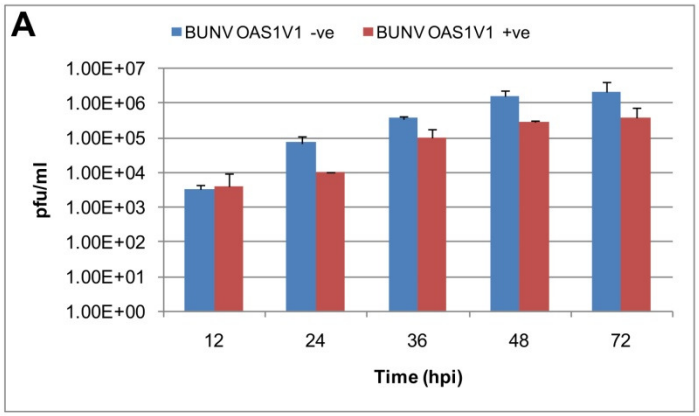

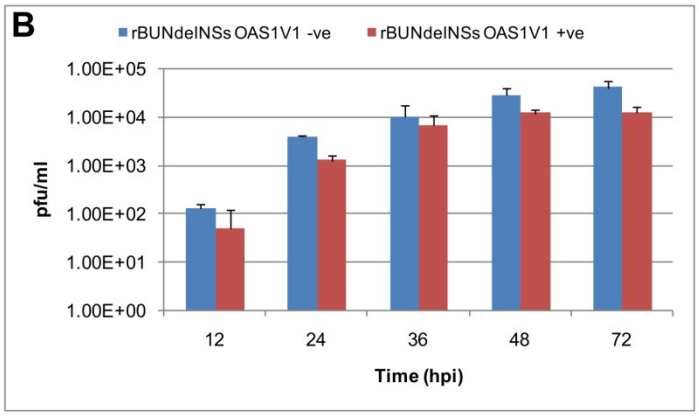

Figure 5.27 : Virus yield from virus infected HEK OAS1V1 cells. Cells were either not induced (-ve) or induced (+ve) and then infected with BUNV **(A)** or rBUNdelNSs **(B)** at 0.01 pfu/cell and at the time points indicated a sample of growth medium was removed and used to determine the virus yield by plaque assay. Each value represents the average of triplicate experiments and the error bars show the standard deviation. hpi denotes hours post infection.

rBUNdelNSs virus gave an overall 3-fold reduction compared with uninduced cells (**Fig 5.27A and 5.27B**). However, the induced HEK OAS1V2 cells showed little difference overall in viral yield when infected with either BUNV or rBUNdelNSs, compared with uninduced cells (**Fig 5.28A and 5.28B**). Furthermore, 2', 5' oligoadenylate synthetase-like (OASL) is similar to OAS1 and, while it does not have 2', 5' OAS activity, it does bind to RNA and DNA. Infection of induced HEK OASLV1 cells with the three GFP-tagged viruses showed no inhibition of N protein accumulation compared with uninduced cells (**Fig 5.29**).

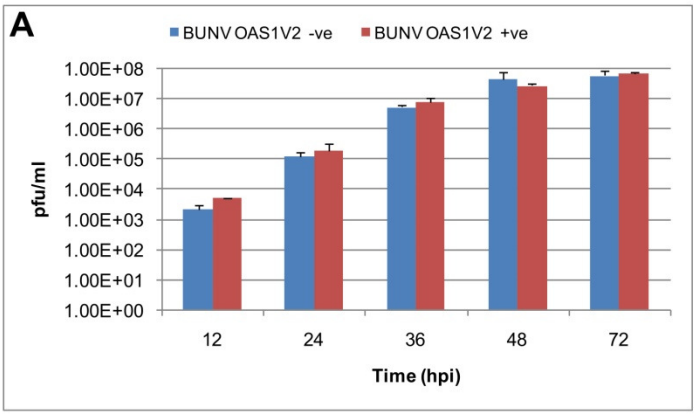

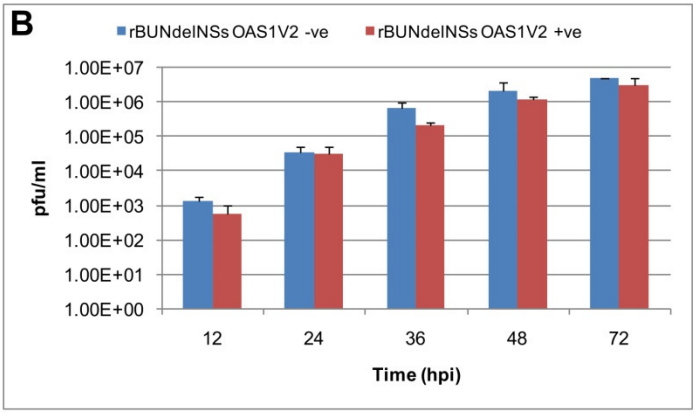

Figure 5.28 : Virus yield from virus infected HEK OAS1V2 cells. Cells were either not induced (-ve) or induced (+ve) and then infected with BUNV **(A)** or rBUNdelNSs **(B)** at 0.01 pfu/cell and at the time points indicated a sample of growth medium was removed and used to determine the virus yield by plaque assay. Each value represents the average of triplicate experiments and the error bars show the standard deviation. hpi denotes hours post infection.

Figure 5.29 : Viral N protein synthesis from virus infected HEK OASLV1 cells. Uninduced (-Tet) or induced (+Tet) cells were either mock infected or infected with either rBUNGc-eGFP, rBUNM-NSm-EGFP, or rBUNM-NSm-EGFP-DelNSs at 1 pfu/cell. Twenty four hours later the cells were lysed and 1/30 of the lysate was analysed by SDS-PAGE and transferred to a nitrocellulose membrane and subjected to Western blotting using anti-FLAG (mouse) antibody for ISG detection, and N and tubulin proteins were detected using anti-N (rabbit) antibody and anti-Tubulin (mouse) antibody respectively. Proteins are labelled on the right hand side.

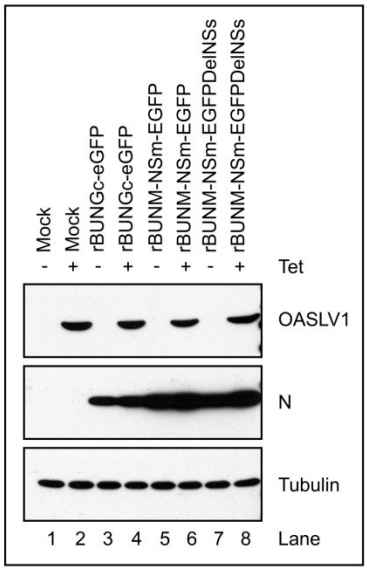

The data collected from virus yield assays and Western blot analysis for each cell line in this section are summarised in table 5.1 below.

Table 5.1: Summary of the effect on viral inhibition by induced HEK ISG cell lines.

HEK293 ISG-expressing cell line	Inhibition* on BUNV yield †	Inhibition* on rBUNdelNSs virus yield †	Inhibition of N protein †	GenBank accession number
CAT	-	-	-	
ISG 9-27	-	-	-	003641
ISG12a	-	+	-	BN000227
ISG15	-	-	NDC	005101
ISG20	NDC	NDC	NDC	002201
ISG56	-	-	-	001548
1-8D	-	-	-	006435
1-8U	-	-	-	021034
ADAR1	-	-	-	001111
MTAP44	+	+	-	D28915
GBP1	-	-	NDC	002053
MAPK8	-	-	NDC	002750
Viperin	+	+	+	AF442151
VPM1	-	-	-	
PKR	+	+	+	AH008429
PKRM	-	-	-	
SAMHD1	NDC	NDC	-	015474
STAF50	-	-	-	X82200
BST2	-	-	-	004335
FLJ20637	NDC	NDC	-	AK000644
FLJ38348	-	-	-	AK095667
FLJ20035	-	-	-	AK000042
PLSCR1	-	-	-	021105
PLSCR2	-	-	NDC	
UBE2L6	-	-	-	004223
USP18	-	-	-	017414
OAS1V1	-	-	NDC	016816
OAS1V2	-	-	NDC	002534
OASLV1	NDC	NDC	-	003733

* Inhibition of 10-fold or higher.
† + indicates the ISG inhibits the virus.
NDC denotes no data collected.

Screening by immunofluorescence

To further assess the utility of the three GFP-tagged viruses for screening cell lines for their anti-BUNV properties, immunofluorescence was used. An immunofluorescence protocol that is fast and reliable would enable high throughput screening of cells and compounds of interest.

The immunofluorescence experiments in this section were carried out as described in Chapter Two and at an MOI of 1, and infected cells were visualized using a confocal microscope. The cells were fixed 24 hours after infection and the FLAG-tagged ISGs and the viral N protein were detected by indirect immunofluorescence, whereas the GFP-tagged proteins were observed by their

autofluorescence. To determine the extent of infection, the percentage of infected cells was calculated by counting the number of GFP-positive cells out of 1000 cells. Under the confocal microscope rBUNGc-eGFP produces punctate bright green dots when the chimeric GcGFP protein is expressed. However, expression of the NSmGFP chimeric protein from the two NSm GFP-tagged viruses is significantly less bright and more evenly distributed.

HEK 38348: The induced mock cells clearly showed that this protein was located in the nucleus and was not detected without Tet induction (**Fig 5.30**, panel 1 and 2). Both uninduced and induced cells showed 100% infection by all

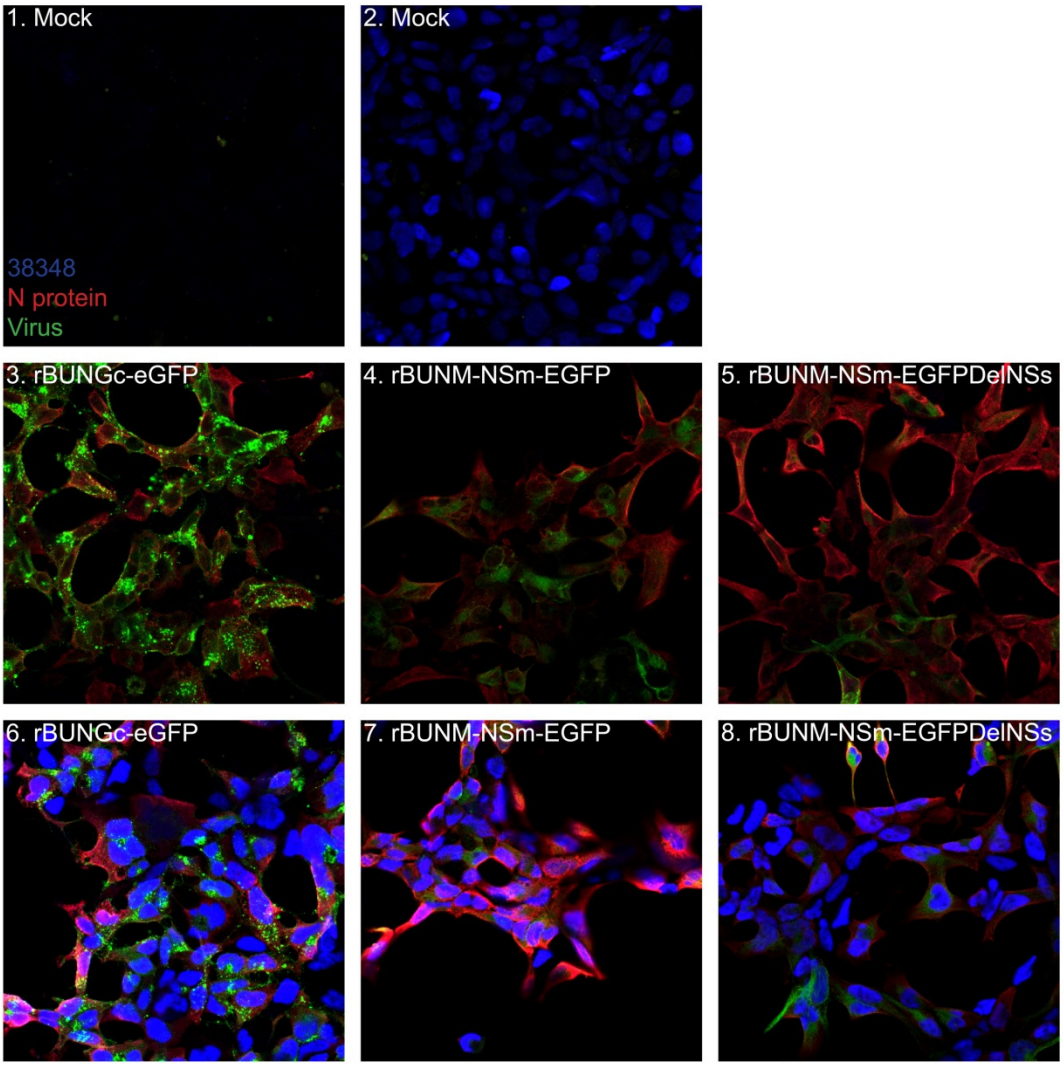

Figure 5.30 : Immunofluorescence of HEK 38348 cells infected with GFP tagged rBUNV. HEK 38348 cells uninduced (**1, 3, 4, 5**) or induced (**2, 6, 7, 8**) were mock infected or infected with rBUNGc-eGFP or rBUNM-NSm-EGFP or rBUNM-NSm-EGFPDelNSs at an MOI of 1 for 24 hours at which point the cells were fixed with 4% paraformaldehyde. Viral infection was determined by autofluorescence of GFP (green) and or indirect immunofluorescence using an anti-N Texas Red conjugated antibody (red). Induction of the ISG 38348 was detected by indirect immunofluorescence using an anti-FLAG Cy5 conjugated antibody (blue).

three GFP-tagged viruses (**Fig 5.30**, panels 3-8) and panels 6-8 show that cells were simultaneously induced and infected. The data correlate with the earlier

virus yield assay and Western blot data showing no effect on BUNV. Additionally, BUNV replicates in the cytoplasm and the 38348 protein clearly locates in the nucleus.

HEK PKR: The mock cells when induced did show a clear signal compared with the uninduced cells (**Fig 5.31**, panel 1 and 2). Similarly with other cell lines the uninduced cells were 100% infected by each of the three GFP-tagged viruses (**Fig 5.31**, panels 3, 4 and 5). Panel 3 shows many infected cells with numerous bright green and punctate dots showing the synthesis of the chimeric GcGFP proteins which may have already been assembled into virions (Shi *et al.*, 2010). Panel 4 also shows many green cells due to the synthesis of the

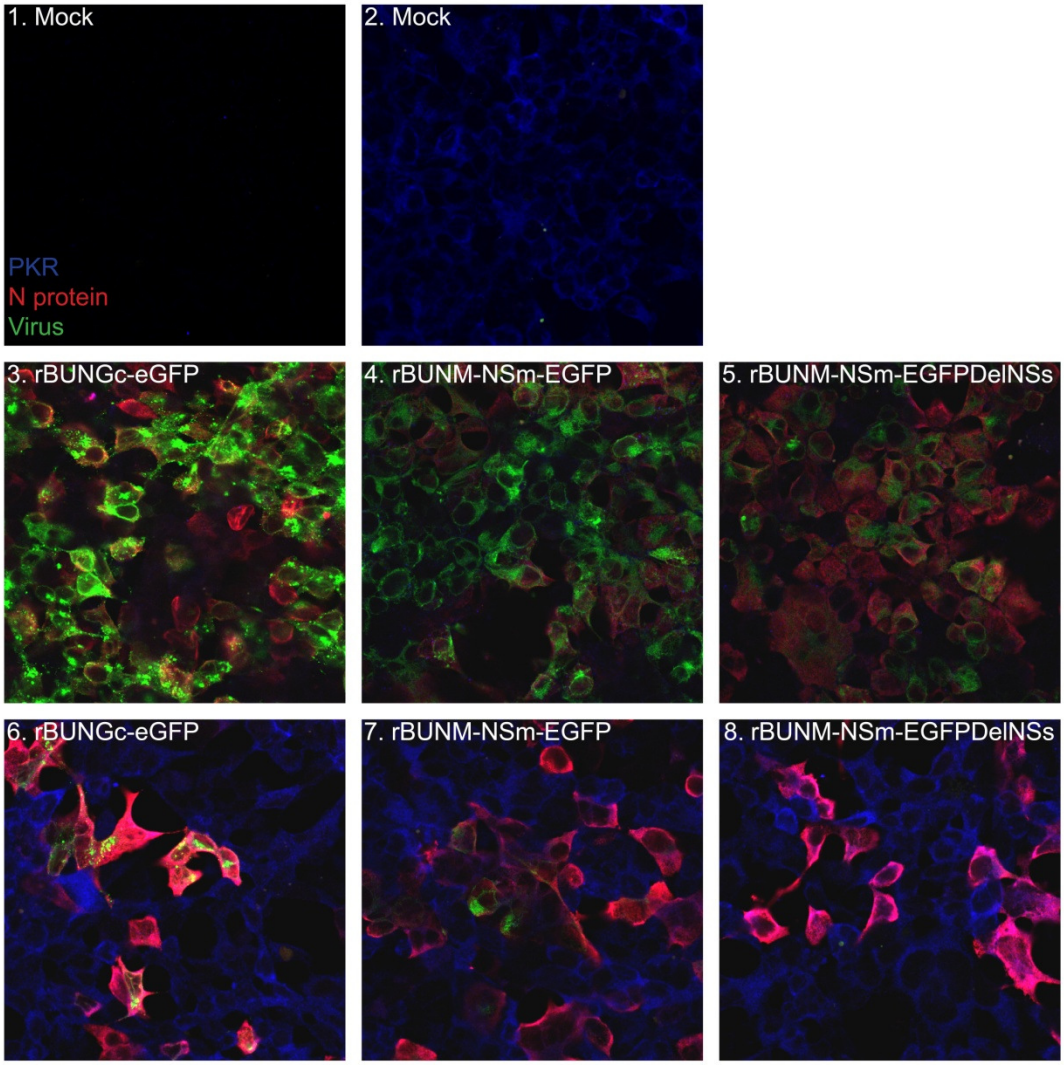

Figure 5.31 : Immunofluorescence of HEK PKR cells infected with GFP tagged rBUNV. HEK PKR cells uninduced (**1, 3, 4, 5**) or induced (**2, 6, 7, 8**) were mock infected or infected with rBUNGc-eGFP or rBUNM-NSm-EGFP or rBUNM-NSm-EGFPDelNSs at an MOI of 1 for 24 hours at which point the cells were fixed with 4% paraformaldehyde. Viral infection was determined by autofluorescence of GFP (green) and or indirect immunofluorescence using an anti-N Texas Red conjugated antibody (red). Induction of the ISG PKR was detected by indirect immunofluorescence using an anti-FLAG Cy5 conjugated antibody (blue).

chimeric NSmGFP protein which will be used by the virus during morphogenesis but is not packaged and as the virus is far into the replicative cycle this is why there was less N protein. NSmGFPdel is even more attenuated than the other GFP-tagged viruses thus the infected cells in panel 5 have not progressed as far as in panels 3 and 4 (**Fig 5.31**). In comparison,

panels 6, 7 and 8 show considerably less chimeric GFP protein than N protein as they are not as far into their replicative cycle compared with panels 3 and 4 (**Fig 5.31**). In the induced cells, however, 40% of the cells showed evidence of infection for each virus (**Fig 5.31**, panels 6, 7 and 8), supporting the earlier findings of lower viral yield and reduced N protein synthesis (**Fig 5.4**). The attenuated NSmGFPdel virus was unable to synthesise detectable chimeric NSmGFP proteins by 24 hours post infection (**Fig 5.31**, panel 8).

HEK ISG9-27: Induction of the mock cells resulted in a bright and intense signal from the FLAG-tagged ISG9-27 stained with anti-FLAG antibody that was not present in the uninduced mock cells (**Fig 5.32**, panel 1 and 2). Infection of the uninduced cells with each of the GFP-tagged viruses resulted in 100% of

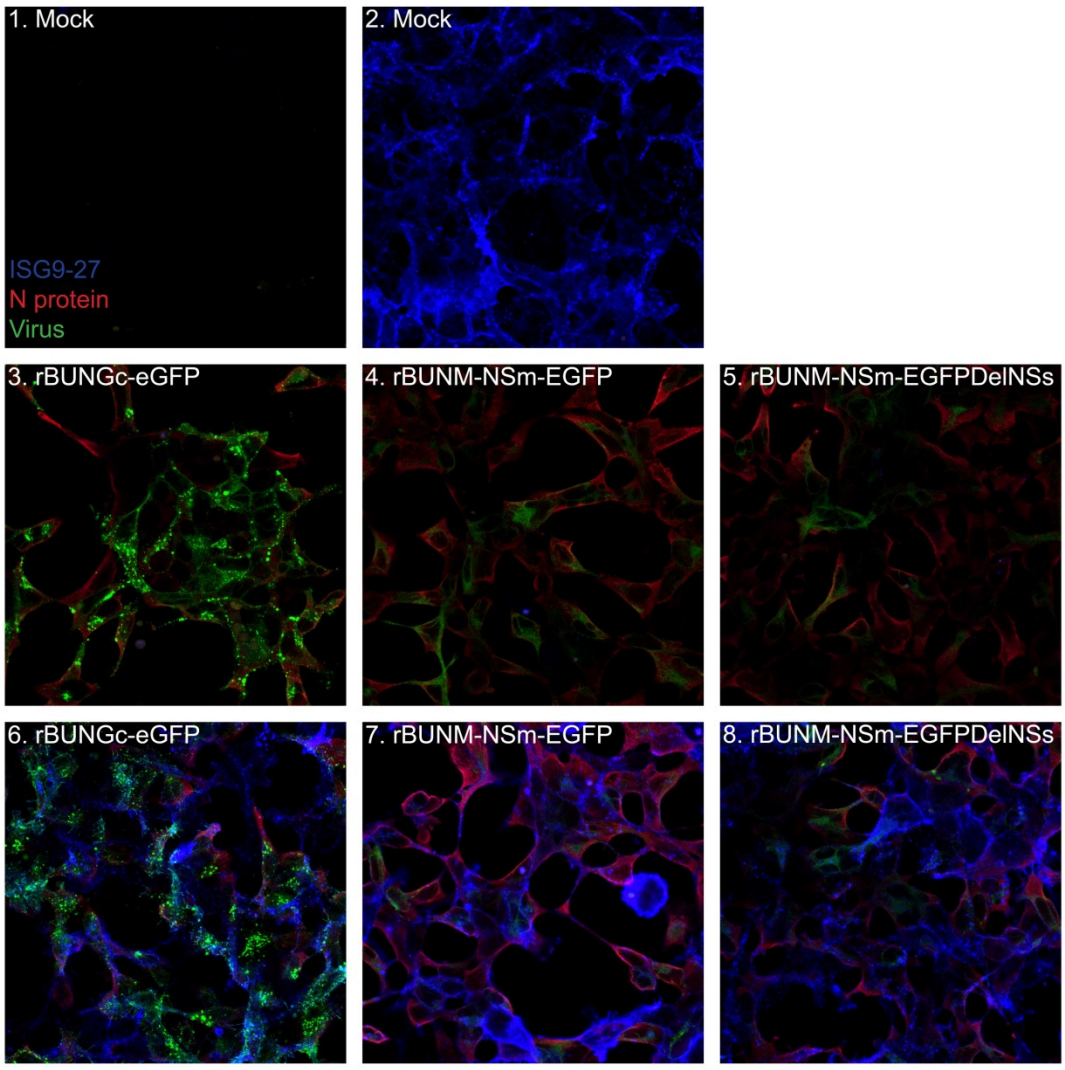

Figure 5.32 : Immunofluorescence of HEK 9-27 cells infected with GFP tagged rBUNV. HEK 9-27 cells uninduced (**1, 3, 4, 5**) or induced (**2, 6, 7, 8**) were mock infected or infected with rBUNGc-eGFP or rBUNM-NSm-EGFP or rBUNM-NSm-EGFPDelNSs at an MOI of 1 for 24 hours at which point the cells were fixed with 4% paraformaldehyde. Viral infection was determined by autofluorescence of GFP (green) and or indirect immunofluorescence using an anti-N Texas Red conjugated antibody (red). Induction of the ISG 9-27 was detected by indirect immunofluorescence using an anti-FLAG Cy5 conjugated antibody (blue).

the cells being infected (**Fig 5.32**, panels 3, 4 and 5), however in the induced cells the number of infected cells was 90% (**Fig 5.3**, panels 6, 7 and 8) and further supports the slight reduction in viral yield observed earlier by viral yield assays (**Fig 5.23**). The N protein signal was weaker than in other cell lines but was equally visible in both uninduced and induced cells. Panels 6, 7 and 8 (**Fig 5.32)** also show the simultaneous induction and infection of the cells and, as the ISG9-27 protein is normally located in the plasma membrane, it was not observed in the nucleus.

HEK 1-8D: A strong and bright signal from the FLAG-tagged ISG 1-8D stained with anti-FLAG antibody was observed in the induced mock cells compared with the uninduced cells (**Fig 5.33**, panel 1 and 2). Infection with any of the three GFP-tagged viruses resulted in 100% of the uninduced cells being infected (**Fig**

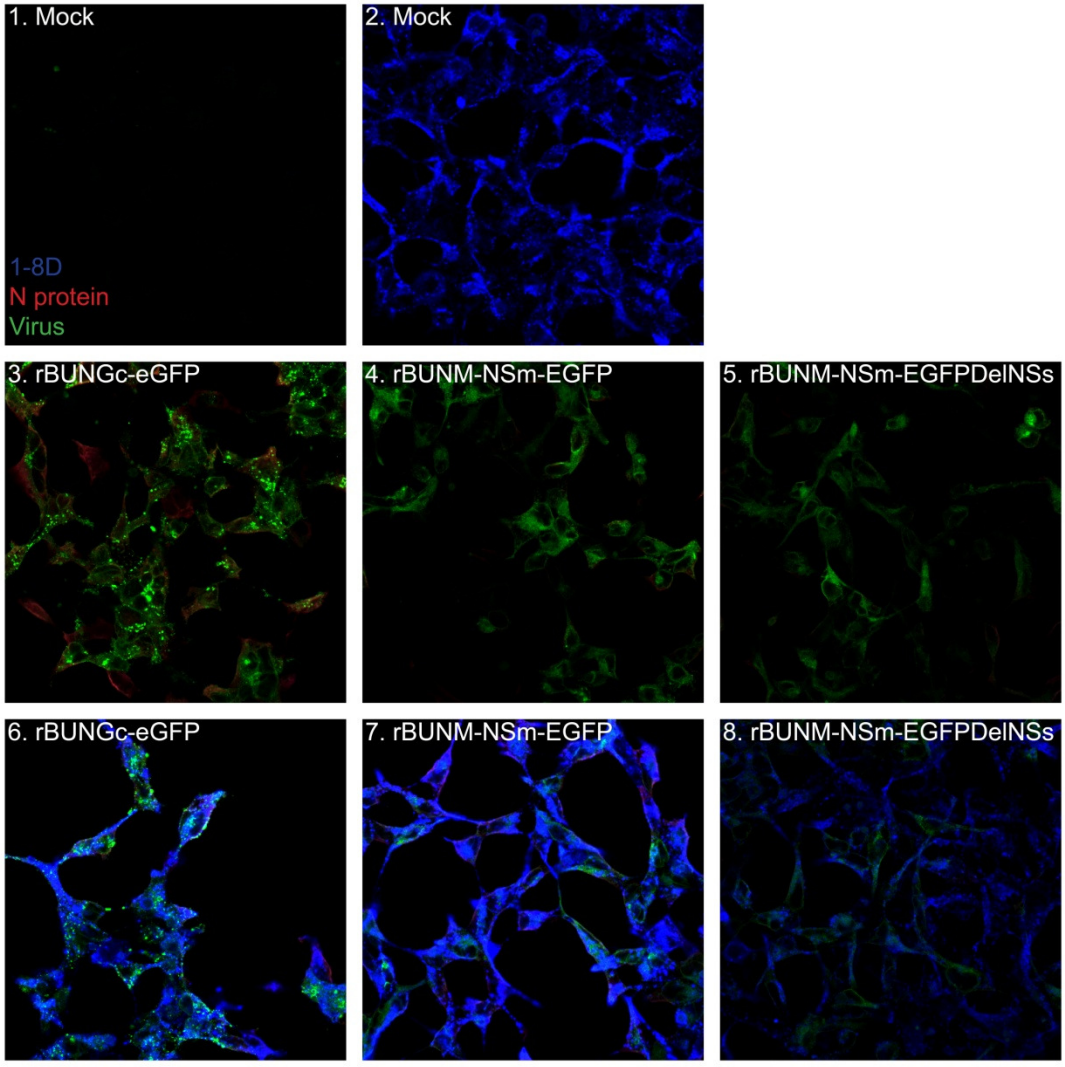

Figure 5.33 : Immunofluorescence of HEK 1-8D cells infected with GFP tagged rBUNV. HEK 1-8D cells uninduced (**1, 3, 4, 5**) or induced (**2, 6, 7, 8**) were mock infected or infected with rBUNGc-eGFP or rBUNM-NSm-EGFP or rBUNM-NSm-EGFPDelNSs at an MOI of 1 for 24 hours at which point the cells were fixed with 4% paraformaldehyde. Viral infection was determined by autofluorescence of GFP (green) and or indirect immunofluorescence using an anti-N Texas Red conjugated antibody (red). Induction of the ISG 1-8D was detected by indirect immunofluorescence using an anti-FLAG Cy5 conjugated antibody (blue).

5.33, panels 3, 4 and 5). Furthermore, induction of the cells conferred no inhibitory effects on the viruses as 100% of the cells were infected which was observed by the GFP signal as the N protein signal was weak in comparison, particularly in panels 5 and 8 (**Fig 5.33**), demonstrating the advantage of using the GFP-tagged viruses. This corresponds with the earlier findings from viral yield assays and Western blot analysis that showed no inhibitory effect by the 1-8D protein on BUNV (**Fig 5.25**).

HEK 1-8U: There was no observed signal in the mock uninduced cells and a strong and bright signal from the FLAG-tagged ISG 1-8U stained with anti-FLAG antibody in the induced mock cells (**Fig 5.34**, panels 1 and 2). When infected with any of the three GFP-tagged viruses the uninduced cells were

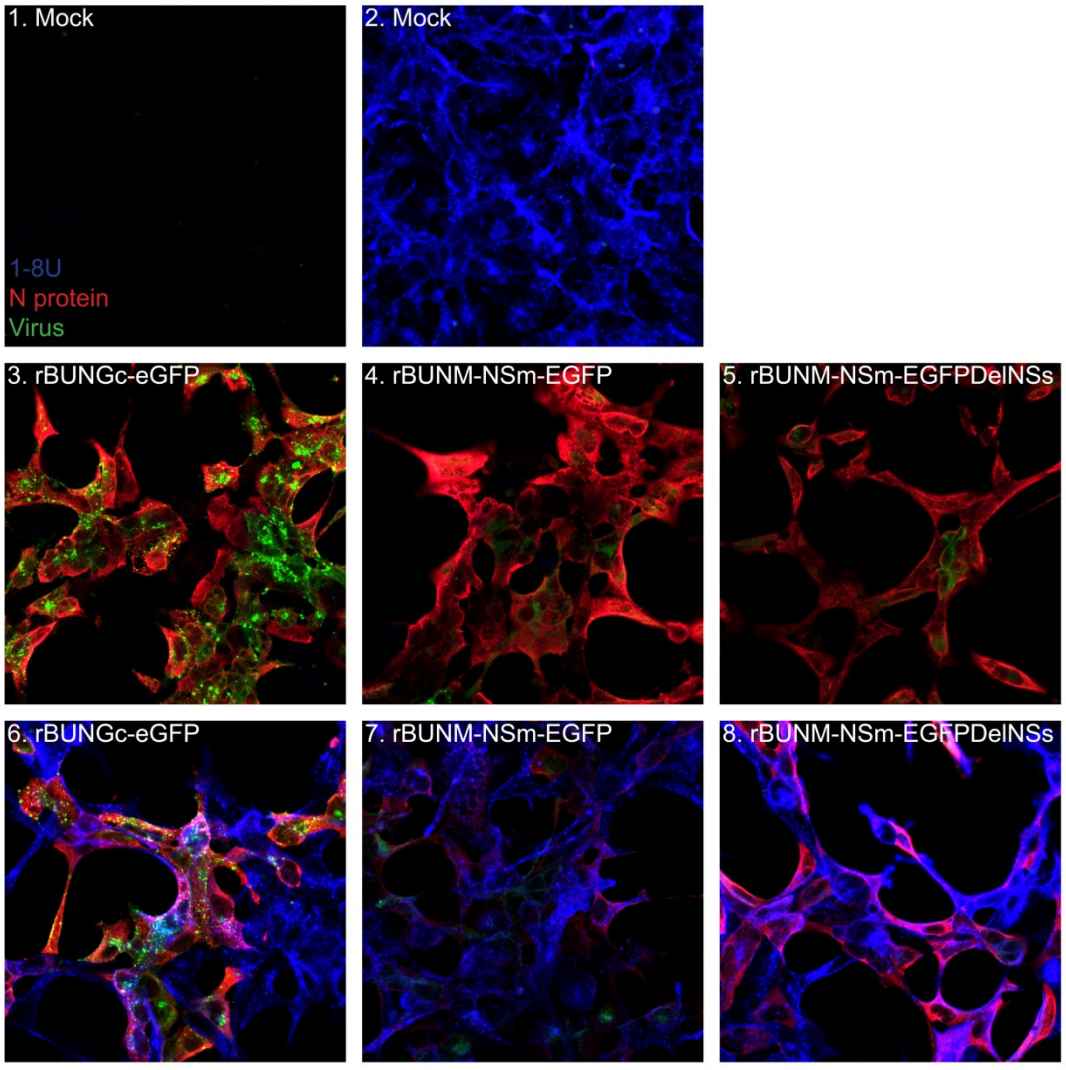

Figure 5.34 : Immunofluorescence of HEK 1-8U cells infected with GFP tagged rBUNV. HEK 1-8U cells uninduced (**1, 3, 4, 5**) or induced (**2, 6, 7, 8**) were mock infected or infected with rBUNGc-eGFP or rBUNM-NSm-EGFP or rBUNM-NSm-EGFPDelNSs at an MOI of 1 for 24 hours at which point the cells were fixed with 4% paraformaldehyde. Viral infection was determined by autofluorescence of GFP (green) and or indirect immunofluorescence using an anti-N Texas Red conjugated antibody (red). Induction of the ISG 1-8U was detected by indirect immunofluorescence using an anti-FLAG Cy5 conjugated antibody (blue).

100% infected (**Fig 5.34**, panels 3, 4 and 5). **Figure 5.34** shows simultaneous ISG induction and infection (panels 6, 7 and 8), and when the cells were induced they showed no restriction on any of the three viruses. All of these data directly relate to the Western blot analysis described earlier (**Fig 5.24**) that showed no restriction on virus replication by the 1-8U protein.

HEK PLSCR1: Induction of the mock cells showed a clear signal compared with the uninduced cells, although it was not very bright (**Fig 5.35**, panels 1 and 2). When infected with each of the GFP-tagged viruses the uninduced cells were completely infected (**Fig 5.35**, panels 3, 4 and 5) and the induced cells

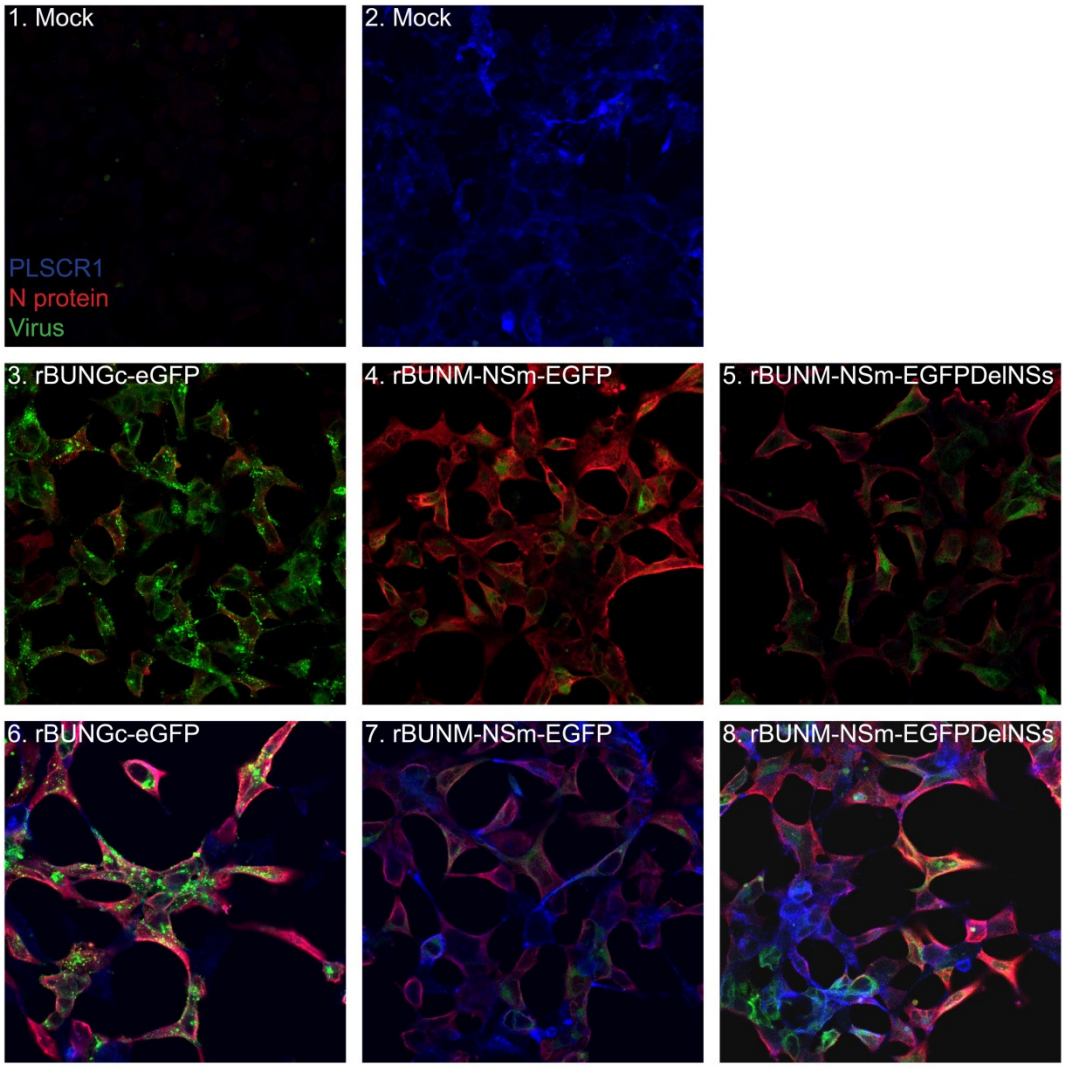

Figure 5.35 : Immunofluorescence of HEK PLSCR1 cells infected with GFP tagged rBUNV. HEK PLSCR1 cells uninduced (**1, 3, 4, 5**) or induced (**2, 6, 7, 8**) were mock infected or infected with rBUNGc-eGFP or rBUNM-NSm-EGFP or rBUNM-NSm-EGFPDelNSs at an MOI of 1 for 24 hours at which point the cells were fixed with 4% paraformaldehyde. Viral infection was determined by autofluorescence of GFP (green) and or indirect immunofluorescence using an anti-N Texas Red conjugated antibody (red). Induction of the ISG PLSCR1 was detected by indirect immunofluorescence using an anti-FLAG Cy5 conjugated antibody (blue).

also showed 100% infection, as well as the simultaneous induction and infection of the cells (**Fig 5.35**, panels 6, 7 and 8). Furthermore, the data shown here correlate with both the virus yield assays and Western blot analysis described earlier (**Fig 5.7**).

Table 5.2 shows the empirical data collected from the immunofluorescence experiments in the form of the % of infected cells out of 1000 that were counted.

Table 5.2: Percentage of infected cells out of 1000 observed using immunofluorescence microscopy.

Cell line / Virus	HEK 38348		HEK PKR		HEK 9-27		HEK 1-8D		HEK 1-8U		HEK PLSCR1	
	-	+	-	+	-	+	-	+	-	+	-	+
rBUNGc-eGFP	100	100	100	40	100	90	100	100	100	100	100	100
BUNGFP	100	100	100	40	100	90	100	100	100	100	100	100
NSmGFP del	100	100	100	40	100	90	100	100	100	100	100	100

- denotes uninduced cells
+ denotes induced cells

Discussion

The screening of these cell lines using immunofluorescence proved to be a useful and accurate tool. Of the six cell lines used, four (38348, 1-8D, 1-8U and PLSCR1) showed no visible inhibition as all were 100% infected by 24 hours post infection which was further reflected in the absence of change observed in Western blot analysis and viral yield assays. Of the other two cell lines, ISG9-27 showed a 10% reduction of cells infected, which correlates with a 5-fold reduction in viral yield at 24 hours. However there was no effect on the amount of N protein synthesised suggesting that ISG9-27s inhibitory effect is early on in the replicative cycle of BUNV. The last cell line analysed by immunofluorescence was HEK PKR which showed a significant reduction of 60% in infected cells which was further illustrated by the detection of less N protein on the Western blot and in a lower viral yield. However, the reduction observed was of infected cells as opposed to all cells infected but viral replication reduced by 60%. This suggests that the over-expression of PKR inhibits viral infection before translation of detectable N or chimeric GFP proteins, which is consistent with PKRs antiviral mechanism. It could be that the cells were infected but the infection detection methods (staining and autofluorescence of translated proteins) used were unable to detect infected cells in stages of viral replication prior to translation. Chen *et al*. (Chen *et al*., 2010) showed that heterocellular IFNβ induction occurs in BUNV infected cells, therefore PKR expression may induce other antiviral mechanisms that further inhibit the early stages of BUNV replication, which is consistent with the role of PKR as a PRR. Thus this fluorescence technique, that utilised the GFP tagged viruses, is useful for screening cell lines for their anti-BUNV properties by showing the one cell line (HEK PKR) out of six that was found (by viral yield assay and Western blot) to be able to considerably inhibit BUNV replication.

Further, the visible 10% reduction in infection of HEK ISG9-27 cells correlated with a reduction in viral yield. Importantly the method produces data four days before plaque assays and is less time consuming. Furthermore, with the use of fluorescence microscopes and plate readers this time can be cut to real-time analysis as the GFP fluorescence can be observed in vivo and the cells returned to the incubator for later time observations or further fixed for staining and confocal microscopy or lysed for Western blot analysis. Thus this would enable an efficient screening process.

Suitability of GFP-tagged viruses for screening: Comparisons of the viral yields from BUNV, rBUNdelNSs and the three GFP-tagged viruses in HEK 38348 cells showed that, though attenuated, the GFP viruses followed a similar growth pattern as BUNV and rBUNdelNSs. Using HEK PKR cells further corroborated this finding by showing a similar pattern in viral yield across both uninduced and induced cells, thus demonstrating that the detection of GFP from the GFP-tagged viruses was representative of the viral inhibition that was shown to be occurring. However, there was variability in virus yield observed across many of the uninduced HEK ISG cell lines, most likely attributable to virus preparation using different cell lines. Elite virus stocks are, usually, amplified and titred using BHK cells. Therefore the titre may be different when infecting HEK cells, thereby explaining the observed fluctuations in viral yield from uninduced cells expressing different ISGs. For these reasons the GFP-tagged viruses are suitable for screening as observations by immunofluorescence match those of more classical virology. However, further thought is required to consider the location of the GFP tags and the subsequent consequences. Despite many years of fruitful research on orthobunyaviruses, there is still much to learn, and all the ramifications of inserting GFP into the NSm protein or of replacing part of the N-terminal of the Gc protein with GFP are not yet known. These manipulations may have useful or detrimental effects on each of the stages of replication from entry to egress, which is emphasised by the attenuation of the tagged viruses, and therefore the viruses should be used for screening in conjunction with other assays that can confirm any effects that are or are not found.

One concern with studies using cells engineered to over-express ISG proteins is the dependency of some proteins on other ISGs and or cellular factors for their antiviral effect. For example ISG15 is dependent on proteins in the entire ISGylation pathway such as UBE1L, UBE2L6, HerC5 and USP18 which are responsible for activation, conjugation, ligation and de-ISGylation of ISG15 respectively, thus each is vital for the pathway. Therefore over-expression of just one of these individual proteins may not be sufficient for the successful inhibition of virus. Versteeg *et al.* (2010) showed that in their system substitution of either ISG15, E1, E2, or E3 with GFP resulted in the loss of ISG15-conjugate formation. However, over-expression of UBE1L may lead to

increased activation of ISG15 and the subsequent hyper stimulation of the ISGylation pathway. Likewise over-expression of the rate limiting factor in the pathway may increase the efficiency of the whole process.

De-ISGylation requires deconjugation enzymes and studies have identified five classes of de-ubiquitinating proteolytic enzymes, one of which is the ovarian tumour (OTU) domain family. Several mammalian proteins which have an OTU domain have been shown to be involved in deconjugation of ubiquitin, such as the NF-κB activation inhibitor A20 which down regulates TNF-α signalling *via* TRAF6 de-ubiquitination (Boone *et al.*, 2004; Evans *et al.*, 2004). The nairovirus CCHFV L protein contains an OTU domain and has been shown to reduce the level of ISGylated proteins almost as well as UBP43 (USP18), thus counteracting the effects of ISG15 (Frias-Staheli *et al.*, 2007). An OTU domain was found in other nairovirus L proteins but not in any other viral L proteins of the four remaining genera in the *Bunyaviridae* (Frias-Staheli *et al.*, 2007), although the existence of other OTU-like domains cannot be dismissed.

In this study the significant level of virus inhibition was taken to be 10-fold or greater because many ISGs appear to show low level restriction which demonstrates the combined antiviral strategy employed by cells. This does not lower the importance of the role, in combination, that each ISG plays in the antiviral response to BUNV infection but merely enables identification of the ISGs that have a more involved function in the antiviral response. Three cell lines showed a > 10-fold reduction in viral yield; HEK MTAP44, HEK viperin and HEK PKR. The viperin- and PKR-expressing cells further showed a reduction in N protein levels, suggesting a larger role in inhibition of BUNV replication. Several cell lines showed a < 10-fold reduction in viral yield but none of these cells inhibited the amount of N protein detected. A negative effect of viperin, PKR and ISG20 has been described on HCV replicons (Jiang *et al.*, 2008) whereas my preliminary data regarding ISG20 suggest no effect on BUNV but data on rBUNdelNSs have not yet been collected. The inhibition of BUNV and rBUNdelNSs by the over-expression of PKR and viperin will be discussed further in Chapter Six and Chapter Seven, respectively.

The induced HEK MTAP44 cell line showed significant restriction (> 10-fold) by 36 hours post-infection in BUNV and by 48 hours in rBUNdelNSs infected cells. Little is known about the function of this protein but it has been shown to aggregate with microtubules and thus, this may affect the early viral transport in the cell. A previous study showed MTAP44 to be localised in the cytoplasm after IFN induction and that it contains a GTP binding site (Hallen *et al.*, 2007). This led them to suggest that MTAP44 binds to intracellular GTP *ergo* depleting the cytoplasmic levels of GTP and ultimately leading to the inhibition of cell division/growth. The depletion of GTP by MTAP44 does not however appear to inhibit N protein synthesis.

In addition to the PKR, viperin and MTAP44 cell lines, several other lines showed some level of restriction (20035, 20637, ISG9-27, ISG12a, ISG15, ISG56, OAS1V1, BST2) while the rest (MAPK8, USP18, UBE2L6, 1-8U, 1-8D, ADAR1, PLSCR1, PLSCR2, GBP1, STAF50, SAMHD1, 38348, OAS1V2, OASLV1) showed no detected restrictive effect at all.

The reduction in viral yield but not in N protein level observed from induced HEK 9-27 cells suggests slight inhibition at an early stage of the BUNV replication cycle. As stated earlier recent studies have shown ISG9-27 to inhibit IAV, the two filoviruses EBOV and MARV, and two major flavivirus pathogens DENV and WNV, by an as yet unknown mechanism that involves the late stages of endocytosis (Brass *et al.*, 2009; Huang *et al.*, 2011). Thus, this may account for the slight restriction in viral yield observed as BUNV entry requires acidification of the late endocytic vesicles. There was even less restriction on rBUNdelNSs suggesting the ablation of NSs is advantageous in counteracting ISG9-27 mediated viral inhibition. Furthermore, as the restriction was only seen in the viral yield assays and not on the amount of N protein, it suggests that the deletion of the N-terminus of the Gc protein may have interfered with the antiviral mechanism of ISG9-27 on BUNV. Of the two other IFITM proteins, 1-8D and 1-8U, 1-8D appears not to have any restrictive capabilities on BUNV and rBUNdelNSs, whereas 1-8U showed slight restriction of rBUNGc-eGFP virus, which further corresponds with the distinct antiviral properties of each of the IFITM proteins seen elsewhere.

ISG12a induces apoptosis and therefore the slight restriction of viral replication observed in induced BUNV infected cells could be due to the cells becoming apoptotic. This is exacerbated in rBUNdelNSs virus infected cells as the NSs protein would normally inhibit apoptosis by interacting with IRF3 (see Chapter One). Consequently, apoptosis was possibly triggered by two independent mechanisms in HEK ISG12a-induced and rBUNdelNSs-infected cells: the over-expression of the pro-apoptotic ISG12a and the absence of the anti-apoptotic NSs protein. Furthermore, the spike of viral yield observed at 48 hours could be explained by more cells being infected in the uninduced cells, leading to greater cell death and thus, fewer cells would be available for infection. This can be observed by the extensive cell death seen in rBUNdelNSs infected cells compared with ISG12a induced cells.

Four cell lines (ISG15, ISG56, OAS1V1, and BST2) showed low inhibition in the viral yield assays, although ISG56 expression only inhibited rBUNdelNSs. Together these data imply an overall antiviral effect against BUNV is achieved through several independent inhibitory mechanisms acting synergistically. Some ISGs, such as PKR, viperin and MTAP44, play a larger role in the inhibition of BUNV replication but no single ISG has been found as yet that causes the extent of inhibition on the level such observed in other systems, such as in the inhibition of HIV replication by BST2.

Summary

This chapter shows:

- The effects of 26 (plus 2 mutated ISGs) ISG expressing cell lines.
- That PKR and Viperin show inhibitory effects on BUNV.
- That MTAP44 has restrictive effects on BUNV.
- The screening of six ISG expressing cell lines with tagged GFP viruses using immunofluorescence.
- The GFP-tagged viruses can be used for screening cell lines in conjunction with other techniques.

6 PKR inhibition of Bunyamwera virus

Introduction

PKR was discussed in detail in Chapter One. The previous chapter investigated the growth kinetics of BUNV and rBUNdelNSs in HEK PKR cells and showed that the over-expression of PKR resulted in a ten-fold reduction in viral yield and a significant reduction in the synthesis of N protein from those cells. Therefore, the aim of this chapter was to investigate the inhibitory effects of PKR on BUNV replication in more detail.

Protein expression in HEK PKR cells

To further investigate the effect of over-expressed PKR on BUNV, HEK PKR cells were infected at an MOI of 0.01 pfu/cell with BUNV or rBUNdelNSs and labelled with [^{35}S]-methionine for one hour at different times over a 72 hour period. The cell lysates were then analysed by SDS-PAGE followed by autoradiography (**Fig 6.1**). Comparison of the uninduced and induced mock cells demonstrated that over-expression of PKR and the subsequent translational inhibition results in some non-viral host cell protein shut-off (**Fig 6.1A**, Mock). Both uninduced and induced cells infected with BUNV showed an

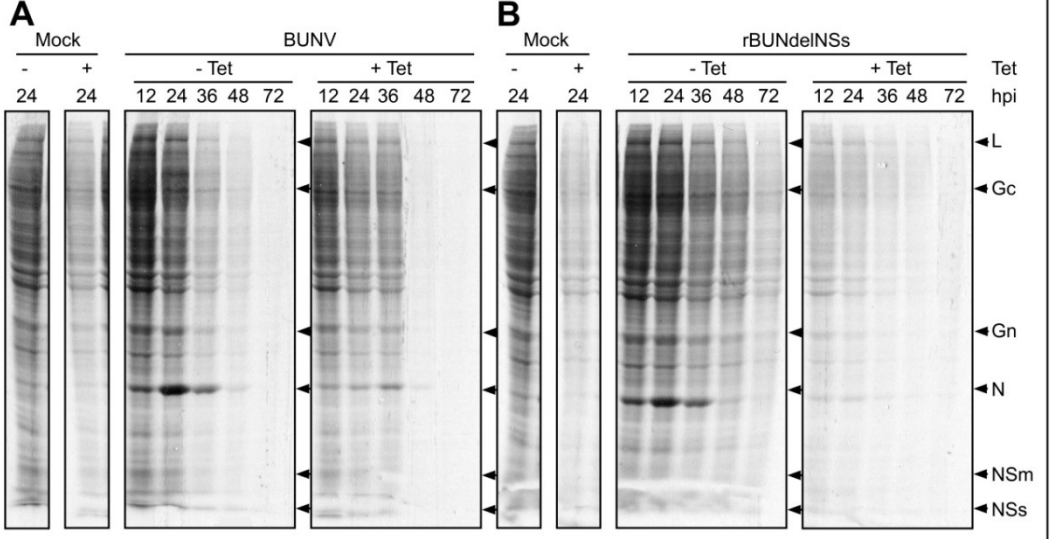

Figure 6.1 : In vivo protein labelling of HEK PKR cells mock infected or infected with BUNV (A) or rBUNdelNSs (B). Cells were either not induced (-) or induced (+) and then infected at an MOI of 0.01 pfu/cell and labelling with [^{35}S]-methionine was carried out for 1 hour prior to the time points indicated, and then the cells were lysed. 1/30 of the volume of the lysate was loaded per well and analysed by SDS-PAGE and autoradiography. The positions of viral proteins are indicated on the right (with arrows in the centre). Tet denotes tetracycline and hpi denotes the hours post infection.

increase in the viral L, Gc and N proteins with the N protein peaking at 24 hours, and clear host protein synthesis shut-off occurring by 24 hours and progressively increasing thereafter. However, the induced cells showed significantly less intense protein bands for the viral proteins L, Gc and N confirming the inhibitory effect on protein synthesis by PKR, and shut-off appeared stronger and earlier at around 12 hours. Infection of uninduced cells

with rBUNdelNSs yielded a similar viral protein synthesis pattern to BUNV with L, Gc and N protein synthesis increasing up to 24 hours post infection, however, host protein synthesis shut-off was not clearly visible until 36 and 48 hours post infection (**Fig 6.1B**). There was no NSs protein expression thus the mechanism of shut-off observed in rBUNdelNSs infected cells was likely due to cap snatching by the L protein resulting in degradation/instability of decapped mRNAs. rBUNdelNSs infected induced cells showed a huge reduction in overall protein synthesis which is attributable to increased PKR expression. The viral L, Gc and N proteins were discernible but their intensities were low compared with the uninduced cells. Western blot analysis was carried out to monitor the accumulation of viral proteins (**Fig 6.2**). In the uninduced cells infected with BUNV there was little increase in the amount of N protein accumulated after 36 hours (**Fig 6.2A**) which correlates with the protein

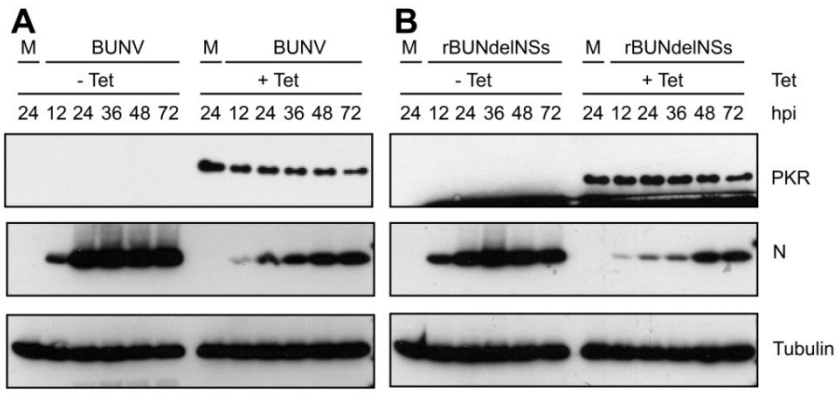

Figure 6.2 : Western blot analysis of HEK PKR cells mock (M) infected or infected with BUNV (A) or rBUNdelNSs (B). Cells were either not induced (-) or induced (+) and then infected at an MOI of 0.01 pfu/cell and lysed at the time points indicated. 1/30 of the lysate was analysed by SDS-PAGE and then transferred to a nitrocellulose membrane and subjected to Western blotting. PKR was detected using anti-FLAG (mouse) antibody, N protein (N) was detected using anti-N (rabbit) antibody and tubulin was detected using anti-Tubulin (mouse) antibody. Tet denotes tetracycline and hpi denotes the hours post infection.

labelling data that showed N protein synthesis peaked at 24 hours (**Fig 6.1A**). Western blot analysis of induced cells, however, showed that N protein synthesis continued until at least 48 hours post infection as the amount of N protein continually increased (**Fig 6.2**), but the total amount of N protein was considerably less than in uninduced cells. When infected with rBUNdelNSs, uninduced cells showed a reduction in N protein accumulation after 36 hours (**Fig 6.2B**), most likely attributable to virus-induced apoptosis (Kohl *et al.*, 2003). However, induced cells showed a continual increase in viral N protein over 72 hours confirming that viral protein synthesis continued even after induction of PKR and thus that over-expression of PKR did not prevent but merely slowed the course of infection. In agreement with this, the overall level of N protein accumulation even at its peak was lower in the induced than the uninduced cells, showing that expression of PKR attenuates viral replication and protein synthesis.

RNA analysis in HEK PKR cells

To investigate the viral RNA profile, HEK PKR cells, both uninduced and induced, were infected with either BUNV or rBUNdelNSs at an MOI of 0.01 pfu/cell. RNA was extracted at different times after infection and analysed by Northern blotting. RNA extracted from uninduced BUNV-infected cells showed the predicted pattern of L, M and S genomic RNA segments (**Fig 6.3A**). RNA from induced cells was significantly reduced for each segment, with a strong S segment signal whereas the L and M segments were barely detected. When

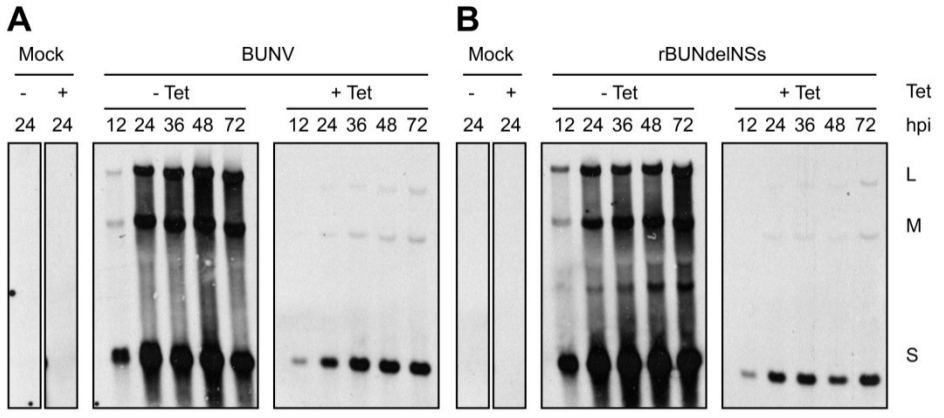

Fig 6.3 : Analysis of viral genomic RNA from HEK PKR cells. Cells were either not induced (-) or induced (+) and the cells were then mock infected or infected with BUNV **(A)** or rBUNdelNSs **(B)** at an MOI of 0.01 pfu/cell. Total RNA was extracted using Trizol at the time points indicated and 10 µg per well was analysed by Northern blotting using probes complementary to genomic RNA (+ve probes). Viral RNAs are identified on the right. Tet denotes tetracycline and hpi denotes the hours post infection.

infected with rBUNdelNSs the uninduced cells showed the predicted pattern for each segment whereas in the induced cells viral RNA synthesis was significantly lower (**Fig 6.3B**). Thus these two sets of data showed that over-expression of PKR considerably reduced but did not abrogate the synthesis of viral genomic RNA.

It is not possible to resolve the BUNV anti-genomic RNA and mRNA species for the L and M segment by Northern blotting. It is, however, possible to resolve the two positive sense RNA species for the S segment because there is a difference in size between anti-genomic RNA (961 nt) and mRNA (850 nt) of approximately 11.5%. The uninduced cells infected with either BUNV or rBUNdelNSs showed the predicted migrations and strong signals for each viral segment (**Fig 6.4A and B**). However, viral synthesis of positive sense RNA was significantly reduced for both BUNV and rBUNdelNSs.

The reductions in viral RNA synthesis seen here correlate with the observed reduction in viral protein synthesis discussed earlier. Thus, it is apparent that induction of PKR expression in HEK PKR cells attenuated viral replication by inhibiting both viral RNA and protein expression.

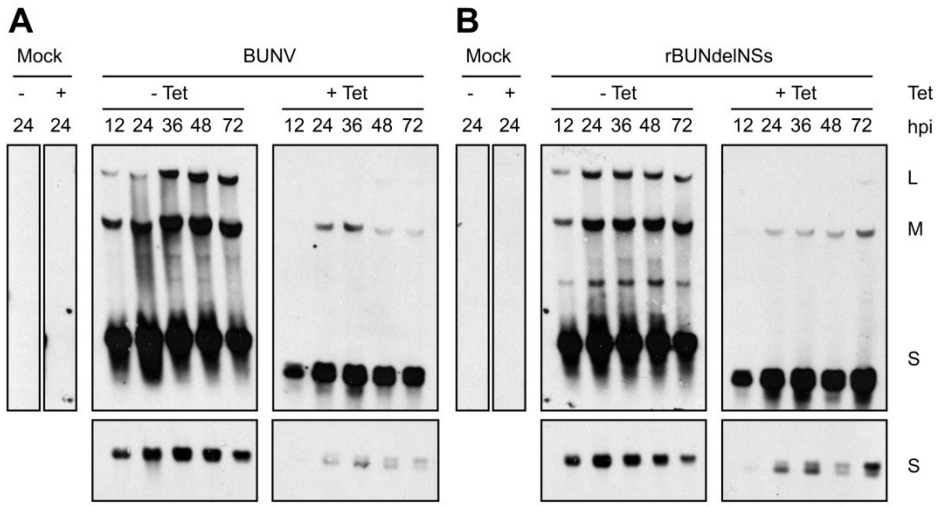

Figure 6.4 : Analysis of viral anti-genomic RNA from HEK PKR cells. Cells were either not induced (-) or induced (+) and the cells were then mock infected or infected with BUNV **(A)** or rBUNdelNSs **(B)** at an MOI of 0.01 pfu/cell. Total RNA was extracted using Trizol at the time points indicated and 10 µg per well was analysed by Northern blotting using probes complementary to anti-genomic RNA (-ve probes). Viral RNAs are identified on the right. The extra panels below are shorter exposures of the S segment. Tet denotes tetracycline and hpi denotes the hours post infection.

BUNV replication in PKR knockdown cells

To investigate the role of PKR in the innate immune response to viral infection, I used a human A549 cell line engineered to express shRNA against PKR (A549shPKR cells (kindly donated by Rick Randall, University of St Andrews, UK)).

Growth kinetics in A549shPKR cells

To investigate the growth kinetics of wild-type and NSs deletion mutant viruses in A549shPKR cells, the cells were either not treated or pre-treated with IFNβ for 24 hours and then infected at an MOI of 1 pfu/cell. Virus released into the growth medium was collected at various times and titrated by plaque assay. In both the untreated and treated cells the BUNV titre increased until 24 hours but

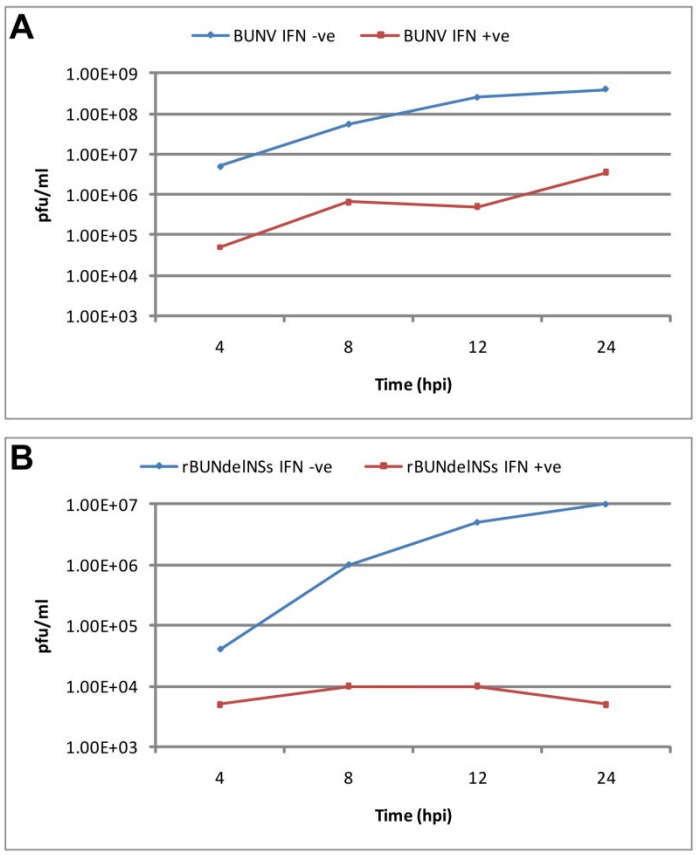

Figure 6.5 : Comparison of BUNV (A) and rBUNdelNSs (B) growth in untreated and IFNβ pre-treated A549shPKR cells. At 37°C, cells were either untreated (-ve) with or pre-treated (+ve) with IFNβ (1000 U/ml) 24 hours prior to infection. The cells were then infected at an MOI of 1 pfu/cell and at the time points indicated virus in the cell supernatants was collected and titrated by plaque assay. Graphs show a representative growth curve.

in the treated cells the titre was ~100-fold lower than the untreated cells, at all time points (**Fig 6.5A**). The data shown here contrast with the data described earlier in Figure 3.7, which showed no increase in BUNV titre in cells pre-treated with IFNβ.

However, the untreated cells infected with rBUNdelNSs produced 1000-fold higher titre than IFNβ treated cells by 24 hours (**Fig 6.5B**). Thus, the knockdown of PKR restored BUNV, but not rBUNdelNSs, replication in IFNβ pre-treated cells.

Protein expression in A549shPKR cells

Earlier data shown in Chapter Three showed that IFN pre-treatment (in A549 and Vero cells) blocked detectable viral protein synthesis (**Fig 3.8, 3.9, 3.12**), thus *in vivo* labelling was used here to determine whether the knockdown of PKR under the same conditions could alter that finding. Untreated and IFNβ pre-treated A549shPKR cells were infected with either BUNV or rBUNdelNSs at an MOI of 1 pfu/cell, labelled with [^{35}S]-methionine for 1 hour at different times over a 24 hour period, and then analysed by SDS-PAGE and autoradiography (**Fig 6.6**). Untreated cells infected with BUNV showed a clear increase in viral protein synthesis from 4 to 12 hours post infection, and host cell protein shut-off was clearly observed by 24 hours (**Fig 6.6A**, middle panel). Conversely, the

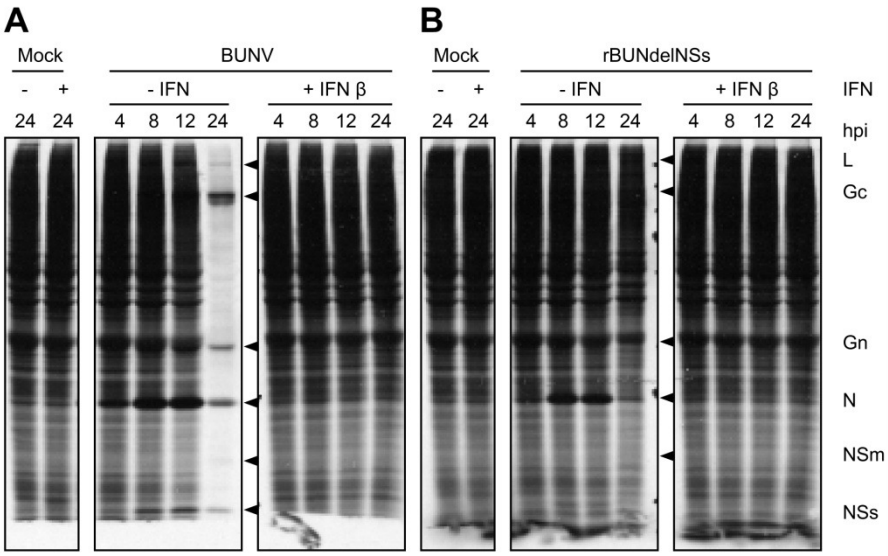

Figure 6.6 : In vivo labelling of A549shPKR cells untreated or pre-treated with IFNβ and infected with BUNV (A) or rBUNdelNSs (B). At 37°C, cells were either not treated with (-) or pre-treated with (+) IFNβ (1000 U/ml) 24 hours prior to infection. The cells were then infected at an MOI of 1 pfu/cell and labelling with ^{35}[S]-methionine was carried out for 1 hour prior to the time points indicated, and then the cells were lysed. 1/30 of the volume of the lysate was loaded per well and analysed by SDS-PAGE and autoradiography. The positions of viral proteins are indicated on the right (with arrows in the centre). IFN denotes interferon and hpi denotes the hours post infection.

cells treated with IFNβ showed a significant reduction in viral protein synthesis with no viral proteins visible throughout the 24 hours (**Fig 6.6A**, right panel). Furthermore, there was no observable virus induced host protein shut-off in the same samples. Infection with rBUNdelNSs resulted in a similar pattern of viral protein synthesis; in the untreated cells viral proteins were visible by 8 hours and remained constant through 12 hours and then reduced by 24 hours but in the treated cells there were no visible viral proteins. Thus, pre-treatment with IFNβ was able to block viral protein synthesis and prevent virus-induced protein shut-off by BUNV.

To further understand viral protein synthesis under these conditions, the labelled cell lysates were immunoprecipitated with anti-BUN antibody and then analysed by SDS-PAGE and autoradiography (**Fig 6.7A**). BUNV infected untreated cells showed viral protein synthesis was underway for Gc and N protein by 4 hours and for L protein by 8 hours. Protein synthesis increased and plateaued at 12 hours and reduced again by 24 hours, which is consistent with the data described above. The treated BUNV infected cells showed weak

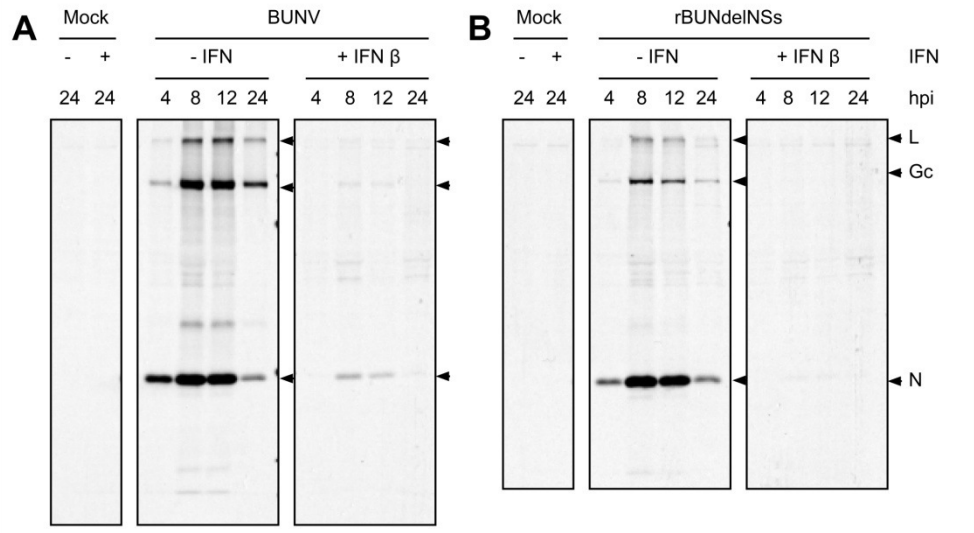

Figure 6.7 : Immunoprecipitation of A549shPKR cells untreated or pre-treated with IFNβ and infected with BUNV (A) or rBUNdelNSs (B). At 37°C, cells were either not treated with (-) or pre-treated with (+) IFNβ (1000 U/ml) 24 hours prior to infection. The cells were then infected at an MOI of 1 pfu/cell and labelling with ^{35}[S]-methionine was carried out for 1 hour prior to the time points indicated, and then the cells were lysed. Using 1/3 of the lysate the soluble antigen extracts were immunoprecipitated with anti-BUN antibody, and the precipitates were analysed by SDS-PAGE and autoradiography. The positions of viral proteins are indicated on the right (with arrows in the centre). IFN denotes interferon and hpi denotes the hours post infection.

N protein expression at 8 and 12 hours (**Fig 6.7A**). rBUNdelNSs infected but untreated cells produced a similar protein synthesis pattern to BUNV but the L and Gc protein levels were less, however protein synthesis in the treated cells was undetectable (**Fig 6.7B**).

These data correlate with the viral titres described in Figure 6.5 and show that there was protein synthesis occurring in Figure 6.6 but at a level undetectable by the method described there.

Western blot analysis to detect N protein showed a significant increase, from 4 hours through to 24 hours, in the amount of N protein expressed by untreated BUNV infected cells (**Fig 6.8**). In contrast, the IFN pre-treated cells not only showed a large reduction in detectable protein but also that N protein levels peaked at 12 hours and were reduced by 24 hours, indicative of protein degradation. Compared with BUNV-infected cells, those infected with rBUNdelNSs showed less intense N protein signals which were detectable at 4 hours, peaked at 12 hours and then reduced by 24 hours (**Fig 6.8**). In contrast,

there was no detectable N protein from the IFN-treated cells. The tubulin blots confirm not only protein loading controls for the Western analyses but also for the *in vivo* labelling experiments. Thus, IFN pre-treatment inhibited viral protein synthesis by both BUNV and rBUNdelNSs, as determined by monitoring N protein production.

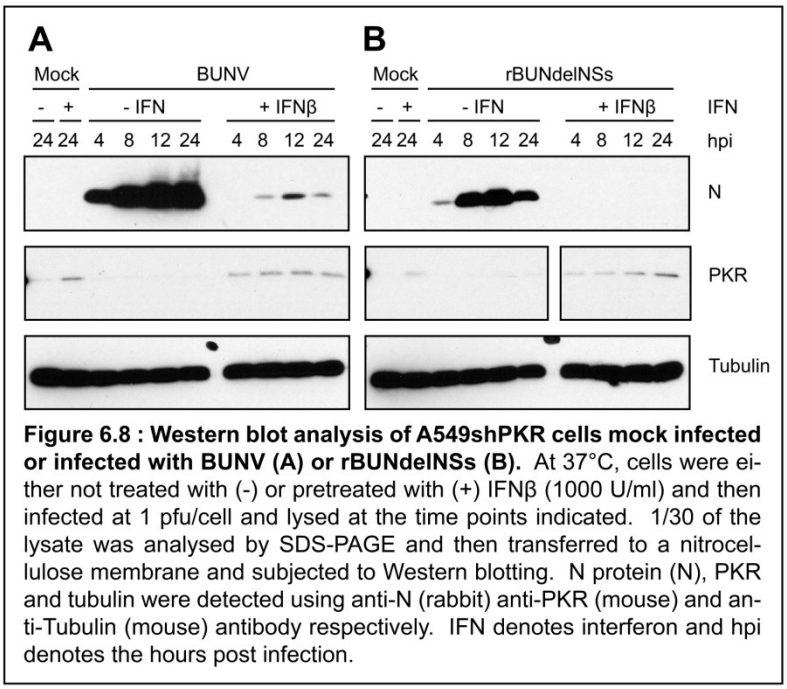

Figure 6.8 : Western blot analysis of A549shPKR cells mock infected or infected with BUNV (A) or rBUNdelNSs (B). At 37°C, cells were either not treated with (-) or pretreated with (+) IFNβ (1000 U/ml) and then infected at 1 pfu/cell and lysed at the time points indicated. 1/30 of the lysate was analysed by SDS-PAGE and then transferred to a nitrocellulose membrane and subjected to Western blotting. N protein (N), PKR and tubulin were detected using anti-N (rabbit) anti-PKR (mouse) and anti-Tubulin (mouse) antibody respectively. IFN denotes interferon and hpi denotes the hours post infection.

RNA analysis in A549shPKR cells

Activation of PKR leads to a reduction in host cell protein synthesis *via* inhibition of translation. Therefore, in the absence of PKR, the cellular restriction mechanism(s) of IFNβ on BUNV replication may involve transcriptional inhibition, either for primary transcription or genome amplification. To investigate this further, untreated and pre-treated A549shPKR cells were infected at an MOI of 1 pfu/cell, total RNA extracted at several time points after infection, and then analysed by Northern blotting. Using probes complementary to genomic viral RNA, it was clear that pre-treatment with IFNβ significantly restricted BUNV and completely restricted rBUNdelNSs (**Fig 6.9**). From

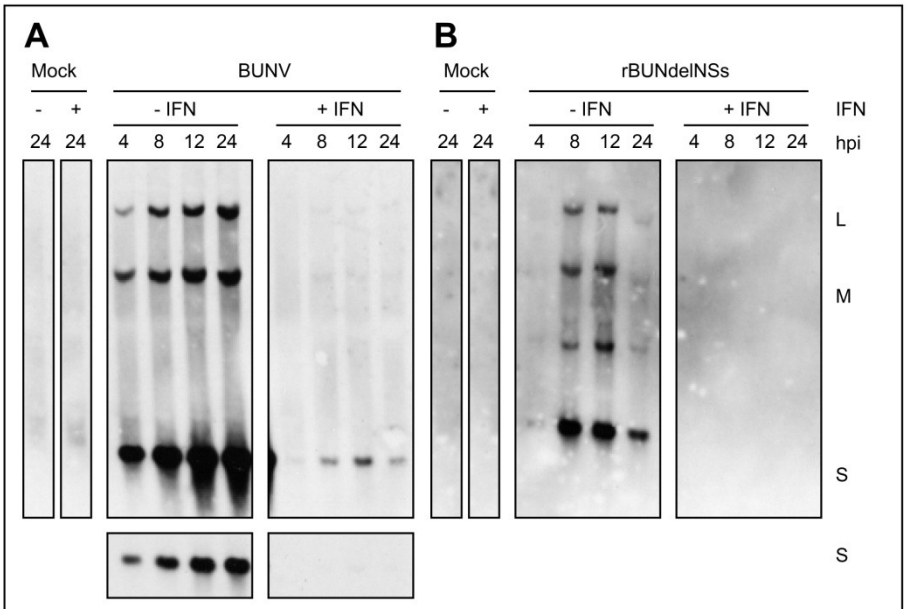

Figure 6.9 : Analysis of viral genomic RNA from A549shPKR cells. At 37°C, cells were either not treated with (-) or pre-treated with (+) IFNβ (1000 U/ml) 24 hours prior to infection. The cells were then mock infected or infected with BUNV **(A)** or rBUNdelNSs **(B)** at an MOI of 1 pfu/cell. Total RNA was extracted using Trizol at the time points indicated and 10 µg per well was analysed by Northern blotting using probes complementary to genomic RNA (+ve probes). Viral RNAs are identified on the right. The extra panels below are shorter exposures of the S segment. IFN denotes interferon and hpi denotes the hours post infection.

untreated BUNV infected cells, genomic S, M and L segments were detected at 4 hours and the intensity of each segment increased throughout the 24-hour experiment, correlating with data discussed above. However, when pre-treated with IFNβ, there was a large reduction in detectable viral RNA: while there was detectable S genomic RNA and faint (clearer on longer exposure) bands for the M and L segments, the overall level of RNA was greatly reduced (**Fig 6.9A**). Untreated cells infected with rBUNdelNSs also showed detectable S and M genomic RNA at 4 hours, both of which increased through 8 and 12 hours and then were reduced by 24 hours. Whereas the L segment was not detected until 8 hours and then increased slightly by 12 hours, and was also reduced by 24 hours post infection. Unlike BUNV-infected cells however, treatment with IFNβ resulted in no detectable viral genomic RNA (**Fig 6.9B**).

Using probes that were complementary to anti-genomic viral RNA, it was clear that pre-treatment with IFNβ severely restricted viral RNA synthesis but, as with genomic RNA, it was barely detectable from either BUNV or rBUNdelNSs (**Fig 6.10**). BUNV infected untreated cells showed signals for positive sense S, M and L segment RNA at 4 hours post infection and the signal from all three segments increased throughout the 24 hour experiment (**Fig 6.10A**). Due to the small difference in size between mRNA and anti-genomic RNA of the M and L

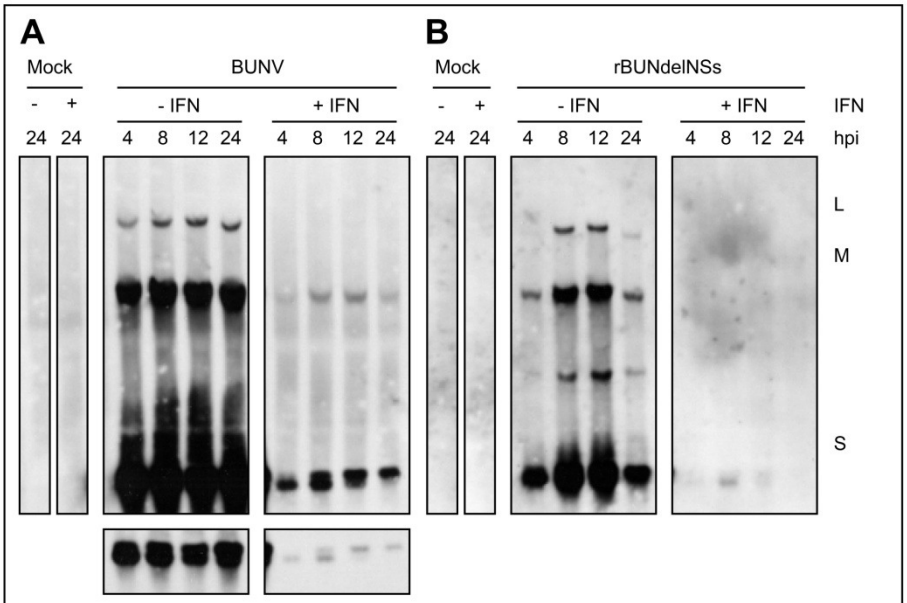

Figure 6.10 : Analysis of viral anti-genomic RNA from A549shPKR cells. At 37°C, cells were either not treated with (-) or pre-treated with (+) IFNβ (1000 U/ml) 24 hours prior to infection. The cells were then mock infected or infected with BUNV **(A)** or rBUNdelNSs **(B)** at an MOI of 1 pfu/cell. Total RNA was extracted using Trizol at the time points indicated and 10 µg per well was analysed by Northern blotting using probes complementary to anti-genomic RNA (-ve probes). Viral RNAs are identified on the right. The extra panels below are shorter exposures of the S segment. IFN denotes interferon and hpi denotes the hours post infection.

segments they do not resolve using this system but it is possible to resolve the S segment RNA species. There did not appear to be any BUNV S segment mRNA or anti-genomic RNA specific inhibition in the treated cells, compared with the untreated cells, although the band separation was not optimal (**Fig 6.10A**).

In untreated cells, rBUNdelNSs S and M segment RNA was detected at 4 hours and increased up to 12 hours but was then reduced (**Fig 6.10B**). The L segment was not detected until 8 hours post-infection and then the level increased until 12 hours, after which it was reduced by 24 hours. However, pre-treated cells infected with rBUNdelNSs produced significantly less positive stranded RNA and S, but not M or L, segment RNA was weakly detected. Neither positive sense M or L segment RNA was detected from treated cells even after longer exposures. These data from both viruses correlate with the data observed in Figure 6.9.

Additionally, *naïve* A549 cells were infected with either BUNV or rBUNdelNSs and immediately treated (synchronous treatment) with IFNβ. While PKR is present in an inactivated state in cells all the time, its expression was upregulated following IFN treatment at 12 hours post treatment (**Fig 6.11**, Mock). In contrast, infection with BUNV did not induce an increase in PKR expression and, moreover, BUNV was even able to restrict PKR expression after IFN treatment (**Fig 6.11**, BUN). Thus there was no increase in PKR levels

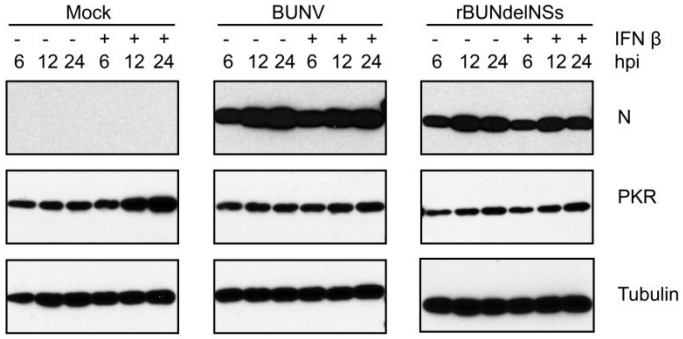

Figure 6.11 : Western blot analysis of A549 cells mock infected or infected with BUNV or rBUNdelNSs. At 37°C, cells were infected at an MOI of 5 pfu/cell and then either not treated with (-) or treated with (+) IFNβ (1000 U/ml) and then lysed at the time points indicated. 1/30 of the lysate was analysed by SDS-PAGE and then transferred to a nitrocellulose membrane and subjected to Western blotting. N, PKR and tubulin were detected using anti-N (rabbit), anti-PKR (mouse) and anti-tubulin (mouse) antibody respectively. IFN denotes interferon and hpi denotes the hours post infection.

observed in BUNV infected cells. Infection with rBUNdelNSs induced a slight increase in expression of PKR in the absence of IFN which was enhanced by the addition of IFNβ (**Fig 6.11**, rBUNdelNSs). However, the slight increase in expression of PKR from rBUNdelNSs infected cells also in the presence of IFN was not as much as was observed from mock infected IFNβ treated cells, suggesting that rBUNdelNSs also inhibits IFN-induced PKR.

Discussion

PKR is a critical molecule in antiviral immunity, since it acts both as a PRR that is able to detect viral dsRNA, and as an ISG that inhibits host cell protein synthesis by phosphorylating eIF2α (Garcia *et al.*, 2006). Therefore, it is not surprising that cells with activated PKR are likely in a state of reduced translation and protein synthesis and this was clearly demonstrated in the mock infected cells in Figure 6.1. This mechanism can be an extremely potent way of blocking viral protein synthesis and for several viruses PKR is blocked in order to permit replication. There are various methods of blocking PKR utilised by different viruses, such as direct interaction with PKR, degradation of PKR, sequestration of dsRNA and the dephosphorylation of eIF2α (Garcia *et al.*, 2006; Langland *et al.*, 2006). The HIV1 TAT protein sequesters dsRNA, thereby removing the PAMP recognised by PKR, and TAT also directly interacts with PKR to prevent its autophosphorylation (Clerzius *et al.*, 2011). Therefore,

over-expression of PKR in cells should make the cells highly sensitive to dsRNA and enhance the effects of the subsequent activation of PKR on host cell protein synthesis.

Streitenfeld *et al.* (2003) demonstrated that in MEF cells both BUNV and rBUNdelNSs activate PKR but this activation does not confer any resistance to the viruses in cell culture. However, using PKR knockout mice they found that PKR does show some weak protection *in vivo* to BUNV infection. Thus, perhaps activation of PKR is ultimately beneficial to BUNV once the infection becomes established. The mechanism of the primary IFN antagonist NSs of BUNV is to inhibit host cell protein synthesis at a transcriptional level by blocking RNA polymerase II mediated transcription (Chapter One). It may be the case that normal expression of PKR is beneficial to BUNV replication by enhancing the effect of host cell protein synthesis shut-off by blocking further cellular protein translation. This PKR-induced translational inhibition, along with cap snatching, may allow for increased viral protein translation as NSs blocks de novo cellular mRNA synthesis and cap snatching reduces cellular levels of mRNA. At the same time viral mRNA and translation is able to increase because the cellular translational machinery has been liberated from cellular mRNAs. In the induced HEK PKR cells, both BUNV and rBUNdelNSs proteins were less intense and cellular protein synthesis was clearly lower. Likewise, even though the level of N protein expression was less in the induced cells it still increased thereby showing that the virus was restricted but not stopped by PKR. Clearly PKR over-expression attenuates but does not stop viral replication for either virus. Further, even in the absence of NSs, there is some viral replication, suggesting that there is more to BUNV inhibition of the IFN response than just NSs. These data also correlated with the RNA analysis that showed restriction by PKR of both genomic and anti-genomic viral RNA but not abrogation. Data in Chapter Five (**Fig 5.4**) showed that both BUNV and rBUNdelNSs were restricted by a factor of 10 in plaque assay by the over-expression of PKR, which also significantly reduced the amount of N protein, thus correlating with the data from this chapter also.

As seen previously in Chapter Three, pre-treatment with IFNβ completely inhibited BUNV replication but this was partially reversed here by knocking down PKR with shRNA which shows that PKR is not a major factor but just one part of the IFN response that inhibits BUNV replication. However, rBUNdelNSs was more restricted than BUNV in protein and RNA synthesis and particularly in the virus titre showing that the NSs protein is still vital for overcoming the IFN response and enabling successful viral replication in the absence of PKR.

The phlebovirus RVFV also encodes a NSs protein on the S segment but in an ambisense coding strategy. RVFV is highly pathogenic, predominantly because of the action of the NSs protein which, like BUNV, blocks IFN induction at a transcriptional level but *via* a different mechanism to BUNV and the NSs-

deletion mutants are IFN inducers and thus attenuated. Habjan *et al.* (2009) and Ikegami *et al.* (2009) demonstrated that not only does RVFV inhibit PKR expression but the virus also targets PKR for proteasomal degradation which is unlike any other bunyavirus and not observed here for BUNV. Thus, other bunyaviruses target PKR likely by different mechanisms compared to BUNV.

Research investigating the mechanisms behind the action of PKR, both as a dsRNA sensor and as an antiviral protein, is constantly updating the complex pathways and cellular proteins involved in the PKR-dependent antiviral response. The ISG ADAR1 has been shown to actually inhibit PKR activation, thereby suppressing the phosphorylation of eIF2α and enhancing the replication of VSV (Li *et al.*, 2010). Also, PKR inhibited HIV replication can be returned to normal by the expression of ADAR1 and the inhibition of ADAR1 expression results in inhibition of HIV expression (Clerzius *et al.*, 2009). Thus some viruses are able to inhibit the PKR response but also are helped by cellular factors that are most likely there to regulate the PKR response. As yet it is unknown whether ADAR1 or other ISGs enhance BUNV replication by inhibiting PKR. Further work is needed to elucidate the mechanism by which BUNV is able to block PKR in order to facilitate viral replication.

Summary

This chapter shows:

- Over-expression of PKR inhibits viral protein synthesis.
- Furthermore, over-expression of PKR inhibits overall viral RNA synthesis.
- Knockdown of PKR in A549 cells rescued BUNV replication.
- However, knockdown of PKR in A549 cells did not rescue rBUNdelNSs replication but did enable detection of some protein and RNA synthesis.

7 Viperin inhibition of Bunyamwera virus

Introduction

Viperin (Virus inhibitory protein, endoplasmic reticulum-associated, IFN-inducible) was initially identified as cig5 in human primary skin cells infected with HCMV (Zhu *et al.*, 1997a) and later the homologues vig1 and mvig were identified in rainbow trout leukocytes infected with the rhabdovirus viral haemorrhagic septicaemia virus (VHSV) (Boudinot *et al.*, 1999) and murine dendritic cells infected with VSV or pseudorabies virus (Boudinot *et al.*, 2000), respectively. Chin and Cresswell (2001) went on to show that viperin was highly induced by both type I and II IFNs and had antiviral activity against HCMV. More recently, viperin has been found to be induced by several different viruses and shown to have antiviral activity against various viruses including IAV, HCV, and HIV (Helbig *et al.*, 2005; Jiang *et al.*, 2010; Rivieccio *et al.*, 2006; Severa *et al.*, 2006; Wang *et al.*, 2007).

Viperin is a 361 amino acid protein with a predicted molecular mass of 42.2 kDa, containing an amphipathic α-helix at its N terminus followed by a CX_3CX_2C motif in the middle and a C terminal conserved domain (Jiang *et al.*, 2008). Hinson (2009a) showed that viperin self-associates and that the 42 amino acid amphipathic α-helix is responsible for viperin localisation to the cytosolic face of the ER and inhibition of soluble protein secretion. Further to this Hinson (2009b) found that the N terminal amphipathic α-helix was necessary for localisation to lipid droplets. Duschene (2010) confirmed that the CX_3CX_2C motif enables viperin to bind iron-sulphur ([4Fe-4S]) clusters and catalyse the reductive cleavage of SAM, thus viperin is also called radical S-adenosyl methionine (SAM) domain-containing 2 (RSAD2) .

Complete understanding of the antiviral mechanism of viperin has yet to be elucidated, although insights into the specific action of viperin-mediated restriction on some viruses has been shown previously. Wang *et al.* (2007) demonstrated that viperin interacts with farnesyl diphosphate synthase (FPPS) and inhibits the enzymatic function of FPPS in lipid metabolism which results in the disruption of lipid raft formation. Lipid rafts play a vital role in the replication cycle of IAV as the envelope of IAV is enriched in lipid rafts and the ensuing accumulation of viral envelope proteins stimulates the budding process of IAV particles (Scheiffele *et al.*, 1999). Thus viperin restricts IAV by blocking viral release and causing a “daisy chain” budding effect. Viperin inhibits HCV replication by associating with lipid droplets, a vital part of the HCV replication cycle, and interfering with HCV in an as yet unidentified manner (Hinson & Cresswell, 2009a). Both SINV and JEV induce viperin expression but SINV induced expression is in an IFN-dependent manner whereas JEV directly activates the viperin promoter *via* IRF3 and AP-1 (Chan *et al.*, 2008). Additionally, SINV replication was significantly reduced by the over-expression

of viperin but JEV was not restricted unless the proteasomal inhibitor MG132 was also added. RNAi knockdown of viperin enhanced SINV replication but did not affect JEV replication, thus JEV may induce viperin but is able to neutralise the antiviral effect of viperin by targeting viperin for degradation. Therefore understanding of the full role that viperin plays in antiviral immunity is incomplete and research into the antiviral mechanism of viperin is ongoing.

As described in Chapter Five a second cell line showed inhibitory effects on BUNV in virus yield assays. The HEK Viperin cell line over-expresses viperin when induced with tetracycline and was found to inhibit BUNV and rBUNdelNSs yields by 100- and 1000-fold respectively which further correlated with a reduction in the amount of N protein synthesis seen by Western blot analysis. This Chapter investigates the effects of viperin in more detail.

Viral protein expression in HEK viperin cells

Initially, to look at the protein expression of BUNV in HEK viperin cells they were infected at an MOI of 0.01 pfu/cell with either BUNV or rBUNdelNSs. The infected cells were labelled with [^{35}S]-methionine for one hour at different times and then whole-cell lysates were analysed by SDS-PAGE and autoradiography.

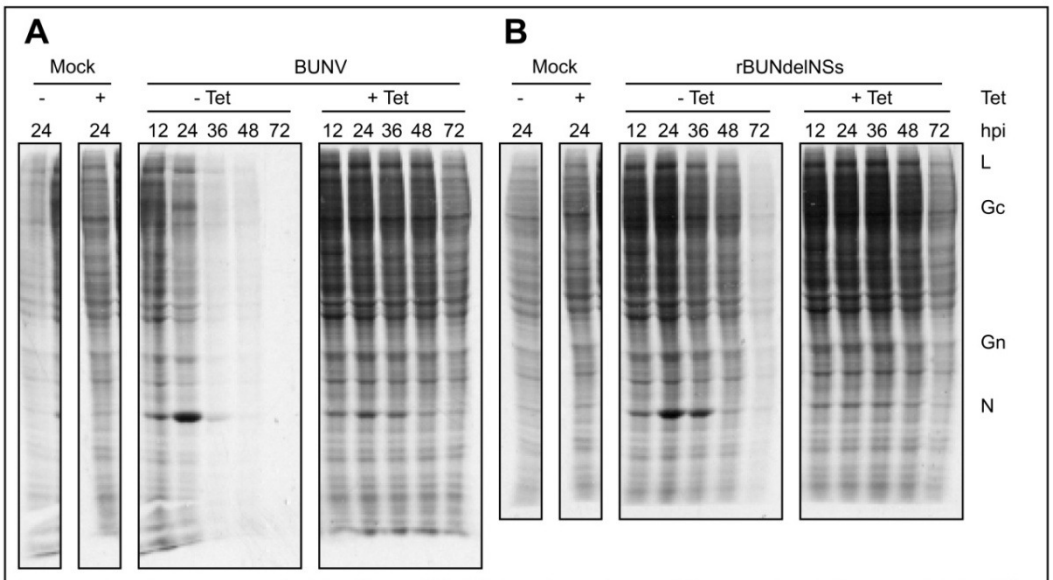

Figure 7.1 : In vivo protein labelling of HEK Viperin cells mock infected or infected with BUNV (A) or rBUNdelNSs (B). Cells were either not induced (-) or induced (+) and then infected at an MOI of 0.01 pfu/cell and labelling with [^{35}S]-methionine was carried out for 1 hour prior to the time points indicated, and then the cells were lysed. 1/30 of the volume of the lysate was loaded per well and analysed by SDS-PAGE and autoradiography. The positions of viral proteins are indicated on the right. Tet denotes tetracycline and hpi denotes the hours post infection.

The N protein signal increased in intensity from 12 to 24 hours and reduced thereafter in the uninduced HEK viperin cells infected with BUNV (**Fig 7.1A**). Host cell protein synthesis shut-off was observed by 24 hours, however shut-off was drastically reduced in BUNV-infected induced HEK viperin cells and was only slightly observed even by 72 hours. The N protein signal was significantly reduced at 12 and 24 hours in comparison with uninduced cells, and a host

band comigrated with N (**Fig 7.1A**), therefore Western blot analysis was needed to confirm the identity of N. Infection of uninduced cells with rBUNdelNSs showed N protein expression increasing from 12 to 24 hours and reducing thereafter, as well as a reduction in host protein synthesis after 36 hours (**Fig 7.1B**). In the induced cells infected with rBUNdelNSs there was no observed viral protein expression.

Analysis of the protein labelling experiment indicated that BUNV had no difficulty replicating in the uninduced cells. In contrast, in the induced cells, the signal for the N protein was considerably reduced and was difficult to discern from cellular proteins (**Fig 7.1A**). Western blot analysis confirmed that BUNV N protein synthesis peaked at 24 hours and the signal for the N protein remained around the same level up to 72 hours (**Fig 7.2A**). Furthermore, the Western

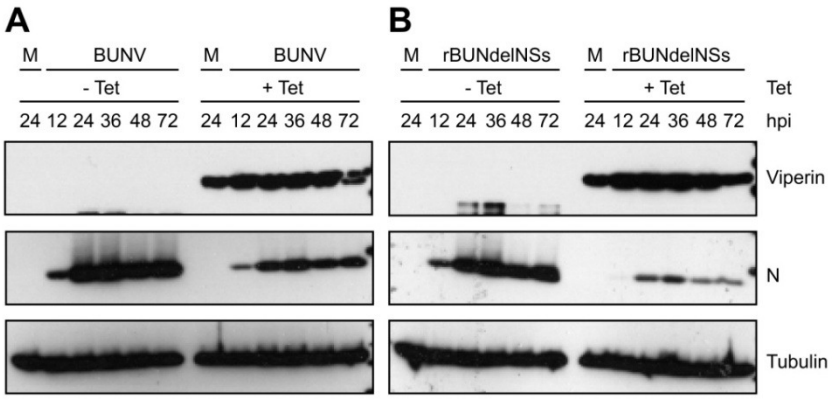

Figure 7.2 : Western blot analysis of HEK Viperin cells mock (M) infected or infected with BUNV (A) or rBUNdelNSs (B). Cells were either not induced (-) or induced (+) and then infected at an MOI of 0.01 pfu/cell and lysed at the time points indicated. 1/30 of the lysate was analysed by SDS-PAGE and then transferred to a nitrocellulose membrane and subjected to Western blotting. Viperin was detected using anti-FLAG (mouse) antibody, N protein (N) was detected using anti-N (rabbit) antibody and tubulin was detected using anti-Tubulin (mouse) antibody. Tet denotes tetracycline and hpi denotes the hours post infection.

blot confirmed that N protein was being synthesised in the induced cells by 12 hours and the amount of N protein then increased until 36 hours, which correlates with the protein labelling experiment. The amount of N protein observed by Western blot from the uninduced cells infected with rBUNdelNSs followed a similar pattern to that of BUNV, being detectable by 12 hours, increasing through 24 and 36 hours and then decreasing (**Fig 7.2B**). A similar pattern to BUNV was also observed for the induced cells infected with rBUNdelNSs but there was significantly less protein detected overall, with the N band intensity peaking at 36 hours and decreasing by 48 hours. Viperin expression following Tet induction was confirmed by Western blotting and was slightly elevated after viral infection, suggesting increased stimulation of viperin expression (**Fig 7.2A and B**).

RNA analysis: HEK Viperin and VPM1 cells

Over-expression of viperin clearly affects the levels of viral protein synthesis. To determine if the restriction was at the transcriptional level, HEK viperin cells were infected with either BUNV or rBUNdelNSs at an MOI of 0.01 pfu/cell and, at various times, total cell RNA was extracted and analysed by Northern blotting.

Essentially, the over-expression of viperin significantly reduced the amount of genomic RNA detected from both BUNV and rBUNdelNSs infected cells. The uninduced BUNV infected cells showed strong signals for each segment by 24 hours whereas the induced cells significantly reduced the amount of detectable

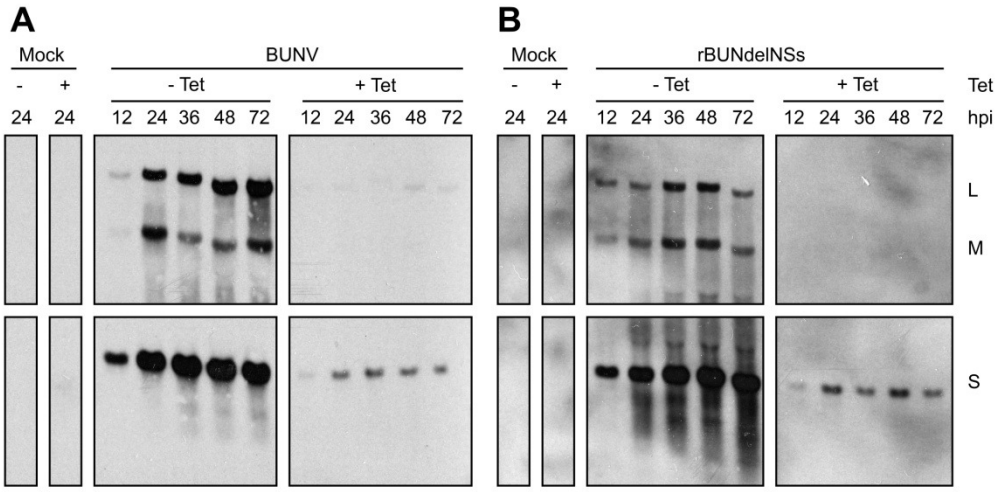

Figure 7.3 : Analysis of viral genomic RNA from HEK Viperin cells. Cells were either not induced (-) or induced (+) and the cells were then mock infected or infected with BUNV **(A)** or rBUNdelNSs **(B)** at an MOI of 0.01 pfu/cell. Total RNA was extracted using Trizol at the time points indicated and 10 µg per well was analysed by Northern blotting using probes complementary to genomic RNA (+ve probes). Viral RNAs are identified on the right. Tet denotes tetracycline and hpi denotes the hours post infection.

genomic RNA (**Fig 7.3A**). The uninduced cells infected with rBUNdelNSs also showed strong signals for each genomic RNA segment by 24 hours and a significant decrease in the level of genomic RNA detected (**Fig 7.3B**).

As with the genomic RNA analysis, the viral mRNA and anti-genomic RNA showed strong signals and the predicted migrations for each segment in the uninduced cells, and in the induced cells there was a significant decrease in the overall amount of RNA detected. To see the L and M segments the blots had to be over-exposed. This could be due to the lower activity of the L and M probes or to less than optimal transfer of those segment RNAs. The size difference between the S segment mRNA and anti-genomic RNA is about 11.5%, making it possible to resolve the two S segment RNA species by electrophoresis, but not the L and M segment RNAs. Therefore, the RNA analysis shown here is focussed on the S segment. The uninduced BUNV infected cells showed the amount of mRNA increased from 12 hours up to 36 hours and then decreased, whereas the amount of genomic RNA increased throughout the course of

infection (**Fig 7.4A**, -Tet lower panel). However, in the induced cells infected with BUNV (**Fig 7.4A**, +Tet upper panel) the amount of mRNA followed a similar pattern as from the uninduced cells but the amount of genomic RNA was reduced. This suggests that there was a block in anti-genomic RNA either

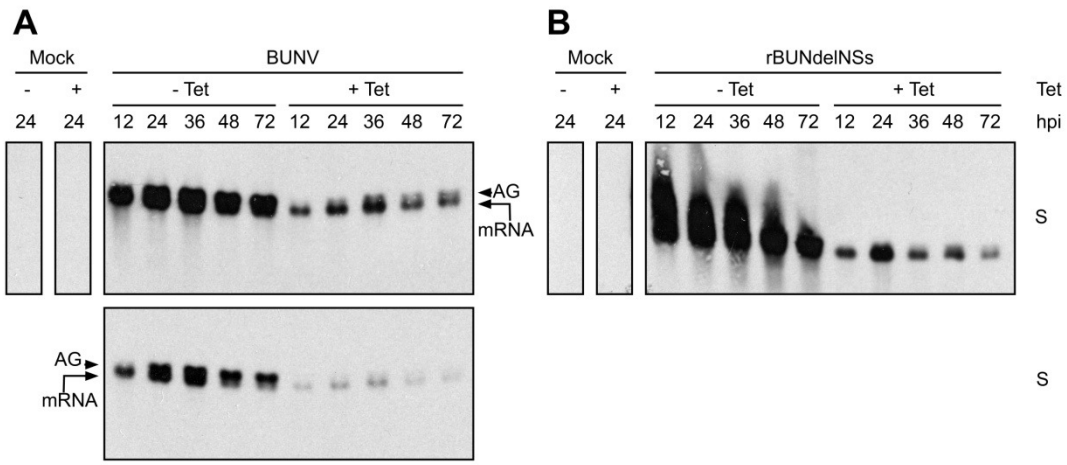

Figure 7.4 : Analysis of viral S segment anti-genomic RNA from HEK Viperin cells. Cells were either not induced (-) or induced (+) and the cells were then mock infected or infected with BUNV **(A)** or rBUNdelNSs **(B)** at an MOI of 0.01 pfu/cell. Total RNA was extracted using Trizol at the time points indicated and 10 µg per well was analysed by Northern blotting using probes complementary to anti-genomic RNA (-ve probes). Viral RNAs are identified on the right. The extra panel below is a shorter exposure. Tet denotes tetracycline, hpi denotes the hours post infection and AG denotes antigenomic RNA.

transcriptionally or post transcriptionally, and could explain the reduction in genomic RNA described earlier. The induced cells infected with rBUNdelNSs showed considerably less positive sense RNA than the uninduced cells but anti-genomic and mRNA could not be separately distinguished (**Fig 7.4B**).

To further confirm that over-expression of viperin caused inhibition of anti-genome transcription, cells that over-express a mutant form of viperin (HEK VPM1 cells) in which the enzymatic capability of viperin was removed, were infected with BUNV at an MOI of 0.01 pfu/cell. At different times the total cellular RNA was extracted and analysed by Northern blotting (**Fig 7.5**). The genomic RNA for each segment from the uninduced cells had been detected by 36 hours and the level increased for each segment throughout the course of infection (**Fig 7.5A**, -Tet). Exactly the same pattern of detected genomic RNA was observed in the induced cells but the signal was slightly less intense (**Fig 7.5A**, +Tet). Positive-stranded S and M segment RNA from the uninduced cells was detected at 24 hours and increased up to 36 hours whereas the L segment RNA was detected at 36 hours and increased thereafter (**Fig 7.5B**, -Tet). Thus, loss of the enzymatic function of viperin in these cells abrogated the inhibitory effect of viperin on BUNV RNA synthesis.

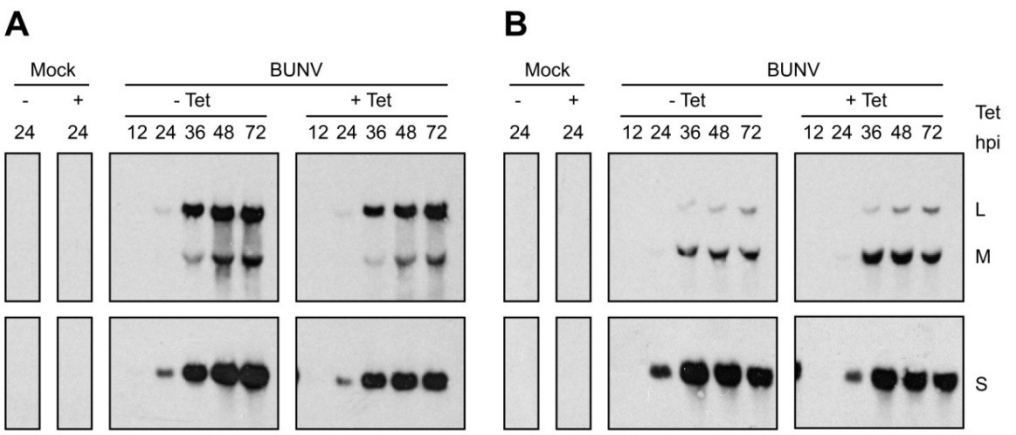

Figure 7.5 : Analysis of viral genomic (A) and anti-genomic (B) RNA from HEK VPM1 cells. Cells were either not induced (-) or induced (+) and the cells were then mock infected or infected with BUNV at an MOI of 0.01 pfu/cell. Total RNA was extracted using Trizol at the time points indicated and 10 µg per well was analysed by Northern blotting using; **(A)** probes complementary to genomic RNA (+ve probes) or **(B)** probes complementary to anti-genomic RNA (-ve probes). Viral RNAs are identified on the right. Tet denotes tetracycline and hpi denotes the hours post infection.

Viperin induction

Over-expression of viperin clearly restricts BUNV replication but it is unknown whether viperin is induced in *naïve* cells following infection with BUNV. To address this question, *naïve* A549 cells were infected with BUNV or rBUNdelNSs at an MOI of 5 pfu/cell and subjected to synchronous IFNβ treatment. At different time points over a 24 hour period, the cells were harvested, lysed and then analysed by Western blotting (**Fig 7.6**). As expected, the amount of N protein produced by both BUNV and rBUNdelNSs increased throughout the experiment in the IFNβ untreated cells (**Fig 7.6**, BUNV and rBUNdelNSs N panel) and for both viruses less N protein was detected when exogenous IFNβ was added at the time of infection (as seen earlier in Chapter Three).

The human ISG MxA is only induced by IFN and is therefore a reliable marker of successful IFN induction and signalling. Mock infected cells showed strong induction of MxA by the addition of IFNβ (**Fig 7.6**, Mock MxA panel). However, BUNV infection alone did not induce MxA, although MxA was induced in BUNV-infected cells treated with exogenous IFNβ but to a lower level than that observed in IFNβ-treated mock cells (**Fig 7.6**, BUNV MxA panel). Thus, BUNV was able to inhibit MxA induction by IFNβ as seen by the considerably reduced signal compared with mock IFNβ treated cells. In contrast, rBUNdelNSs induced MxA expression on its own and the level of MxA observed was higher following the addition of IFNβ (**Fig 7.6**, rBUNdelNSs MxA panel). The level of induction by rBUNdelNSs in the absence of IFNβ was slightly more than in BUNV infected IFNβ treated cells and, in the presence of IFNβ, was only slightly increased, thereby demonstrating the ability of rBUNdelNSs to inhibit MxA despite not expressing an NSs protein.

Viperin expression in A549 cells was confirmed by the signal observed when the cells were treated with IFNβ (**Fig 7.6**, Mock viperin panel) and, while viperin expression peaked by 12 hours, it did remain constant up to 24 hours. The viperin antibody also detected an as yet unknown band just below viperin. BUNV did not however induce viperin in the absence of exogenous IFNβ, but in the presence of exogenous IFNβ viperin was induced to the same level as observed in the mock-infected cells (**Fig 7.6**, BUNV viperin panel). Additionally, BUNV was not able to inhibit viperin expression induced by exogenous IFNβ although it was able to inhibit MxA expression under the same conditions. Unlike BUNV, rBUNdelNSs induced viperin in the absence of IFNβ although not quite as strongly as observed in mock IFNβ treated cells (**Fig 7.6**, rBUNdelNSs viperin panel). Exogenous IFNβ treatment of rBUNdelNSs infected cells

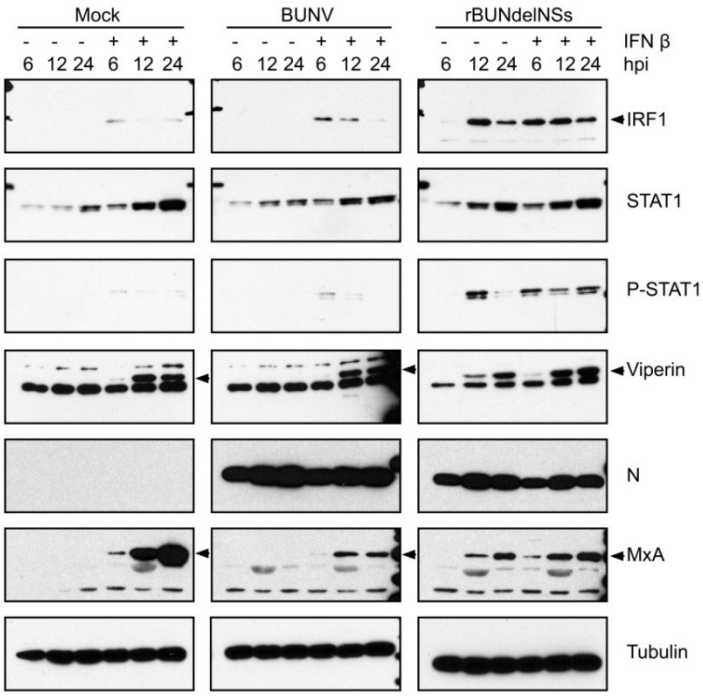

Figure 7.6 : Western blot analysis of A549 cells mock infected or infected with BUNV or rBUNdelNSs. Cells were infected at an MOI of 5 pfu/cell and then either not treated with (-) or treated with (+) IFNβ (1000 U/ml) and then lysed at the time points indicated. 1/30 of the lysate was analysed by SDS-PAGE and then transferred to a nitrocellulose membrane and subjected to Western blotting. IRF1, STAT1, P-STAT1, Viperin, N, MxA and tubulin were detected using anti-IRF1 (rabbit), anti-STAT1 (rabbit), anti-P-STAT1 (rabbit), anti-viperin (rabbit), anti-N (rabbit), anti-MxA (rabbit) and anti-tubulin (mouse) antibody respectively. IFN denotes interferon and hpi denotes the hours post infection, while the arrows indicate specific protein bands.

induced viperin expression although the induction was slightly higher than in either mock or BUNV-infected IFNβ-treated cells, showing that not only are IFNβ and rBUNdelNSs capable of inducing viperin, but they also have a combined cumulative effect on viperin expression (**Fig 7.6**, rBUNdelNSs viperin panel).

Stirnweiss *et al.* (2010) showed that induction of viperin can be by two different pathways: the first is *via* induction of IFNβ that then induces ISGF3 which mediates the induction of ISGs such as viperin; the second is *via* the transcriptional induction of IRF1 which can directly activate the viperin promoter. Western blot analysis showed that IRF1 was weakly upregulated by IFNβ in mock infected cells (**Fig 7.6**, Mock IRF1 panel) and also by BUNV treated with IFNβ (**Fig 7.6**, BUNV IRF1 panel). However, rBUNdelNSs was a good inducer of IRF1 independently of IFNβ addition (**Fig 7.6**, rBUNdelNSs IRF1 panel).

STAT1 is expressed constitutively in cells and both pathways mentioned above are dependent on the activation (by phosphorylation) of STAT1: the first as ISGF3 is a complex comprising STAT1/STAT2/IRF3; and the second as STAT1 directly activates IRF1. Consequently, IFNβ treatment stimulates STAT1 expression (**Fig 7.6**, Mock STAT1 panel) whereas BUNV infection does not induce STAT1 expression unless in the presence of IFNβ and even then expression is reduced due to expression of BUNV NSs protein (**Fig 7.6**, BUNV STAT1 panel). In contrast to BUNV, rBUNdelNSs did induce STAT1 but not quite as strongly as IFNβ (**Fig 7.6**, rBUNdelNSs STAT1 panel). In the mock and BUNV infected cells phosphorylation of STAT1 was weakly detected after addition of exogenous IFNβ (**Fig 7.6**, Mock and BUNV P-STAT1 panel). rBUNdelNSs however, was a strong inducer of STAT1 phosphorylation independently of IFNβ addition (**Fig 7.6**, rBUNdelNSs P-STAT1).

Discussion

The HEK VPM1 cell line over-expresses a viperin mutant that has had the three cysteine residues in the CX_3CX_2C motif 1 replaced with three alanine residues, thus eliminating its viperin-like enzymatic capability. Chapter Five showed that over-expression of VPM1 had no effect on viral yield and further by Western blot that N protein synthesis was unaffected. The inhibitory effect of viperin on BUNV was taken further here by Northern blotting which showed viperin to inhibit BUNV RNA synthesis. Additionally, this RNA restriction was not seen in the mutant viperin VPM1 cells suggesting the RNA restriction is also dependent on the enzymatic action of CX_3CX_2C motif 1 of viperin.

Also, in this system host protein synthesis shut-off was drastically impaired in BUNV-infected induced viperin cells, even more so than in the uninduced cells infected with the NSs deletion virus rBUNdelNSs. The level of host protein synthesis shut-off was similar between induced cells infected with either BUNV or rBUNdelNSs, suggesting the antiviral mechanism of viperin involves NSs. Perhaps viperin interferes with the transport of NSs thereby allowing the time required by the IFN system to respond to BUNV infection. Multiplicity of infection must be considered when discussing shut-off and the low MOI used was required to ensure that the experiment was not stopped early due to immense cell death induced by rBUNdelNSs.

Investigations into the effects of IFN on BUNV infection have found that over-expression of viperin clearly restricts BUNV replication. IFNβ and rBUNdelNSs induce viperin expression and therefore the remaining question is whether viperin is part of the global cellular response to BUNV infection or a more specialised attack on one stage of the BUNV replication cycle. BUNV was found to inhibit viperin expression, probably due to the expression of BUNV NSs blocking host cell protein synthesis. However, it may be that, like JEV, BUNV induces viperin expression and then targets viperin for proteasomal degradation. As BUNV NSs is extremely efficient at host cell protein shut-off, targeting viperin for degradation is unlikely to be required. However, NSs is itself degraded in a proteasome- and ubiquitination-dependent manner (Ingeborg van Knippenberg, personal communication), therefore perhaps viperin is either targeted by NSs for degradation or is co-degraded with NSs. Further work is required to establish if and how BUNV induces viperin and whether NSs restricts or induces viperin degradation.

As Wang *et al.* (2007) showed that viperin expression restricts IAV budding and release, it was hypothesised that viperin may restrict BUNV by interfering with the lipid structure around the Golgi, possibly including lipid rafts. It is unknown whether BUNV uses lipid rafts or even how lipid composition affects BUNV replication. Therefore further investigation into the lipid composition and structure of BUNV particles from 293 cells and HEK viperin cells would begin to address this. Preliminary data from infected 293 cells suggests the lipid composition can be ascertained (data not shown) and thus the method could reveal the effect of viperin over-expression on the lipid composition of BUNV particles.

In Chapter Five the HEK PLSCR1 cell line, which over-expresses the scramblase enzyme PLSCR1 was shown to have no effect on BUNV yield. This scramblase enzyme is involved in the translocation of lipids between the lipid bilayer of the cell membrane thus, as BUNV buds from the Golgi and not the cell membrane PLSCR1-mediated lipid trafficking does not affect BUNV replication. Additionally, PLSCR2 appeared to enhance the viral yield of rBUNdelNSs. Therefore, lipid trafficking and composition could play an important function in the BUNV replication cycle.

Summary

This chapter shows:

- Over-expression of viperin restricts viral protein synthesis and virus induced host protein synthesis shut-off.
- Viperin inhibits overall RNA synthesis.
- The restrictive capability of viperin is dependent on its CX_3CX_2C motif 1.
- BUNV inhibits viperin expression whereas rBUNdelNSs induces viperin expression.

8 Final thoughts

The data presented in this study has furthered the understanding of the effects of IFN on the BUNV replication cycle and may provide insight into potential treatment for bunyavirus infections. The viral protein NSs was already known to be an IFN antagonist and the engineered rBUNdelNSs has been shown to be a strong IFN inducer (Bridgen *et al.*, 2001; Weber *et al.*, 2002). The primary function of the IFN system is to detect and nullify viral infections. Therefore the IFN system relies on being able to detect viral infections quickly and to then rapidly signal the host cell's antiviral defence system and to signal neighbouring cells to go into the antiviral state. Once in the antiviral state, the cells are primed for rapid detection of viral infection and to mount the appropriate antiviral response.

The initial aim for this project had two parts: firstly to advance the understanding of the effects of IFN on BUNV replication; and secondly, to identify specific ISGs that affect the BUNV replication cycle. Chapter Three showed that priming cells first with IFN appears to fully restrict BUNV and that treating the cells with IFNβ after infection appears to have little effect on the virus. It was further shown here that synchronous treatment with IFNβ immediately following infection had a significant effect on viral replication. This treatment caused an overall drastic reduction in synthesis of N and Gc proteins, probably due to a block in translation as there was an increase in positive-stranded viral RNA, but not in genomic RNA. A previous study rescued 57 viable recombinant BUN viruses with a mutated N protein and these could be used in IFNβ studies to establish the importance of the N protein in the successful IFNβ response to BUNV infection (Eifan & Elliott, 2009). Further to this, viral polymerases have been shown to be involved in the antagonism of the IFN response (Iwai *et al.*, 2010; Wang & Ryu, 2010; Yu *et al.*, 2010), and the BUNV L protein contributes to host cell protein synthesis shut-off by cap snatching. It should be investigated in more detail for other IFN antagonistic properties. As the polymerase protein is present within virions, it is feasible that the polymerase plays an important role in the early phase of host cell innate immune antagonism and not only by cap snatching. Finally, an important point to note is that Vero cells are not able to produce type I IFNs due to a spontaneous mutation and they also have a relatively inefficient IRF3 response but they are able to synthesise type III (IFNλs) IFNs (Chew *et al.*, 2009; Emeny & Morgan, 1979). Vero cells do have IFNARs and therefore can respond to type I IFNs, but they have been shown to be highly responsive to IFNλs. Moreover, IFNλ expression and function is very similar to type I IFNs in that they activate the JAK/STAT signalling pathway which activates ISGF3 and subsequently results in the expression of many ISGs. Recently the hantaviruses SNV, ANDV and Prospect Hill virus (PHV) were shown to induce IFNλ in Vero cells, and hantaviruses are not thought to

be detected by MDA5 but both HTNV and BUNV are detected by RIG-I (Lee *et al.*, 2011).

The IFN system involves many cellular proteins and pathways that are interlinked and enable rapid detection of viral infections. The PRRs detect various viral PAMPs and subsequently signal the induction of the IFNβ promoter. Secreted IFNβ acts in both an autocrine and a paracrine manner, triggering the host cell's antiviral defence mechanisms while the surrounding cells enter the antiviral state. Numerous ISGs are upregulated and can impede viral infection although some have been shown to enhance the viral infection.

The second angle on the initial aim of the study was to determine the role, if any, that particular ISGs played in restricting BUNV replication. Chapters Five, Six and Seven addressed this. Chapter Five tested 26 ISG inducible cell lines for restrictive capabilities on BUNV replication and found three showed inhibitory effects ten-fold or greater; MTAP44, PKR and viperin. No further work was undertaken on MTAP44 here but both PKR and viperin were further investigated (Chapter Six and Seven respectively).

PKR has been previously shown to be induced by BUNV infection and to have only marginal inhibitory effects on BUNV replication (Streitenfeld *et al.*, 2003). This study quantified the restriction of PKR, as well as examining the role of another ISG, viperin. Prior to this study viperin was unknown to inhibit bunyaviruses. The role of viperin in controlling the lipid composition of lipid rafts and lipid droplets has been investigated regarding IAV and HCV respectively and may play an essential role in BUNV replication inhibition as BUNV buds into the Golgi (Hinson & Cresswell, 2009a; Wang *et al.*, 2007). Detailed lipidomic studies would reveal the specific lipid composition of bunyavirus virions and determine if they utilise lipid microdomains.

PKR and viperin act synergistically on BUNV: as BUNV infects cells, PRRs (such as PKR and RIG-I) detect the virus and trigger the IFN system leading to the upregulation of the IFNβ promoter and subsequently the expression of antiviral proteins such as PKR and viperin. An increase in PKR expression further enhances viral detection and inhibition of host cell protein synthesis. BUNV primary transcription and NSs expression occurs and the NSs protein interacts with the Mediator complex and subsequently blocks RNA polymerase II mediated host cell transcription. Thus, while the virus fights to control cellular transcription *via* NSs, the cell fights to control BUNV *via* the action of viperin and PKR (and other innate antiviral mechanisms and ISGs). However, when antiviral proteins are already expressed (either by IFN induction or in a transduced cell line) it is very difficult for BUNV to overcome the antiviral state as the cells are primed to restrict the expression of viral proteins, such as NSs. Furthermore, if viperin targets NSs and is already expressed at the time of infection then it may prevent NSs from blocking host cell transcription.

However, BUNV was still able to enter the cells and to replicate at low levels, suggesting there is a mechanism for overcoming expressed antiviral proteins. Perhaps a low level of expression of NSs is enough for the virus to gain the advantage over the innate immune response. Other viruses, such as PIV5, are known to be able to dismantle the IFN-induced antiviral state (Carlos *et al.*, 2005).

Further useful studies to be done would be to engineer three cell lines: one that over-expresses both viperin and PKR; one that expresses shRNA for viperin knockdown; and one that expresses shRNA for both viperin and PKR knockdown. These could be used to quantify the effects of both viperin and PKR together on BUNV as well as to see whether PKR and viperin shRNA knockdown rescues virus replication in IFNβ pre-treated cells, as discussed in Chapter Six. Additionally, these Tet-inducible ISG-expressing cell lines could be used to look at the effect of ISG induction post-infection to establish whether either viperin or PKR over-expression is able to inhibit BUNV replication once it has been established. This study has presented data showing post-infection treatment with IFNβ has limited restrictive effects on BUNV replication (Chapter Three) but perhaps the rapid over-expression of known BUNV inhibitors (such as PKR and viperin) after infection may result in some BUNV restriction.

The reverse genetics system established by Bridgen *et al.* (1996) and later improved by Lowen *et al.* (2005) has enabled the engineering of many recombinant viruses with the aim of further understanding the BUNV replication cycle. These engineering studies resulted in the production of several fluorescently tagged viruses that were able to carry out successful replication cycles although they were somewhat attenuated (Shi *et al.*, 2010; Shi *et al.*, 2009; Shi *et al.*, 2006). In this study, three GFP-tagged viruses were used to investigate the efficacy of using them to screen the ISG-expressing cell lines for their anti-BUNV characteristics. There are two viruses with their NSm protein tagged with GFP; BUNM-NSM-EGFP and BUNM-NSM-EGFPDelNSs. However, there is only one Gc-GFP tagged virus and the study of the effects of IFN (and subsequent ISGs) on BUNV is more easily carried out in comparison with rBUNdelNSs in parallel. Therefore, an additional objective for this project was to engineer rBUNdelNSs to express GFP fused to the Gc protein (as in BUNGc-eGFP) and to characterise the virus, which was achieved and documented in Chapter Four. Subsequently, Chapter Five showed the efficacy of using three of the recombinant viruses for screening ISG-expressing cell lines for their anti-BUNV characteristics. The data presented from viral yield assays, fluorescence and Western blot analyses correlated and distinguished between non-inhibitory and inhibitory ISGs and demonstrated the usefulness of the fluorescently tagged viruses in screening the cell lines. Furthermore, with the use of inverted fluorescence microscopes, cell lines could be set up in multi-well plates and used for imaging of live cells infected with fluorescently tagged

viruses in real-time over many time points. Indeed, a recent study generated over 380 ISG and red fluorescent protein expressing cell lines which were used to analyse the effects on the replicative cycle of the expressed ISG on several different GFP-tagged viruses by fluorescence activated cell sorting (FACS) (Schoggins *et al.*, 2011). The study highlighted several broadly acting ISGs and that a common mechanism of ISG mediated inhibition was at the translational level.

There is little or no cytopathogenicity caused by viruses in the *Orthobunyavirus* genus infecting invertebrate cells but many are cytolytic in their respective vertebrate hosts. The most successful viruses are able to infect the target cell and replicate without destroying the host organism as this enables further propagation of the virus. Measles virus is highly contagious and is spread *via* aerosol and is therefore able to infect many people within the same room (Griffin, 2007). The mortality rate from measles virus infection in developed countries is low so the virus is able to spread easily and rapidly (if the population were not vaccinated). The mortality rate from filovirus infection, such as Ebola virus, can be as high as 90% and therefore the population is often decimated in rural areas before the virus can spread to highly populated areas (Geisbert & Hensley, 2004). Some of the more pathogenic bunyaviruses that infect humans, such as CCHFV and HTNV have mortality rates that can be as high as 30% and 15%, respectively (Whitehouse, 2004; Wichmann *et al.*, 2002). The mortality rate of RVFV is approximately 1% but has been as high as 29% in hospitalised cases (Bouloy & Weber, 2010) and the orthobunyavirus LACV has a mortality rate up to 1.9% (Haddow & Odoi, 2009). The NSs protein of bunyaviruses is very efficient at antagonising the IFN response by causing host cell protein synthesis shut-off, therefore it may be that BUNV has evolved to be less pathogenic in order to enhance the longevity of the virus population. This is evidenced by the relatively low mortality rate from disease outbreaks caused by many members of the *Bunyaviridae*. Perhaps BUNV is able to persistently infect an as yet unidentified mammalian cell line. HTNV causes asymptomatic persistent infections in rodents whilst it can be highly pathogenic in humans (Zeier *et al.*, 2005). Hantaviruses are spread horizontally in rodents often by biting, but also, and for human transmission by aerosolised excreta, *ergo* they are not arboviruses. Perhaps the reason other members of the *Bunyaviridae* are unable to cause persistent infections in humans is that they are transmitted by arthropods. Polymerase (both transcriptase and endonuclease) activity in arthropods may be reduced which could result in less damage to the host cell thereby allowing for low level viral replication as a persistent infection (Carvalho *et al.*, 1986; Rossier *et al.*, 1988). Furthermore, the production of non-classical (sub-genomic) DIs with truncated L proteins or that are temperature sensitive, could have limited the polymerase activity. Renewed interest in DIs has emerged from studies showing that it is the DIs themselves that are detected as PAMPs and lead to the induction of the IFN response (Killip *et al.*, 2011). Thus,

perhaps successful persistent infections in arthropods are not hindered by DI synthesis, but infection of mammalian cells by the same viruses results in strong IFNβ activation due to DI synthesis (Elliott, 1996; Scallan & Elliott, 1992).

IFN is a potent inducer of the antiviral response and is used to treat several viral infections such as HCV and hepatitis B virus (HBV) but IFN treatment has several adverse effects such as headache, muscle pain, convulsions, dizziness, hair thinning and depression. Therefore new methods of treating viral infections are constantly being sought. Identifying particular ISGs that inhibit BUNV may reveal broadly acting ISGs with inhibitory effects on other highly pathogenic bunyaviruses, such as HTNV, CCHFV and RVFV. Alternatively, the inhibitory ISGs could be virus specific but acting on a homologous viral replication mechanism, such as reverse transcription, thus highlighting areas for research. Furthermore, several ISGs are able to exhibit their antiviral effect without irreversibly damaging the host cell. Therefore isolating an ISG that has a combination of known viral antagonist (broadly or specifically) and low cellular damage would be commercially useful as an antiviral as it has potential to be administered without damaging side effects.

Understanding the host cell innate immune response to BUNV infection and how this response targets BUNV makes it possible to envision the engineering of viruses that are attenuated whilst at the same time able to elicit a strong immune response. Thus such viruses could be used to treat already infected individuals to prime their immune response to the established viral infection and ameliorate disease. This knowledge further facilitates the production of more effective vaccines as the viral proteins not targeted internally can be used to elicit a strong and rapid humoral immune response.

References

Abe, T., Hemmi, H., Miyamoto, H., Moriishi, K., Tamura, S., Takaku, H., Akira, S. & Matsuura, Y. (2005). Involvement of the Toll-like receptor 9 signaling pathway in the induction of innate immunity by baculovirus. *J Virol* 79, 2847-2858.

Abramovich, C., Shulman, L. M., Ratovitski, E., Harroch, S., Tovey, M., Eid, P. & Revel, M. (1994). Differential tyrosine phosphorylation of the IFNAR chain of the type I interferon receptor and of an associated surface protein in response to IFN-alpha and IFN-beta. *Embo J* 13, 5871-5877.

Accola, M. A., Huang, B., Al Masri, A. & McNiven, M. A. (2002). The antiviral dynamin family member, MxA, tubulates lipids and localizes to the smooth endoplasmic reticulum. *J Biol Chem* 277, 21829-21835.

Ahmad, S., Alsayed, Y. M., Druker, B. J. & Platanias, L. C. (1997). The type I interferon receptor mediates tyrosine phosphorylation of the CrkL adaptor protein. *J Biol Chem* 272, 29991-29994.

Ahmed, M. & Lyles, D. S. (1998). Effect of vesicular stomatitis virus matrix protein on transcription directed by host RNA polymerases I, II, and III. *J Virol* 72, 8413-8419.

Ahn, S. H., Kim, M. & Buratowski, S. (2004). Phosphorylation of serine 2 within the RNA polymerase II C-terminal domain couples transcription and 3' end processing. *Mol Cell* 13, 67-76.

Alber, D. & Staeheli, P. (1996). Partial inhibition of vesicular stomatitis virus by the interferon-induced human 9-27 protein. *J Interferon Cytokine Res* 16, 375-380.

Alcami, A. & Smith, G. L. (1995). Vaccinia, cowpox, and camelpox viruses encode soluble gamma interferon receptors with novel broad species specificity. *J Virol* 69, 4633-4639.

Alcami, A., Symons, J. A. & Smith, G. L. (2000). The vaccinia virus soluble alpha/beta interferon (IFN) receptor binds to the cell surface and protects cells from the antiviral effects of IFN. *J Virol* 74, 11230-11239.

Alexopoulou, L., Holt, A. C., Medzhitov, R. & Flavell, R. A. (2001). Recognition of double-stranded RNA and activation of NF-kappaB by Toll-like receptor 3. *Nature* 413, 732-738.

Alfadhli, A., Steel, E., Finlay, L., Bachinger, H. P. & Barklis, E. (2002). Hantavirus nucleocapsid protein coiled-coil domains. *J Biol Chem* 277, 27103-27108.

Alff, P. J., Sen, N., Gorbunova, E., Gavrilovskaya, I. N. & Mackow, E. R. (2008). The NY-1 hantavirus Gn cytoplasmic tail coprecipitates TRAF3 and inhibits cellular interferon responses by disrupting TBK1-TRAF3 complex formation. *J Virol* 82, 9115-9122.

Alff, P. J., Gavrilovskaya, I. N., Gorbunova, E., Endriss, K., Chong, Y., Geimonen, E., Sen, N., Reich, N. C. & Mackow, E. R. (2006). The pathogenic NY-1 hantavirus G1 cytoplasmic tail inhibits RIG-I- and TBK-1-directed interferon responses. *J Virol* 80, 9676-9686.

Alminaite, A., Backstrom, V., Vaheri, A. & Plyusnin, A. (2008). Oligomerization of hantaviral nucleocapsid protein: charged residues in the N-terminal coiled-coil domain contribute to intermolecular interactions. *J Gen Virol* 89, 2167-2174.

Anderson, G. W., Jr. & Smith, J. F. (1987). Immunoelectron microscopy of Rift Valley fever viral morphogenesis in primary rat hepatocytes. *Virology* 161, 91-100.

Andersson, I., Lundkvist, A., Haller, O. & Mirazimi, A. (2006). Type I interferon inhibits Crimean-Congo hemorrhagic fever virus in human target cells. *J Med Virol* 78, 216-222.

Andersson, I., Bladh, L., Mousavi-Jazi, M., Magnusson, K. E., Lundkvist, A., Haller, O. & Mirazimi, A. (2004). Human MxA protein inhibits the replication of Crimean-Congo hemorrhagic fever virus. *J Virol* 78, 4323-4329.

Andrejeva, J., Young, D. F., Goodbourn, S. & Randall, R. E. (2002). Degradation of STAT1 and STAT2 by the V proteins of simian virus 5 and human parainfluenza virus type 2, respectively: consequences for virus replication in the presence of alpha/beta and gamma interferons. *J Virol* 76, 2159-2167.

Andrejeva, J., Childs, K. S., Young, D. F., Carlos, T. S., Stock, N., Goodbourn, S. & Randall, R. E. (2004). The V proteins of paramyxoviruses bind the IFN-inducible RNA helicase, mda-5, and inhibit its activation of the IFN-beta promoter. *Proc Natl Acad Sci U S A* 101, 17264-17269.

Arimoto, K., Takahashi, H., Hishiki, T., Konishi, H., Fujita, T. & Shimotohno, K. (2007). Negative regulation of the RIG-I signaling by the ubiquitin ligase RNF125. *Proc Natl Acad Sci U S A* 104, 7500-7505.

Bach, E. A., Aguet, M. & Schreiber, R. D. (1997). The IFN gamma receptor: a paradigm for cytokine receptor signaling. *Annu Rev Immunol* 15, 563-591.

Balachandran, S., Roberts, P. C., Kipperman, T., Bhalla, K. N., Compans, R. W., Archer, D. R. & Barber, G. N. (2000). Alpha/beta interferons potentiate virus-induced apoptosis through activation of the FADD/Caspase-8 death signaling pathway. *J Virol* 74, 1513-1523.

Banninger, G. & Reich, N. C. (2004). STAT2 nuclear trafficking. *J Biol Chem* 279, 39199-39206.

Barber, G. N., Edelhoff, S., Katze, M. G. & Disteche, C. M. (1993). Chromosomal assignment of the interferon-inducible double-stranded RNA-dependent protein kinase (PRKR) to human chromosome 2p21-p22 and mouse chromosome 17 E2. *Genomics* 16, 765-767.

Barnard, P. & McMillan, N. A. (1999). The human papillomavirus E7 oncoprotein abrogates signaling mediated by interferon-alpha. *Virology* 259, 305-313.

Barnes, B. J., Richards, J., Mancl, M., Hanash, S., Beretta, L. & Pitha, P. M. (2004). Global and distinct targets of IRF-5 and IRF-7 during innate response to viral infection. *J Biol Chem* 279, 45194-45207.

Barr, J. N. & Wertz, G. W. (2004). Bunyamwera bunyavirus RNA synthesis requires cooperation of 3'- and 5'-terminal sequences. *J Virol* 78, 1129-1138.

Barr, J. N. & Wertz, G. W. (2005). Role of the conserved nucleotide mismatch within 3'- and 5'-terminal regions of Bunyamwera virus in signaling transcription. *J Virol* 79, 3586-3594.

Barr, J. N., Rodgers, J. W. & Wertz, G. W. (2006). Identification of the Bunyamwera bunyavirus transcription termination signal. *J Gen Virol* 87, 189-198.

Barr, J. N., Elliott, R. M., Dunn, E. F. & Wertz, G. W. (2003). Segment-specific terminal sequences of Bunyamwera bunyavirus regulate genome replication. *Virology* 311, 326-338.

Barr, S. D., Smiley, J. R. & Bushman, F. D. (2008). The interferon response inhibits HIV particle production by induction of TRIM22. *PLoS Pathog* 4, e1000007.

Bauhofer, O., Summerfield, A., Sakoda, Y., Tratschin, J. D., Hofmann, M. A. & Ruggli, N. (2007). Classical swine fever virus Npro interacts with interferon regulatory factor 3 and induces its proteasomal degradation. *J Virol* 81, 3087-3096.

Beaty, B. J. & Calisher, C. H. (1991). Bunyaviridae--natural history. *Curr Top Microbiol Immunol* 169, 27-78.

Bellocq, C. & Kolakofsky, D. (1987). Translational requirement for La Crosse virus S-mRNA synthesis: a possible mechanism. *J Virol* 61, 3960-3967.

Bergeron, E., Vincent, M. J. & Nichol, S. T. (2007). Crimean-Congo hemorrhagic fever virus glycoprotein processing by the endoprotease SKI-1/S1P is critical for virus infectivity. *J Virol* 81, 13271-13276.

Berghall, H., Siren, J., Sarkar, D., Julkunen, I., Fisher, P. B., Vainionpaa, R. & Matikainen, S. (2006). The interferon-inducible RNA helicase, mda-5, is involved in measles virus-induced expression of antiviral cytokines. *Microbes Infect*.

Bertolotti-Ciarlet, A., Smith, J., Strecker, K., Paragas, J., Altamura, L. A., McFalls, J. M., Frias-Staheli, N., Garcia-Sastre, A., Schmaljohn, C. S. & other authors (2005). Cellular localization and antigenic characterization of crimean-congo hemorrhagic fever virus glycoproteins. *J Virol* 79, 6152-6161.

Bhattacharya, S. & Schindler, C. (2003). Regulation of Stat3 nuclear export. *J Clin Invest* 111, 553-559.

Bhattacharya, S., Eckner, R., Grossman, S., Oldread, E., Arany, Z., D'Andrea, A. & Livingston, D. M. (1996). Cooperation of Stat2 and p300/CBP in signalling induced by interferon-alpha. *Nature* 383, 344-347.

Bigger, C. B., Guerra, B., Brasky, K. M., Hubbard, G., Beard, M. R., Luxon, B. A., Lemon, S. M. & Lanford, R. E. (2004). Intrahepatic gene expression during chronic hepatitis C virus infection in chimpanzees. *J Virol* 78, 13779-13792.

Billecocq, A., Gauliard, N., Le May, N., Elliott, R. M., Flick, R. & Bouloy, M. (2008). RNA polymerase I-mediated expression of viral RNA for the rescue of infectious virulent and avirulent Rift Valley fever viruses. *Virology* 378, 377-384.

Biron, C. A., Ganes, C.S. (2007). *Innate responses to viral infections. In "Field's Virology" (D. M Knipe and P. M. Howley, eds)*, 5 edn, vol. 1.

Bishop, D. H., Gay, M. E. & Matsuoko, Y. (1983). Nonviral heterogeneous sequences are present at the 5' ends of one species of snowshoe hare bunyavirus S complementary RNA. *Nucleic Acids Res* 11, 6409-6418.

Bishop, D. H., Gould, K. G., Akashi, H. & Clerx-van Haaster, C. M. (1982). The complete sequence and coding content of snowshoe hare bunyavirus small (S) viral RNA species. *Nucleic Acids Res* 10, 3703-3713.

Black, B. L. & Lyles, D. S. (1992). Vesicular stomatitis virus matrix protein inhibits host cell-directed transcription of target genes in vivo. *J Virol* 66, 4058-4064.

Blakqori, G. & Weber, F. (2005). Efficient cDNA-based rescue of La Crosse bunyaviruses expressing or lacking the nonstructural protein NSs. *J Virol* 79, 10420-10428.

Blakqori, G., van Knippenberg, I. & Elliott, R. M. (2009). Bunyamwera orthobunyavirus S-segment untranslated regions mediate poly(A) tail-independent translation. *J Virol* 83, 3637-3646.

Blakqori, G., Kochs, G., Haller, O. & Weber, F. (2003). Functional L polymerase of La Crosse virus allows in vivo reconstitution of recombinant nucleocapsids. *J Gen Virol* 84, 1207-1214.

Blazek, E., Mittler, G. & Meisterernst, M. (2005). The mediator of RNA polymerase II. *Chromosoma* 113, 399-408.

Boone, D. L., Turer, E. E., Lee, E. G., Ahmad, R. C., Wheeler, M. T., Tsui, C., Hurley, P., Chien, M., Chai, S. & other authors (2004). The ubiquitin-modifying enzyme A20 is required for termination of Toll-like receptor responses. *Nat Immunol* 5, 1052-1060.

Bosch, B. J., de Haan, C. A. & Rottier, P. J. (2004). Coronavirus spike glycoprotein, extended at the carboxy terminus with green fluorescent protein, is assembly competent. *J Virol* 78, 7369-7378.

Boudinot, P., Massin, P., Blanco, M., Riffault, S. & Benmansour, A. (1999). vig-1, a new fish gene induced by the rhabdovirus glycoprotein, has a virus-induced homologue in humans and shares conserved motifs with the MoaA family. *J Virol* 73, 1846-1852.

Boudinot, P., Riffault, S., Salhi, S., Carrat, C., Sedlik, C., Mahmoudi, N., Charley, B. & Benmansour, A. (2000). Vesicular stomatitis virus and pseudorabies virus induce a vig1/cig5 homologue in mouse dendritic cells via different pathways. *J Gen Virol* 81, 2675-2682.

Bouloy, M. (1991). Bunyaviridae: genome organization and replication strategies. *Adv Virus Res* 40, 235-275.

Bouloy, M. & Hannoun, C. (1976). Studies on lumbo virus replication. I. RNA-dependent RNA polymerase associated with virions. *Virology* 69, 258-264.

Bouloy, M. & Weber, F. (2010). Molecular biology of rift valley Fever virus. *Open Virol J* 4, 8-14.

Bouloy, M., Janzen, C., Vialat, P., Khun, H., Pavlovic, J., Huerre, M. & Haller, O. (2001). Genetic evidence for an interferon-antagonistic function of rift valley fever virus nonstructural protein NSs. *J Virol* 75, 1371-1377.

Braciale, T. J., Hahn, Y.S., Burton, D.R. (2007). *The adaptive immune response to viruses. In "Field's Virology" (D. M Knipe and P. M. Howley, eds)*

5edn, vol. 1.

Brass, A. L., Huang, I. C., Benita, Y., John, S. P., Krishnan, M. N., Feeley, E. M., Ryan, B. J., Weyer, J. L., van der Weyden, L. & other authors (2009). The IFITM proteins mediate cellular resistance to influenza A H1N1 virus, West Nile virus, and dengue virus. *Cell* 139, 1243-1254.

Braunstein, J., Brutsaert, S., Olson, R. & Schindler, C. (2003). STATs dimerize in the absence of phosphorylation. *J Biol Chem* 278, 34133-34140.

Bridgen, A. & Elliott, R. M. (1996). Rescue of a segmented negative-strand RNA virus entirely from cloned complementary DNAs. *Proc Natl Acad Sci U S A* 93, 15400-15404.

Bridgen, A., Weber, F., Fazakerley, J. K. & Elliott, R. M. (2001). Bunyamwera bunyavirus nonstructural protein NSs is a nonessential gene product that contributes to viral pathogenesis. *Proc Natl Acad Sci U S A* 98, 664-669.

Bridgen, A., Dalrymple, D. A., Weber, F. & Elliott, R. M. (2004). Inhibition of Dugbe nairovirus replication by human MxA protein. *Virus Res* 99, 47-50.

Briese, T., Kapoor, V. & Lipkin, W. I. (2007). Natural M-segment reassortment in Potosi and Main Drain viruses: implications for the evolution of orthobunyaviruses. *Arch Virol* 152, 2237-2247.

Briese, T., Bird, B., Kapoor, V., Nichol, S. T. & Lipkin, W. I. (2006). Batai and Ngari viruses: M segment reassortment and association with severe febrile disease outbreaks in East Africa. *J Virol* 80, 5627-5630.

Brzozka, K., Finke, S. & Conzelmann, K. K. (2005). Identification of the rabies virus alpha/beta interferon antagonist: phosphoprotein P interferes with phosphorylation of interferon regulatory factor 3. *J Virol* 79, 7673-7681.

Buchholz, U. J., Finke, S. & Conzelmann, K. K. (1999). Generation of bovine respiratory syncytial virus (BRSV) from cDNA: BRSV NS2 is not essential for virus replication in tissue culture, and the human RSV leader region acts as a functional BRSV genome promoter. *J Virol* 73, 251-259.

Burfoot, M. S., Rogers, N. C., Watling, D., Smith, J. M., Pons, S., Paonessaw, G., Pellegrini, S., White, M. F. & Kerr, I. M. (1997). Janus kinase-dependent activation of insulin receptor substrate 1 in response to interleukin-4, oncostatin M, and the interferons. *J Biol Chem* 272, 24183-24190.

Cardenas, W. B., Loo, Y. M., Gale, M., Jr., Hartman, A. L., Kimberlin, C. R., Martinez-Sobrido, L., Saphire, E. O. & Basler, C. F. (2006). Ebola virus VP35 protein binds double-stranded RNA and inhibits alpha/beta interferon production induced by RIG-I signaling. *J Virol* 80, 5168-5178.

Carlos, T. S., Fearns, R. & Randall, R. E. (2005). Interferon-induced alterations in the pattern of parainfluenza virus 5 transcription and protein synthesis and the induction of virus inclusion bodies. *J Virol* 79, 14112-14121.

Carlos, T. S., Young, D. F., Schneider, M., Simas, J. P. & Randall, R. E. (2009). Parainfluenza virus 5 genomes are located in viral cytoplasmic bodies whilst the virus dismantles the interferon-induced antiviral state of cells. *J Gen Virol* 90, 2147-2156.

Carroll, S. A., Bird, B. H., Rollin, P. E. & Nichol, S. T. (2010). Ancient common ancestry of Crimean-Congo hemorrhagic fever virus. *Mol Phylogenet Evol* 55, 1103-1110.

Carvalho, M. G., Frugulhetti, I. C. & Rebello, M. A. (1986). Marituba (Bunyaviridae) virus replication in cultured Aedes albopictus cells and in L-A9 cells. *Arch Virol* 90, 325-335.

Chadick, J. Z. & Asturias, F. J. (2005). Structure of eukaryotic Mediator complexes. *Trends Biochem Sci* 30, 264-271.

Chan, Y. L., Chang, T. H., Liao, C. L. & Lin, Y. L. (2008). The cellular antiviral protein viperin is attenuated by proteasome-mediated protein degradation in Japanese encephalitis virus-infected cells. *J Virol* 82, 10455-10464.

Chang, H. W., Watson, J. C. & Jacobs, B. L. (1992). The E3L gene of vaccinia virus encodes an inhibitor of the interferon-induced, double-stranded RNA-dependent protein kinase. *Proc Natl Acad Sci U S A* 89, 4825-4829.

Chariot, A., Leonardi, A., Muller, J., Bonif, M., Brown, K. & Siebenlist, U. (2002). Association of the adaptor TANK with the I kappa B kinase (IKK) regulator NEMO connects IKK complexes with IKK epsilon and TBK1 kinases. *J Biol Chem* 277, 37029-37036.

Chen, J., Baig, E. & Fish, E. N. (2004). Diversity and relatedness among the type I interferons. *J Interferon Cytokine Res* 24, 687-698.

Chen, M., Cheng, A., Chen, Y. Q., Hymel, A., Hanson, E. P., Kimmel, L., Minami, Y., Taniguchi, T., Changelian, P. S. & other authors (1997). The amino terminus of JAK3 is necessary and sufficient for binding to the common gamma chain and confers the ability to transmit interleukin 2-mediated signals. *Proc Natl Acad Sci U S A* 94, 6910-6915.

Chen, S., Short, J. A., Young, D. F., Killip, M. J., Schneider, M., Goodbourn, S. & Randall, R. E. (2010). Heterocellular induction of interferon by negative-sense RNA viruses. *Virology* 407, 247-255.

Chen, Z. J. (2005). Ubiquitin signalling in the NF-kappaB pathway. *Nat Cell Biol* 7, 758-765.

Chew, T., Noyce, R., Collins, S. E., Hancock, M. H. & Mossman, K. L. (2009). Characterization of the interferon regulatory factor 3-mediated antiviral response in a cell line deficient for IFN production. *Mol Immunol* 46, 393-399.

Childs, J. E., Ksiazek, T. G., Spiropoulou, C. F., Krebs, J. W., Morzunov, S., Maupin, G. O., Gage, K. L., Rollin, P. E., Sarisky, J. & other authors (1994). Serologic and genetic identification of Peromyscus maniculatus as the primary rodent reservoir for a new hantavirus in the southwestern United States. *J Infect Dis* 169, 1271-1280.

Childs, K., Stock, N., Ross, C., Andrejeva, J., Hilton, L., Skinner, M., Randall, R. & Goodbourn, S. (2007). mda-5, but not RIG-I, is a common target for paramyxovirus V proteins. *Virology* 359, 190-200.

Chin, K. C. & Cresswell, P. (2001). Viperin (cig5), an IFN-inducible antiviral protein directly induced by human cytomegalovirus. *Proc Natl Acad Sci U S A* 98, 15125-15130.

Chin, Y. E., Kitagawa, M., Kuida, K., Flavell, R. A. & Fu, X. Y. (1997). Activation of the STAT signaling pathway can cause expression of caspase 1 and apoptosis. *Mol Cell Biol* 17, 5328-5337.

Chinsangaram, J., Piccone, M. E. & Grubman, M. J. (1999). Ability of foot-and-mouth disease virus to form plaques in cell culture is associated with suppression of alpha/beta interferon. *J Virol* 73, 9891-9898.

Chung, S. I., Livingston, C. W., Jr., Edwards, J. F., Crandell, R. W., Shope, R. E., Shelton, M. J. & Collisson, E. W. (1990). Evidence that Cache Valley virus induces congenital malformations in sheep. *Vet Microbiol* 21, 297-307.

Clarke, P., Meintzer, S. M., Wang, Y., Moffitt, L. A., Richardson-Burns, S. M., Johnson, G. L. & Tyler, K. L. (2004). JNK regulates the release of proapoptotic mitochondrial factors in reovirus-infected cells. *J Virol* 78, 13132-13138.

Clerzius, G., Gelinas, J. F. & Gatignol, A. (2011). Multiple levels of PKR inhibition during HIV-1 replication. *Rev Med Virol* 21, 42-53.

Clerzius, G., Gelinas, J. F., Daher, A., Bonnet, M., Meurs, E. F. & Gatignol, A. (2009). ADAR1 interacts with PKR during human immunodeficiency virus infection of lymphocytes and contributes to viral replication. *J Virol* 83, 10119-10128.

Collins, P. L., Hill, M. G., Camargo, E., Grosfeld, H., Chanock, R. M. & Murphy, B. R. (1995). Production of infectious human respiratory syncytial virus from cloned cDNA confirms an essential role for the transcription elongation factor from the 5' proximal open reading frame of the M2 mRNA in gene expression and provides a capability for vaccine development. *Proc Natl Acad Sci U S A* 92, 11563-11567.

Colonna, M., Trinchieri, G. & Liu, Y. J. (2004). Plasmacytoid dendritic cells in immunity. *Nat Immunol* 5, 1219-1226.

Conaway, R. C., Sato, S., Tomomori-Sato, C., Yao, T. & Conaway, J. W. (2005). The mammalian Mediator complex and its role in transcriptional regulation. *Trends Biochem Sci* 30, 250-255.

Conzelmann, K. K. (2005). Transcriptional activation of alpha/beta interferon genes: interference by nonsegmented negative-strand RNA viruses. *J Virol* 79, 5241-5248.

Crozat, K. & Beutler, B. (2004). TLR7: A new sensor of viral infection. *Proc Natl Acad Sci U S A* 101, 6835-6836.

Cusson-Hermance, N., Khurana, S., Lee, T. H., Fitzgerald, K. A. & Kelliher, M. A. (2005). Rip1 mediates the Trif-dependent toll-like receptor 3- and 4-induced NF-{kappa}B activation but does not contribute to interferon regulatory factor 3 activation. *J Biol Chem* 280, 36560-36566.

D'Agostino P, M., Amenta, J. J. & Reiss, C. S. (2009). IFN-beta-induced alteration of VSV protein phosphorylation in neuronal cells. *Viral Immunol* 22, 353-369.

D'Cunha, J., Ramanujam, S., Wagner, R. J., Witt, P. L., Knight, E., Jr. & Borden, E. C. (1996). In vitro and in vivo secretion of human ISG15, an IFN-induced immunomodulatory cytokine. *J Immunol* 157, 4100-4108.

Dar, A. C., Dever, T. E. & Sicheri, F. (2005). Higher-order substrate recognition of eIF2alpha by the RNA-dependent protein kinase PKR. *Cell* 122, 887-900.

Dastur, A., Beaudenon, S., Kelley, M., Krug, R. M. & Huibregtse, J. M. (2006). Herc5, an interferon-induced HECT E3 enzyme, is required for conjugation of ISG15 in human cells. *J Biol Chem* 281, 4334-4338.

Davies, F. G. (1997). Tick virus diseases of sheep and goats. *Parassitologia* 39, 91-94.

de Bouteiller, O., Merck, E., Hasan, U. A., Hubac, S., Benguigui, B., Trinchieri, G., Bates, E. E. & Caux, C. (2005). Recognition of double-stranded RNA by human toll-like receptor 3 and downstream receptor signaling requires multimerization and an acidic pH. *J Biol Chem* 280, 38133-38145.

de Haan, P., Kormelink, R., de Oliveira Resende, R., van Poelwijk, F., Peters, D. & Goldbach, R. (1991). Tomato spotted wilt virus L RNA encodes a putative RNA polymerase. *J Gen Virol* 72 (Pt 9), 2207-2216.

de Lang, A., Osterhaus, A. D. & Haagmans, B. L. (2006). Interferon-gamma and interleukin-4 downregulate expression of the SARS coronavirus receptor ACE2 in Vero E6 cells. *Virology* 353, 474-481.

de Veer, M. J., Holko, M., Frevel, M., Walker, E., Der, S., Paranjape, J. M., Silverman, R. H. & Williams, B. R. (2001). Functional classification of interferon-stimulated genes identified using microarrays. *J Leukoc Biol* 69, 912-920.

Decker, T., Lew, D. J. & Darnell, J. E., Jr. (1991a). Two distinct alpha-interferon-dependent signal transduction pathways may contribute to activation of transcription of the guanylate-binding protein gene. *Mol Cell Biol* 11, 5147-5153.

Decker, T., Lew, D. J., Mirkovitch, J. & Darnell, J. E., Jr. (1991b). Cytoplasmic activation of GAF, an IFN-gamma-regulated DNA-binding factor. *Embo J* 10, 927-932.

Degols, G., Eldin, P. & Mechti, N. (2007). ISG20, an actor of the innate immune response. *Biochimie* 89, 831-835.

Deng, L., Wang, C., Spencer, E., Yang, L., Braun, A., You, J., Slaughter, C., Pickart, C. & Chen, Z. J. (2000). Activation of the IkappaB kinase complex by TRAF6 requires a dimeric ubiquitin-conjugating enzyme complex and a unique polyubiquitin chain. *Cell* 103, 351-361.

Der, S. D., Zhou, A., Williams, B. R. & Silverman, R. H. (1998). Identification of genes differentially regulated by interferon alpha, beta, or gamma using oligonucleotide arrays. *Proc Natl Acad Sci U S A* 95, 15623-15628.

Diao, F., Li, S., Tian, Y., Zhang, M., Xu, L. G., Zhang, Y., Wang, R. P., Chen, D., Zhai, Z. & other authors (2007). Negative regulation of MDA5- but not RIG-I-mediated innate antiviral signaling by the dihydroxyacetone kinase. *Proc Natl Acad Sci U S A* 104, 11706-11711.

DiDonato, J. A., Hayakawa, M., Rothwarf, D. M., Zandi, E. & Karin, M. (1997). A cytokine-responsive IkappaB kinase that activates the transcription factor NF-kappaB. *Nature* 388, 548-554.

Diebold, S. S., Kaisho, T., Hemmi, H., Akira, S. & Reis e Sousa, C. (2004). Innate antiviral responses by means of TLR7-mediated recognition of single-stranded RNA. *Science* 303, 1529-1531.

Djavani, M., Rodas, J., Lukashevich, I. S., Horejsh, D., Pandolfi, P. P., Borden, K. L. & Salvato, M. S. (2001). Role of the promyelocytic leukemia protein PML in the interferon sensitivity of lymphocytic choriomeningitis virus. *J Virol* 75, 6204-6208.

Dong, B., Zhou, Q., Zhao, J., Zhou, A., Harty, R. N., Bose, S., Banerjee, A., Slee, R., Guenther, J. & other authors (2004). Phospholipid scramblase 1 potentiates the antiviral activity of interferon. *J Virol* 78, 8983-8993.

Dong, C., Davis, R. J. & Flavell, R. A. (2002). MAP kinases in the immune response. *Annu Rev Immunol* 20, 55-72.

Dotson, M. R., Yuan, C. X., Roeder, R. G., Myers, L. C., Gustafsson, C. M., Jiang, Y. W., Li, Y., Kornberg, R. D. & Asturias, F. J. (2000). Structural organization of yeast and mammalian mediator complexes. *Proc Natl Acad Sci U S A* 97, 14307-14310.

Douglass, R. J., Calisher, C. H. & Bradley, K. C. (2005). State-by-state incidences of hantavirus pulmonary syndrome in the United States, 1993-2004. *Vector Borne Zoonotic Dis* 5, 189-192.

Dumoutier, L., Tounsi, A., Michiels, T., Sommereyns, C., Kotenko, S. V. & Renauld, J. C. (2004). Role of the interleukin (IL)-28 receptor tyrosine residues for antiviral and antiproliferative activity of IL-29/interferon-lambda 1: similarities with type I interferon signaling. *J Biol Chem* 279, 32269-32274.

Dunn, E. F., Pritlove, D. C. & Elliott, R. M. (1994). The S RNA genome segments of Batai, Cache Valley, Guaroa, Kairi, Lumbo, Main Drain and Northway bunyaviruses: sequence determination and analysis. *J Gen Virol* 75 (Pt 3), 597-608.

Dunn, E. F., Pritlove, D. C., Jin, H. & Elliott, R. M. (1995). Transcription of a recombinant bunyavirus RNA template by transiently expressed bunyavirus proteins. *Virology* 211, 133-143.

Duschene, K. S. & Broderick, J. B. (2010). The antiviral protein viperin is a radical SAM enzyme. *FEBS Lett* 584, 1263-1267.

Ea, C. K., Deng, L., Xia, Z. P., Pineda, G. & Chen, Z. J. (2006). Activation of IKK by TNFalpha requires site-specific ubiquitination of RIP1 and polyubiquitin binding by NEMO. *Mol Cell* 22, 245-257.

Edelmann, K. H., Richardson-Burns, S., Alexopoulou, L., Tyler, K. L., Flavell, R. A. & Oldstone, M. B. (2004). Does Toll-like receptor 3 play a biological role in virus infections? *Virology* 322, 231-238.

Eifan, S. A. & Elliott, R. M. (2009). Mutational analysis of the Bunyamwera orthobunyavirus nucleocapsid protein gene. *J Virol* 83, 11307-11317.

Elliott, R. M. (1989). Nucleotide sequence analysis of the large (L) genomic RNA segment of Bunyamwera virus, the prototype of the family Bunyaviridae. *Virology* 173, 426-436.

Elliott, R. M. (1990). Molecular biology of the Bunyaviridae. *J Gen Virol* 71 (Pt 3), 501-522.

Elliott, R. M. (1996). The Bunyaviridae: concluding remarks and future prospects. In *The Bunyaviridae*, pp. 295-332. Edited by R. M. Elliott. New York: Plenum Press.

Elliott, R. M. (1997). Emerging viruses: The Bunyaviridae. *Molecular Medecine* 3, 572-577.

Emeny, J. M. & Morgan, M. J. (1979). Regulation of the interferon system: evidence that Vero cells have a genetic defect in interferon production. *J Gen Virol* 43, 247-252.

Erickson, B. R., Deyde, V., Sanchez, A. J., Vincent, M. J. & Nichol, S. T. (2007). N-linked glycosylation of Gn (but not Gc) is important for Crimean Congo hemorrhagic fever virus glycoprotein localization and transport. *Virology* 361, 348-355.

Erlandsson, L., Blumenthal, R., Eloranta, M. L., Engel, H., Alm, G., Weiss, S. & Leanderson, T. (1998). Interferon-beta is required for interferon-alpha production in mouse fibroblasts. *Curr Biol* 8, 223-226.

Evans, P. C., Ovaa, H., Hamon, M., Kilshaw, P. J., Hamm, S., Bauer, S., Ploegh, H. L. & Smith, T. S. (2004). Zinc-finger protein A20, a regulator of inflammation and cell survival, has de-ubiquitinating activity. *Biochem J* 378, 727-734.

Everett, R. D. & Chelbi-Alix, M. K. (2007). PML and PML nuclear bodies: implications in antiviral defence. *Biochimie* 89, 819-830.

Fagerlund, R., Melen, K., Kinnunen, L. & Julkunen, I. (2002). Arginine/lysine-rich nuclear localization signals mediate interactions between dimeric STATs and importin alpha 5. *J Biol Chem* 277, 30072-30078.

Farrar, J. D., Smith, J. D., Murphy, T. L. & Murphy, K. M. (2000). Recruitment of Stat4 to the human interferon-alpha/beta receptor requires activated Stat2. *J Biol Chem* 275, 2693-2697.

Feller, S. M. (2001). Crk family adaptors-signalling complex formation and biological roles. *Oncogene* 20, 6348-6371.

Fenner, F. (1976). The classification and nomenclature of viruses. Summary of results of meetings of the International Committee on Taxonomy of Viruses in Madrid, September 1975. *Virology* 71, 371-378.

Fensterl, V. & Sen, G. C. (2011). The ISG56/IFIT1 gene family. *J Interferon Cytokine Res* 31, 71-78.

Fitzgerald, K. A., McWhirter, S. M., Faia, K. L., Rowe, D. C., Latz, E., Golenbock, D. T., Coyle, A. J., Liao, S. M. & Maniatis, T. (2003). IKKepsilon and TBK1 are essential components of the IRF3 signaling pathway. *Nat Immunol* 4, 491-496.

Flick, K., Katz, A., Overby, A., Feldmann, H., Pettersson, R. F. & Flick, R. (2004). Functional analysis of the noncoding regions of the Uukuniemi virus (Bunyaviridae) RNA segments. *J Virol* 78, 11726-11738.

Fodor, E., Devenish, L., Engelhardt, O. G., Palese, P., Brownlee, G. G. & Garcia-Sastre, A. (1999). Rescue of influenza A virus from recombinant DNA. *J Virol* 73, 9679-9682.

Fontana, J., Lopez-Montero, N., Elliott, R. M., Fernandez, J. J. & Risco, C. (2008). The unique architecture of Bunyamwera virus factories around the Golgi complex. *Cell Microbiol* 10, 2012-2028.

Frese, M., Kochs, G., Feldmann, H., Hertkorn, C. & Haller, O. (1996). Inhibition of bunyaviruses, phleboviruses, and hantaviruses by human MxA protein. *J Virol* 70, 915-923.

Frias-Staheli, N., Giannakopoulos, N. V., Kikkert, M., Taylor, S. L., Bridgen, A., Paragas, J., Richt, J. A., Rowland, R. R., Schmaljohn, C. S. & other authors (2007). Ovarian tumor domain-containing viral proteases evade ubiquitin- and ISG15-dependent innate immune responses. *Cell Host Microbe* 2, 404-416.

Fu, Y., Comella, N., Tognazzi, K., Brown, L. F., Dvorak, H. F. & Kocher, O. (1999). Cloning of DLM-1, a novel gene that is up-regulated in activated macrophages, using RNA differential display. *Gene* 240, 157-163.

Gack, M. U., Shin, Y. C., Joo, C. H., Urano, T., Liang, C., Sun, L., Takeuchi, O., Akira, S., Chen, Z. & other authors (2007). TRIM25 RING-finger E3 ubiquitin ligase is essential for RIG-I-mediated antiviral activity. *Nature* 446, 916-920.

Garcia, M. A., Gil, J., Ventoso, I., Guerra, S., Domingo, E., Rivas, C. & Esteban, M. (2006). Impact of protein kinase PKR in cell biology: from antiviral to antiproliferative action. *Microbiol Mol Biol Rev* 70, 1032-1060.

Garcin, D., Pelet, T., Calain, P., Roux, L., Curran, J. & Kolakofsky, D. (1995a). A highly recombinogenic system for the recovery of infectious Sendai paramyxovirus from cDNA: generation of a novel copy-back nondefective interfering virus. *Embo J* 14, 6087-6094.

Garcin, D., Lezzi, M., Dobbs, M., Elliott, R. M., Schmaljohn, C., Kang, C. Y. & Kolakofsky, D. (1995b). The 5' ends of Hantaan virus (Bunyaviridae) RNAs suggest a prime-and-realign mechanism for the initiation of RNA synthesis. *J Virol* 69, 5754-5762.

Gavrilovskaya, I. N., Brown, E. J., Ginsberg, M. H. & Mackow, E. R. (1999). Cellular entry of hantaviruses which cause hemorrhagic fever with renal syndrome is mediated by beta3 integrins. *J Virol* 73, 3951-3959.

Geisbert, T. W. & Hensley, L. E. (2004). Ebola virus: new insights into disease aetiopathology and possible therapeutic interventions. *Expert Rev Mol Med* 6, 1-24.

Gelinas, J. F., Clerzius, G., Shaw, E. & Gatignol, A. (2011). Enhancement of Replication of RNA Viruses by ADAR1 via RNA Editing and Inhibition of RNA-Activated Protein Kinase. *J Virol* 85, 8460-8466.

Gerrard, S. R. & Nichol, S. T. (2002). Characterization of the Golgi retention motif of Rift Valley fever virus G(N) glycoprotein. *J Virol* 76, 12200-12210.

Gerrard, S. R., Li, L., Barrett, A. D. & Nichol, S. T. (2004). Ngari virus is a Bunyamwera virus reassortant that can be associated with large outbreaks of hemorrhagic fever in Africa. *J Virol* 78, 8922-8926.

Gerrard, S. R., Bird, B. H., Albarino, C. G. & Nichol, S. T. (2007). The NSm proteins of Rift Valley fever virus are dispensable for maturation, replication and infection. *Virology* 359, 459-465.

Giorgi, C., Accardi, L., Nicoletti, L., Gro, M. C., Takehara, K., Hilditch, C., Morikawa, S. & Bishop, D. H. (1991). Sequences and coding strategies of the S RNAs of Toscana and Rift Valley fever viruses compared to those of Punta Toro, Sicilian Sandfly fever, and Uukuniemi viruses. *Virology* 180, 738-753.

Gitlin, L., Barchet, W., Gilfillan, S., Cella, M., Beutler, B., Flavell, R. A., Diamond, M. S. & Colonna, M. (2006). Essential role of mda-5 in type I IFN responses to polyriboinosinic:polyribocytidylic acid and encephalomyocarditis picornavirus. *Proc Natl Acad Sci U S A* 103, 8459-8464.

Goldsmith, C. S., Elliott, L. H., Peters, C. J. & Zaki, S. R. (1995). Ultrastructural characteristics of Sin Nombre virus, causative agent of hantavirus pulmonary syndrome. *Arch Virol* 140, 2107-2122.

Gonzalez-Scarano, F., Bupp, K., and Nathanson, N. (1996). *Pathogenesis of diseases caused by viruses of the Bunyavirus genus.*: Plenum press, New York.

Goodbourn, S., Didcock, L. & Randall, R. E. (2000). Interferons: cell signalling, immune modulation, antiviral response and virus countermeasures. *J Gen Virol* 81, 2341-2364.

Gorchakov, R., Frolova, E., Williams, B. R., Rice, C. M. & Frolov, I. (2004). PKR-dependent and -independent mechanisms are involved in translational shutoff during Sindbis virus infection. *J Virol* 78, 8455-8467.

Goujon, C. & Malim, M. H. (2010). Characterization of the alpha interferon-induced postentry block to HIV-1 infection in primary human macrophages and T cells. *J Virol* 84, 9254-9266.

Griffin, D. E. (2007). *Measles virus. In "Fields virology" 5th edition (D. M Knipe and P. M. Howley, eds).* 5th edn, vol. II.

Groot, H., Oya, A., Bernal, C. & Barreto-Reyes, P. (1959). Guaroa virus, a new agent isolated in Colombia, South America. *Am J Trop Med Hyg* 8, 604-609.

Habjan, M., Penski, N., Spiegel, M. & Weber, F. (2008). T7 RNA polymerase-dependent and -independent systems for cDNA-based rescue of Rift Valley fever virus. *J Gen Virol* 89, 2157-2166.

Habjan, M., Pichlmair, A., Elliott, R. M., Overby, A. K., Glatter, T., Gstaiger, M., Superti-Furga, G., Unger, H. & Weber, F. (2009). NSs protein of rift valley fever virus

induces the specific degradation of the double-stranded RNA-dependent protein kinase. *J Virol* 83, 4365-4375.

Hacker, H., Redecke, V., Blagoev, B., Kratchmarova, I., Hsu, L. C., Wang, G. G., Kamps, M. P., Raz, E., Wagner, H. & other authors (2006). Specificity in Toll-like receptor signalling through distinct effector functions of TRAF3 and TRAF6. *Nature* 439, 204-207.

Haddow, A. D. & Odoi, A. (2009). The incidence risk, clustering, and clinical presentation of La Crosse virus infections in the eastern United States, 2003-2007. *PLoS One* 4, e6145.

Haferkamp, S., Fernando, L., Schwarz, T. F., Feldmann, H. & Flick, R. (2005). Intracellular localization of Crimean-Congo Hemorrhagic Fever (CCHF) virus glycoproteins. *Virol J* 2, 42.

Hale, B. G., Knebel, A., Botting, C. H., Galloway, C. S., Precious, B. L., Jackson, D., Elliott, R. M. & Randall, R. E. (2009). CDK/ERK-mediated phosphorylation of the human influenza A virus NS1 protein at threonine-215. *Virology* 383, 6-11.

Hallen, L. C., Burki, Y., Ebeling, M., Broger, C., Siegrist, F., Oroszlan-Szovik, K., Bohrmann, B., Certa, U. & Foser, S. (2007). Antiproliferative activity of the human IFN-alpha-inducible protein IFI44. *J Interferon Cytokine Res* 27, 675-680.

Haller, O., Arnheiter, H., Gresser, I. & Lindenmann, J. (1979). Genetically determined, interferon-dependent resistance to influenza virus in mice. *J Exp Med* 149, 601-612.

Haller, O., Arnheiter, H., Lindenmann, J. & Gresser, I. (1980). Host gene influences sensitivity to interferon action selectively for influenza virus. *Nature* 283, 660-662.

Haller, O., Frese, M., Rost, D., Nuttall, P. A. & Kochs, G. (1995). Tick-borne thogoto virus infection in mice is inhibited by the orthomyxovirus resistance gene product Mx1. *J Virol* 69, 2596-2601.

Haller, O., Gao, S., von der Malsburg, A., Daumke, O. & Kochs, G. (2010). Dynamin-like MxA GTPase: structural insights into oligomerization and implications for antiviral activity. *J Biol Chem* 285, 28419-28424.

Hartman, A. L., Dover, J. E., Towner, J. S. & Nichol, S. T. (2006). Reverse genetic generation of recombinant Zaire Ebola viruses containing disrupted IRF-3 inhibitory domains results in attenuated virus growth in vitro and higher levels of IRF-3 activation without inhibiting viral transcription or replication. *J Virol* 80, 6430-6440.

Hawkins, P. T., Anderson, K. E., Davidson, K. & Stephens, L. R. (2006). Signalling through Class I PI3Ks in mammalian cells. *Biochem Soc Trans* 34, 647-662.

He, B., Paterson, R. G., Stock, N., Durbin, J. E., Durbin, R. K., Goodbourn, S., Randall, R. E. & Lamb, R. A. (2002). Recovery of paramyxovirus simian virus 5 with a V protein lacking the conserved cysteine-rich domain: the multifunctional V protein blocks both interferon-beta induction and interferon signaling. *Virology* 303, 15-32.

Heil, F., Hemmi, H., Hochrein, H., Ampenberger, F., Kirschning, C., Akira, S., Lipford, G., Wagner, H. & Bauer, S. (2004). Species-specific recognition of single-stranded RNA via toll-like receptor 7 and 8. *Science* 303, 1526-1529.

Helbig, K. J., Lau, D. T., Semendric, L., Harley, H. A. & Beard, M. R. (2005). Analysis of ISG expression in chronic hepatitis C identifies viperin as a potential antiviral effector. *Hepatology* 42, 702-710.

Hemmi, H., Takeuchi, O., Sato, S., Yamamoto, M., Kaisho, T., Sanjo, H., Kawai, T., Hoshino, K., Takeda, K. & other authors (2004). The roles of two IkappaB kinase-related kinases in lipopolysaccharide and double stranded RNA signaling and viral infection. *J Exp Med* 199, 1641-1650.

Hemmi, H., Takeuchi, O., Kawai, T., Kaisho, T., Sato, S., Sanjo, H., Matsumoto, M., Hoshino, K., Wagner, H. & other authors (2000). A Toll-like receptor recognizes bacterial DNA. *Nature* 408, 740-745.

Hershey, J. W. (1991). Translational control in mammalian cells. *Annu Rev Biochem* 60, 717-755.

Hewlett, M. J., Pettersson, R. F. & Baltimore, D. (1977). Circular forms of Uukuniemi virion RNA: an electron microscopic study. *J Virol* 21, 1085-1093.

Hilton, L., Moganeradj, K., Zhang, G., Chen, Y. H., Randall, R. E., McCauley, J. W. & Goodbourn, S. (2006). The NPro product of bovine viral diarrhea virus inhibits DNA binding by interferon regulatory factor 3 and targets it for proteasomal degradation. *J Virol* 80, 11723-11732.

Hinson, E. R. & Cresswell, P. (2009a). The antiviral protein, viperin, localizes to lipid droplets via its N-terminal amphipathic alpha-helix. *Proc Natl Acad Sci U S A* 106, 20452-20457.

Hinson, E. R. & Cresswell, P. (2009b). The N-terminal amphipathic alpha-helix of viperin mediates localization to the cytosolic face of the endoplasmic reticulum and inhibits protein secretion. *J Biol Chem* 284, 4705-4712.

Ho, L. J., Hung, L. F., Weng, C. Y., Wu, W. L., Chou, P., Lin, Y. L., Chang, D. M., Tai, T. Y. & Lai, J. H. (2005). Dengue virus type 2 antagonizes IFN-alpha but not IFN-gamma antiviral effect via down-regulating Tyk2-STAT signaling in the human dendritic cell. *J Immunol* 174, 8163-8172.

Hochrainer, K., Mayer, H., Baranyi, U., Binder, B., Lipp, J. & Kroismayr, R. (2005). The human HERC family of ubiquitin ligases: novel members, genomic organization, expression profiling, and evolutionary aspects. *Genomics* 85, 153-164.

Hoebe, K., Du, X., Georgel, P., Janssen, E., Tabeta, K., Kim, S. O., Goode, J., Lin, P., Mann, N. & other authors (2003). Identification of Lps2 as a key transducer of MyD88-independent TIR signalling. *Nature* 424, 743-748.

Hoenen, A., Liu, W., Kochs, G., Khromykh, A. A. & Mackenzie, J. M. (2007). West Nile virus-induced cytoplasmic membrane structures provide partial protection against the interferon-induced antiviral MxA protein. *J Gen Virol* 88, 3013-3017.

Honda, K., Ohba, Y., Yanai, H., Negishi, H., Mizutani, T., Takaoka, A., Taya, C. & Taniguchi, T. (2005). Spatiotemporal regulation of MyD88-IRF-7 signalling for robust type-I interferon induction. *Nature* 434, 1035-1040.

Honda, K., Yanai, H., Mizutani, T., Negishi, H., Shimada, N., Suzuki, N., Ohba, Y., Takaoka, A., Yeh, W. C. & other authors (2004). Role of a transductional-transcriptional processor complex involving MyD88 and IRF-7 in Toll-like receptor signaling. *Proc Natl Acad Sci U S A* 101, 15416-15421.

Hornung, V., Ellegast, J., Kim, S., Brzozka, K., Jung, A., Kato, H., Poeck, H., Akira, S., Conzelmann, K. K. & other authors (2006). 5'-Triphosphate RNA is the ligand for RIG-I. *Science* 314, 994-997.

Horvath, C. M. (2004). Silencing STATs: lessons from paramyxovirus interferon evasion. *Cytokine Growth Factor Rev* 15, 117-127.

Hu, W., Hofstetter, W., Guo, W., Li, H., Pataer, A., Peng, H. H., Guo, Z. S., Bartlett, D. L., Lin, A. & other authors (2008). JNK-deficiency enhanced oncolytic vaccinia virus replication and blocked activation of double-stranded RNA-dependent protein kinase. *Cancer Gene Ther* 15, 616-624.

Huang, I. C., Bailey, C. C., Weyer, J. L., Radoshitzky, S. R., Becker, M. M., Chiang, J. J., Brass, A. L., Ahmed, A. A., Chi, X. & other authors (2011). Distinct patterns of IFITM-mediated restriction of filoviruses, SARS coronavirus, and influenza A virus. *PLoS Pathog* 7, e1001258.

Huang, S., Hendriks, W., Althage, A., Hemmi, S., Bluethmann, H., Kamijo, R., Vilcek, J., Zinkernagel, R. M. & Aguet, M. (1993). Immune response in mice that lack the interferon-gamma receptor. *Science* 259, 1742-1745.

Hui, D. J., Bhasker, C. R., Merrick, W. C. & Sen, G. C. (2003). Viral stress-inducible protein p56 inhibits translation by blocking the interaction of eIF3 with the ternary complex eIF2.GTP.Met-tRNAi. *J Biol Chem* 278, 39477-39482.

Huiskonen, J. T., Overby, A. K., Weber, F. & Grunewald, K. (2009). Electron cryo-microscopy and single-particle averaging of Rift Valley fever virus: evidence for GN-GC glycoprotein heterodimers. *J Virol* 83, 3762-3769.

Hutchinson, K. L., Peters, C. J. & Nichol, S. T. (1996). Sin Nombre virus mRNA synthesis. *Virology* 224, 139-149.

Huye, L. E., Ning, S., Kelliher, M. & Pagano, J. S. (2007). Interferon regulatory factor 7 is activated by a viral oncoprotein through RIP-dependent ubiquitination. *Mol Cell Biol* 27, 2910-2918.

Hwang, S. Y., Hertzog, P. J., Holland, K. A., Sumarsono, S. H., Tymms, M. J., Hamilton, J. A., Whitty, G., Bertoncello, I. & Kola, I. (1995). A null mutation in the gene encoding a type I interferon receptor component eliminates antiproliferative and antiviral responses to interferons alpha and beta and alters macrophage responses. *Proc Natl Acad Sci U S A* 92, 11284-11288.

Ikegami, T., Won, S., Peters, C. J. & Makino, S. (2005). Rift Valley fever virus NSs mRNA is transcribed from an incoming anti-viral-sense S RNA segment. *J Virol* 79, 12106-12111.

Ikegami, T., Won, S., Peters, C. J. & Makino, S. (2006). Rescue of infectious rift valley fever virus entirely from cDNA, analysis of virus lacking the NSs gene, and expression of a foreign gene. *J Virol* 80, 2933-2940.

Ikegami, T., Narayanan, K., Won, S., Kamitani, W., Peters, C. J. & Makino, S. (2009). Dual functions of Rift Valley fever virus NSs protein: inhibition of host mRNA transcription and post-transcriptional downregulation of protein kinase PKR. *Ann N Y Acad Sci* 1171 Suppl 1, E75-85.

Isaacs, A. & Lindenmann, J. (1987). Virus interference. I. The interferon. By A. Isaacs and J. Lindenmann, 1957. *J Interferon Res* 7, 429-438.

Ishii, K. J. & Akira, S. (2005). TLR ignores methylated RNA? *Immunity* 23, 111-113.

Ishii, K. J., Coban, C., Kato, H., Takahashi, K., Torii, Y., Takeshita, F., Ludwig, H., Sutter, G., Suzuki, K. & other authors (2006). A Toll-like receptor-independent antiviral response induced by double-stranded B-form DNA. *Nat Immunol* 7, 40-48.

Ishikawa, H. & Barber, G. N. (2008). STING is an endoplasmic reticulum adaptor that facilitates innate immune signalling. *Nature* 455, 674-678.

Itsui, Y., Sakamoto, N., Kurosaki, M., Kanazawa, N., Tanabe, Y., Koyama, T., Takeda, Y., Nakagawa, M., Kakinuma, S. & other authors (2006). Expressional screening of interferon-stimulated genes for antiviral activity against hepatitis C virus replication. *J Viral Hepat* 13, 690-700.

Itsui, Y., Sakamoto, N., Kakinuma, S., Nakagawa, M., Sekine-Osajima, Y., Tasaka-Fujita, M., Nishimura-Sakurai, Y., Suda, G., Karakama, Y. & other authors (2009). Antiviral effects of the interferon-induced protein guanylate binding protein 1 and its interaction with the hepatitis C virus NS5B protein. *Hepatology* 50, 1727-1737.

Iwai, A., Shiozaki, T., Kawai, T., Akira, S., Kawaoka, Y., Takada, A., Kida, H. & Miyazaki, T. (2010). Influenza A virus polymerase inhibits type I interferon induction by binding to interferon beta promoter stimulator 1. *J Biol Chem* 285, 32064-32074.

Iwasaki, A. (2007). Role of autophagy in innate viral recognition. *Autophagy* 3, 354-356.

Janknecht, R. & Hunter, T. (1996). Transcription. A growing coactivator network. *Nature* 383, 22-23.

Jarrossay, D., Napolitani, G., Colonna, M., Sallusto, F. & Lanzavecchia, A. (2001). Specialization and complementarity in microbial molecule recognition by human myeloid and plasmacytoid dendritic cells. *Eur J Immunol* 31, 3388-3393.

Jennings, S., Martinez-Sobrido, L., Garcia-Sastre, A., Weber, F. & Kochs, G. (2005). Thogoto virus ML protein suppresses IRF3 function. *Virology* 331, 63-72.

Jiang, D., Guo, H., Xu, C., Chang, J., Gu, B., Wang, L., Block, T. M. & Guo, J. T. (2008). Identification of three interferon-inducible cellular enzymes that inhibit the replication of hepatitis C virus. *J Virol* 82, 1665-1678.

Jiang, D., Weidner, J. M., Qing, M., Pan, X. B., Guo, H., Xu, C., Zhang, X., Birk, A., Chang, J. & other authors (2010). Identification of five interferon-induced cellular proteins that inhibit west nile virus and dengue virus infections. *J Virol* 84, 8332-8341.

Jiang, Z., Mak, T. W., Sen, G. & Li, X. (2004). Toll-like receptor 3-mediated activation of NF-kappaB and IRF3 diverges at Toll-IL-1 receptor domain-containing adapter inducing IFN-beta. *Proc Natl Acad Sci U S A* 101, 3533-3538.

Jin, H. & Elliott, R. M. (1991). Expression of functional Bunyamwera virus L protein by recombinant vaccinia viruses. *J Virol* 65, 4182-4189.

Jin, H. & Elliott, R. M. (1993). Characterization of Bunyamwera virus S RNA that is transcribed and replicated by the L protein expressed from recombinant vaccinia virus. *J Virol* 67, 1396-1404.

Johnsen, I. B., Nguyen, T. T., Ringdal, M., Tryggestad, A. M., Bakke, O., Lien, E., Espevik, T. & Anthonsen, M. W. (2006). Toll-like receptor 3 associates with c-Src tyrosine kinase on endosomes to initiate antiviral signaling. *Embo J* 25, 3335-3346.

Jounai, N., Takeshita, F., Kobiyama, K., Sawano, A., Miyawaki, A., Xin, K. Q., Ishii, K. J., Kawai, T., Akira, S. & other authors (2007). The Atg5 Atg12 conjugate associates with innate antiviral immune responses. *Proc Natl Acad Sci U S A* 104, 14050-14055.

Kadowaki, N., Ho, S., Antonenko, S., Malefyt, R. W., Kastelein, R. A., Bazan, F. & Liu, Y. J. (2001). Subsets of human dendritic cell precursors express different toll-like receptors and respond to different microbial antigens. *J Exp Med* 194, 863-869.

Kainz, M., Hilson, P., Sweeney, L., Derose, E. & German, T. L. (2004). Interaction Between Tomato spotted wilt virus N Protein Monomers Involves Nonelectrostatic Forces Governed by Multiple Distinct Regions in the Primary Structure. *Phytopathology* 94, 759-765.

Kajaste-Rudnitski, A., Pultrone, C., Marzetta, F., Ghezzi, S., Coradin, T. & Vicenzi, E. (2010). Restriction factors of retroviral replication: the example of Tripartite Motif (TRIM) protein 5 alpha and 22. *Amino Acids* 39, 1-9.

Kakach, L. T., Suzich, J. A. & Collett, M. S. (1989). Rift Valley fever virus M segment: phlebovirus expression strategy and protein glycosylation. *Virology* 170, 505-510.

Kaletsky, R. L., Francica, J. R., Agrawal-Gamse, C. & Bates, P. (2009). Tetherin-mediated restriction of filovirus budding is antagonized by the Ebola glycoprotein. *Proc Natl Acad Sci U S A* 106, 2886-2891.

Kanayama, A., Seth, R. B., Sun, L., Ea, C. K., Hong, M., Shaito, A., Chiu, Y. H., Deng, L. & Chen, Z. J. (2004). TAB2 and TAB3 activate the NF-kappaB pathway through binding to polyubiquitin chains. *Mol Cell* 15, 535-548.

Kanerva, M., Melen, K., Vaheri, A. & Julkunen, I. (1996). Inhibition of puumala and tula hantaviruses in Vero cells by MxA protein. *Virology* 224, 55-62.

Karaghiosoff, M., Neubauer, H., Lassnig, C., Kovarik, P., Schindler, H., Pircher, H., McCoy, B., Bogdan, C., Decker, T. & other authors (2000). Partial impairment of cytokine responses in Tyk2-deficient mice. *Immunity* 13, 549-560.

Kariko, K., Buckstein, M., Ni, H. & Weissman, D. (2005). Suppression of RNA recognition by Toll-like receptors: the impact of nucleoside modification and the evolutionary origin of RNA. *Immunity* 23, 165-175.

Kariwa, H., Tanabe, H., Mizutani, T., Kon, Y., Lokugamage, K., Lokugamage, N., Iwasa, M. A., Hagiya, T., Araki, K. & other authors (2003). Synthesis of Seoul virus RNA and structural proteins in cultured cells. *Arch Virol* 148, 1671-1685.

Kato, H., Takeuchi, O., Sato, S., Yoneyama, M., Yamamoto, M., Matsui, K., Uematsu, S., Jung, A., Kawai, T. & other authors (2006). Differential roles of MDA5 and RIG-I helicases in the recognition of RNA viruses. *Nature* 441, 101-105.

Kawai, T., Takahashi, K., Sato, S., Coban, C., Kumar, H., Kato, H., Ishii, K. J., Takeuchi, O. & Akira, S. (2005). IPS-1, an adaptor triggering RIG-I- and Mda5-mediated type I interferon induction. *Nat Immunol* 6, 981-988.

Kawai, T., Sato, S., Ishii, K. J., Coban, C., Hemmi, H., Yamamoto, M., Terai, K., Matsuda, M., Inoue, J. & other authors (2004). Interferon-alpha induction through Toll-like receptors involves a direct interaction of IRF7 with MyD88 and TRAF6. *Nat Immunol* 5, 1061-1068.

Kerr, I. M., Brown, R. E. & Hovanessian, A. G. (1977). Nature of inhibitor of cell-free protein synthesis formed in response to interferon and double-stranded RNA. *Nature* 268, 540-542.

Kessler, D. S., Veals, S. A., Fu, X. Y. & Levy, D. E. (1990). Interferon-alpha regulates nuclear translocation and DNA-binding affinity of ISGF3, a multimeric transcriptional activator. *Genes Dev* 4, 1753-1765.

Khan, A. S., Khabbaz, R. F., Armstrong, L. R., Holman, R. C., Bauer, S. P., Graber, J., Strine, T., Miller, G., Reef, S. & other authors (1996). Hantavirus pulmonary syndrome: the first 100 US cases. *J Infect Dis* 173, 1297-1303.

Kikkert, M., Van Lent, J., Storms, M., Bodegom, P., Kormelink, R. & Goldbach, R. (1999). Tomato spotted wilt virus particle morphogenesis in plant cells. *J Virol* 73, 2288-2297.

Killip, M. J., Young, D. F., Ross, C. S., Chen, S., Goodbourn, S. & Randall, R. E. (2011). Failure to activate the IFN-beta promoter by a paramyxovirus lacking an interferon antagonist. *Virology* 415, 39-46.

Kim, M. J., Hwang, S. Y., Imaizumi, T. & Yoo, J. Y. (2008). Negative feedback regulation of RIG-I-mediated antiviral signaling by interferon-induced ISG15 conjugation. *J Virol* 82, 1474-1483.

Kitajima, E. W., Resende, R. D., de Avila, A. C., Goldbach, R. W. & Peters, D. (1992). Immuno-electron microscopical detection of tomato spotted wilt virus and its nucleocapsids in crude plant extracts. *J Virol Methods* 38, 313-322.

Kobayashi, T., Yanase, T., Yamakawa, M., Kato, T., Yoshida, K. & Tsuda, T. (2007). Genetic diversity and reassortments among Akabane virus field isolates. *Virus Res* 130, 162-171.

Kobor, M. S. & Greenblatt, J. (2002). Regulation of transcription elongation by phosphorylation. *Biochim Biophys Acta* 1577, 261-275.

Kochs, G. & Haller, O. (1999). Interferon-induced human MxA GTPase blocks nuclear import of Thogoto virus nucleocapsids. *Proc Natl Acad Sci U S A* 96, 2082-2086.

Kochs, G., Garcia-Sastre, A. & Martinez-Sobrido, L. (2007). Multiple anti-interferon actions of the influenza A virus NS1 protein. *J Virol* 81, 7011-7021.

Kohl, A., Dunn, E. F., Lowen, A. C. & Elliott, R. M. (2004). Complementarity, sequence and structural elements within the 3' and 5' non-coding regions of the Bunyamwera orthobunyavirus S segment determine promoter strength. *J Gen Virol* 85, 3269-3278.

Kohl, A., Clayton, R. F., Weber, F., Bridgen, A., Randall, R. E. & Elliott, R. M. (2003). Bunyamwera Virus Nonstructural Protein NSs Counteracts Interferon Regulatory Factor 3-Mediated Induction of Early Cell Death. *J Virol* 77, 7999-8008.

Kohlhuber, F., Rogers, N. C., Watling, D., Feng, J., Guschin, D., Briscoe, J., Witthuhn, B. A., Kotenko, S. V., Pestka, S. & other authors (1997). A JAK1/JAK2 chimera can sustain alpha and gamma interferon responses. *Mol Cell Biol* 17, 695-706.

Kolakofsky, D. & Hacker, D. (1991). Bunyavirus RNA synthesis: genome transcription and replication. *Curr Top Microbiol Immunol* 169, 143-159.

Komarnitsky, P., Cho, E. J. & Buratowski, S. (2000). Different phosphorylated forms of RNA polymerase II and associated mRNA processing factors during transcription. *Genes Dev* 14, 2452-2460.

Kormelink, R., de Haan, P., Peters, D. & Goldbach, R. (1992a). Viral RNA synthesis in tomato spotted wilt virus-infected Nicotiana rustica plants. *J Gen Virol* 73 (Pt 3), 687-693.

Kormelink, R., de Haan, P., Meurs, C., Peters, D. & Goldbach, R. (1992b). The nucleotide sequence of the M RNA segment of tomato spotted wilt virus, a bunyavirus with two ambisense RNA segments. *J Gen Virol* 73 (Pt 11), 2795-2804.

Kormelink, R., Storms, M., Van Lent, J., Peters, D. & Goldbach, R. (1994). Expression and subcellular location of the NSM protein of tomato spotted wilt virus (TSWV), a putative viral movement protein. *Virology* 200, 56-65.

Kornberg, R. D. (2005). Mediator and the mechanism of transcriptional activation. *Trends Biochem Sci* 30, 235-239.

Kotenko, S. V., Gallagher, G., Baurin, V. V., Lewis-Antes, A., Shen, M., Shah, N. K., Langer, J. A., Sheikh, F., Dickensheets, H. & other authors (2003). IFN-lambdas mediate antiviral protection through a distinct class II cytokine receptor complex. *Nat Immunol* 4, 69-77.

Krug, A., French, A. R., Barchet, W., Fischer, J. A., Dzionek, A., Pingel, J. T., Orihuela, M. M., Akira, S., Yokoyama, W. M. & other authors (2004). TLR9-dependent recognition of MCMV by IPC and DC generates coordinated cytokine responses that activate antiviral NK cell function. *Immunity* 21, 107-119.

Kuismanen, E., Hedman, K., Saraste, J. & Pettersson, R. F. (1982). Uukuniemi virus maturation: accumulation of virus particles and viral antigens in the Golgi complex. *Mol Cell Biol* 2, 1444-1458.

Kumar, A., Haque, J., Lacoste, J., Hiscott, J. & Williams, B. R. (1994). Double-stranded RNA-dependent protein kinase activates transcription factor NF-kappa B by phosphorylating I kappa B. *Proc Natl Acad Sci U S A* 91, 6288-6292.

Kumar, P. P., Bischof, O., Purbey, P. K., Notani, D., Urlaub, H., Dejean, A. & Galande, S. (2007). Functional interaction between PML and SATB1 regulates chromatin-loop architecture and transcription of the MHC class I locus. *Nat Cell Biol* 9, 45-56.

Lachmann, P. J. & Davies, A. (1997). Complement and immunity to viruses. *Immunol Rev* 159, 69-77.

Lamb, J. R., Tugendreich, S. & Hieter, P. (1995). Tetratrico peptide repeat interactions: to TPR or not to TPR? *Trends Biochem Sci* 20, 257-259.

Lamb, R. A. a. P., G. D. (2007). *Paramyxoviridae: The viruses and their replication. In Fileds Virology 5th edition.*, vol. Vol 2. Lippincott Williams and Wilkins, New York.

Langland, J. O., Cameron, J. M., Heck, M. C., Jancovich, J. K. & Jacobs, B. L. (2006). Inhibition of PKR by RNA and DNA viruses. *Virus Res* 119, 100-110.

Lappin, D. F., Nakitare, G. W., Palfreyman, J. W. & Elliott, R. M. (1994). Localization of Bunyamwera bunyavirus G1 glycoprotein to the Golgi requires association with G2 but not with NSm. *J Gen Virol* 75 (Pt 12), 3441-3451.

Lawson, N. D., Stillman, E. A., Whitt, M. A. & Rose, J. K. (1995). Recombinant vesicular stomatitis viruses from DNA. *Proc Natl Acad Sci U S A* 92, 4477-4481.

Le May, N., Gauliard, N., Billecocq, A. & Bouloy, M. (2005). The N terminus of Rift Valley fever virus nucleoprotein is essential for dimerization. *J Virol* 79, 11974-11980.

Le May, N., Dubaele, S., Proietti De Santis, L., Billecocq, A., Bouloy, M. & Egly, J. M. (2004). TFIIH transcription factor, a target for the Rift Valley hemorrhagic fever virus. *Cell* 116, 541-550.

Le May, N., Mansuroglu, Z., Leger, P., Josse, T., Blot, G., Billecocq, A., Flick, R., Jacob, Y., Bonnefoy, E. & other authors (2008). A SAP30 complex inhibits IFN-beta expression in Rift Valley fever virus infected cells. *PLoS Pathog* 4, e13.

Leaman, D. W., Salvekar, A., Patel, R., Sen, G. C. & Stark, G. R. (1998). A mutant cell line defective in response to double-stranded RNA and in regulating basal expression of interferon-stimulated genes. *Proc Natl Acad Sci U S A* 95, 9442-9447.

Lee, H. K., Lund, J. M., Ramanathan, B., Mizushima, N. & Iwasaki, A. (2007). Autophagy-dependent viral recognition by plasmacytoid dendritic cells. *Science* 315, 1398-1401.

Lee, H. W. (1989). Hemorrhagic fever with renal syndrome in Korea. *Rev Infect Dis* 11 Suppl 4, S864-876.

Lee, M. H., Lalwani, P., Raftery, M. J., Matthaei, M., Lutteke, N., Kirsanovs, S., Binder, M., Ulrich, R. G., Giese, T. & other authors (2011). RNA helicase retinoic acid-inducible gene I as a sensor of Hantaan virus replication. *J Gen Virol* 92, 2191-2200.

Lee, Y. F., Nomoto, A., Detjen, B. M. & Wimmer, E. (1977). A protein covalently linked to poliovirus genome RNA. *Proc Natl Acad Sci U S A* 74, 59-63.

Lees, J. F., Pringle, C. R. & Elliott, R. M. (1986). Nucleotide sequence of the Bunyamwera virus M RNA segment: conservation of structural features in the Bunyavirus glycoprotein gene product. *Virology* 148, 1-14.

Lenschow, D. J., Giannakopoulos, N. V., Gunn, L. J., Johnston, C., O'Guin, A. K., Schmidt, R. E., Levine, B. & Virgin, H. W. t. (2005). Identification of interferon-stimulated gene 15 as an antiviral molecule during Sindbis virus infection in vivo. *J Virol* 79, 13974-13983.

Leonard, V. H., Kohl, A., Hart, T. J. & Elliott, R. M. (2006). Interaction of Bunyamwera Orthobunyavirus NSs protein with mediator protein MED8: a mechanism for inhibiting the interferon response. *J Virol* 80, 9667-9675.

Leonard, V. H., Kohl, A., Osborne, J. C., McLees, A. & Elliott, R. M. (2005). Homotypic interaction of Bunyamwera virus nucleocapsid protein. *J Virol* 79, 13166-13172.

Leung, S., Qureshi, S. A., Kerr, I. M., Darnell, J. E., Jr. & Stark, G. R. (1995). Role of STAT2 in the alpha interferon signaling pathway. *Mol Cell Biol* 15, 1312-1317.

Levine, J. R., Prescott, J., Brown, K. S., Best, S. M., Ebihara, H. & Feldmann, H. (2010). Antagonism of type I interferon responses by new world hantaviruses. *J Virol* 84, 11790-11801.

Levy, D. E., Kessler, D. S., Pine, R. & Darnell, J. E., Jr. (1989). Cytoplasmic activation of ISGF3, the positive regulator of interferon-alpha-stimulated transcription, reconstituted in vitro. *Genes Dev* 3, 1362-1371.

Levy, D. E., Marie, I., Smith, E. & Prakash, A. (2002). Enhancement and diversification of IFN induction by IRF-7-mediated positive feedback. *J Interferon Cytokine Res* 22, 87-93.

Lewin, A. R., Reid, L. E., McMahon, M., Stark, G. R. & Kerr, I. M. (1991). Molecular analysis of a human interferon-inducible gene family. *Eur J Biochem* 199, 417-423.

Li, C., Ni, C. Z., Havert, M. L., Cabezas, E., He, J., Kaiser, D., Reed, J. C., Satterthwait, A. C., Cheng, G. & other authors (2002). Downstream regulator TANK binds to the CD40 recognition site on TRAF3. *Structure* 10, 403-411.

Li, H., Kobayashi, M., Blonska, M., You, Y. & Lin, X. (2006a). Ubiquitination of RIP is required for tumor necrosis factor alpha-induced NF-kappaB activation. *J Biol Chem* 281, 13636-13643.

Li, K., Foy, E., Ferreon, J. C., Nakamura, M., Ferreon, A. C., Ikeda, M., Ray, S. C., Gale, M., Jr. & Lemon, S. M. (2005a). Immune evasion by hepatitis C virus NS3/4A protease-mediated cleavage of the Toll-like receptor 3 adaptor protein TRIF. *Proc Natl Acad Sci U S A* 102, 2992-2997.

Li, S., Min, J. Y., Krug, R. M. & Sen, G. C. (2006b). Binding of the influenza A virus NS1 protein to PKR mediates the inhibition of its activation by either PACT or double-stranded RNA. *Virology* 349, 13-21.

Li, X. D., Sun, L., Seth, R. B., Pineda, G. & Chen, Z. J. (2005b). Hepatitis C virus protease NS3/4A cleaves mitochondrial antiviral signaling protein off the mitochondria to evade innate immunity. *Proc Natl Acad Sci U S A* 102, 17717-17722.

Li, Z., Wolff, K. C. & Samuel, C. E. (2010). RNA adenosine deaminase ADAR1 deficiency leads to increased activation of protein kinase PKR and reduced vesicular stomatitis virus growth following interferon treatment. *Virology* 396, 316-322.

Lin, R. J., Chang, B. L., Yu, H. P., Liao, C. L. & Lin, Y. L. (2006). Blocking of interferon-induced Jak-Stat signaling by Japanese encephalitis virus NS5 through a protein tyrosine phosphatase-mediated mechanism. *J Virol* 80, 5908-5918.

Lindenmann, J. (1960). [Interferon and inverse interference.]. *Z Haut Geschlechtskr* 146, 287-309.

Liu, B., Liao, J., Rao, X., Kushner, S. A., Chung, C. D., Chang, D. D. & Shuai, K. (1998). Inhibition of Stat1-mediated gene activation by PIAS1. *Proc Natl Acad Sci U S A* 95, 10626-10631.

Livonesi, M. C., de Sousa, R. L., Badra, S. J. & Figueiredo, L. T. (2007). In vitro and in vivo studies of the Interferon-alpha action on distinct Orthobunyavirus. *Antiviral Res* 75, 121-128.

Loeb, K. R. & Haas, A. L. (1992). The interferon-inducible 15-kDa ubiquitin homolog conjugates to intracellular proteins. *J Biol Chem* 267, 7806-7813.

Loeb, K. R. & Haas, A. L. (1994). Conjugates of ubiquitin cross-reactive protein distribute in a cytoskeletal pattern. *Mol Cell Biol* 14, 8408-8419.

Loo, Y. M., Fornek, J., Crochet, N., Bajwa, G., Perwitasari, O., Martinez-Sobrido, L., Akira, S., Gill, M. A., Garcia-Sastre, A. & other authors (2008). Distinct RIG-I and MDA5 signaling by RNA viruses in innate immunity. *J Virol* 82, 335-345.

Lopez, N., Muller, R., Prehaud, C. & Bouloy, M. (1995). The L protein of Rift Valley fever virus can rescue viral ribonucleoproteins and transcribe synthetic genome-like RNA molecules. *J Virol* 69, 3972-3979.

Lowen, A. C. & Elliott, R. M. (2005). Mutational analyses of the nonconserved sequences in the Bunyamwera Orthobunyavirus S segment untranslated regions. *J Virol* 79, 12861-12870.

Lowen, A. C., Noonan, C., McLees, A. & Elliott, R. M. (2004). Efficient bunyavirus rescue from cloned cDNA. *Virology* 330, 493-500.

Lu, G., Reinert, J. T., Pitha-Rowe, I., Okumura, A., Kellum, M., Knobeloch, K. P., Hassel, B. & Pitha, P. M. (2006). ISG15 enhances the innate antiviral response by inhibition of IRF-3 degradation. *Cell Mol Biol (Noisy-le-grand)* 52, 29-41.

Lu, Y., Wambach, M., Katze, M. G. & Krug, R. M. (1995). Binding of the influenza virus NS1 protein to double-stranded RNA inhibits the activation of the protein kinase that phosphorylates the eIF-2 translation initiation factor. *Virology* 214, 222-228.

Lund, J., Sato, A., Akira, S., Medzhitov, R. & Iwasaki, A. (2003). Toll-like receptor 9-mediated recognition of Herpes simplex virus-2 by plasmacytoid dendritic cells. *J Exp Med* 198, 513-520.

Lund, J. M., Alexopoulou, L., Sato, A., Karow, M., Adams, N. C., Gale, N. W., Iwasaki, A. & Flavell, R. A. (2004). Recognition of single-stranded RNA viruses by Toll-like receptor 7. *Proc Natl Acad Sci U S A* 101, 5598-5603.

Luo, H., Rose, P., Barber, D., Hanratty, W. P., Lee, S., Roberts, T. M., D'Andrea, A. D. & Dearolf, C. R. (1997). Mutation in the Jak kinase JH2 domain hyperactivates Drosophila and mammalian Jak-Stat pathways. *Mol Cell Biol* 17, 1562-1571.

Lyles, D. S. a. R., C. E. (2007). *Rhabdoviridae. In Fields Virology 5th edition.*, vol. Vol 2. Lippincott Williams and Wilkins, New York.

Macpherson, I. & Stoker, M. (1962). Polyoma transformation of hamster cell clones--an investigation of genetic factors affecting cell competence. *Virology* 16, 147-151.

Madoff, D. H. & Lenard, J. (1982). A membrane glycoprotein that accumulates intracellularly: cellular processing of the large glycoprotein of LaCrosse virus. *Cell* 28, 821-829.

Malakhov, M. P., Malakhova, O. A., Kim, K. I., Ritchie, K. J. & Zhang, D. E. (2002). UBP43 (USP18) specifically removes ISG15 from conjugated proteins. *J Biol Chem* 277, 9976-9981.

Malakhov, M. P., Kim, K. I., Malakhova, O. A., Jacobs, B. S., Borden, E. C. & Zhang, D. E. (2003). High-throughput immunoblotting. Ubiquitiin-like protein ISG15 modifies key regulators of signal transduction. *J Biol Chem* 278, 16608-16613.

Malakhova, O. A., Yan, M., Malakhov, M. P., Yuan, Y., Ritchie, K. J., Kim, K. I., Peterson, L. F., Shuai, K. & Zhang, D. E. (2003). Protein ISGylation modulates the JAK-STAT signaling pathway. *Genes Dev* 17, 455-460.

Malathi, K., Dong, B., Gale, M., Jr. & Silverman, R. H. (2007). Small self-RNA generated by RNase L amplifies antiviral innate immunity. *Nature* 448, 816-819.

Mao, X., Ren, Z., Parker, G. N., Sondermann, H., Pastorello, M. A., Wang, W., McMurray, J. S., Demeler, B., Darnell, J. E., Jr. & other authors (2005). Structural bases of unphosphorylated STAT1 association and receptor binding. *Mol Cell* 17, 761-771.

Marcus, P. I. (1983). Interferon induction by viruses: one molecule of dsRNA as the threshold for interferon induction. *Interferon* 5, 115-180.

Marczinke, B. I. & Nichol, S. T. (2002). Nairobi sheep disease virus, an important tick-borne pathogen of sheep and goats in Africa, is also present in Asia. *Virology* 303, 146-151.

Marie, I., Durbin, J. E. & Levy, D. E. (1998). Differential viral induction of distinct interferon-alpha genes by positive feedback through interferon regulatory factor-7. *Embo J* 17, 6660-6669.

Marriott, A. C. & Nuttall, P. A. (1996). Large RNA segment of Dugbe nairovirus encodes the putative RNA polymerase. *J Gen Virol* 77 (Pt 8), 1775-1780.

Marriott, A. C., el-Ghorr, A. A. & Nuttall, P. A. (1992). Dugbe Nairovirus M RNA: nucleotide sequence and coding strategy. *Virology* 190, 606-615.

Martin, M. L., Lindsey-Regnery, H., Sasso, D. R., McCormick, J. B. & Palmer, E. (1985). Distinction between Bunyaviridae genera by surface structure and comparison with Hantaan virus using negative stain electron microscopy. *Arch Virol* 86, 17-28.

Martinand, C., Montavon, C., Salehzada, T., Silhol, M., Lebleu, B. & Bisbal, C. (1999). RNase L inhibitor is induced during human immunodeficiency virus type 1 infection and down regulates the 2-5A/RNase L pathway in human T cells. *J Virol* 73, 290-296.

Martinez-Moczygemba, M., Gutch, M. J., French, D. L. & Reich, N. C. (1997). Distinct STAT structure promotes interaction of STAT2 with the p48 subunit of the interferon-alpha-stimulated transcription factor ISGF3. *J Biol Chem* 272, 20070-20076.

Matsumoto, M., Kikkawa, S., Kohase, M., Miyake, K. & Seya, T. (2002). Establishment of a monoclonal antibody against human Toll-like receptor 3 that blocks double-stranded RNA-mediated signaling. *Biochem Biophys Res Commun* 293, 1364-1369.

Matsumoto, M., Funami, K., Tanabe, M., Oshiumi, H., Shingai, M., Seto, Y., Yamamoto, A. & Seya, T. (2003). Subcellular localization of Toll-like receptor 3 in human dendritic cells. *J Immunol* 171, 3154-3162.

Matsuoka, Y., Chen, S. Y. & Compans, R. W. (1994). A signal for Golgi retention in the bunyavirus G1 glycoprotein. *J Biol Chem* 269, 22565-22573.

Matsuoka, Y., Ihara, T., Bishop, D. H. & Compans, R. W. (1988). Intracellular accumulation of Punta Toro virus glycoproteins expressed from cloned cDNA. *Virology* 167, 251-260.

Matthys, V., Gorbunova, E. E., Gavrilovskaya, I. N., Pepini, T. & Mackow, E. R. (2011). The C-terminal 42 residues of the Tula virus Gn protein regulate interferon induction. *J Virol* 85, 4752-4760.

McBride, K. M. & Reich, N. C. (2003). The ins and outs of STAT1 nuclear transport. *Sci STKE* 2003, RE13.

McBride, K. M., McDonald, C. & Reich, N. C. (2000). Nuclear export signal located within theDNA-binding domain of the STAT1transcription factor. *Embo J* 19, 6196-6206.

Meager, A., Visvalingam, K., Dilger, P., Bryan, D. & Wadhwa, M. (2005). Biological activity of interleukins-28 and -29: comparison with type I interferons. *Cytokine* 31, 109-118.

Melchjorsen, J., Jensen, S. B., Malmgaard, L., Rasmussen, S. B., Weber, F., Bowie, A. G., Matikainen, S. & Paludan, S. R. (2005). Activation of innate defense against a paramyxovirus is mediated by RIG-I and TLR7 and TLR8 in a cell-type-specific manner. *J Virol* 79, 12944-12951.

Melen, K., Fagerlund, R., Franke, J., Kohler, M., Kinnunen, L. & Julkunen, I. (2003). Importin alpha nuclear localization signal binding sites for STAT1, STAT2, and influenza A virus nucleoprotein. *J Biol Chem* 278, 28193-28200.

Mercurio, F., Zhu, H., Murray, B. W., Shevchenko, A., Bennett, B. L., Li, J., Young, D. B., Barbosa, M., Mann, M. & other authors (1997). IKK-1 and IKK-2: cytokine-activated IkappaB kinases essential for NF-kappaB activation. *Science* 278, 860-866.

Metz, D. H. & Esteban, M. (1972). Interferon inhibits viral protein synthesis in L cells infected with vaccinia virus. *Nature* 238, 385-388.

Meylan, E., Burns, K., Hofmann, K., Blancheteau, V., Martinon, F., Kelliher, M. & Tschopp, J. (2004). RIP1 is an essential mediator of Toll-like receptor 3-induced NF-kappa B activation. *Nat Immunol* 5, 503-507.

Meylan, E., Curran, J., Hofmann, K., Moradpour, D., Binder, M., Bartenschlager, R. & Tschopp, J. (2005). Cardif is an adaptor protein in the RIG-I antiviral pathway and is targeted by hepatitis C virus. *Nature* 437, 1167-1172.

Mibayashi, M., Martinez-Sobrido, L., Loo, Y. M., Cardenas, W. B., Gale, M., Jr. & Garcia-Sastre, A. (2007). Inhibition of retinoic acid-inducible gene I-mediated induction of beta interferon by the NS1 protein of influenza A virus. *J Virol* 81, 514-524.

Michallet, M. C., Meylan, E., Ermolaeva, M. A., Vazquez, J., Rebsamen, M., Curran, J., Poeck, H., Bscheider, M., Hartmann, G. & other authors (2008). TRADD protein is an essential component of the RIG-like helicase antiviral pathway. *Immunity* 28, 651-661.

Min, J. Y. & Krug, R. M. (2006). The primary function of RNA binding by the influenza A virus NS1 protein in infected cells: Inhibiting the 2'-5' oligo (A) synthetase/RNase L pathway. *Proc Natl Acad Sci U S A* 103, 7100-7105.

Mohl, B. P. & Barr, J. N. (2009). Investigating the specificity and stoichiometry of RNA binding by the nucleocapsid protein of Bunyamwera virus. *RNA* 15, 391-399.

Muller, M., Briscoe, J., Laxton, C., Guschin, D., Ziemiecki, A., Silvennoinen, O., Harpur, A. G., Barbieri, G., Witthuhn, B. A. & other authors (1993). The protein tyrosine kinase JAK1 complements defects in interferon-alpha/beta and -gamma signal transduction. *Nature* 366, 129-135.

Muller, R., Argentini, C., Bouloy, M., Prehaud, C. & Bishop, D. H. (1991). Completion of the genome sequence of Rift Valley fever phlebovirus indicates that the L RNA is negative sense and codes for a putative transcriptase-replicase [corrected]. *Nucleic Acids Res* 19, 5433.

Muller, R., Poch, O., Delarue, M., Bishop, D. H. & Bouloy, M. (1994). Rift Valley fever virus L segment: correction of the sequence and possible functional role of newly identified regions conserved in RNA-dependent polymerases. *J Gen Virol* 75 (Pt 6), 1345-1352.

Murphy, F. A., Whitfield, S. G., Coleman, P. H., Calisher, C. H., Rabin, E. R., Jenson, A. B., Melnick, J. L., Edwards, M. R. & Whitney, E. (1968). California group arboviruses: electron microscopic studies. *Exp Mol Pathol* 9, 44-56.

Mustelin, T., Vang, T. & Bottini, N. (2005). Protein tyrosine phosphatases and the immune response. *Nat Rev Immunol* 5, 43-57.

Myers, L. C., Gustafsson, C. M., Bushnell, D. A., Lui, M., Erdjument-Bromage, H., Tempst, P. & Kornberg, R. D. (1998). The Med proteins of yeast and their function through the RNA polymerase II carboxy-terminal domain. *Genes Dev* 12, 45-54.

Nagai, K., Wong, A. H., Li, S., Tam, W. N., Cuddihy, A. R., Sonenberg, N., Mathews, M. B., Hiscott, J., Wainberg, M. A. & other authors (1997). Induction of CD4 expression and human immunodeficiency virus type 1 replication by mutants of the interferon-inducible protein kinase PKR. *J Virol* 71, 1718-1725.

Nagai, Y. & Kato, A. (2004). Accessory genes of the paramyxoviridae, a large family of nonsegmented negative-strand RNA viruses, as a focus of active investigation by reverse genetics. *Curr Top Microbiol Immunol* 283, 197-248.

Nanduri, S., Carpick, B. W., Yang, Y., Williams, B. R. & Qin, J. (1998). Structure of the double-stranded RNA-binding domain of the protein kinase PKR reveals the molecular basis of its dsRNA-mediated activation. *Embo J* 17, 5458-5465.

Neil, S. J., Sandrin, V., Sundquist, W. I. & Bieniasz, P. D. (2007). An interferon-alpha-induced tethering mechanism inhibits HIV-1 and Ebola virus particle release but is counteracted by the HIV-1 Vpu protein. *Cell Host Microbe* 2, 193-203.

Neumann, G., Watanabe, T., Ito, H., Watanabe, S., Goto, H., Gao, P., Hughes, M., Perez, D. R., Donis, R. & other authors (1999). Generation of influenza A viruses entirely from cloned cDNAs. *Proc Natl Acad Sci U S A* 96, 9345-9350.

Nguyen, K. B., Watford, W. T., Salomon, R., Hofmann, S. R., Pien, G. C., Morinobu, A., Gadina, M., O'Shea, J. J. & Biron, C. A. (2002). Critical role for STAT4 activation by type 1 interferons in the interferon-gamma response to viral infection. *Science* 297, 2063-2066.

Nichol, S. T., Beaty, B., Elliott, R. M., Goldbach, R., Plyusnin, A., Schmaljohn, A. L. & Tesh, R. B. (2005). *Bunyaviridae.* In *In Virus Taxonomy: Eighth Report of the International Committee on Taxonomy of Viruses*, pp. pp.695-716. Edited by M. A. M. Edited by C. M. Fauquet, J. Maniloff, U. Desselberger and L. A. Ball.

Nichol, S. T., Spiropoulou, C. F., Morzunov, S., Rollin, P. E., Ksiazek, T. G., Feldmann, H., Sanchez, A., Childs, J., Zaki, S. & other authors (1993). Genetic identification of a hantavirus associated with an outbreak of acute respiratory illness. *Science* 262, 914-917.

Niklasson, B., Leduc, J., Nystrom, K. & Nyman, L. (1987). Nephropathia epidemica: incidence of clinical cases and antibody prevalence in an endemic area of Sweden. *Epidemiol Infect* 99, 559-562.

Noguchi, T., Satoh, S., Noshi, T., Hatada, E., Fukuda, R., Kawai, A., Ikeda, S., Hijikata, M. & Shimotohno, K. (2001). Effects of mutation in hepatitis C virus nonstructural protein 5A on interferon resistance mediated by inhibition of PKR kinase activity in mammalian cells. *Microbiol Immunol* 45, 829-840.

Novick, D., Cohen, B. & Rubinstein, M. (1994). The human interferon alpha/beta receptor: characterization and molecular cloning. *Cell* 77, 391-400.

Novoa, R. R., Calderita, G., Cabezas, P., Elliott, R. M. & Risco, C. (2005a). Key Golgi factors for structural and functional maturation of bunyamwera virus. *J Virol* 79, 10852-10863.

Novoa, R. R., Calderita, G., Arranz, R., Fontana, J., Granzow, H. & Risco, C. (2005b). Virus factories: associations of cell organelles for viral replication and morphogenesis. *Biol Cell* 97, 147-172.

Obijeski, J. F., Bishop, D. H., Murphy, F. A. & Palmer, E. L. (1976a). Structural proteins of La Crosse virus. *J Virol* 19, 985-997.

Obijeski, J. F., Bishop, D. H., Palmer, E. L. & Murphy, F. A. (1976b). Segmented genome and nucleocapsid of La Crosse virus. *J Virol* 20, 664-675.

Ochsenbein, A. F., Fehr, T., Lutz, C., Suter, M., Brombacher, F., Hengartner, H. & Zinkernagel, R. M. (1999). Control of early viral and bacterial distribution and disease by natural antibodies. *Science* 286, 2156-2159.

Ogawa, Y., Sugiura, K., Kato, K., Tohya, Y. & Akashi, H. (2007). Rescue of Akabane virus (family Bunyaviridae) entirely from cloned cDNAs by using RNA polymerase I. *J Gen Virol* 88, 3385-3390.

Onoguchi, K., Yoneyama, M., Takemura, A., Akira, S., Taniguchi, T., Namiki, H. & Fujita, T. (2007). Viral infections activate types I and III interferon genes through a common mechanism. *J Biol Chem* 282, 7576-7581.

Osborne, J. C. & Elliott, R. M. (2000). RNA binding properties of bunyamwera virus nucleocapsid protein and selective binding to an element in the 5' terminus of the negative-sense S segment. *J Virol* 74, 9946-9952.

Osiak, A., Utermohlen, O., Niendorf, S., Horak, I. & Knobeloch, K. P. (2005). ISG15, an interferon-stimulated ubiquitin-like protein, is not essential for STAT1 signaling and responses against vesicular stomatitis and lymphocytic choriomeningitis virus. *Mol Cell Biol* 25, 6338-6345.

Overby, A. K., Pettersson, R. F. & Neve, E. P. (2007). The glycoprotein cytoplasmic tail of Uukuniemi virus (Bunyaviridae) interacts with ribonucleoproteins and is critical for genome packaging. *J Virol* 81, 3198-3205.

Overby, A. K., Pettersson, R. F., Grunewald, K. & Huiskonen, J. T. (2008). Insights into bunyavirus architecture from electron cryotomography of Uukuniemi virus. *Proc Natl Acad Sci U S A* 105, 2375-2379.

Pardigon, N., Vialat, P., Girard, M. & Bouloy, M. (1982). Panhandles and hairpin structures at the termini of germiston virus RNAs (Bunyavirus). *Virology* 122, 191-197.

Park, G. S., Morris, K. L., Hallett, R. G., Bloom, M. E. & Best, S. M. (2007). Identification of residues critical for the interferon antagonist function of Langat virus NS5 reveals a role for the RNA-dependent RNA polymerase domain. *J Virol* 81, 6936-6946.

Park, S. Y., Saijo, K., Takahashi, T., Osawa, M., Arase, H., Hirayama, N., Miyake, K., Nakauchi, H., Shirasawa, T. & other authors (1995). Developmental defects of lymphoid cells in Jak3 kinase-deficient mice. *Immunity* 3, 771-782.

Patterson, J. L. & Kolakofsky, D. (1984). Characterization of La Crosse virus small-genome transcripts. *J Virol* 49, 680-685.

Patterson, J. L., Holloway, B. & Kolakofsky, D. (1984). La Crosse virions contain a primer-stimulated RNA polymerase and a methylated cap-dependent endonuclease. *J Virol* 52, 215-222.

Patterson, J. L., Kolakofsky, D., Holloway, B. P. & Obijeski, J. F. (1983). Isolation of the ends of La Crosse virus small RNA as a double-stranded structure. *J Virol* 45, 882-884.

Pellegrini, S., John, J., Shearer, M., Kerr, I. M. & Stark, G. R. (1989). Use of a selectable marker regulated by alpha interferon to obtain mutations in the signaling pathway. *Mol Cell Biol* 9, 4605-4612.

Pennington, T. H., Pringle, C. R. & McCrae, M. A. (1977). Bunyamwera virus-induced polypeptide synthesis. *J Virol* 24, 397-400.

Pestka, S., Krause, C. D. & Walter, M. R. (2004). Interferons, interferon-like cytokines, and their receptors. *Immunol Rev* 202, 8-32.

Petersen, J. M., Her, L. S., Varvel, V., Lund, E. & Dahlberg, J. E. (2000). The matrix protein of vesicular stomatitis virus inhibits nucleocytoplasmic transport when it is in the nucleus and associated with nuclear pore complexes. *Mol Cell Biol* 20, 8590-8601.

Pettersson, R. F. (1974). Effect of Uukuniemi virus infection on host cell macromolecule synthesis. *Med Biol* 52, 90-97.

Pettersson, R. F. (1991). Protein localization and virus assembly at intracellular membranes. *Curr Top Microbiol Immunol* 170, 67-106.

Pichlmair, A., Schulz, O., Tan, C. P., Naslund, T. I., Liljestrom, P., Weber, F. & Reis e Sousa, C. (2006). RIG-I-mediated antiviral responses to single-stranded RNA bearing 5'-phosphates. *Science* 314, 997-1001.

Plassmeyer, M. L., Soldan, S. S., Stachelek, K. M., Martin-Garcia, J. & Gonzalez-Scarano, F. (2005). California serogroup Gc (G1) glycoprotein is the principal determinant of pH-dependent cell fusion and entry. *Virology* 338, 121-132.

Platanias, L. C. (2005). Mechanisms of type-I- and type-II-interferon-mediated signalling. *Nat Rev Immunol* 5, 375-386.

Platanias, L. C., Uddin, S., Yetter, A., Sun, X. J. & White, M. F. (1996). The type I interferon receptor mediates tyrosine phosphorylation of insulin receptor substrate 2. *J Biol Chem* 271, 278-282.

Prakash, B., Praefcke, G. J., Renault, L., Wittinghofer, A. & Herrmann, C. (2000). Structure of human guanylate-binding protein 1 representing a unique class of GTP-binding proteins. *Nature* 403, 567-571.

Precious, B., Childs, K., Fitzpatrick-Swallow, V., Goodbourn, S. & Randall, R. E. (2005). Simian virus 5 V protein acts as an adaptor, linking DDB1 to STAT2, to facilitate the ubiquitination of STAT1. *J Virol* 79, 13434-13441.

Precious, B. L., Carlos, T. S., Goodbourn, S. & Randall, R. E. (2007). Catalytic turnover of STAT1 allows PIV5 to dismantle the interferon-induced anti-viral state of cells. *Virology* 368, 114-121.

Prehaud, C., Lopez, N., Blok, M. J., Obry, V. & Bouloy, M. (1997). Analysis of the 3' terminal sequence recognized by the Rift Valley fever virus transcription complex in its ambisense S segment. *Virology* 227, 189-197.

Qanungo, K. R., Shaji, D., Mathur, M. & Banerjee, A. K. (2004). Two RNA polymerase complexes from vesicular stomatitis virus-infected cells that carry out transcription and replication of genome RNA. *Proc Natl Acad Sci U S A* 101, 5952-5957.

Radecke, F., Spielhofer, P., Schneider, H., Kaelin, K., Huber, M., Dotsch, C., Christiansen, G. & Billeter, M. A. (1995). Rescue of measles viruses from cloned DNA. *Embo J* 14, 5773-5784.

Rahaus, M., Desloges, N. & Wolff, M. H. (2004). Replication of varicella-zoster virus is influenced by the levels of JNK/SAPK and p38/MAPK activation. *J Gen Virol* 85, 3529-3540.

Raju, R. & Kolakofsky, D. (1986). Inhibitors of protein synthesis inhibit both La Crosse virus S-mRNA and S genome syntheses in vivo. *Virus Res* 5, 1-9.

Raju, R. & Kolakofsky, D. (1989). The ends of La Crosse virus genome and antigenome RNAs within nucleocapsids are base paired. *J Virol* 63, 122-128.

Randall, G., Chen, L., Panis, M., Fischer, A. K., Lindenbach, B. D., Sun, J., Heathcote, J., Rice, C. M., Edwards, A. M. & other authors (2006). Silencing of USP18 potentiates the antiviral activity of interferon against hepatitis C virus infection. *Gastroenterology* 131, 1584-1591.

Randall, R. E. & Goodbourn, S. (2008). Interferons and viruses: an interplay between induction, signalling, antiviral responses and virus countermeasures. *J Gen Virol* 89, 1-47.

Rane, S. G. & Reddy, E. P. (2000). Janus kinases: components of multiple signaling pathways. *Oncogene* 19, 5662-5679.

Rani, M. R., Shrock, J., Appachi, S., Rudick, R. A., Williams, B. R. & Ransohoff, R. M. (2007). Novel interferon-beta-induced gene expression in peripheral blood cells. *J Leukoc Biol* 82, 1353-1360.

Rathinam, V. A., Jiang, Z., Waggoner, S. N., Sharma, S., Cole, L. E., Waggoner, L., Vanaja, S. K., Monks, B. G., Ganesan, S. & other authors (2010). The AIM2 inflammasome is essential for host defense against cytosolic bacteria and DNA viruses. *Nat Immunol* 11, 395-402.

Ravkov, E. V., Nichol, S. T. & Compans, R. W. (1997). Polarized entry and release in epithelial cells of Black Creek Canal virus, a New World hantavirus. *J Virol* 71, 1147-1154.

Rebouillat, D. & Hovanessian, A. G. (1999). The human 2',5'-oligoadenylate synthetase family: interferon-induced proteins with unique enzymatic properties. *J Interferon Cytokine Res* 19, 295-308.

Reese, S. M., Blitvich, B. J., Blair, C. D., Geske, D., Beaty, B. J. & Black, W. C. t. (2008). Potential for La Crosse virus segment reassortment in nature. *Virol J* 5, 164.

Reid, S. P., Leung, L. W., Hartman, A. L., Martinez, O., Shaw, M. L., Carbonnelle, C., Volchkov, V. E., Nichol, S. T. & Basler, C. F. (2006). Ebola virus VP24 binds karyopherin alpha1 and blocks STAT1 nuclear accumulation. *J Virol* 80, 5156-5167.

Rice, G. I., Bond, J., Asipu, A., Brunette, R. L., Manfield, I. W., Carr, I. M., Fuller, J. C., Jackson, R. M., Lamb, T. & other authors (2009). Mutations involved in Aicardi-Goutieres syndrome implicate SAMHD1 as regulator of the innate immune response. *Nat Genet* 41, 829-832.

Rivieccio, M. A., Suh, H. S., Zhao, Y., Zhao, M. L., Chin, K. C., Lee, S. C. & Brosnan, C. F. (2006). TLR3 ligation activates an antiviral response in human fetal astrocytes: a role for viperin/cig5. *J Immunol* 177, 4735-4741.

Roberts, W. K., Hovanessian, A., Brown, R. E., Clemens, M. J. & Kerr, I. M. (1976). Interferon-mediated protein kinase and low-molecular-weight inhibitor of protein synthesis. *Nature* 264, 477-480.

Rodig, S. J., Meraz, M. A., White, J. M., Lampe, P. A., Riley, J. K., Arthur, C. D., King, K. L., Sheehan, K. C., Yin, L. & other authors (1998). Disruption of the Jak1 gene demonstrates obligatory and nonredundant roles of the Jaks in cytokine-induced biologic responses. *Cell* 93, 373-383.

Rosebeck, S. & Leaman, D. W. (2008). Mitochondrial localization and pro-apoptotic effects of the interferon-inducible protein ISG12a. *Apoptosis* 13, 562-572.

Rossier, C., Raju, R. & Kolakofsky, D. (1988). LaCrosse virus gene expression in mammalian and mosquito cells. *Virology* 165, 539-548.

Rothenfusser, S., Goutagny, N., DiPerna, G., Gong, M., Monks, B. G., Schoenemeyer, A., Yamamoto, M., Akira, S. & Fitzgerald, K. A. (2005). The RNA helicase Lgp2 inhibits TLR-independent sensing of viral replication by retinoic acid-inducible gene-I. *J Immunol* 175, 5260-5268.

Rothwarf, D. M., Zandi, E., Natoli, G. & Karin, M. (1998). IKK-gamma is an essential regulatory subunit of the IkappaB kinase complex. *Nature* 395, 297-300.

Rui, L., Yuan, M., Frantz, D., Shoelson, S. & White, M. F. (2002). SOCS-1 and SOCS-3 block insulin signaling by ubiquitin-mediated degradation of IRS1 and IRS2. *J Biol Chem* 277, 42394-42398.

Rutz, M., Metzger, J., Gellert, T., Luppa, P., Lipford, G. B., Wagner, H. & Bauer, S. (2004). Toll-like receptor 9 binds single-stranded CpG-DNA in a sequence- and pH-dependent manner. *Eur J Immunol* 34, 2541-2550.

Sadler, A. J. & Williams, B. R. (2008). Interferon-inducible antiviral effectors. *Nat Rev Immunol* 8, 559-568.

Saharinen, P., Takaluoma, K. & Silvennoinen, O. (2000). Regulation of the Jak2 tyrosine kinase by its pseudokinase domain. *Mol Cell Biol* 20, 3387-3395.

Sahu, S. K., Gummadi, S. N., Manoj, N. & Aradhyam, G. K. (2007). Phospholipid scramblases: an overview. *Arch Biochem Biophys* 462, 103-114.

Salanueva, I. J., Novoa, R. R., Cabezas, P., Lopez-Iglesias, C., Carrascosa, J. L., Elliott, R. M. & Risco, C. (2003). Polymorphism and structural maturation of bunyamwera virus in Golgi and post-Golgi compartments. *J Virol* 77, 1368-1381.

Sall, A. A., de, A. Z. P. M., Zeller, H. G., Digoutte, J. P., Thiongane, Y. & Bouloy, M. (1997). Variability of the NS(S) protein among Rift Valley fever virus isolates. *J Gen Virol* 78 (Pt 11), 2853-2858.

Samso, A., Bouloy, M. & Hannoun, C. (1975). [Circular ribonucleoproteins in the virus Lumbo (Bunyavirus)]. *C R Acad Sci Hebd Seances Acad Sci D* 280, 779-782.

Samuel, C. E. (2011). Adenosine deaminases acting on RNA (ADARs) are both antiviral and proviral. *Virology* 411, 180-193.

Samuel, M. A., Whitby, K., Keller, B. C., Marri, A., Barchet, W., Williams, B. R., Silverman, R. H., Gale, M., Jr. & Diamond, M. S. (2006). PKR and RNase L contribute to protection against lethal West Nile Virus infection by controlling early viral spread in the periphery and replication in neurons. *J Virol* 80, 7009-7019.

Santos, R. I., Rodrigues, A. H., Silva, M. L., Mortara, R. A., Rossi, M. A., Jamur, M. C., Oliver, C. & Arruda, E. (2008). Oropouche virus entry into HeLa cells involves clathrin and requires endosomal acidification. *Virus Res* 138, 139-143.

Sarkar, S. N., Peters, K. L., Elco, C. P., Sakamoto, S., Pal, S. & Sen, G. C. (2004). Novel roles of TLR3 tyrosine phosphorylation and PI3 kinase in double-stranded RNA signaling. *Nat Struct Mol Biol* 11, 1060-1067.

Sasaki, A., Yasukawa, H., Suzuki, A., Kamizono, S., Syoda, T., Kinjyo, I., Sasaki, M., Johnston, J. A. & Yoshimura, A. (1999). Cytokine-inducible SH2 protein-3 (CIS3/SOCS3) inhibits Janus tyrosine kinase by binding through the N-terminal kinase inhibitory region as well as SH2 domain. *Genes Cells* 4, 339-351.

Sato, S., Sugiyama, M., Yamamoto, M., Watanabe, Y., Kawai, T., Takeda, K. & Akira, S. (2003). Toll/IL-1 receptor domain-containing adaptor inducing IFN-beta (TRIF) associates with TNF receptor-associated factor 6 and TANK-binding kinase 1, and activates two distinct transcription factors, NF-kappa B and IFN-regulatory factor-3, in the Toll-like receptor signaling. *J Immunol* 171, 4304-4310.

Satoh, T., Kato, H., Kumagai, Y., Yoneyama, M., Sato, S., Matsushita, K., Tsujimura, T., Fujita, T., Akira, S. & other authors (2010). LGP2 is a positive regulator of RIG-I-

and MDA5-mediated antiviral responses. *Proc Natl Acad Sci U S A* 107, 1512-1517.

Scallan, M. F. & Elliott, R. M. (1992). Defective RNAs in mosquito cells persistently infected with Bunyamwera virus. *J Gen Virol* 73 (Pt 1), 53-60.

Scheiffele, P., Rietveld, A., Wilk, T. & Simons, K. (1999). Influenza viruses select ordered lipid domains during budding from the plasma membrane. *J Biol Chem* 274, 2038-2044.

Schindler, C. (1998). STATs as activators of apoptosis. *Trends Cell Biol* 8, 97-98.

Schindler, C. & Plumlee, C. (2008). Inteferons pen the JAK-STAT pathway. *Semin Cell Dev Biol* 19, 311-318.

Schindler, C., Levy, D. E. & Decker, T. (2007). JAK-STAT signaling: from interferons to cytokines. *J Biol Chem* 282, 20059-20063.

Schmaljohn, C. S. (1990). Nucleotide sequence of the L genome segment of Hantaan virus. *Nucleic Acids Res* 18, 6728.

Schmaljohn, C. S., and Nichol, S. T. (2007). *Bunyaviridae. In "Field's Virology" 5th edition (D. M Knipe and P. M. Howley, eds)*, 5 edn, vol. 2.

Schmitz, F., Heit, A., Guggemoos, S., Krug, A., Mages, J., Schiemann, M., Adler, H., Drexler, I., Haas, T. & other authors (2007). Interferon-regulatory-factor 1 controls Toll-like receptor 9-mediated IFN-beta production in myeloid dendritic cells. *Eur J Immunol* 37, 315-327.

Schnell, M. J., Mebatsion, T. & Conzelmann, K. K. (1994). Infectious rabies viruses from cloned cDNA. *Embo J* 13, 4195-4203.

Schnettler, E., Hemmes, H., Huismann, R., Goldbach, R., Prins, M. & Kormelink, R. (2010). Diverging affinity of tospovirus RNA silencing suppressor proteins, NSs, for various RNA duplex molecules. *J Virol*.

Schoggins, J. W., Wilson, S. J., Panis, M., Murphy, M. Y., Jones, C. T., Bieniasz, P. & Rice, C. M. (2011). A diverse range of gene products are effectors of the type I interferon antiviral response. *Nature* 472, 481-485.

Seth, R. B., Sun, L., Ea, C. K. & Chen, Z. J. (2005). Identification and characterization of MAVS, a mitochondrial antiviral signaling protein that activates NF-kappaB and IRF 3. *Cell* 122, 669-682.

Severa, M., Coccia, E. M. & Fitzgerald, K. A. (2006). Toll-like receptor-dependent and -independent viperin gene expression and counter-regulation by PRDI-binding factor-1/BLIMP1. *J Biol Chem* 281, 26188-26195.

Sharma, S., tenOever, B. R., Grandvaux, N., Zhou, G. P., Lin, R. & Hiscott, J. (2003). Triggering the interferon antiviral response through an IKK-related pathway. *Science* 300, 1148-1151.

Sherman, M. B., Freiberg, A. N., Holbrook, M. R. & Watowich, S. J. (2009). Single-particle cryo-electron microscopy of Rift Valley fever virus. *Virology* 387, 11-15.

Shi, X. & Elliott, R. M. (2002). Golgi localization of Hantaan virus glycoproteins requires coexpression of G1 and G2. *Virology* 300, 31-38.

Shi, X. & Elliott, R. M. (2004). Analysis of N-linked glycosylation of hantaan virus glycoproteins and the role of oligosaccharide side chains in protein folding and intracellular trafficking. *J Virol* 78, 5414-5422.

Shi, X. & Elliott, R. M. (2009). Generation and analysis of recombinant Bunyamwera orthobunyaviruses expressing V5 epitope-tagged L proteins. *J Gen Virol* 90, 297-306.

Shi, X., Lappin, D. F. & Elliott, R. M. (2004). Mapping the Golgi targeting and retention signal of Bunyamwera virus glycoproteins. *J Virol* 78, 10793-10802.

Shi, X., Brauburger, K. & Elliott, R. M. (2005). Role of N-linked glycans on bunyamwera virus glycoproteins in intracellular trafficking, protein folding, and virus infectivity. *J Virol* 79, 13725-13734.

Shi, X., Kohl, A., Li, P. & Elliott, R. M. (2007). Role of the cytoplasmic tail domains of Bunyamwera orthobunyavirus glycoproteins Gn and Gc in virus assembly and morphogenesis. *J Virol* 81, 10151-10160.

Shi, X., van Mierlo, J. T., French, A. & Elliott, R. M. (2010). Visualizing the replication cycle of bunyamwera orthobunyavirus expressing fluorescent protein-tagged Gc glycoprotein. *J Virol* 84, 8460-8469.

Shi, X., Goli, J., Clark, G., Brauburger, K. & Elliott, R. M. (2009). Functional analysis of the Bunyamwera orthobunyavirus Gc glycoprotein. *J Gen Virol* 90, 2483-2492.

Shi, X., Kohl, A., Leonard, V. H., Li, P., McLees, A. & Elliott, R. M. (2006). Requirement of the N-terminal region of orthobunyavirus nonstructural protein NSm for virus assembly and morphogenesis. *J Virol* 80, 8089-8099.

Shuai, K., Horvath, C. M., Huang, L. H., Qureshi, S. A., Cowburn, D. & Darnell, J. E., Jr. (1994). Interferon activation of the transcription factor Stat91 involves dimerization through SH2-phosphotyrosyl peptide interactions. *Cell* 76, 821-828.

Silverman, R. H. (2007). Viral encounters with 2',5'-oligoadenylate synthetase and RNase L during the interferon antiviral response. *J Virol* 81, 12720-12729.

Simon, M., Johansson, C. & Mirazimi, A. (2009). Crimean-Congo hemorrhagic fever virus entry and replication is clathrin-, pH- and cholesterol-dependent. *J Gen Virol* 90, 210-215.

Simons, J. F., Hellman, U. & Pettersson, R. F. (1990). Uukuniemi virus S RNA segment: ambisense coding strategy, packaging of complementary strands into virions, and homology to members of the genus Phlebovirus. *J Virol* 64, 247-255.

Sin, S. H., McNulty, B. C., Kennedy, G. G. & Moyer, J. W. (2005). Viral genetic determinants for thrips transmission of Tomato spotted wilt virus. *Proc Natl Acad Sci U S A* 102, 5168-5173.

Singh, S. M., Yanagawa, H., Hanibuchi, M., Miki, T., Okamura, H. & Sone, S. (2000). Augmentation by interleukin-18 of MHC-nonrestricted killer activity of human peripheral blood mononuclear cells in response to interleukin-12. *Int J Immunopharmacol* 22, 35-43.

Smith, J. F. & Pifat, D. Y. (1982). Morphogenesis of sandfly viruses (Bunyaviridae family). *Virology* 121, 61-81.

Smithburn, K. C., Haddow, A. J. & Mahaffy, A. F. (1946). A neurotropic virus isolated from Aedes mosquitoes caught in the Semliki forest. *Am J Trop Med Hyg* 26, 189-208.

Smithee, L., Bos, J., Mallonee, S., Nisbett, R. A. & Crutcher, J. M. (2007). Update on hantavirus in Oklahoma: are we missing cases? *J Okla State Med Assoc* 100, 145-148.

Soros, V. B. & Greene, W. C. (2007). APOBEC3G and HIV-1: strike and counterstrike. *Curr HIV/AIDS Rep* 4, 3-9.

Stark, G. R., Kerr, I. M., Williams, B. R., Silverman, R. H. & Schreiber, R. D. (1998). How cells respond to interferons. *Annu Rev Biochem* 67, 227-264.

Stetson, D. B. & Medzhitov, R. (2006). Recognition of cytosolic DNA activates an IRF3-dependent innate immune response. *Immunity* 24, 93-103.

Stirnweiss, A., Ksienzyk, A., Klages, K., Rand, U., Grashoff, M., Hauser, H. & Kroger, A. (2010). IFN regulatory factor-1 bypasses IFN-mediated antiviral effects through viperin gene induction. *J Immunol* 184, 5179-5185.

Strahle, L., Garcin, D. & Kolakofsky, D. (2006). Sendai virus defective-interfering genomes and the activation of interferon-beta. *Virology* 351, 101-111.

Streitenfeld, H., Boyd, A., Fazakerley, J. K., Bridgen, A., Elliott, R. M. & Weber, F. (2003). Activation of PKR by Bunyamwera Virus Is Independent of the Viral Interferon Antagonist NSs. *J Virol* 77, 5507-5511.

Struthers, J. K., Swanepoel, R. & Shepherd, S. P. (1984). Protein synthesis in Rift Valley fever virus-infected cells. *Virology* 134, 118-124.

Subramaniam, P. S., Cruz, P. E., Hobeika, A. C. & Johnson, H. M. (1998). Type I interferon induction of the Cdk-inhibitor p21WAF1 is accompanied by ordered G1 arrest, differentiation and apoptosis of the Daudi B-cell line. *Oncogene* 16, 1885-1890.

Symons, J. A., Alcami, A. & Smith, G. L. (1995). Vaccinia virus encodes a soluble type I interferon receptor of novel structure and broad species specificity. *Cell* 81, 551-560.

Tabeta, K., Georgel, P., Janssen, E., Du, X., Hoebe, K., Crozat, K., Mudd, S., Shamel, L., Sovath, S. & other authors (2004). Toll-like receptors 9 and 3 as essential components of innate immune defense against mouse cytomegalovirus infection. *Proc Natl Acad Sci U S A* 101, 3516-3521.

Takaoka, A. & Yanai, H. (2006). Interferon signalling network in innate defence. *Cell Microbiol* 8, 907-922.

Takaoka, A., Wang, Z., Choi, M. K., Yanai, H., Negishi, H., Ban, T., Lu, Y., Miyagishi, M., Kodama, T. & other authors (2007). DAI (DLM-1/ZBP1) is a cytosolic DNA sensor and an activator of innate immune response. *Nature* 448, 501-505.

Takeda, K. & Akira, S. (2005). Toll-like receptors in innate immunity. *Int Immunol* 17, 1-14.

Talmon, Y., Prasad, B. V., Clerx, J. P., Wang, G. J., Chiu, W. & Hewlett, M. J. (1987). Electron microscopy of vitrified-hydrated La Crosse virus. *J Virol* 61, 2319-2321.

Tang, X., Gao, J. S., Guan, Y. J., McLane, K. E., Yuan, Z. L., Ramratnam, B. & Chin, Y. E. (2007). Acetylation-dependent signal transduction for type I interferon receptor. *Cell* 131, 93-105.

Tauro, L. B., Diaz, L. A., Almiron, W. R. & Contigiani, M. S. (2009). Infection by Bunyamwera virus (Orthobunyavirus) in free ranging birds of Cordoba city (Argentina). *Vet Microbiol* 139, 153-155.

Thomas, D., Blakqori, G., Wagner, V., Banholzer, M., Kessler, N., Elliott, R. M., Haller, O. & Weber, F. (2004). Inhibition of RNA polymerase II phosphorylation by a viral interferon antagonist. *J Biol Chem* 279, 31471-31477.

Thompson, W. H. & Beaty, B. J. (1977). Venereal transmission of La Crosse (California encephalitis) arbovirus in Aedes triseriatus mosquitoes. *Science* 196, 530-531.

Thompson, W. H., Kalfayan, B. & Anslow, R. O. (1965). ISOLATION OF CALIFORNIA ENCEPHALITIS GROUP VIRUS FROM A FATAL HUMAN ILLNESS. *Am J Epidemiol* 81, 245-253.

Torpey, N., Maher, S. E., Bothwell, A. L. & Pober, J. S. (2004). Interferon alpha but not interleukin 12 activates STAT4 signaling in human vascular endothelial cells. *J Biol Chem* 279, 26789-26796.

Towers, G. J. (2007). The control of viral infection by tripartite motif proteins and cyclophilin A. *Retrovirology* 4, 40.

Turan, K., Mibayashi, M., Sugiyama, K., Saito, S., Numajiri, A. & Nagata, K. (2004). Nuclear MxA proteins form a complex with influenza virus NP and inhibit the transcription of the engineered influenza virus genome. *Nucleic Acids Res* 32, 643-652.

Uematsu, S., Sato, S., Yamamoto, M., Hirotani, T., Kato, H., Takeshita, F., Matsuda, M., Coban, C., Ishii, K. J. & other authors (2005). Interleukin-1 receptor-associated kinase-1 plays an essential role for Toll-like receptor (TLR)7- and TLR9-mediated interferon-{alpha} induction. *J Exp Med* 201, 915-923.

Uhrig, J. F., Soellick, T. R., Minke, C. J., Philipp, C., Kellmann, J. W. & Schreier, P. H. (1999). Homotypic interaction and multimerization of nucleocapsid protein of tomato spotted wilt tospovirus: identification and characterization of two interacting domains. *Proc Natl Acad Sci U S A* 96, 55-60.

van Knippenberg, I., Carlton-Smith, C. & Elliott, R. M. (2010). The N-terminus of Bunyamwera orthobunyavirus NSs protein is essential for interferon antagonism. *J Gen Virol* 91, 2002-2006.

Veals, S. A., Schindler, C., Leonard, D., Fu, X. Y., Aebersold, R., Darnell, J. E., Jr. & Levy, D. E. (1992). Subunit of an alpha-interferon-responsive transcription factor is related to interferon regulatory factor and Myb families of DNA-binding proteins. *Mol Cell Biol* 12, 3315-3324.

Venkataraman, T., Valdes, M., Elsby, R., Kakuta, S., Caceres, G., Saijo, S., Iwakura, Y. & Barber, G. N. (2007). Loss of DExD/H box RNA helicase LGP2 manifests disparate antiviral responses. *J Immunol* 178, 6444-6455.

Versteeg, G. A., Hale, B. G., van Boheemen, S., Wolff, T., Lenschow, D. J. & Garcia-Sastre, A. (2010). Species-specific antagonism of host ISGylation by the influenza B virus NS1 protein. *J Virol* 84, 5423-5430.

Vidy, A., El Bougrini, J., Chelbi-Alix, M. K. & Blondel, D. (2007). The nucleocytoplasmic rabies virus P protein counteracts interferon signaling by inhibiting both nuclear accumulation and DNA binding of STAT1. *J Virol* 81, 4255-4263.

Wang, C., Deng, L., Hong, M., Akkaraju, G. R., Inoue, J. & Chen, Z. J. (2001). TAK1 is a ubiquitin-dependent kinase of MKK and IKK. *Nature* 412, 346-351.

Wang, H. & Ryu, W. S. (2010). Hepatitis B virus polymerase blocks pattern recognition receptor signaling via interaction with DDX3: implications for immune evasion. *PLoS Pathog* 6, e1000986.

Wang, X., Hinson, E. R. & Cresswell, P. (2007). The interferon-inducible protein viperin inhibits influenza virus release by perturbing lipid rafts. *Cell Host Microbe* 2, 96-105.

Wang, Z., Choi, M. K., Ban, T., Yanai, H., Negishi, H., Lu, Y., Tamura, T., Takaoka, A., Nishikura, K. & other authors (2008). Regulation of innate immune responses by DAI (DLM-1/ZBP1) and other DNA-sensing molecules. *Proc Natl Acad Sci U S A* 105, 5477-5482.

Ward, B. M. & Moss, B. (2001). Visualization of intracellular movement of vaccinia virus virions containing a green fluorescent protein-B5R membrane protein chimera. *J Virol* 75, 4802-4813.

Watts, D. M., Pantuwatana, S., Yuill, T. M., DeFoliart, G. R., Thompson, W. H. & Hanson, R. P. (1975). Transovarial transmission of LaCrosse virus in Aedes triseriatus. *Ann N Y Acad Sci* 266, 135-143.

Weber, F., Dunn, E. F., Bridgen, A. & Elliott, R. M. (2001). The Bunyamwera virus nonstructural protein NSs inhibits viral RNA synthesis in a minireplicon system. *Virology* 281, 67-74.

Weber, F., Wagner, V., Rasmussen, S. B., Hartmann, R. & Paludan, S. R. (2006). Double-stranded RNA is produced by positive-strand RNA viruses and DNA viruses but not in detectable amounts by negative-strand RNA viruses. *J Virol* 80, 5059-5064.

Weber, F., Bridgen, A., Fazakerley, J. K., Streitenfeld, H., Kessler, N., Randall, R. E. & Elliott, R. M. (2002). Bunyamwera bunyavirus nonstructural protein NSs counteracts the induction of alpha/beta interferon. *J Virol* 76, 7949-7955.

Weihua, X., Ramanujam, S., Lindner, D. J., Kudaravalli, R. D., Freund, R. & Kalvakolanu, D. V. (1998). The polyoma virus T antigen interferes with interferon-inducible gene expression. *Proc Natl Acad Sci U S A* 95, 1085-1090.

Whitehouse, C. A. (2004). Crimean-Congo hemorrhagic fever. *Antiviral Res* 64, 145-160.

Wichmann, D., Grone, H. J., Frese, M., Pavlovic, J., Anheier, B., Haller, O., Klenk, H. D. & Feldmann, H. (2002). Hantaan virus infection causes an acute neurological disease that is fatal in adult laboratory mice. *J Virol* 76, 8890-8899.

Wijkamp, I., van Lent, J., Kormelink, R., Goldbach, R. & Peters, D. (1993). Multiplication of tomato spotted wilt virus in its insect vector, Frankliniella occidentalis. *J Gen Virol* 74 (Pt 3), 341-349.

Wu, C. J., Conze, D. B., Li, T., Srinivasula, S. M. & Ashwell, J. D. (2006). Sensing of Lys 63-linked polyubiquitination by NEMO is a key event in NF-kappaB activation [corrected]. *Nat Cell Biol* 8, 398-406.

Xu, L. G., Wang, Y. Y., Han, K. J., Li, L. Y., Zhai, Z. & Shu, H. B. (2005). VISA is an adapter protein required for virus-triggered IFN-beta signaling. *Mol Cell* 19, 727-740.

Yamamoto, M., Sato, S., Mori, K., Hoshino, K., Takeuchi, O., Takeda, K. & Akira, S. (2002). Cutting edge: a novel Toll/IL-1 receptor domain-containing adapter that preferentially activates the IFN-beta promoter in the Toll-like receptor signaling. *J Immunol* 169, 6668-6672.

Yamamoto, M., Sato, S., Hemmi, H., Hoshino, K., Kaisho, T., Sanjo, H., Takeuchi, O., Sugiyama, M., Okabe, M. & other authors (2003). Role of adaptor TRIF in the MyD88-independent toll-like receptor signaling pathway. *Science* 301, 640-643.

Yamashita, K., Imaizumi, T., Taima, K., Fujita, T., Ishikawa, A., Yoshida, H., Oyama, C. & Satoh, K. (2005). Polyinosinic-polycytidylic acid induces the expression of GRO-alpha in BEAS-2B cells. *Inflammation* 29, 17-21.

Yanai, H., Chen, H. M., Inuzuka, T., Kondo, S., Mak, T. W., Takaoka, A., Honda, K. & Taniguchi, T. (2007). Role of IFN regulatory factor 5 transcription factor in antiviral immunity and tumor suppression. *Proc Natl Acad Sci U S A* 104, 3402-3407.

Yasuda, K., Richez, C., Maciaszek, J. W., Agrawal, N., Akira, S., Marshak-Rothstein, A. & Rifkin, I. R. (2007). Murine dendritic cell type I IFN production induced by human IgG-RNA immune complexes is IFN regulatory factor (IRF)5 and IRF7 dependent and is required for IL-6 production. *J Immunol* 178, 6876-6885.

Yasukawa, H., Misawa, H., Sakamoto, H., Masuhara, M., Sasaki, A., Wakioka, T., Ohtsuka, S., Imaizumi, T., Matsuda, T. & other authors (1999). The JAK-binding protein JAB inhibits Janus tyrosine kinase activity through binding in the activation loop. *Embo J* 18, 1309-1320.

Yeung, M. C., Chang, D. L., Camantigue, R. E. & Lau, A. S. (1999). Inhibitory role of the host apoptogenic gene PKR in the establishment of persistent infection by encephalomyocarditis virus in U937 cells. *Proc Natl Acad Sci U S A* 96, 11860-11865.

Ying, S., Zhang, X., Sarkis, P. T., Xu, R. & Yu, X. (2007). Cell-specific regulation of APOBEC3F by interferons. *Acta Biochim Biophys Sin (Shanghai)* 39, 297-304.

Yokota, S., Yokosawa, N., Okabayashi, T., Suzutani, T., Miura, S., Jimbow, K. & Fujii, N. (2004). Induction of suppressor of cytokine signaling-3 by herpes simplex virus type 1 contributes to inhibition of the interferon signaling pathway. *J Virol* 78, 6282-6286.

Yondola, M. A., Fernandes, F., Belicha-Villanueva, A., Uccelini, M., Gao, Q., Carter, C. & Palese, P. (2011). Budding capability of the influenza virus neuraminidase can be modulated by tetherin. *J Virol* 85, 2480-2491.

Yoneyama, M., Kikuchi, M., Natsukawa, T., Shinobu, N., Imaizumi, T., Miyagishi, M., Taira, K., Akira, S. & Fujita, T. (2004). The RNA helicase RIG-I has an essential function in double-stranded RNA-induced innate antiviral responses. *Nat Immunol* 5, 730-737.

Yoneyama, M., Kikuchi, M., Matsumoto, K., Imaizumi, T., Miyagishi, M., Taira, K., Foy, E., Loo, Y. M., Gale, M., Jr. & other authors (2005). Shared and unique functions of the DExD/H-box helicases RIG-I, MDA5, and LGP2 in antiviral innate immunity. *J Immunol* 175, 2851-2858.

Yoshimatsu, K., Lee, B. H., Araki, K., Morimatsu, M., Ogino, M., Ebihara, H. & Arikawa, J. (2003). The multimerization of hantavirus nucleocapsid protein depends on type-specific epitopes. *J Virol* 77, 943-952.

Young, D. F., Andrejeva, L., Livingstone, A., Goodbourn, S., Lamb, R. A., Collins, P. L., Elliott, R. M. & Randall, R. E. (2003). Virus replication in engineered human cells that do not respond to interferons. *J Virol* 77, 2174-2181.

Young, H. A. (1996). Regulation of interferon-gamma gene expression. *J Interferon Cytokine Res* 16, 563-568.

Yu, S., Chen, J., Wu, M., Chen, H., Kato, N. & Yuan, Z. (2010). Hepatitis B virus polymerase inhibits RIG-I- and Toll-like receptor 3-mediated beta interferon induction in human hepatocytes through interference with interferon regulatory

factor 3 activation and dampening of the interaction between TBK1/IKKepsilon and DDX3. *J Gen Virol* 91, 2080-2090.

Yuan, W. & Krug, R. M. (2001). Influenza B virus NS1 protein inhibits conjugation of the interferon (IFN)-induced ubiquitin-like ISG15 protein. *Embo J* 20, 362-371.

Zahn, R. C., Schelp, I., Utermohlen, O. & von Laer, D. (2007). A-to-G hypermutation in the genome of lymphocytic choriomeningitis virus. *J Virol* 81, 457-464.

Zandi, E., Chen, Y. & Karin, M. (1998). Direct phosphorylation of IkappaB by IKKalpha and IKKbeta: discrimination between free and NF-kappaB-bound substrate. *Science* 281, 1360-1363.

Zeier, M., Handermann, M., Bahr, U., Rensch, B., Muller, S., Kehm, R., Muranyi, W. & Darai, G. (2005). New ecological aspects of hantavirus infection: a change of a paradigm and a challenge of prevention--a review. *Virus Genes* 30, 157-180.

Zhang, D. & Zhang, D. E. (2011). Interferon-stimulated gene 15 and the protein ISGylation system. *J Interferon Cytokine Res* 31, 119-130.

Zhao, C., Denison, C., Huibregtse, J. M., Gygi, S. & Krug, R. M. (2005). Human ISG15 conjugation targets both IFN-induced and constitutively expressed proteins functioning in diverse cellular pathways. *Proc Natl Acad Sci U S A* 102, 10200-10205.

Zhao, C., Beaudenon, S. L., Kelley, M. L., Waddell, M. B., Yuan, W., Schulman, B. A., Huibregtse, J. M. & Krug, R. M. (2004). The UbcH8 ubiquitin E2 enzyme is also the E2 enzyme for ISG15, an IFN-alpha/beta-induced ubiquitin-like protein. *Proc Natl Acad Sci U S A* 101, 7578-7582.

Zhao, T., Yang, L., Sun, Q., Arguello, M., Ballard, D. W., Hiscott, J. & Lin, R. (2007). The NEMO adaptor bridges the nuclear factor-kappaB and interferon regulatory factor signaling pathways. *Nat Immunol* 8, 592-600.

Zhou, A., Hassel, B. A. & Silverman, R. H. (1993). Expression cloning of 2-5A-dependent RNAase: a uniquely regulated mediator of interferon action. *Cell* 72, 753-765.

Zhou, A., Paranjape, J. M., Der, S. D., Williams, B. R. & Silverman, R. H. (1999). Interferon action in triply deficient mice reveals the existence of alternative antiviral pathways. *Virology* 258, 435-440.

Zhu, H., Cong, J. P. & Shenk, T. (1997a). Use of differential display analysis to assess the effect of human cytomegalovirus infection on the accumulation of cellular RNAs: induction of interferon-responsive RNAs. *Proc Natl Acad Sci U S A* 94, 13985-13990.

Zhu, M., John, S., Berg, M. & Leonard, W. J. (1999). Functional association of Nmi with Stat5 and Stat1 in IL-2- and IFNgamma-mediated signaling. *Cell* 96, 121-130.

Zhu, S., Romano, P. R. & Wek, R. C. (1997b). Ribosome targeting of PKR is mediated by two double-stranded RNA-binding domains and facilitates in vivo phosphorylation of eukaryotic initiation factor-2. *J Biol Chem* 272, 14434-14441.

Appendix

Publications

Van Knippenberg, I., **Carlton-Smith, C**., and Elliott, R.M. (2010). **The N-terminus of Bunyamwera virus NSs protein is essential for interferon antagonism**. J Gen Virol 91, 2002-2006.

Presentations

Carlton-Smith, C., and Elliott, R.M. '**Interferon inhibition of Bunyamwera virus Replication**'. ASV 2010, Bozeman, Montana, USA July 2010

Carlton-Smith, C., and Elliott, R.M. '**Interferon inhibition of Bunyavirus replication**'. Controlling Emerging Infectious Diseases in the 21st Century Conference, Texas, USA, Feb 2010

Acknowledgements

My greatest thanks and appreciation goes to Richard for his never-ending patience, guidance and open door throughout my PhD.

Thank you to all members, past and present, of the Elliott lab for their interesting and helpful discussions as well as many enjoyable social adventures, particularly Angela, Agnieszka, Gjon, Ing, Ping and Xiaohong.

I also thank past and present members of the BMS for their help and friendship.

Thank you to the technical staff in the BMS who provided invaluable support throughout the research process, all in a friendly and jovial manner.

I thank my family; parents, brothers and Hanna for their support.